5-2014

Using Ultra Performance Liquid Chromatography-Mass Spectrometric Based Metabolomics to Determine the Metabolic Differences due to Low Temperature or Genetic Mutation in *Salmonella enterica*

Nicole Rhonda Mooney
University of Tennessee - Knoxville, nmooney@utk.edu

To the Graduate Council:

I am submitting herewith a thesis written by Nicole Rhonda Mooney entitled "Using Ultra Performance Liquid Chromatography-Mass Spectrometric Based Metabolomics to Determine the Metabolic Differences due to Low Temperature or Genetic Mutation in *Salmonella enterica*." I have examined the final electronic copy of this thesis for form and content and recommend that it be accepted in partial fulfillment of the requirements for the degree of Master of Science, with a major in Chemistry.

Shawn R. Campagna, Major Professor

We have read this thesis and recommend its acceptance:

Michael J. Sepaniak, John E. Bartmess, Elizabeth Fozo

Accepted for the Council:
Carolyn R. Hodges

Vice Provost and Dean of the Graduate School

(Original signatures are on file with official student records.)

Using Ultra Performance Liquid Chromatography-Mass Spectrometric Based Metabolomics to Determine the Metabolic Differences due to Low Temperature or Genetic Mutation in *Salmonella enterica*

A Thesis Presented for the

Master of Science

Degree

The University of Tennessee, Knoxville

Nicole Rhonda Mooney

May 2014

ACKNOWLEDGEMENTS

Thank you all to my advisor, Dr. Shawn Campagna, for his help and guidance. Thank you to my committee members, Dr. Fozo, Dr. Sepaniak, and Dr. Bartmess for their support. Thank you to my lab mates, Amanda May, Stephen Dearth, Carson Prevatte, Abigail Tester, Hector Castro, Jamie Dillon-Rash, Allen Bourdon, Brandon Kennedy, Jesse Middleton, and Maggie Lookadoo for their help and company through the past year. Thank you to our collaborator's the Downs lab from the University of Georgia, Dr. Downs and Dr. Bazurto, for their help in the *purH* mutation study. Thank you also to my friends and family for keeping my spirits high and providing support when I needed it the most.

ABSTRACT

Metabolomics aims to identify and quantify all of the small molecules within a cell. The relative concentrations of metabolites within cells grown under different experimental conditions, or different species, can be compared using pool size data. Exposing cellular cultures to isotopically labeled compounds allows the progress of metabolites through metabolic pathways to be tracked, known as flux. In the first experiment, the metabolic effects of exposure to lower than optimal temperatures in wild type *Salmonella enterica*, i.e. cold shock, were determined. The metabolites involved in glycolysis, the citric acid cycle, and the pentose phosphate pathway had less efficient labeling and smaller pool sizes at lower temperatures. Most of the amino acids detected showed less efficient labeling and larger pool sizes at lower temperatures, perhaps indicating that proteins were being broken down into amino acids. Alternatively, the less efficient labeling may be due to enzymes denaturing reducing the catalytic abilities of the cells, a slowdown in the rate of transcription or in the rate of translation. It is important to study cold shock in *Salmonella enterica*, at three temperatures in which contamination with the pathogen occurs, in order to see if there is a way to kill the pathogenic species more efficiently and limit the people who get ill from consuming *Salmonella enterica* from food contamination.

The second experiment compared the *purH* mutant and the wild type strain of *Salmonella enterica*. The *purH* mutant had the gene that codes for the enzyme AICAR transformylase/IMP cyclohydrolase removed. AICAR is important to study since it is involved in many pathways in diverse organisms, activates AMP-activated protein kinase in mammals, which affects energy balance and the response to metabolic stress, and AICAR accumulation has been linked to an inhibition of the proliferation of cancer cells. Metabolites in glycolysis and the citric acid cycle were found to label less efficiently or have smaller pool sizes in the *purH* mutant, with the exceptions of those compounds involved in other pathways. The pentose phosphate pathway showed similar labeling patterns and larger pool sizes in the *purH* mutant, indicating that sugars may be going through the pathway.

TABLE OF CONTENTS

LIST OF TABLES

LIST OF FIGURES

CHAPTER 1 INTRODUCTION

Systems Biology

Systems biology attempts to understand how each and every component interacts in the system being studied as a whole i.e. the system is more than simply the sum of its components. The system is studied by examining the system structures, the system dynamics, and the control method. The system structures encompass the actual biochemical pathways, the gene networks, and the ways in which the gene network and biochemical pathways regulate phenotypes. The system dynamics encompasses the changes that occur due to a disturbance. The control method involves looking at regulatory portions of the system.[1] It is important to study metabolomics on a systems biology level, because the genes, metabolites, and phenotypes are all interconnected in a vast web that is not fully understood. Changing one gene theoretically may only remove the ability to make one protein, enzyme, or metabolite; however, the changes seen on a systems level show that a domino effect is often seen by a seemingly simple alteration to the genome.[2]

Metabolomics

Metabolomics is the study of all of the small molecules (molecules with molecular masses less than 1000 atomic mass units) produced by a cell (metabolites).[3, 4] Metabolomics allows a snapshot of cellular biochemistry, showing the concentrations of various metabolites, as well as the flow of these metabolites into, out of, and within a cell.[3, 4, 5] Metabolomics can be used not only to determine what a natural state of homeostasis means in terms of metabolite concentration and flow (metabolism), but also how metabolite concentrations and flows can change under various experimental conditions.[4] Metabolomics can even determine how metabolism changes as a result of a genetic mutation.[4, 6] In short, metabolomics allows the metabolism, the deconstruction and construction of molecules, of an organism to be studied in both native and altered states and conditions. Metabolomics is already enhancing the understanding of cellular metabolism, the effects of genetic mutations, and the role diseases, drugs, and bacterial communication have played.[3,7 ,8, 9, 10]

Metabolites can be divided into two groups, lipids or water-soluble metabolites.[3] Lipids are the nonpolar and amphiphilic molecules produced by a cell or organism, such as fats, waxes, sterols, phospholipids, and the fat soluble vitamins. Many lipids are involved in the production

and maintenance of the cellular membranes.[11, 12] The goal of lipidomics is to identify and quantitate lipids found in a given system. Water soluble metabolomics studies, as one would expect, all of the water soluble metabolites within a cell. The water-soluble metabolites exist transiently, often in very low concentrations, and can play well established metabolic roles within the cells or tissues. Water-soluble metabolites include sugars, cofactors, molecules involved in the transfer of electrons, and many other compounds.[3]

Metabolomics can be studied in one of two ways, in a targeted fashion or in an untargeted fashion.[4] In targeted metabolomics, only a specific set of metabolites is searched for and quantitated; whereas in untargeted metabolomics, as many compounds as possible are searched for and detected. [4, 13, 14] Identification of all unknown compounds in untargeted metabolomics studies can be very cumbersome and has not been done fully as of yet.[15] Targeted metabolomics allows screening for biomarkers of disease, illicit drugs, as well as the determination of the concentrations of specific metabolites of interest in routine analysis.[16, 17] Untargeted metabolomics allows a broader screening of metabolism. For instance using untargeted metabolomics, the determination of the metabolic changes due to differing environmental conditions, global changes in metabolism due to disease and drug treatments, or genetic mutations could be discovered and their differences defined.[18,19]

Metabolomics methodology

Metabolomics studies can be done for a wide range of organisms: adherent and non-adherent bacterial cultures, single-cellular organisms such as yeast or plankton, plants, animal tissues or organs, and biological fluids.[20, 7, 19, 21, 16] In the case of bacterial cultures and single-celled organisms, cells are grown in liquid media or on agarose or agar plates.[5] In the case of plants, tissues, and organs, experiments may be performed on the entire organism, and samples may be removed during the experiment or after the organism has been sacrificed.[22] Biological fluids may be removed from organisms in a fairly non-invasive manner after the entire organism has been exposed to the experimental conditions.[16] As bacterial cellular cultures are used in the

experiments presented in this thesis, the rest of this introduction to metabolomics methodology will be based on working with them.

Using bacterial cellular cultures as a model, cells may be grown in liquid media or on media plates. The bacterial cellular cultures may be exposed to the condition during the initial growth phase or after a certain density, or concentration, of cells has been reached.[20] Experimental conditions can vary widely, depending on both the questions being asked by the study and the optimal conditions of the system (organisms or cells) being studied. Cells grown under different conditions may incorporate the components of the media differently into their metabolism, indicating that the cellular metabolism under the new conditions has changed.[20] If the media includes an isotopically labeled compound, such as ^{13}C labeled glucose, its flux can be tracked through various pathways in order to try to determine what changes to metabolism may have occurred due to the experimental conditions.[20] Graphs of the relative percentage of labeled metabolite to unlabeled metabolite over time are known as flux graphs and show the incorporation of labeled nutrient over time.[5, 23, 24, 25] For a given pathway of interest, multiple metabolites are examined to see how the incorporations of the labeled forms are changing, either in pattern or rate.[5, 24, 25] For instance, if the concentration of unlabeled metabolite is decreasing and the concentration of labeled is not increasing, it indicates that there may a chemical reaction somewhere in the pathway that is not able to occur causing the metabolite not to be produced.

To complement this information, data on pool size, which is the concentration of the individual metabolites within a cell, can also be gathered.[24] Pool size can also be thought of as a measure of the intracellular concentration of the metabolites before ^{13}C incorporation, which can help explain the observation of slower labeling. If an experimental group has a larger pool size than the control, then there may be some blockage in the pathway causing it to build up or the metabolite may not be used as quickly under the experimental condition.

In addition, heat maps can be used to compare the effect of conditions.[26] A heat map details the ratio of the relative change in the concentration of a metabolite (pool size data only) in the experimental group to the relative change of a metabolite in the control, or another experimental group.[26] If metabolite has a larger concentration in comparison, then it will appear red, whereas if a metabolite has a smaller relative concentration, it will appear blue. Heat maps

allow a visual representation of the relative changes in metabolites between experimental conditions.[26]

In order to get the information needed to construct flux graphs, pool size plots, and heat maps, the metabolites must be extracted from the cells.[27] In this step it is important to stop metabolism as quickly as possible (quenching), so that the process of extracting the metabolites does not itself affect metabolism.[27] Often the process for quenching metabolism is the same process used to extract the metabolites. Depending on what types of metabolites are being studied, different extraction protocols are used targeting either specific classes of metabolites or as many metabolites as possible. Once metabolism has been quenched and the metabolites have been extracted, they may be detected through gas chromatography-mass spectrometry (GC-MS) or liquid chromatography-mass spectrometry (LC-MS).[28] GC-MS and LC-MS may be used to measure specific metabolites (targeted metabolomics) or as many compounds as possible (untargeted metabolomics).[28]

The instrumental methods gather the raw data that may then be processed and analyzed in order to construct flux graphs, pool size plots, and heat maps. The raw data must be processed using software such as MAVEN, XCMS, or Xcaliber in order to match metabolites to peaks on the spectra by mass to charge ratio (*m/z*) and retention time by comparison with known standards or information from data bases.[29,30] Exact concentrations of metabolites can be determined through the use of internal standards or the relative concentrations between experimental conditions, over time, or among isopomers can be calculated.[25] Once the raw data has been processed and the flux graphs, pool size plots, and heat maps have been generated, the analysis of the metabolic pathways can begin.[31]

Flux graphs and pool size plots can be overlaid onto metabolic pathways to determine locations where metabolism is not functioning optimally or functioning at all. Indications of suboptimal metabolism include if the unlabeled metabolite disappears and labeled metabolite is not present, or if there is a buildup of metabolites further down the metabolic pathway. Suboptimal performance may also be indicated by slower labeling or less complete labeling of a metabolite as compared to the control conditions. If one imagines that metabolic pathways are like assembly lines, the idea of flux can be illustrated. If there is a blockage in the assembly line,

the items before the blockage will build up, while the items after the blockage will disappear. If there is a slow worker on the assembly line, the effect will be similar to the effect of a blockage, but to a lesser extent (some items will make it down the assembly line). If there is a very fast worker on an assembly line, the items before the worker will be used up quickly and passed along the assembly line to the next step just as quickly. After that, the items may reach a more normal speed of movement. Flux can be thought of as the speed at which metabolites (items) are moving through a metabolic pathway (the assembly line). Pool size can be thought of as the amount of items at each station at the beginning of a shift, when there is no movement through the assembly line.

Analytical Instrumentation

Metabolites are largely detected through chromatography-mass spectrometry, due to the ability to detect many metabolites simultaneously and the flexibility that the instrumental method affords.[24] Chromatography is used first to separate compounds based on the retention of the compound (the time it takes for the compound of interest to travel through the column, the time it takes for the compound reaches the mass analyzer in the mass spectrometry portion of the method, or the time it takes for the compound of interest to reach the detector in other analytical methods). Once the compounds have been separated temporally, they are usually injected directly into the ion source of a mass spectrometer. From there, the compounds are ionized and separated based on *m/z* in the mass analyzer portion of the mass spectrometer. The compounds are then detected and the raw data can be processed.[24]

Chromatography

Chromatography is used to separate metabolites based on size, charge, or affinity for certain ligands. Chromatography separates molecules based upon how much the compounds interact with the coating on the column (stationary phase). The mobile phase carries the compounds through the column. The competing forces on compounds caused by the stationary phase and mobile phase(s) cause compounds to partition between the stationary phase and

mobile phase, which moves compounds through the column at different speeds, and therefore causes compounds to elute after different amounts of time spent in the column.[32]

There are two highly used ways chromatography can be done, via normal phase or reverse phase chromatography. Normal phase chromatography was used first and consists of a polar stationary phase and a nonpolar mobile phase. Normal phase stationary phases include polar compounds such as silica based polymers and zirconia, and best separates polar compounds. Reverse phase was invented after normal phase and consists of a polar mobile phase and a nonpolar stationary phase. Reverse phase stationary phases include hydrocarbon chains, such as C-18 or C-10, and best separates nonpolar compounds. Within these two ways, there are also various types of chromatography that can be done. Gas chromatography, liquid chromatography, ultra high performance liquid chromatography, and affinity chromatography are common forms of chromatography.

In gas chromatography, volatile and semi-volatile substances are aerosolized and injected into the column. These compounds are then carried through the column by a carrier gas and have the ability to interact with the coating on the column. The compounds are then eluted in an order determined by the boiling point of the compound, the interaction of the compound with the column, and the length of the column. An oven can be used in gas chromatography contains the column and may be heated in a gradient manner in order to expedite the flow of compounds through the column. Compounds that are smaller or have a lower boiling point elute faster in gas chromatography. Gas chromatography is not compatible with nonvolatile substances, compounds with boiling points above 450 °C. Suitable compounds for analysis with gas chromatography have a relatively low molecular weight (usually below 1000 atomic mass units), are thermally stable, have a low boiling point, and are unable to react with the stationary phase or mobile phase. Some nonvolatile compounds can be analyzed using gas chromatography after derivatization.[33] Derivatization may be a long process though and may not work with all molecules, but allows nonvolatile compounds to be volatilized for analysis via gas chromatography.

Liquid chromatography can be used to separate nonvolatile compounds, semi-volatile compounds, and most volatile compounds. Ultra high performance liquid chromatography

(UPLC), affinity chromatography, and ion exchange chromatography are types of the broader category of liquid chromatography. In liquid chromatography a sample is injected into the column, dissolved in the mobile phase, and carried by the mobile phase through the column. One or more solutions may be used as the mobile phase in liquid chromatography. As in gas chromatography, the compounds are partitioned between the mobile phase and the stationary phase. Compounds are eluted from the column based on their size, affinity for the mobile phase and stationary phase, and the length and diameter of the column. Typically, in HPLC typically particle diameters are 5 μm, while in UPLC particle diameters are less than 2 μm.[34] UPLC differs from HPLC due to the ability of the instrumentation to withstand higher back pressures. UPLC allows higher back pressures to be withstood due to the better instrumentation used. This allows a small column packed with small particles (diameters smaller than 2 μm) to be used as the stationary phase, which leads to be a better separation due to van Deemter forces. Due to the small particles size, uniform packing of the particles, and high flow rates sometimes used, the sample is moved through the column at a very high pressure. This allows fast and reproducible separations.

Affinity chromatography works by injecting a sample into a column coated with a compound that will only bind to the compounds of interest. The compounds coating the column attach to a portion of or the entire molecule of interest. The compounds of interest are retained and everything else in the sample is washed through the column. The components coating the column can then be forced to release the molecules of interest by adding a reagent, known as salting the column. Affinity chromatography is very expensive due to the need for ligands capable of binding to the compound of interest, and this method is not flexible as compared to those methods not requiring ligands.

In ion exchange chromatography, the stationary phase consists of a coating of charged particles. A solution of compounds, dissolved in the mobile phase, goes through the column and oppositely charged particles interact with the charged particles in the stationary phase. This allows oppositely charged particles to be retained in the column longer than similarly charged particles, leading to better separation. A type of ion interaction chromatography is ion pairing chromatography. In this case, the ion pairing reagent is added to the mobile phase so that when

the components of the sample are dissolved in the mobile phase those of opposite charge interact with the ion pairing reagent. The addition of the ion pairing reagent allows the analyte molecules to interact with the coating on the column. The interactions between the ion pairing reagents and the oppositely charged particles slow down the movement of the compounds through the column and allow the compounds to have a longer retention time, which leads to better separation.

Mass spectrometry

Gas phase mass spectrometry works by injecting compounds, ionizing the compounds using an ionization source, separating mass to charge ratios (*m/z*), and then detecting the mass to charge.[35] When mass spectrometry is paired to a chromatographic technique, the injection of the compounds into the ionization source is based on their elution from the chromatographic column used. There are a number of ion sources used in mass spectrometry whose purpose is to ionize compounds. Ionization sources include electron ionization (EI), chemical ionization (CI), electron spray ionization (ESI), and matrix assisted laser desorption (MALDI).[35] Some ion sources, such as ESI, accomplish ionization by adding protons (positive mode mass spectrometry) or removing protons (negative mode mass spectrometry).[36] Other ion sources accomplish ionization by bombarding a molecule with a stream of electrons, such as EI.[37] Once ions have been made they are collected and moved into the mass analyzer either once a certain number of ions have been collected or after a certain amount of time has passed.[38] Having two methods of moving ions into the mass spectrometer helps prevents too many ions from getting into the mass analyzer and introducing molecular repulsion, diffusion of the ion band, or ion suppression.[38] The separation by *m/z* is accomplished by utilizing electrical and magnetic fields to guide the ions to the desired location within the mass analyzer.[35] The ions organized by *m/z* are then sent to the mass detector. Detectors also vary widely and can include Faraday cups, electron multiplier tubes, and micro channel plate detectors.[35] Mass spectrometry is one method used for metabolomics analysis since it requires a small samples size, it is relatively easy to manipulate and detect charged particles, it enables accurate identification via *m/z* mass fragmentation patterns, and retention times when paired with chromatography, and has the ability to quantitate the concentration of the metabolites.

Electron ionization sources have a filament that is heated until electrons are ejected from the surface of the metal.[39] The electrons are attracted to an anode set up on the opposite end of the ion source. The sample is vaporized and injected into the ion source perpendicular to the filament and between the filament and the anode.[39] As the electron beam generated by the filament moves towards the anode, the electron beam hits the sample, causing ionization and often fragmentation.[39] The fragmentation caused by electron ionization can be extensive, and less destructive ionization sources are desirable.[39] A schematic for an electron ionization source is shown in Figure 1.1.

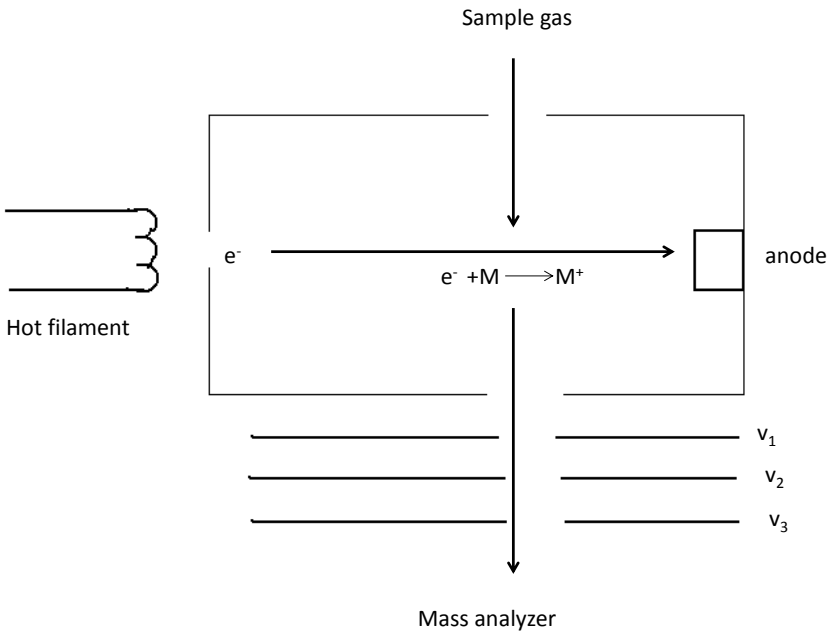

Figure 1-1. Electron ionization sources work through colliding the analyte molecules with a beam of electrons. This is a high energy process and fragmentation often occurs.

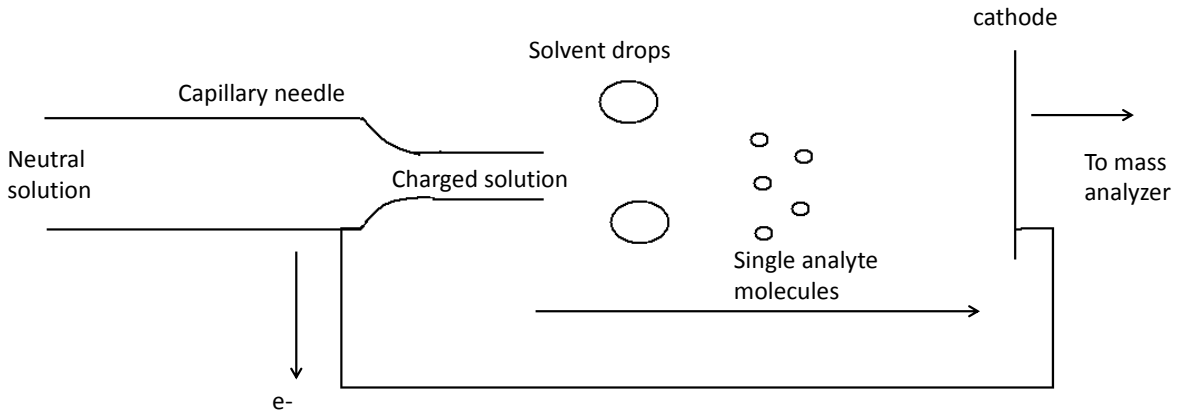

Figure 1-2. An electrospray ionization source produces a fine spray of charged particles via the formation of a Taylor cone and then produces single analyte molecules that are charged via fragmentation.

Electrospray ionization sources work by first injecting the sample into a usually heated capillary or needle.[36] A voltage is applied to the tip of the needle, and an electrode is place across from the needle.[36] The sample forms a Taylor cone as it moves towards the electrode. The Taylor cone eventually gets so small that droplets of the sample form. The solvent evaporates from the droplets due to the heat, sheath gas, and the continuing dispersion of sample drops into smaller drops until single ionized, analyte molecules are produced.[36] As the solvent evaporates from the sample droplets, the charge from the solvent is transferred to the sample droplets. At some critical point, the charges on the sample overcome columbic interactions forcing the droplet to break into two or more droplets. The breaking apart of the droplets theoretically continues until all of the solvent has been removed and only the analytes remain. Electrospray ionization is another soft ionization technique, where fragmentation of the analytes is unlikely to occur.[36] Due to the mechanism of ionization used in electrospray ionization, larger molecules may become multiply charged, allowing their detection with common mass analyzers.[36] Figure 1.2 shows a schematic of an electrospray ionization source.

.

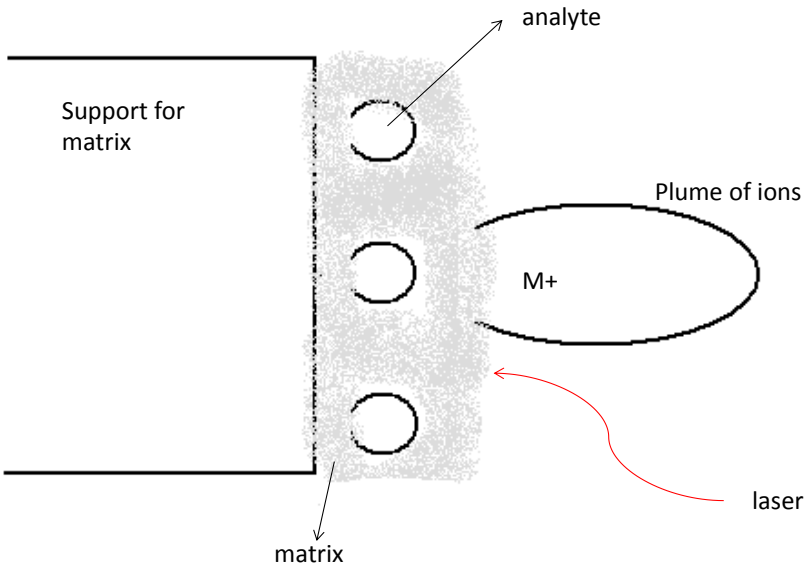

Figure 1-3. A MALDI ion source consists of the sample imbedded in the matrix, a pulsed laser, and an electrostatic field.

MALDI works by first inserting the sample into a matrix of some sort.[40] The matrix is usually chosen so that the matrix strongly absorbs at the wavelength of laser excitation, the analyte should be soluble in the matrix, and the matrix should be stable in a vacuum. Matrices absorb energy from the pulsed laser into the matrix and then transfer the energy to the analyte molecules embedded within the matrix. A laser is then razed across the surface of the matrix-analyte mixture in short bursts, generating plasmas.[40] The plasmas generate ions, often by taking protons away from the matrix and adding them to the analyte molecules.[40] The ions are then carried into the mass analyzer where separation can occur, followed by detection. MALDI is able to ionize compounds that otherwise do not ionize very well, very large or non-volatile compounds, including polymers and proteins.[40] Fragmentation is minimized since the matrix largely absorbs the energy of the laser pulses and transfers the energy to the analyte molecules.[40] Unfortunately reproducibility between laser bursts is poor, finding an appropriate matrix for the sample may be difficult, and quantification is not possible.[40] Figure 1.3 displays how MALDI is set up.

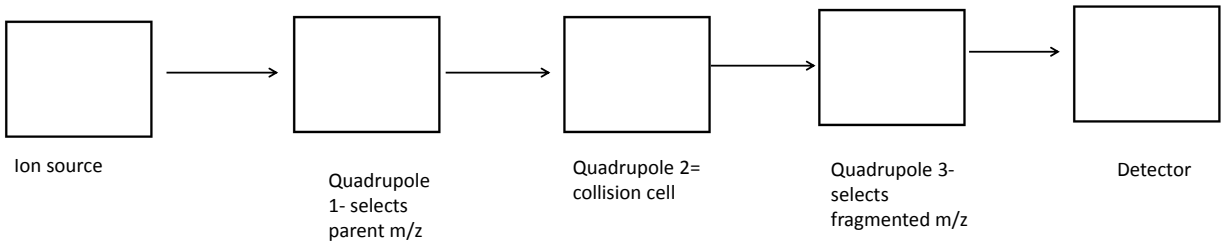

Figure 1-4. Triple quadrupole mass analyzers consist of three quadrupoles. The first and third quadrupoles select ions with the desired range of *m/z.* The second quadrupole collides the ions passed from the first quadrupole with a collision gas, fragmenting the ions further.

Mass analyzers are responsible for separating ions into bands of *m/z*. Some mass analyzers use electromagnetic fields to accomplish the separation, such as the traditional magnetic sector mass analyzer; others use the velocity difference due to mass, such as time-of-flight (TOF) mass analyzers. The types of mass analyzers vary widely, and a few mass analyzers of note are triple quadrupoles (electromagnetic field), time of flight (velocity), reflectron mass analyzers (velocity), and ion traps (electromagnetic field). Triple quadrupole mass analyzers, when used in selected reaction monitoring mode, consist of a series of quadrupoles. The first quadrupole selects ions with a parent *m/z*. The second quadrupole allows fragmentation of the parent ion though collision with an inert gas such as nitrogen. The third quadrupole selects the fragmented ions with the desired *m/z*. The ions are then detected, and a mass spectrum is generated. The instrumental set up of triple quadrupole mass analyzers is shown in Figure 1.4.

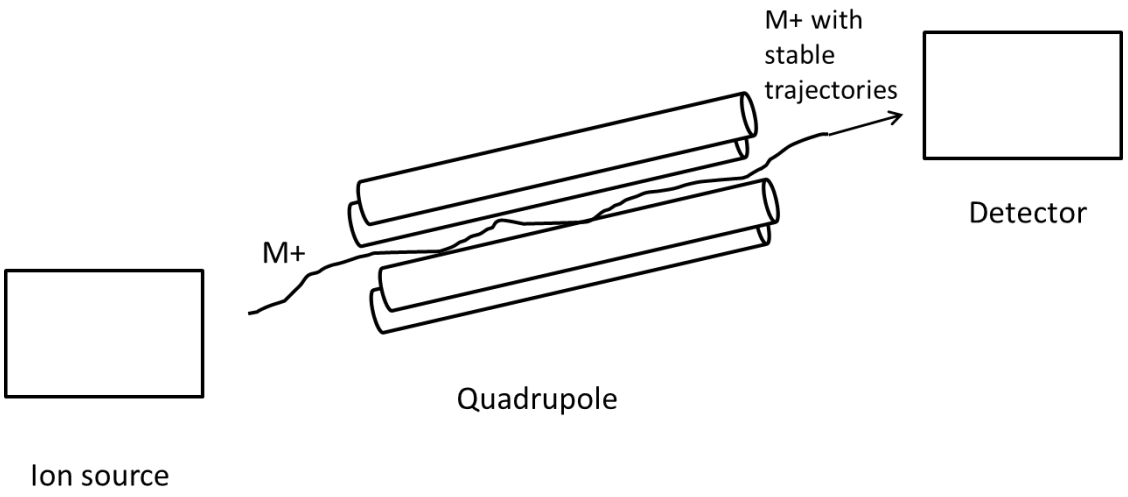

Figure 1-5. Quadrupoles separate ions based on the stability of their flight through the quadrupole. Ions of interest can be selected by changing the voltage and radio frequency applied to the rods.

Quadrupoles consist of four parallel metal rods. A direct current voltage is applied to each of the rods along with a radiofrequency potential. Ions are injected into the quadrupole and will orbit in between the four metal rods with orbits forming based on *m/z*. Ions orbiting closer to the center of the four metal rods will have more stable orbits than ions orbiting further from the center of the rods. Ions with a stable orbit pass through the quadrupole, and the ions selected to pass through the quadrupole can be changed by altering the applied voltage and radiofrequency potential applied to the four rods. If the ions have a *m/z* different than the desired one, the ions crash into the walls of the quadrupole and are not transmitted through the quadrupole.[41] Quadrupole mass analyzers have a mass accuracy of greater than 100 ppm. A quadrupole is shown in Figure 1.5.

Using a triple quadrupole mass analyzer in multiple reactions monitoring mode for targeted metabolomics allows the reliable and reproducible quantitation of metabolites and the ability to absolutely quantify metabolites.[13] The triple quadrupole is also highly robust and sensitive, as well as capable of searching for particular compounds of interest in a high

throughput scenario.[13] This method may require optimization, and a standard calibration curve for an internal standard in order for absolute quantitation of metabolites.[3] Unfortunately since this method relies on mass fragmentation patterns, it is not possible to quantitate unknown compounds.[3]

TOF mass analyzers separate ions by applying an electric field to all of the ions at the same instant in time. The ions are accelerated towards the detector. Larger ions will take longer to reach the detector than smaller ions, thus accomplishing the separation of ions into bands of *m/z*. Ions may be accelerated at different points within the mass analyzer leading to a larger than desirable spread, known as initial spacing distribution, in the bands of *m/z* until the focal point is reached.[42] After the focal point has been reached, all ions of the same *m/z* are moving together. Reflectron mass analyzers work very similarly to time of flight mass analyzers; except that a magnetic field curves the ions back towards the region of acceleration. The reflection of ions is accomplished by a series of reflectrons, which are regions with differential voltages applied. The differential voltages interact with the charges on the ions and turn the ions around. Ions that were accelerated earlier are in effect moving faster and so get turned around in a later series of differential voltage plates. This allows the ions with similar *m/z* to reach the detector in a shorter band of time. TOF mass analyzers have a 2-5 ppm mass accuracy, as do reflectron mass analyzers. Figure 1.6 shows a time of flight mass analyzer, while Figure 1.7 shows a reflectron mass analyzer.

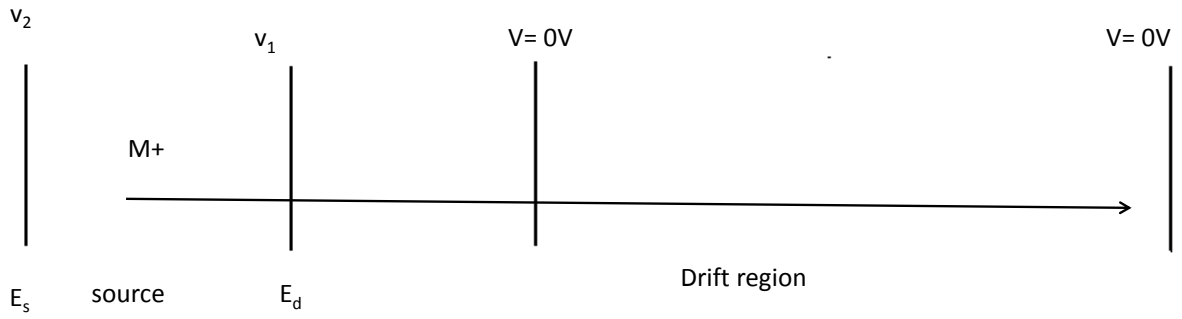

Figure 1-6. A time of flight mass analyzer applies the same acceleration to all ions. Ions with a heavier mass to charge ratio will move at a slower velocity than ions with a lighter *m/z*, thus separating ions into bands of mass to charge ratio.[43]

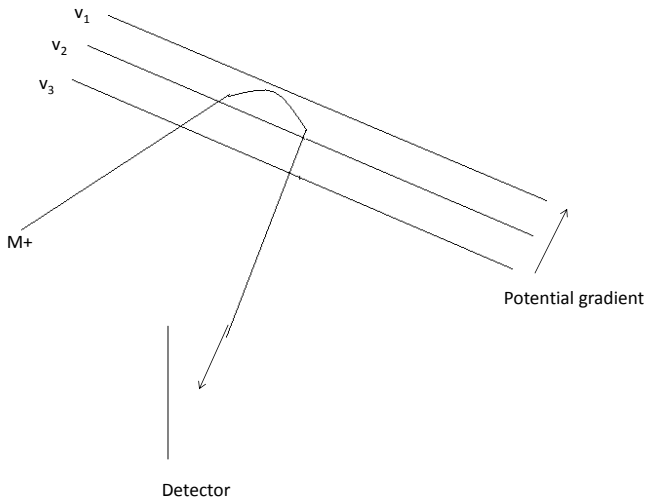

Figure 1-7. Reflectron mass analyzers accelerate ions in the same manner as time of flight mass analyzers, but due to the reflectron of ions back to the detector eliminate the spread of ions due to differential acceleration. The faster the ion is moving the further into the electromagnetic fields the ion will travel before being turned around by the electromagnetic field.

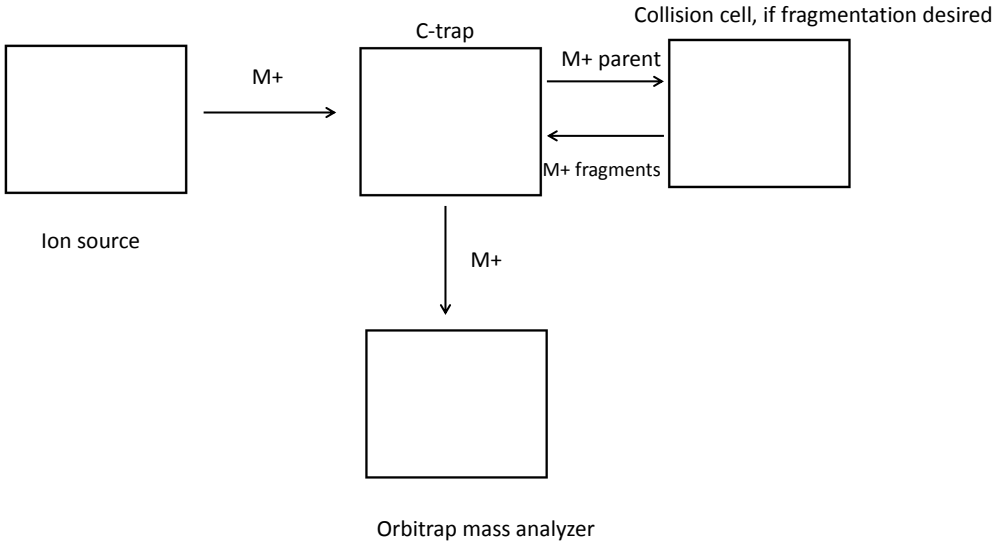

Figure 1-8. Orbitrap mass spectrometers often consist of an ion source, an s-lens, a c-trap, a collision cell, and an orbitrap mass analyzer.[44]

Orbitrap mass spectrometers use an ion trap as a mass analyzer that traps ions using purely electrostatic forces. The Exactive Orbitrap Plus mass spectrometer, used in all of the studies in this thesis, works by first ionizing compounds and the ions are then moved to a c-trap, where they can be transported to either a collision cell for fragmentation or directly to an Orbitrap mass analyzer. Figure 1.8 shows the set up for a typical orbitrap mass spectrometer.

The important distinction between Orbitrap mass spectrometers and other types of mass spectrometers is the specific use of the orbitrap as an ion trap. The Orbitrap ion trap consists of a small central electrode and a large outer electrode.[38] A direct current voltage is applied between the two electrodes, generating an electrostatic field.[38] The ions are injected and consequently trapped in this electrostatic field.[38] Due to the interaction of the charge on the ions and the electrostatic field in which the ions are placed, the ions orbit around the central electrode while also oscillating.[38] The frequency of the oscillations is based only on the *m/z* of the ions and the potential between the electrodes.[38] Since a direct current voltage is applied between the electrodes, the *m/z* actually determines the frequency of oscillations.[38] A series of orbits are

formed around the central electrode, with each orbit having a unique *m/z* and frequency of oscillation.[38] As the ions orbit around the central electrode and pass near the outer electrode, an image charge is generated in the outer electrode.[38] The image charges are Fourier transformed to produce a spectrum of the oscillation frequencies, which can then be transformed into a mass spectrum using available computer software.[38]

The Orbitrap mass spectrometer's main advantage is its high resolution (up to 150,000), which allows metabolites with very small differences in *m/z* to be separated into different peaks.[45] The Orbitrap mass spectrometer is extremely accurate in finding *m/z* (2-5 ppm).[45] Due to the many advantages of using the orbitrap as a mass analyzer, it was used in this series of experiments.

CHAPTER 2 FINDING THE METABOLIC CHANGES IN *SALMONELLA ENTERICA* DUE TO COLD SHOCK

Abstract

Wild type *Salmonella enterica* was grown at three different temperatures in order to determine the metabolic changes associated with cold shock (the condition resulting from exposure to less than ideal temperatures). On three separate days, cultures of *S. enterica* were grown at their optimal temperature of 37 °C until they reached mid-exponential phase. The bacterial cultures were then filtered onto nylon filters and exposed to one of three temperatures, 37 °C, 25 °C, or 3 °C for thirty minutes. The bacterial cultures were switched to ^{13}C labeled glucose media, and the metabolism of the cells was quenched while their contents were simultaneously extracted after the appropriate amount of exposure (0, 2, 5, 15, 30, 60, or 120 min) to isotopically labeled glucose. The cellular extracts were then analyzed using UPLC-MS, and the results analyzed with the use of MAVEN, cluster, and Java Treeview. Metabolites that were detected in glycolysis and the citric acid cycle showed slower or less complete labeling and smaller pool sizes at lower temperatures. Metabolites that were detected in the pentose phosphate pathway showed slower or less complete labeling and smaller pool sizes. Glutamate, glutamine, leucine/ isoleucine, aspartate, and valine showed less complete or slower labeling and larger pool sizes indicating the possible breakdown of proteins into amino acids. Alanine showed slower or less complete labeling and larger pool sizes at lower temperatures. Alternatively, the less efficient labeling may be due to enzymes denaturing, reducing the catalysis abilities of the cells, a slowdown in the rate of transcription of DNA into RNA, or a slowdown in the rate of translation of RNA into proteins. It is important to study the cold shock of *S. enterica* at these three temperatures (body temperature, the temperature of a kitchen countertop, and the temperature of a fridge) in order to see if there is a weakness in the pathogenic bacteria at these three temperatures that can be exploited in order to kill the pathogen more efficiently.

Introduction

Stress metabolomics studies the metabolic effects stress has on metabolism.[46] In essence, organisms are placed in unusual conditions in order to determine how those unusual conditions affect metabolic rates, metabolic pathways, and the concentrations of metabolites. Stress can be caused by a number of different conditions. Heat stress is caused by the placement of organisms, or cells, in an environment with a higher than usual temperature.[47] Cold stress, or cold shock, results from the placement of organisms in lower than usual temperatures.[48] Oxidative stress is caused by the addition of an oxidizing agent, such as hydrogen peroxide, to an environment in which the organism resides.[49] Stress can also be caused by placing organisms in environments with little (hypoxic) or no (anaerobic) oxygen environments when the organism requires oxygen for normal metabolic functions.[50] Osmotic stress can be caused by adding higher than normal concentrations of solutes to an environment, for instance placing a freshwater organism into salt water.[51] Although the responses of organisms to stressors change from species to species and are dependent on the type of stressor, the organisms will alter their metabolism in order to mitigate any damaging effects the stressor may have.[52] Organisms may also alter their metabolism to try to adept to the new circumstances in which they find themselves.[46]

It is generally thought that exposure to a stressor of some sort (abnormal temperatures, low oxygen levels, exposure to higher solute concentrations, and so on) will cause two types of responses from the organism. The first response from the organism is to repair any damage to the cells, or organism as a whole, caused by exposure to the stressor.[46, 53] The second response is generally to slow down the rate of growth and cease or drastically reduce reproduction until more optimal conditions arrive.[46, 53]

Many studies have been done on how cold shock affects organisms such as insects and plants, but all of the metabolic effects of cold shock have not been elucidated for even these groups of organisms.[54,55, 50, 56, 57] A few studies have looked at how cold shock affects model single celled organisms, such as *Escherchi*a *coli* and yeast, and these studies seem to be making headway towards understanding how cold shock affects these two model organisms.[58, 46] However, no studies have been found which look at cold shock in *Salmonella enterica*.

One study of note was done by the Willmitzer group, and studied the effect of heat stress, cold shock, oxidative stress, and nutrient starvation in *E. coli* on the metabolome and the transcriptome. The study looked at how the pool sizes of 93 different metabolites changed after the addition of stress as time passed. The concentrations of 15 metabolites changed significantly after 10 minutes of stress application, as determined by a p value less than or equal to 0.05 and a minimum ratio of 2 between the pool size before stress addition and pool size after stress addition. The pool sizes of 5 more metabolites changed significantly after 40 minutes of stress application. There was a general decrease in pool size after the application of cold shock for the metabolites involved in central carbon metabolism (glycolysis and the citric acid cycle). The pool sizes of many amino acids increased after stress application, any stress application studied, during the course of this study as well. *E. coli* and *S. enterica* are rather similar organisms, based on the size of the genome and the characterization into classes based on physical characteristics. Similar results for the *S. enterica* study to the *E. coli* study are expected due to the similar physical characteristics and genome. The effects of cold shock on some proteins and the transcriptome of *S. enterica* have been studied. The effects of cold shock on the metabolome of *S. enterica* will be discussed here.

Experimental procedures

The wild type strain LT2 of *S. enterica*, provided by the Down's lab at the University of Georgia, were revived from freezer glycerol stocks and streaked onto rich Diffco, agar media plates.[59] The plates were inoculated at 37 °C until single, isolated colonies appeared. The bacterial colonies were removed from the plates and inoculated in rich media for approximately six hours. The bacterial cultures were then centrifuged at 3 °C and 13,200 RPM for one minute. The media was removed, and the *S. enterica* cells were suspended in 2 mL of 8.5% NaCl in sterile water. 100 µL of the cells in NaCl solution was used to inoculate 5 mL of minimal no carbon essential (NCE) media, in order to minimize nutrient carry over from the rich media and

Table 2-1. The components of the minimal NCE media are listed below.

Reagent	Concentration
Glucose	11mM
$MgSO_4$	1mM
Adenine	0.4mM
Thiamine	100nM
Nitrilotriacetic acid	5.3 µM
$MgSO^4$ (anhydrous)	3.75 µM
$MnSO_4$ *$1H_2O$	1.25 µM
NaCl	17.1 µM
$FeSO^4$*$7H_2O$	0.4 µM
$CoCl_2$	0.4 µM
$CaCl_2$ *$2H_2O$	0.7 µM
$ZnSO_4$	0.035 µM
$CuSO_4$ *$5H_2O$	0.04 µM
$Al_2(SO_4)_3$	0.039 µM
H_3BO_3	0.2 µM
Na_2MoO_4 *$2H_2O$	1.2 µM
Potassium phosphate dibasic crystals	0.021 M
Potassium phosphate monobasic crystals	0.027 M
Sodium ammonium phosphate	0.013 M

to minimize the chance of mutations occurring in the strains due to longer incubation periods.[59] The minimal NCE media components are listed in Table 2.1. The growth and extraction of metabolites from cells is based on the findings of the Rabinowitz lab.[60] The cells were allowed to grow overnight at 37 °C with continual shaking at 200 RPM; and the next morning, 1 mL of the overnight minimal NCE media culture was used to inoculate 50 mL of minimal NCE media, in biological triplicate. Once the bacterial cultures reached mid-exponential phase as determined by the optical density at 600 nm (OD_{600} equal to approximately 0.8), 5 mL aliquots of the cultures were filtered onto 47 mm nylon filters (manufactured by Fischer Scientific) and placed on minimal NCE media agarose plates. Growth curves for each strain were done in a previous experiment in order to determine the OD_{650} correlating to mid-exponential phase, the exact OD_{650} are shown in Table 2.2. There were seven time points for each biological triplicate; 0, 2,

Table 2-2. The average optical densities for each experiment are reported.

Culture temperature (°C)	OD_{650}
37	1.42
25	0.77
3	0.80

5, 15, 30, 60, and 120 min of exposure to 7 mM ^{13}C glucose plates. The cultures were allowed to grow on the filters; nutrients are able to diffuse through the filters and into the cells, for a half hour at the desired temperature, 37 °C, 25 °C, or 3 °C. Once that time passed, all but one set of filters were placed onto minimal NCE media agarose plates, containing ^{13}C labeled glucose. The plates were then placed back at the desired temperature until the appropriate amount of exposure to the isotopically labeled plates had passed. The cells then had their metabolisms quenched and the water soluble metabolites were extracted.

The quenching and extracting process is started by scraping any media on the bottom of the filters off and placing the filters cell side down into petri dishes containing 1.3 mL of extraction solvent (40:40:20 HPLC grade methanol: HPLC grade acetonitrile: HPLC grade water with 0.1 M formic acid kept at -20 °C). The filters were placed on ice at -20 °C for fifteen min. The filters were then taken on ice to the cold room, kept at 3 °C, where the filters were flipped over using a serological pipette tip, and the filters were washed with the extraction solvent in the petri dish 15 times while rotating the filter in order to remove the cells from the filter. The extraction solvent was removed from the petri dish and placed in a microcentrifuge tube. 300 µL of chilled extraction solvent was added to the filters, and the filters were washed another 15 times. This extraction solvent was added to the same microcentrifuge tube containing the first round of extraction solvent. The filters were disposed of, and the microcentrifuge tubes were centrifuged at 13,200 RPM at 3 °C for five min. The supernatant was placed in a 1 dram vial and kept at 3 °C, while the cellular pellet was suspended in 50 µL of chilled extraction solvent. The microcentrifuge tubes containing the lysed cells were transported on ice to a -20 °C freezer where they remained for another fifteen min. The microcentrifuge tubes were then transferred on

ice back to the cold room and centrifuged for five min at 3 °C and 13,200 RPM. The supernatant was added to the corresponding 1 dram vial, and the cell pellet was suspended in 50 µL of chilled extraction solvent. The lysed cells were transferred on ice back to the -20 °C freezer and left there for a final fifteen min. The microcentrifuge tubes were then taken back to the cold room on ice, and centrifuged for a final five min at 3 °C and 13,200 RPM. The supernatant was placed in the corresponding 1 dram vial, and the cell pellet was disposed of. The 1 dram vials were then placed in a nitrogen drying apparatus until the contents of the vials were dry. The residues in the vials were suspended at 3 °C with 300 µL of chilled sterile water and the contents were transferred to an autosampler vial. The samples were then ready for detection on the UPLC-MS system. This entire procedure was done on three different days, one day was assigned for each temperature. All three experiments were completed within the same week, and all of the UPLC-MS detection was also accomplished within that week.

The UPLC-MS system was controlled by Xcalibur (Thermo Scientific), and the methods used for separation and detection are those reported by the Rabinowitz lab.[61] The MS was calibrated and tuned by direct injection before use with the use of Thermo Scientific's negative mode ESI standard calibration mix as well as with a mixture of polytyrosine-1,3,6, 1 µM glutamic acid, and 3 µM aspartic acid in HPLC grade water with 0.1 percent formic acid. The separation was accomplished using a Synergy Hydro-RP column (100 mm x 2 mm with 2.5 µm sized particles) and a reverse-phase gradient using tributylamine (TBA) as an ion-pairing reagent. The mobile phase gradient uses varying mixtures of two mobile phases: solvent A consists of 97:3 HPLC grade water: HPLC grade methanol with 10 mM tributylamine and 15 mM acetic acid; while, solvent B is HPLC grade methanol. The gradient lasts 25 min and is: 0.0 min, 0% B; 2.5 min, 0% B; 5.0 min, 20% B; 7.5 min, 20% B; 13 min, 55% B; 15.5 min, 95% B; 18.5 min, 95% B; 19 min, 0% B; 25 min, 0% B. The gradient is summarized in the Figure 2.1 below. The flow rate through the column is held at a constant 200 µL per minute and the temperature of the column is kept at 25°C. The autosampler tray is kept at 4°C, and 10 µL of sample is injected into the UPLC-MS set-up.

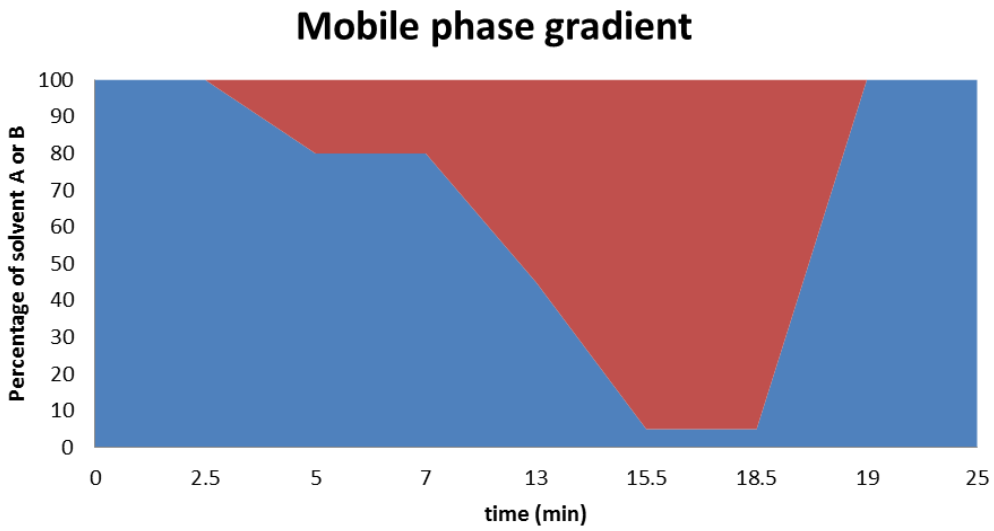

Figure 2-1.The mobile phase gradient is shown. Solvent A (blue) consists of 97:3 water: methanol with 10 mM tributylamine and 15 mM acetic acid; solvent b (red) consists of methanol.

As compounds are eluted from the column they are injected directly into an ESI source. Nitrogen acted as the sheath gas, auxiliary gas, and sweep gas. The flow rates were 25 arbitrary units, 8 arbitrary units, and 3 arbitrary units for the three types of gas, respectively. The spray voltage in the ion source was set to 3 kV, the capillary temperature was set at 325 °C, the capillary voltage was set at -50 V, and the tube lens voltage was set at -100 V.

The MS was set to scan in the following *m/z* at the following times: from 0.0 to 5.0 min, the range of 85 to 800 *m/z* units, from 5.0 to 6.7 min, the range of 100 to 800 *m/z* units, from 6.7 to 6.9 min, the range of 85 to 800 *m/z* units, from 9.0 to 16 min, the range of 110 to 1000 *m/z* units, and from 16 to 24 min, the range of 220 to 1000 *m/z* units. The *m/z* scanning range was raised from 85 to 110 between 9 to 16 minutes in order to allow sulfates and phosphates to elute without entering the mass analyzer and causing space charge effects. The scanning ranges are summarized in the Table 2.3.

The raw data , displayed as a total ion chromatogram in Figure 2.2, was converted to the format of MZML files, using msconvert.[62] The MZML files were then loaded in software program MAVEN, where all peak detection and integration was performed on the data, including the blanks analyzed during the experiments.[63] MAVEN allows large amounts of data to be processed together with visualization of the peaks given by ion count versus retention time for a

given *m/z* windows, an example of which is shown in Figure 2.3.[63] The MZML files were loaded into MAVEN. The peaks were then aligned using the parameters shown in Table 2.4. Automatic peak detection was then performed using the parameters shown in Figure 2.4. The chromatogram is searched for peaks for each metabolite of interest. The correct peaks are chosen by hand based on labeling patterns, pool size information, consistency between replicates, peak shape, and matching of the retention time.

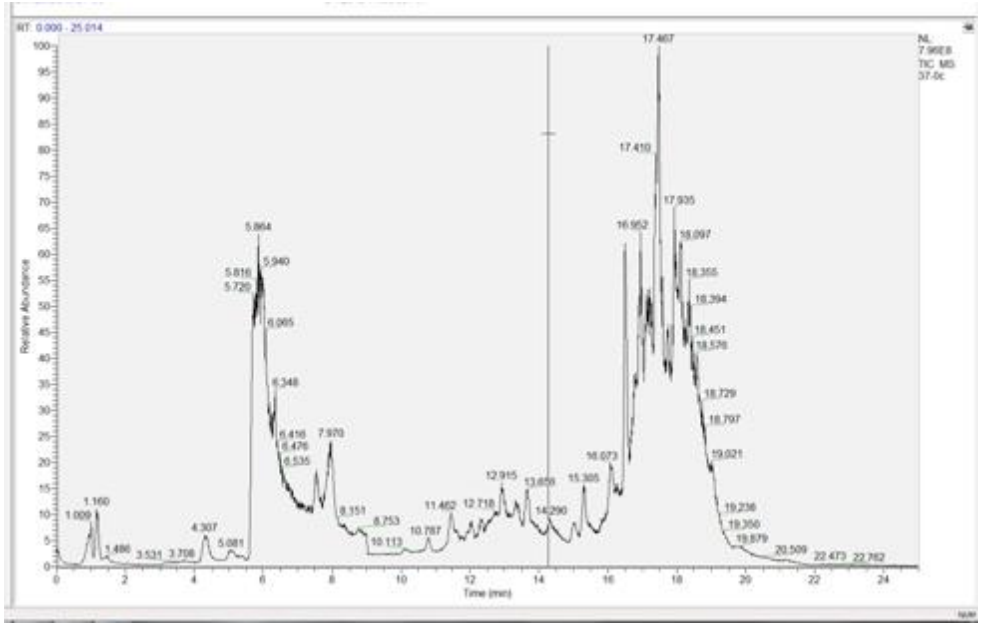

Figure 2-2.The total ion chromatogram can be viewed using Xcaliber. The time point 0 sample for the 37 °C experiment, replicate 2 is shown here.

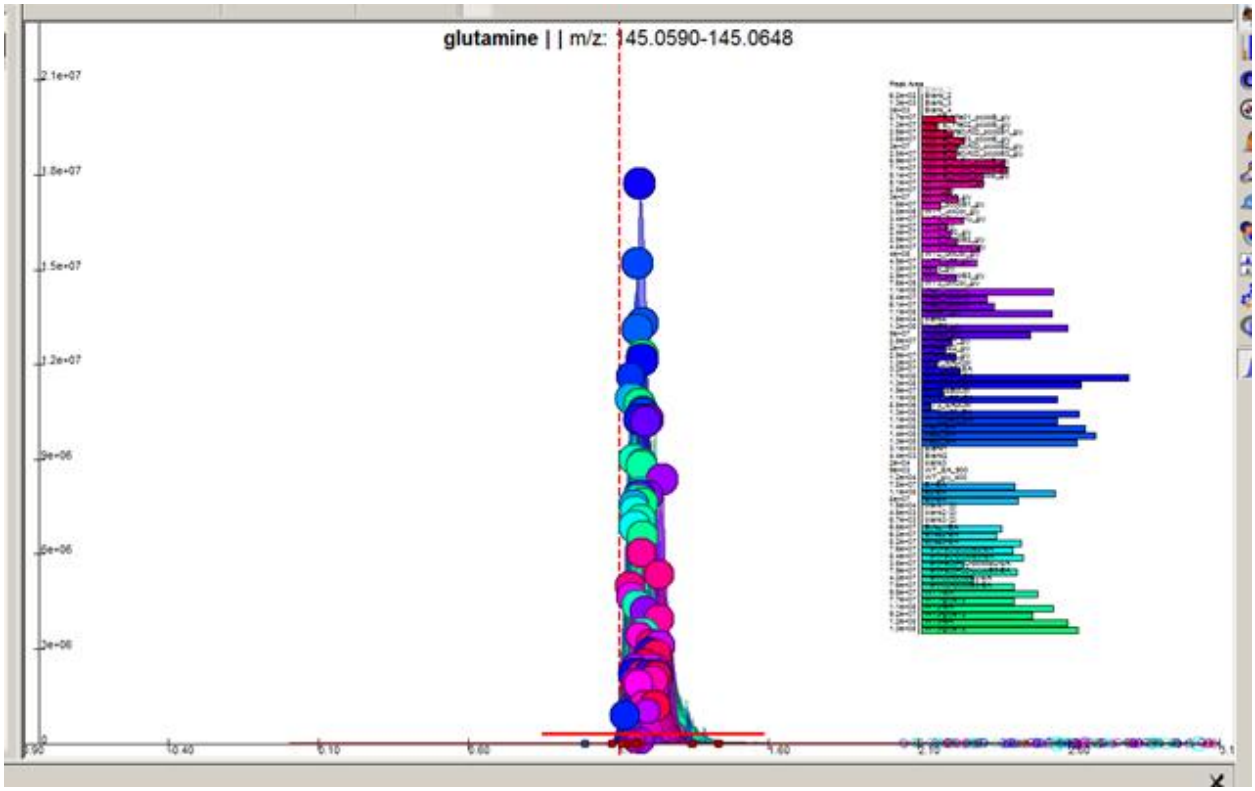

Figure 2-3. The extracted ion chromatogram for glutamine is shown here. MAVEN allows the extraction of a range of m/z values at a given retention time, so that the ion counts of the metabolite can be determined.

Table 2-3. The scanning ranges for each range of retention times are summarized below. The scanning ranges for the mass spectrometer can be set up so as to scan only the relevant mass to charge ratio ranges in a given range of retention times.

Time (min)	Scanning range (*m/z*)
0.0 to 5.0	85.0 to 800
5.0 to 6.7	100 to 800
6.7 to 6.9	85.0 to 800
9.0 to 16	110 to 1000
16 to 24	220 to 1000

Table 2-4.The alignment parameters used in MAVEN are shown.

Parameter	value
Group must contain at least [X] good peaks	2 peaks
Limit total number of groups in alignment to	1000 groups
Peak grouping window	20 scans
Minimum peak intensity	5000.00
Minimum peak S/N	5
Minimum peak width	5 scans
Maximum number of iterations	10
Polynomial degree	5

All of the samples were analyzed with a 20 ppm *m/z* window surrounding the theoretical *m/z* for each metabolite and their isotope labeled partners for flux analysis (theoretical *m/z* ± 20 ppm). The samples taken before the addition of ^{13}C labeled glucose were also analyzed with a 5 ppm window surrounding the theoretical *m/z* of each metabolite in order to generate a heat map.

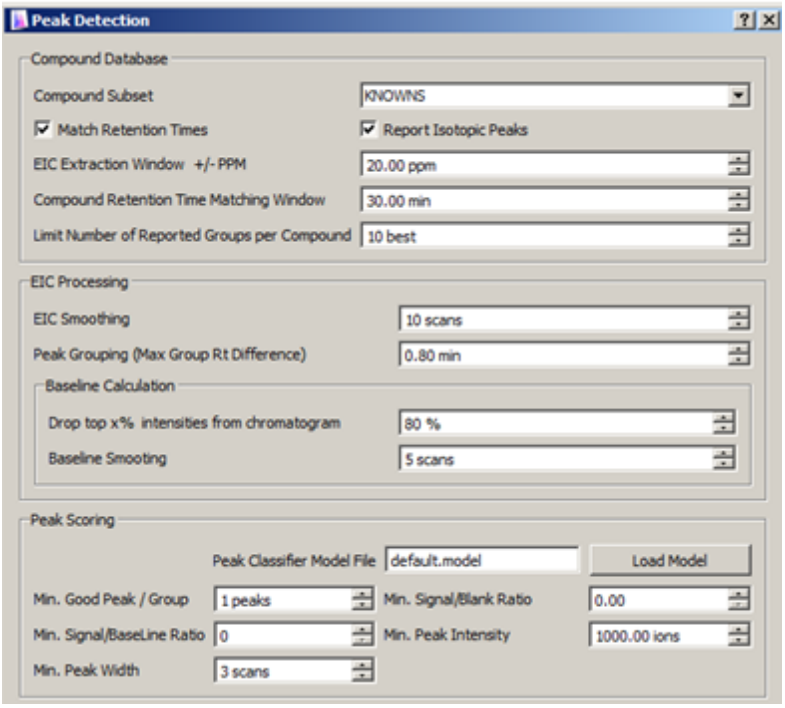

Figure 2-4. The parameters used for automatic peak detection by MAVEN are shown above. Multiple peaks are detected for each metabolite with this method and the best group of peaks for each metabolite is chosen by hand based on labeling patterns, pool size information, consistency between replicates, peak shape, and matching of the retention time.

A spreadsheet of the integrated peaks, *m/z*s and retention times of the peaks, as well as the peak identities were exported into Microsoft Excel where further analysis was done. The flux data was used to make flux graphs showing the relative percentage of the parent compound (unlabeled) and each labeled form of the metabolite versus time of exposure to the isotope for each metabolite. Pool size graphs were also made using the total ion counts from the mass spectra within the *m/z* window at the appropriate retention time for each metabolite, allowing the comparison of the pool sizes of each metabolite between the cultures grown at 37, 25, and 3 °C. P values for the pool size data were determined for all of the metabolites detected. P values are a measure of statistical significance. A p value of 0.01 is considered very significant and correlates to a 99% confidence that the two values are different from one another. The heat map

comparing the log transformed relative changes between the cultures was made by first log transforming and clustering the information with the program Cluster 3.0.[64] Java Treeview then used the information generated by Cluster 3.0 to make a heat map showing the relative changes in concentration before the addition of isotope labeled compound for each metabolite detected.[65] The flux graphs, pool size plots, and heat map were all compared to metabolic pathways using the KEGG database in order to find the differences in the metabolic pathways between the differences between the cultures grown at the three different temperatures.

Results and Discussion

Flux graphs, pool size information, and heat maps have been generated and overlaid onto a number of pathways. The heat map for all of the known metabolites detected is shown in Figure 2.5. In the glycolysis pathway, the lower temperatures show less complete labeling and slower labeling than the warmer temperatures. The colder temperatures also show smaller pool sizes. Glucose-6-phosphate, fructose-6-phosphate, fructose-1,6-bisphophate, 1,3-disphoglycerate, and pyruvate all showed slower or less complete labeling and smaller pool sizes at the lower temperatures. Glyceraldehyde-3-phosphate, dihydroxyacetone (DHA), 3-phospho-glycerate, 2-phosphoglycerate, and phosphoenolpyruvate were not detected in this series of experiments. Metabolites may not be detected if they are at too low of a concentration within the cell, if they are not extracted efficiently with the water soluble extraction procedure, or if the metabolites degrade quickly during extraction or before analysis with the UPLC-MS set up. Glucose/fructose-6-phosphate showed full labeling occurring in only 50% of the molecules detected at 2 min for the 3 °C bacterial cultures, but full labeling occurred for 80% of the molecules detected at 2 min for the two higher temperatures. The pool sizes have a fold change of 0.77 for 37 vs. 25 °C (p value= 0.36) and 0.73 for 37 vs. 3 °C (p value= 0.18). P values are a measure of statistical significance. Fructose-1,6-bisphosphate showed a dramatic decrease in the percentage of molecules detected that showed full labeling in the 3 °C cultures, 50% labeled as opposed to 90% labeling at the higher temperatures. The pool sizes have a fold change of 1.53 for 37 vs. 25 °C (p value= 0.38) and 24.9 for 37 vs. 3 °C (p value= 0.08). 1,3-diphsophoglycerate

follows the same pattern as fructose-1,6-bisphosphate; the 3 °C time point of 2 min shows 50% of the molecules detected fully labeling, while at the higher temperatures 90% of the molecules detected at the 2 min time point show full labeling. The pool sizes have a fold change of 1.31 for 37 vs. 25 °C (p value= 0.41) and 39.2 for 37 vs. 3 °C (p value= 0.03). Pyruvate showed 60% of molecules fully labeling at the 20 min time point for the 3 °C bacterial cultures. The 25 °C bacterial cultures showed 80% of the molecules labeling at 5 min, while the 37 °C showed 90% of the molecules detected at the 2 min time point. The pool sizes have a fold change of 0.73 for 37 vs. 25 °C (p value= 0.66) and 7.17×10^{-4} for 37 vs. 3 °C (p value= 0.18). Metabolites are moving less efficiently through the glycolysis at lower temperatures. Figure 2.6 summarizes the results for glycolysis, Figure 2.7 displays the flux graphs, and Figure 2.8 displays the pool size graphs for the metabolites involved in this pathway.

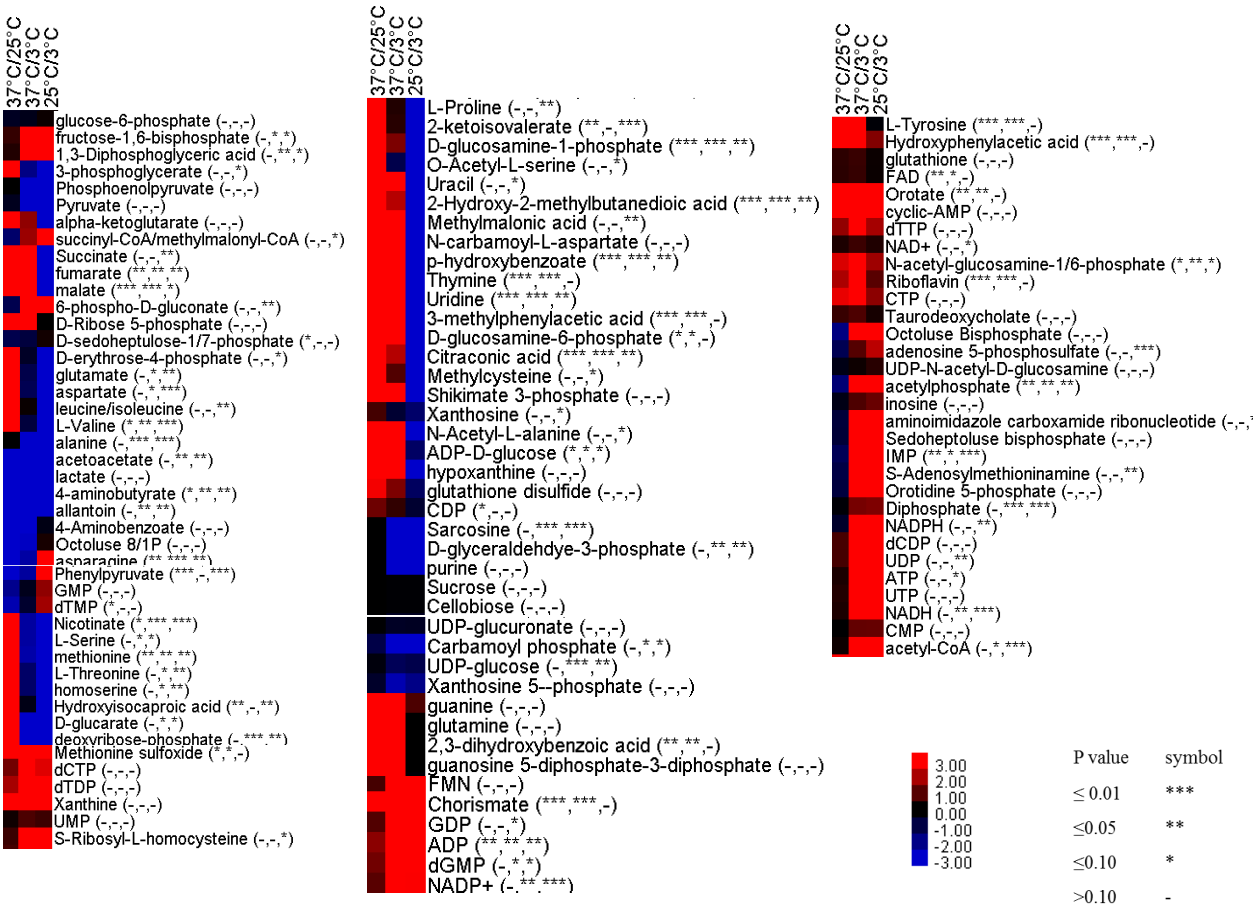

Figure 2-5. Heat map of metabolites detected for the experiment testing cold shock in *S. enterica*. The relative pool sizes for each metabolite is visualized as a heat map, where relative increases in concentration are shown in red and relative decreases in concentration are shown in blue. Metabolites are organized by metabolic pathway through the metabolites discussed here.

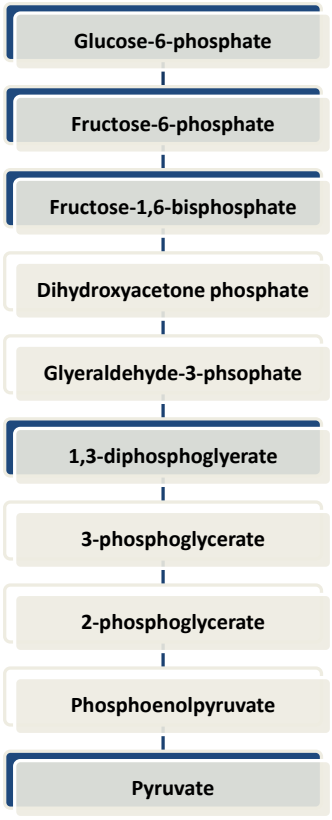

Figure 2-6. The glycolysis pathway is shown. Grey boxes in the cycle indicate metabolites that were not detected. Blue boxes indicate metabolites with slower or less complete labeling and smaller pool size in the lower temperature conditions.

Glucose/ Fructose-6-phosphate

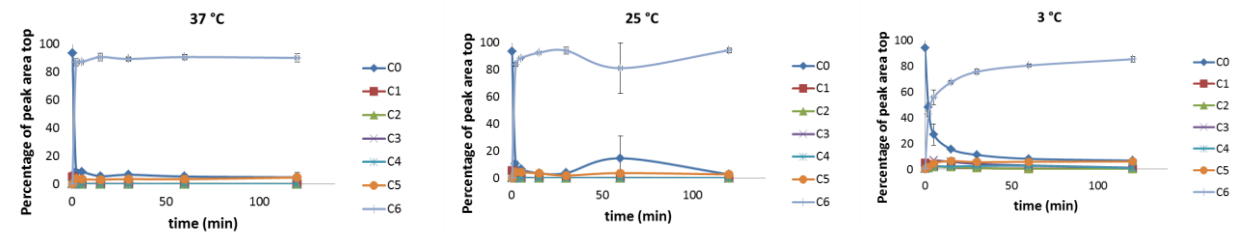

Fructose-1,6-bisphosphate

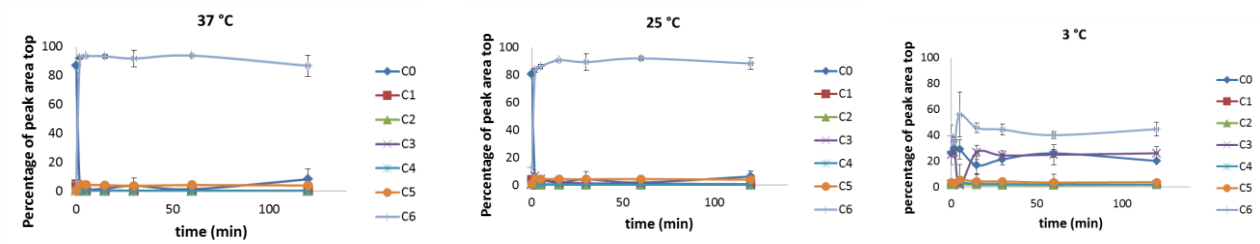

1, 3-diphopshateglycerate

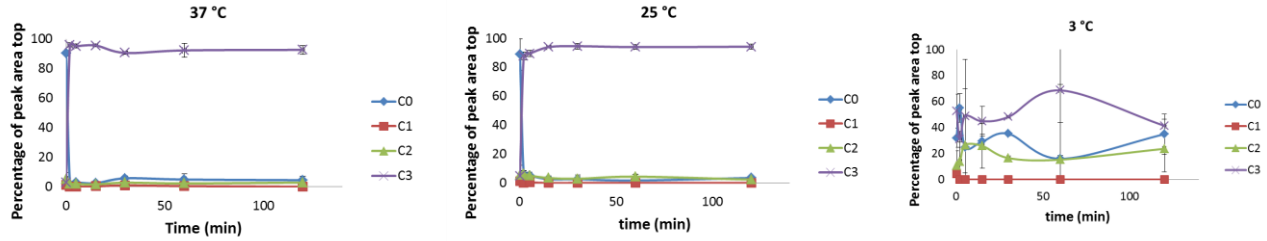

Pyruvate

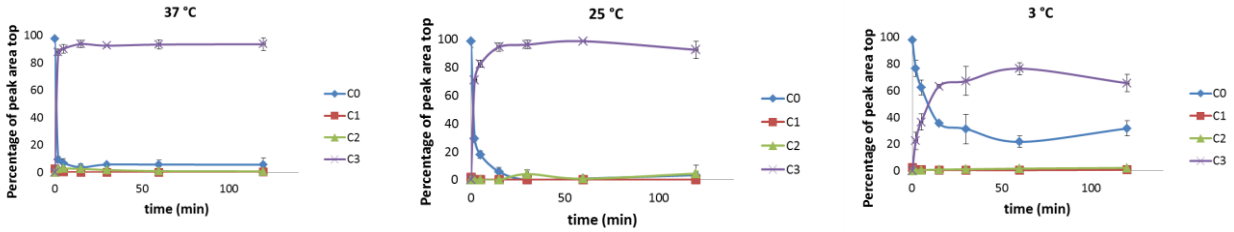

Figure 2-7. The flux graphs for the metabolites involved in glycolysis are shown. C0 refers to the unlabeled metabolite. C1 refers to the metabolite containing 1 ^{13}C, and so on.

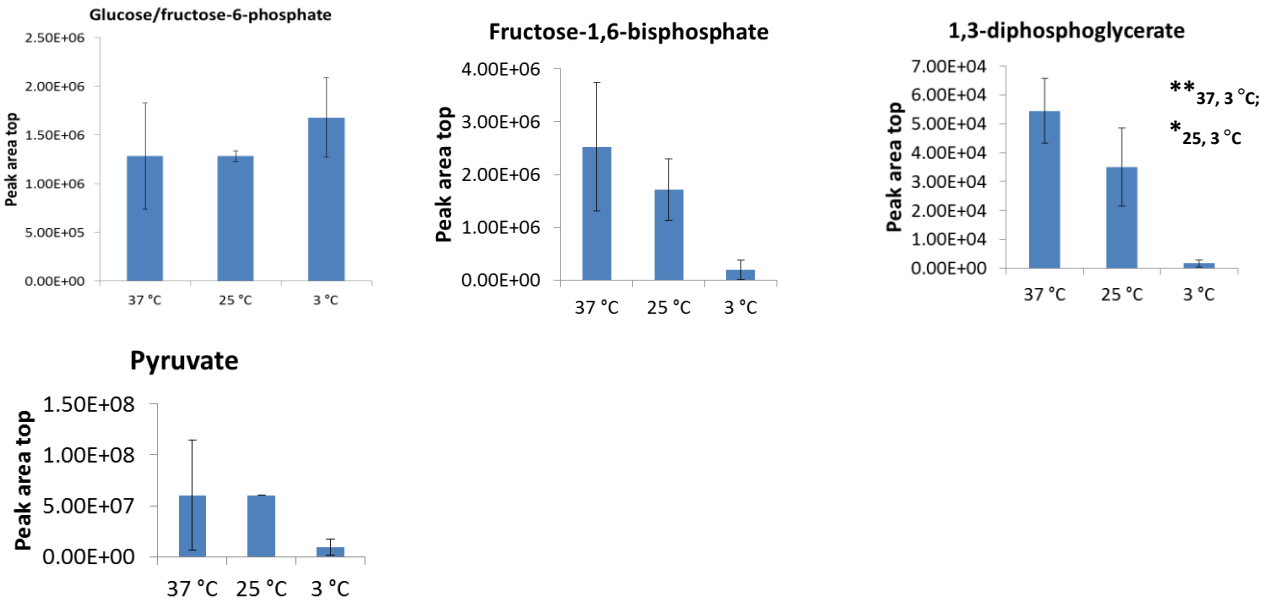

Figure 2-8. The pool size plots for the metabolites involved in glycolysis are shown. *** refers to a comparison with a p value ≤ 0.01. ** refers to a comparison with a p value ≤ 0.05. * refers to a p value ≤ 0.1.

Every metabolite that is detected in the citric acid cycle also shows slower or less efficient labeling and smaller pool sizes. Alpha-ketoglutarate, succinyl-coA, succinate, fumarate, and malate were detected. Citrate, cis-aconitate, isocitrate, and oxaloacetate were not detected in this series of experiments. Alpha-ketoglutarate showed essentially no labeling in the 25 °C bacterial cultures; while the 3 °C bacterial cultures showed 30% of the molecules detected being labeled with 2 ^{13}C after 120 min. The 37 °C bacterial cultures showed 30% full labeling after 5 min and nearly 80% full labeling after 120 min. The pool sizes have a fold change of 6.09×10^4 for 37 vs. 25 °C (p value= 0.13) and 3.25 for 37 vs. 3 °C (p value= 0.23). Succinyl-coA did not show any labeling. The pool sizes have a fold change of 0.34 for 37 vs. 25 °C (p value= 0.15) and 3.57 for 37 vs. 3 °C (p value= 0.34). Labeling with different numbers of ^{13}C indicates that different routes are being utilized to make the metabolites in question. 80% of the succinate molecules detected displayed full labeling after 20 min at 37 °C; while only 5% of the succinate molecules detected display full labeling at 3 °C. The 25 °C bacterial cultures show 70% labeling with 2 ^{13}C at 20 min. The pool sizes have a fold change of 4.10×10^5 for 37 vs. 25 °C (p value= 0.16) and 31.1 for 37 vs. 3 °C (p value= 0.17). Fumarate shows 80% of the molecules detected fully labeled after 20 min at 37 °C. Fumarate was in the noise range in the 25 °C bacterial cultures. In the 3 °C bacterial cultures, 60% of the molecules detected labeled with 3 ^{13}C after 60 min. The pool sizes have a fold change of 13.9 for 37 vs. 3 °C (p value= 0.04). Malate showed 60% of the molecules detected fully labeling after 2 min at 37 °C, but only 40% of the molecules detected labeled with 3 ^{13}C after 20 min at 3 °C. Malate was not detected in the 25 °C bacterial cultures. The pool sizes have a fold change of 2.58×10^5 for 37 vs. 25 °C (p value= 9.09×10^{-4}) and 15.5 for 37 vs. 3 °C (p value= 3.49×10^{-5}). Compounds may not be detected in the case of the 25 °C cultures due to a problem with the extraction or UPLC-MS method, since the three experiments were performed on three different days. Figure 2.9 shows a summary of the metabolites in the citric acid cycle overlaid with colored boxes denoting the less efficient labeling and the smaller pool sizes at lower temperatures, Figure 2.10 displays the flux graphs, and Figure 2.11 displays the pool size graphs for the metabolites involved in the citric acid cycle.

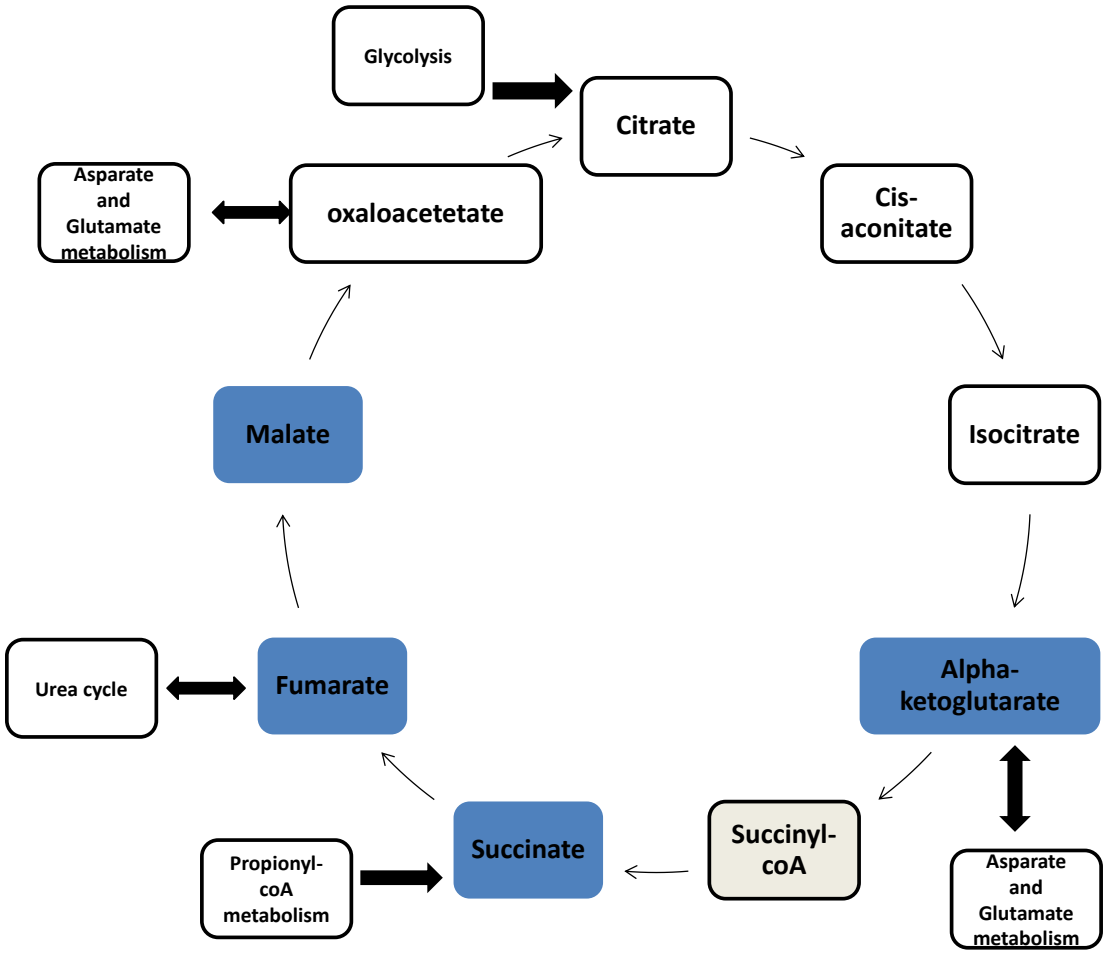

Figure 2-9. The citric acid cycle is shown. White boxes in the cycle indicate metabolites that were not detected. Blue boxes indicate metabolites with slower or less complete labeling and smaller pool size at lower temperature conditions. Grey boxes indicate metabolites that do not differ significantly in labeling patterns or pool size.

Alpha-ketoglutarate

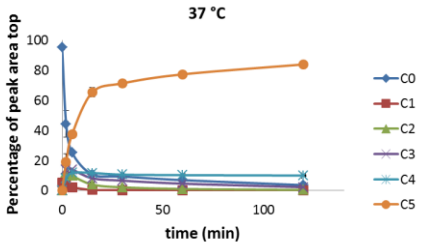

Compound not detected at 25 °C.

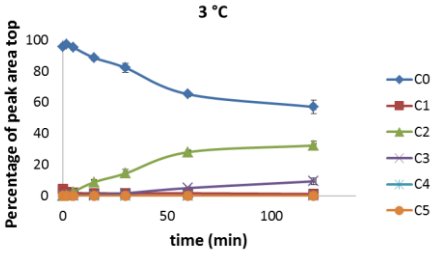

Succinate

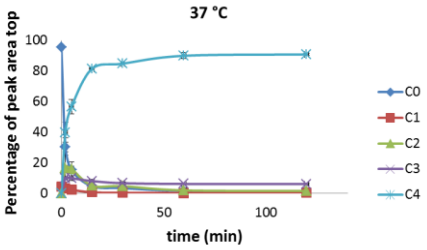

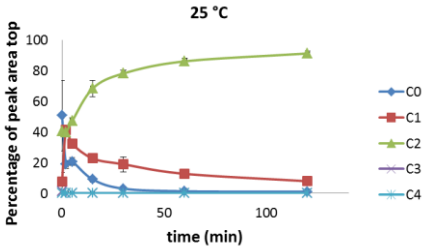

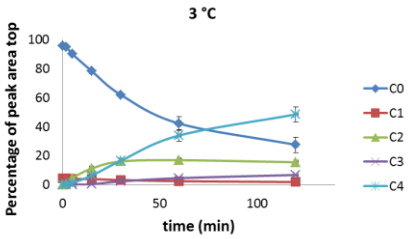

Fumarate

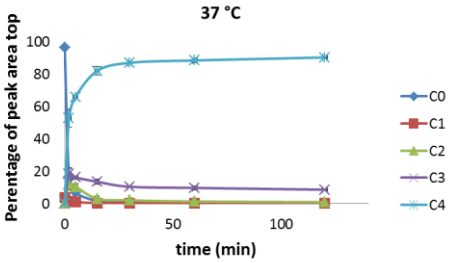

Compound not detected at 25 °C.

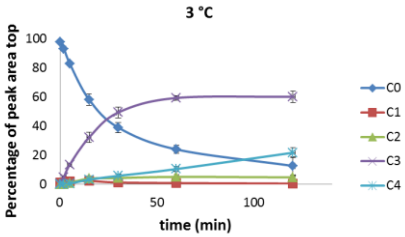

Malate

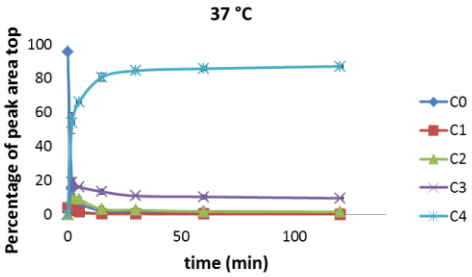

Compound not detected at 25 °C.

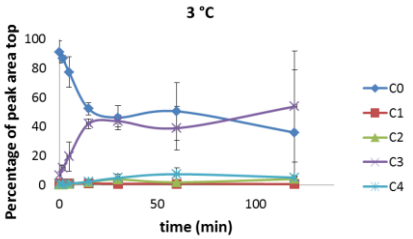

Figure 2-10. The flux graphs for the metabolites involved in the citric acid cycle are shown.

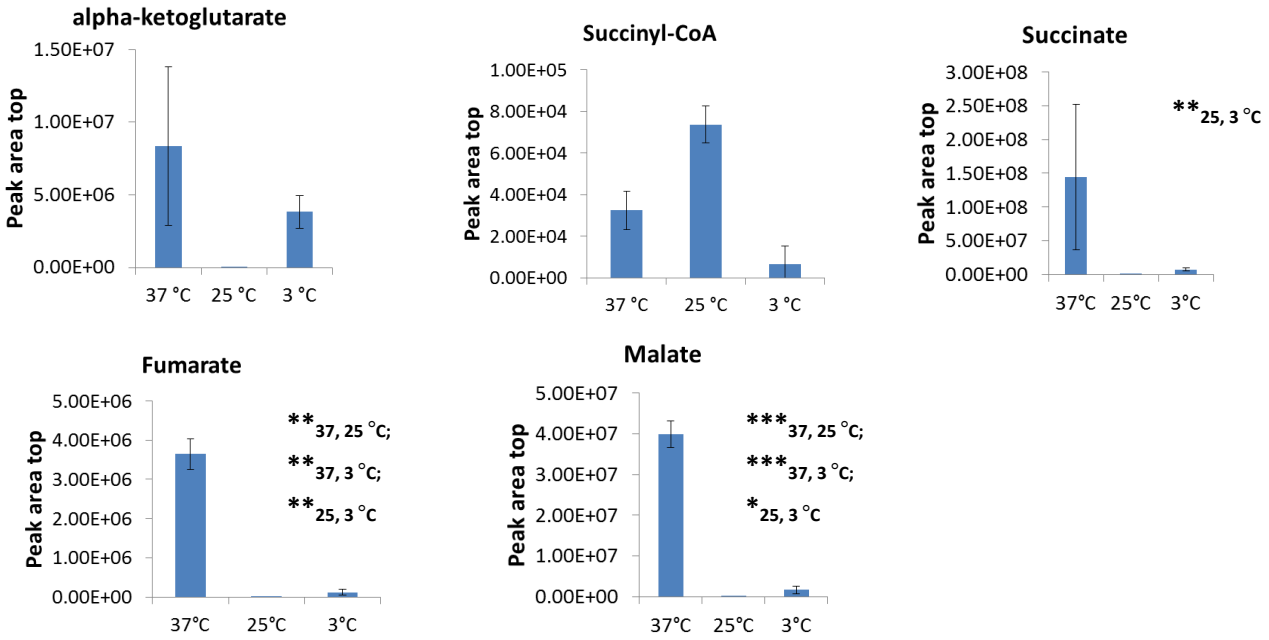

Figure 2-11. The pool size graphs for the metabolites involved in the citric acid cycle are shown. *** refers to a comparison with a p value ≤ 0.01. ** refers to a comparison with a p value ≤ 0.05. * refers to a p value ≤ 0.1.

The pentose phosphate pathway shows smaller pool sizes or less efficient labeling for all compounds detected for the 3 °C cultures, compared to the 37 °C. Glucose-6-phosphate, ribulose-5-phosphate, ribose-5-phosphate, xyulose-5-phosphate, 6-phosphogluconate, sedoheptulose-7-phosphate, and fructose-6-phosphate all show less complete or slower labeling patterns with smaller pool sizes at lower temperatures. Glyceraldehyde-3-phosphate and erythose-4-phosphate were not detected in this series of experiments. 6-phosphogluconate showed full labeling of 90% of the molecules detected after 2 min in the 37 °C and 25 °C bacterial cultures. The 3 °C bacterial cultures were not detected. The pool sizes have a fold change of 0.45 for 37 vs. 25 °C (p value= 0.10) and 157 for 37 vs. 3 °C (p value= 0.17). Ribose/ ribulose/ xyulose-5-phosphate showed full labeling of 90% of the molecules detected after 2 min at 37 °C, but only 30% of the molecules detected showed full labeling after 15 min in the 3 °C bacterial cultures. The 25 °C bacterial cultures for ribose/ribulose/xyulose-5-phosphate were not detected. The pool sizes have a fold change of 4.28×10^{13} for 37 vs. 3 °C (p value= 0.30). Sedoheptulose-1/7-phosphate shows full labeling of 90% of the molecules detected at 37 °C after 2 min and 80% of the molecules detected show full labeling after 2 min at 25 °C. Only 20% of the molecules detected show full labeling at 3 °C after 15 min. The pool sizes have a fold change of 0.45 for 37 vs. 25 °C (p value= 0.23) and 0.53 for 37 vs. 3 °C (p value= 0.19). Figure 2.10 shows the pentose phosphate pathway with colored blocks indicating whether the warmer or colder temperatures had faster or more complete labeling and larger pool size, Figure 2.11 shows the flux and pool size graphs for the metabolites involved in the pentose phosphate pathway.

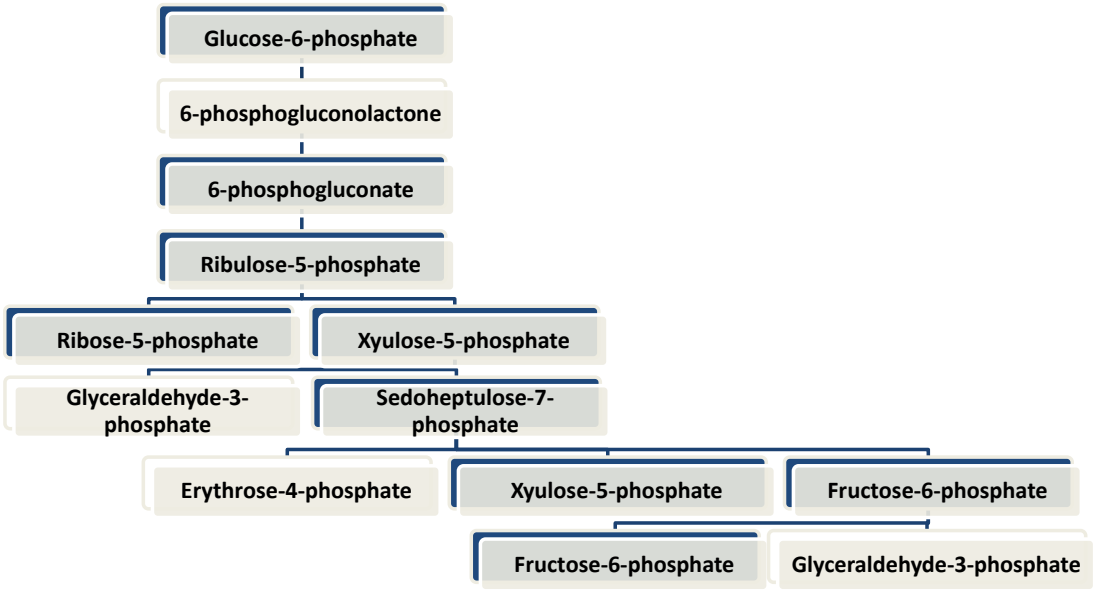

Figure 2-12. The pentose phosphate pathway is shown. Grey boxes in the pathway indicate metabolites that were not detected. Blue boxes indicate metabolites with slower or less complete labeling and smaller pool size in the lower temperature conditions.

6-phosphogluconate

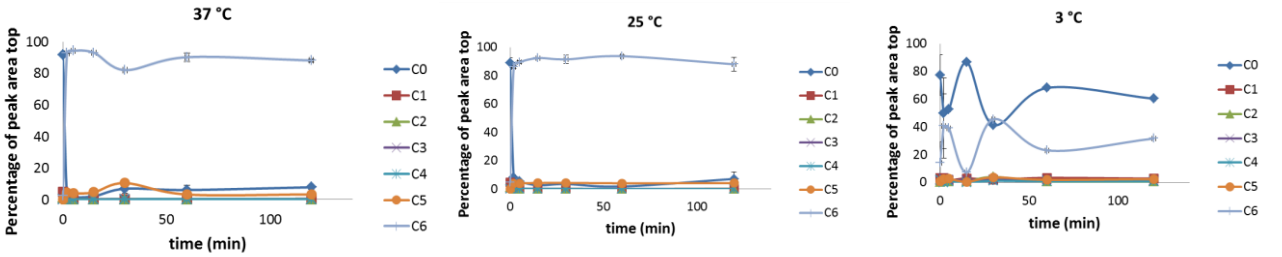

Sedoheptulose-1/7-phosphate

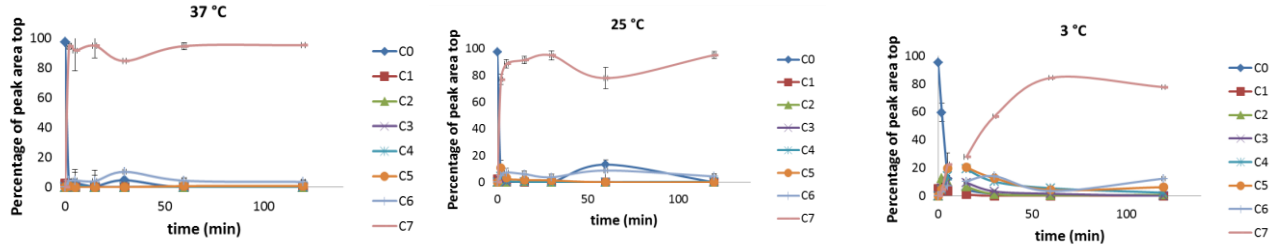

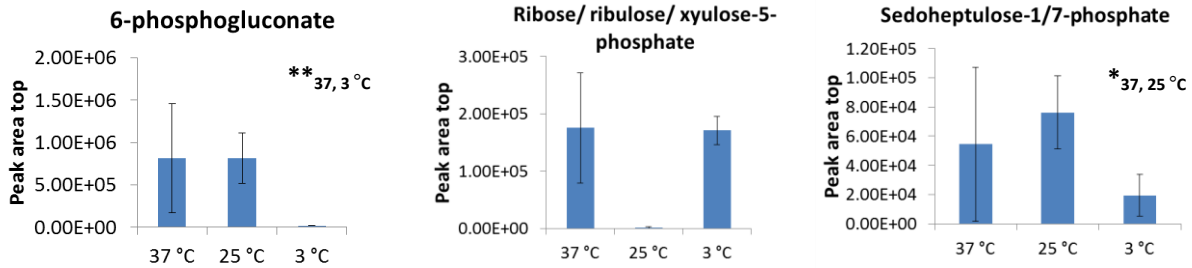

Figure 2-13. The flux graphs for the metabolites involved in the pentose phosphate pathway, excepting those that have already been shown, are shown here. *** refers to a comparison with a p value ≤ 0.01. ** refers to a comparison with a p value ≤ 0.05. * refers to a p value ≤ 0.1.

The amino acids that are detected largely show slower or less complete labeling and larger pool size at lower temperatures, indicating that perhaps more amino acids are being produced by the breakdown of proteins. Alternatively, the less efficient labeling may be due to enzymes denaturing, reducing the catalytic ability of the cells, a slowdown in the rate of transcription, or a slowdown in the rate of translation. Glutamate, glutamine, aspartate, leucine/ isoleucine, and valine all show less complete or slower labeling and larger pool sizes at lower temperatures, indicating that perhaps proteins are being degraded into their amino acids. Alanine showed less complete or slower labeling and smaller pool sizes at lower temperatures. None of the other amino acids were detected in this series of experiments. 70% of the glutamate molecules detected show full labeling after 20 min at 37 °C, while only 15% of the glutamate molecules show labeling with 2 ^{13}C after 20 min at 3 °C. Glutamate was not detected at 25 °C. The pool sizes have a fold change of 0.47 for 37 vs. 3 °C (p value= 0.08). 90% of the glutamine molecules detected showed full labeling after 20 min at 37 °C. 40% of all glutamine molecules showed labeling with 2 ^{13}C after 120 min at 3 °C. Glutamine was not detected at 25 °C. The pool sizes have a fold change of 1.38 x 10^{14} for 37 vs. 3 °C (p value= 0.20). 60% of the aspartate molecules detected showed full labeling after 2 min at 37 °C. 50% of the aspartate molecules detected showed labeling with 3 ^{13}C after 20 min at 3 °C. Aspartate was not detected at 25 °C. The pool sizes have a fold change of 0.43 for 37 vs. 3 °C (p value= 0.06). 90% of the alanine molecules detected showed full labeling after 2 min at 37 °C, while 80% of the alanine molecules detected showed labeling with 2 ^{13}C after 2 min at 3 °C. Alanine was not detected at 37 or 25 °C, but was detected at 3 °C. 80% of the valine molecules detected showed full labeling after 2 min at 37 °C, while only 60% of the valine molecules detected showed full labeling after 120 min at 3 °C. Valine was not detected at 25 °C. The pool sizes have a fold change of 0.53 for 37 vs. 3 °C (p value= 0.05). Full labeling of 60% of the molecules of leucine/ isoleucine was detected after 5 min at 37 °C and only 10% of the molecules detected fully labeling after 120 min at 3 °C. Leucine/ isoleucine was not detected at 25 °C. The pool sizes have a fold change of 1.08 for 37 vs. 3 °C (p value= 0.88). Figure 2.14 shows the flux graphs for the amino acids, and

Figure 2.15 shows the pool size graphs. The labeling and pool size information about the amino acids is summarized in Table 2.5.

Table 2-5. The amino acids are grouped according to their labeling efficiencies and their pools sizes. The fold changes and p values shown here are for the 37 to 3 °C.

Amino acid	Fold change	P value
Glutamate	0.465	0.077
Glutamine	1.38×10^{14}	0.195
Aspartate	0.429	0.0585
Leucine/ Isoleucine	1.08	0.878
Valine	0.534	0.0473

Glutamate

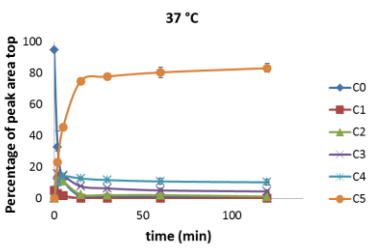

Compound not detected at 25 °C.

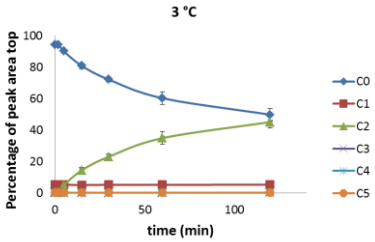

Glutamine

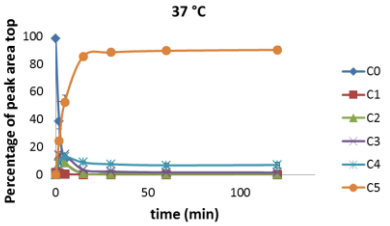

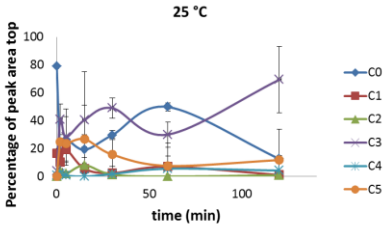

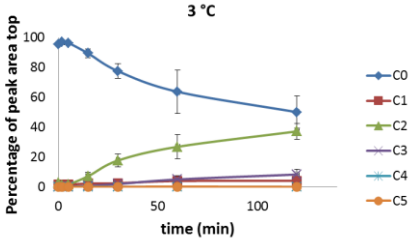

Aspartate

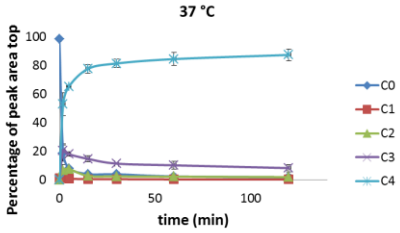

Compound not detected at 25 °C.

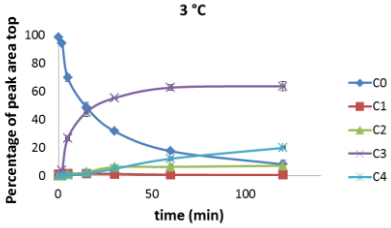

Leucine/ Isoleucine

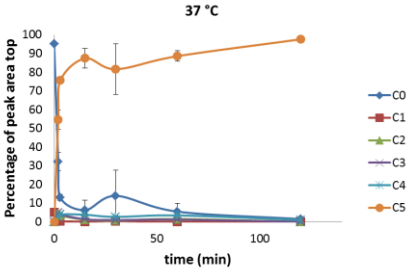

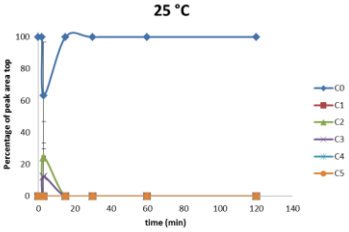

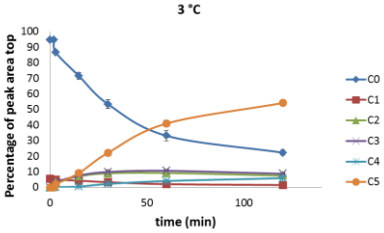

Figure 2-14. The flux graphs for the amino acids are shown here.

Alanine

Leucine/ isoleucine

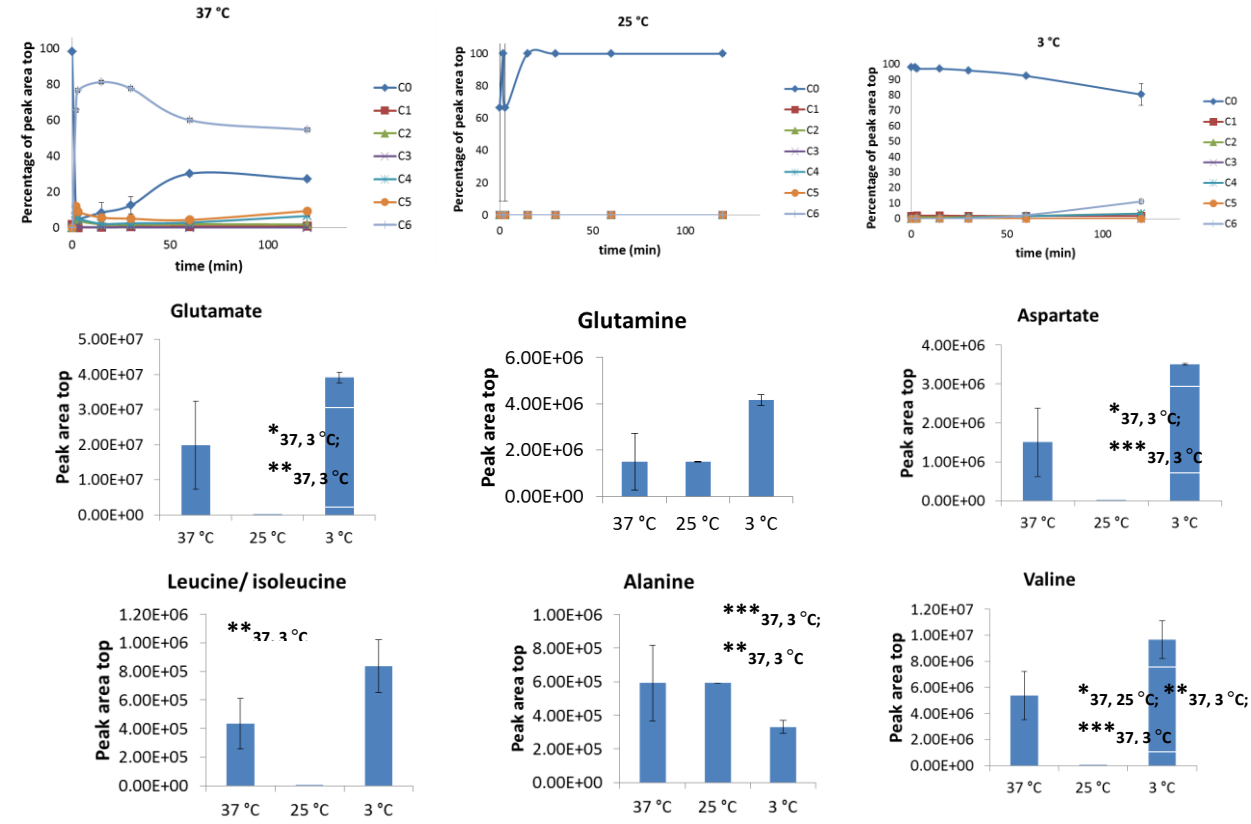

Figure 2-15. The flux graphs for leucine/isoleucine and valine, as well as the pool size graphs for all of the amino acids are shown. *** refers to a comparison with a p value ≤ 0.01. ** refers to a comparison with a p value ≤ 0.05. * refers to a p value ≤ 0.1.

Conclusion

There are metabolic differences between *S. enterica* cultures grown at 37 °C and the cultures grown at 25 and 3 °C. Metabolites that were detected in glycolysis and the citric acid cycle show less efficient labeling and smaller pool sizes at lower temperatures, in agreement with the *E. coli* study done by the Willmitzer lab.[46] Metabolites that were detected in the pentose phosphate pathway show less efficient labeling and smaller pool sizes. Five of the six amino acids detected showed less efficient labeling and larger pool sizes indicating that those amino acids might be produced by the breakdown of proteins, in agreement with the *E. coli* study done by the Willmitzer lab.[46] Conversely, the less efficient labeling may be due to enzymes denaturing, reducing the catalytic ability of the cells, a slowdown in the rate of transcription, or a slowdown in the rate of translation. The remaining amino acid showed less efficient labeling and smaller pool sizes at lower temperatures, indicating the possible conversion into other metabolites. It is important to study cold shock in *S. enterica* in order to kill the pathogenic species more effectively at the three temperatures studied so that contaminated food or surfaces will not make people ill.

CHAPTER 3

FINDING THE DIFFERENCES DUE TO THE *PURH* GENETIC MUTATIONS IN *SALMONELLA ENTERICA*

Abstract

In this set of experiments, the *purH355* mutant, strain DM2, and the LT2 wild type strain of *Salmonella enterica* were compared metabolically via metabolomics and kinetic flux profiling[59]. The *purH* mutant has the genome sequence coding for the production of the enzyme AICAR transformylase/IMP cyclohydrolase changed via the insertion of a thymidine into position 716. The insertion leads to a frame shift mutation that leads to the improper formation of ACIAR transformylase/IMP cyclohydrolase. AICAR transformylase/IMP cyclohydrolas catalyzes the reaction needed to convert aminoimidazole carboxamide ribotide (AICAR) into FICAR. It is important to study AICAR since it is involved in many pathways in diverse organisms, is involved in energy balance and the stress response of the metabolome in mammals, and has been linked to an inhibition in the proliferation of cancer cells. Due to the lack of AICAR transformylase/IMP cyclohydrolase, the *purH* mutant cannot make purines and so can act as a model for humans taking sulfa drugs. Humans taking sulfa drugs as well as the *purH* mutant show the buildup of amino-carboxamide ribonucleotide (AICAR) and the inhibition of purine metabolism.[59] The cellular strains were grown under the same conditions, and their contents were extracted before analysis with UPLC-MS. Metabolites involved in glycolysis and the citric acid cycle were largely found to label slower or have smaller pool sizes in the *purH* mutant. Notable exceptions in the citric acid cycle include those compounds involved in other pathways. The non-oxidative portion of the pentose phosphate pathway shows comparable labeling patterns and larger pool sizes in the *purH* mutant, indicating that sugars may be preferentially traveling through the pentose phosphate pathway instead of glycolysis and the citric acid cycle.

Introduction

Untargeted metabolomics can be used in order to compare different types of organisms, either different species, mutations of species, or the mutated species to the wild type may be compared. Untargeted metabolomics is needed in this type of analysis, since a genomic mutation may affect metabolites that are involved in metabolic pathways intersecting the pathway affected by the mutation.[66] Once species or mutant versions of a single species of interest have been

identified, they may be grown under similar conditions, and their metabolic contents extracted for metabolomic analysis. The relative concentrations of metabolites may be compared to see if one species or mutant produces more of any given metabolite than another. Some metabolites may be found in one species or mutant, but not detected in another. The pathways with which or efficiencies in which species or mutants move compounds through their catabolic or anabolic pathways may also differ. Metabolomics is a useful tool for identifying changes in species and mutants, because metabolites are the second to end result of any differences in the genome, with the phenotypes of the organism being the end result.[66]

Experimental Procedures

The wild type and *purH* mutant strains, provided by the Down's lab at the University of Georgia, were revived from freezer glycerol stocks and streaked onto rich Diffco, agar media plates.[59] The experimental procedure detailed in chapter two was followed for each of the strains, with a few changes. Instead of performing the experiments at three different temperatures, only the optimal temperature for *S. enterica*, 37 °C, was used. The wild time strain of S. enterica was moved onto unlabeled minimal NCE media plates at an average OD_{650} of 0.518 and the *purH* mutant was moved onto unlabeled minimal media plates at an OD_{650} of 0.540. During the analysis phase of the experimentation, automatic peak detection was not utilized using MAVEN. Instead peaks were picked manually using labeling, peak shape, closeness of retention time to the expected retention time, and consistency between replicates. The rest of the experimental procedure and analysis was performed in a similar manner as explained in chapter two.

Results and Discussion

A heat map showing the relative changes in all of the known metabolites detected is shown in Figure 3.1. In the glycolysis pathway, glucose-6-phosphate, fructose-6-phosphate, and fructose-1,6-bisphosphate all show isotopic labeling in both the wild type and the *purH* mutant;

however, pool size in the *purH* strain is higher than in the wild type strain. Glucose/fructose-6-phosphate showed full labeling occurring in 70% of the molecules detected after 2 min in the wild type strain and in the *purH* mutant. The pool sizes have a fold change of 0.66 (p value= 0.04). Approximately 80% of the fructose-1,6-bisphosphate molecules detected showed full labeling after 2 min in both the wild type and the *purH* mutant strains. The pool sizes have a fold change of 1.96 (p value= 6.74×10^{-3}). 1,3-diphosphoglycerate was not detected. In 3-phosphoglycerate and 2-phosphoglycerate (not differentiable in the methods used, so this is probably a combination of the two metabolites), isotopic labeling did not occur in the *purH* mutant. The pool sizes have a fold change of 0.33 (p value= 4.45×10^{-4}). This may indicate that 3-phosphoglycerate and 2-phosphoglycerate are not being synthesized or entirely used in further reactions. Very little isotopic labeling occurred in the wild type strain in the case of 3-phosphoglycerate and 2-phosphoglycerate as well; however, after this point in the glycolysis pathway, the *purH* shows consistently smaller pool sizes. Phosphoenolpyruvate was not detected in this analysis due to the unstable nature of the compound. Pyruvate showed full isotopic labeling in both strains, but was not detected within the 5 ppm window used to look at pool size. This indicated that the flux of pyruvate was slower in the *purH* mutant than in the wild type strain. 80% of the pyruvate molecules detected were fully labeled after 5 min in the wild type strain, while only 60% of the pyruvate molecules detected were fully labeled after 5 min in the *purH* mutant strain. In Figure 3.2, the glycolysis pathway is shown with colored boxes indicating which strain had faster or more complete labeling and larger pool size and Figure 3.3 displays the flux graphs for the metabolites involved in the glycolysis pathway.

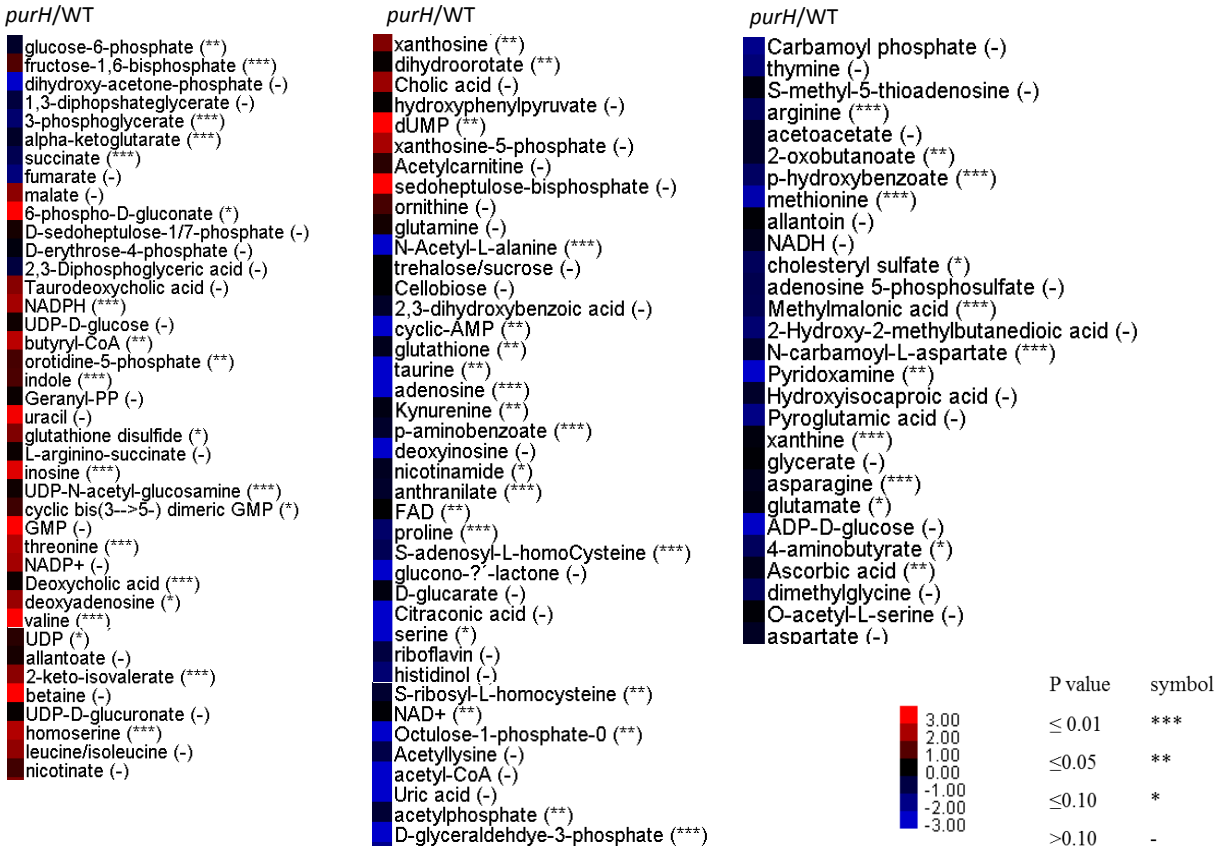

Figure 3-1. The heat map shows the log base 2 concentrations of all known metabolites detected in the *purH* mutant relative to the concentrations of the metabolites found in the wild type strain. The color bar on the lower right hand side shows the colors associated with the relative change in metabolite concentration between the *purH* mutant and the wild type.

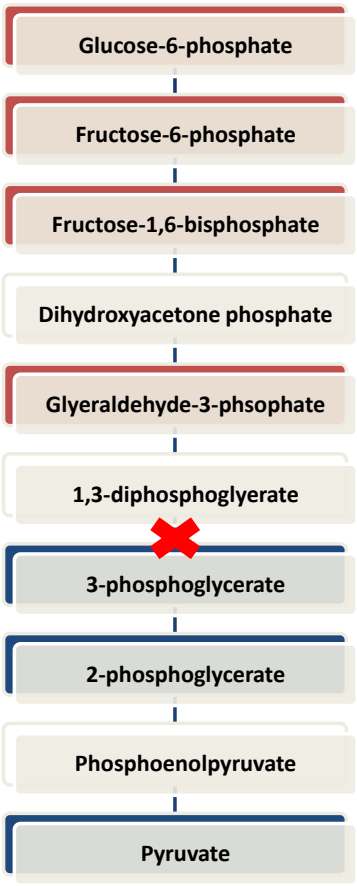

Figure 3-2. The glycolysis pathway is shown. Grey boxes in the cycle indicate metabolites that were not detected. Blue boxes indicate metabolites with slower or less complete labeling and smaller pool size in the *purH* mutant. Red boxes indicate metabolites with faster or more complete labeling and larger pool size in the *purH* mutant. A red "X" denotes the location where the larger relative rates of metabolic flux and pool size change from the *purH* mutant strain to the wild strain of *S. enterica*.

Glucose/fructose-6-phosphate

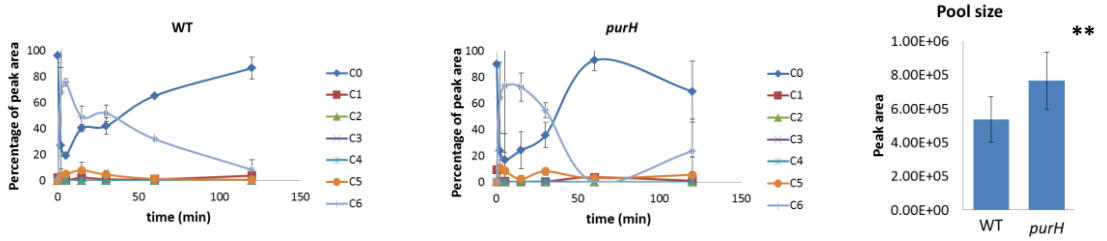

Fructose-1,6-bisphosphate

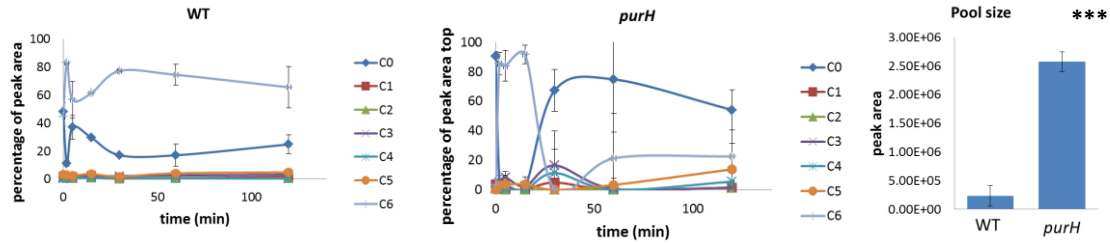

Glyceraldehyde-3-phosphate

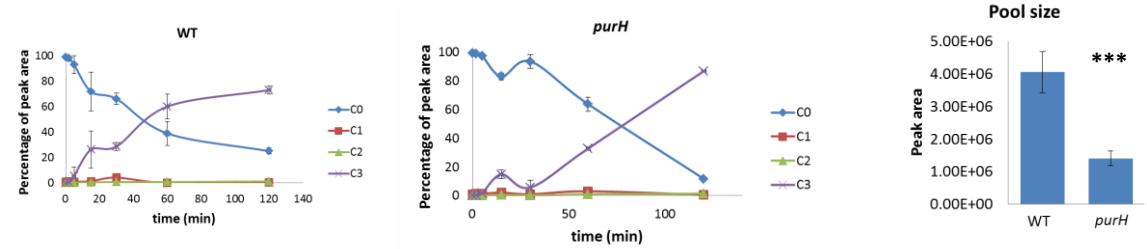

2/3-phosphoglycerate

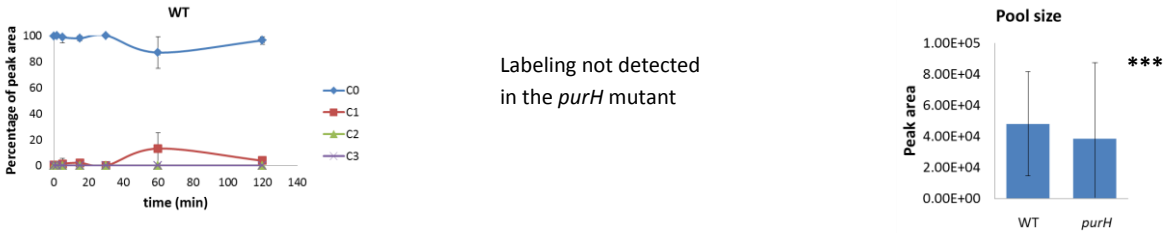

Pyruvate

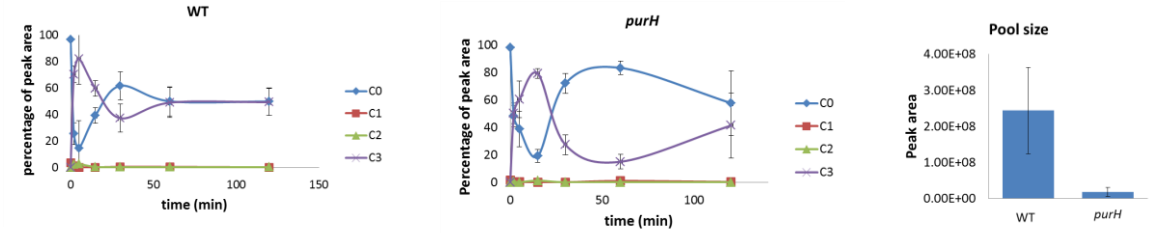

Figure 3-3. The flux and pool size graphs for the metabolites involved in glycolysis are shown. *** refers to a comparison with a p value ≤ 0.01. ** refers to a comparison with a p value ≤ 0.05. * refers to a p value ≤ 0.1.

In the citric acid cycle, the pool sizes for the metabolites are smaller in the *purH* strain than in the mutant strain, except where metabolites are involved in multiple pathways. Entering into the citric acid cycle, pyruvate showed a smaller pool size in the *purH* mutant. Cis-asconitate and isocitrate were not detected in these experiments. Alpha-ketoglutarate and succinate also showed full isotopic labeling in the wild type and the *purH* mutant, as well as a smaller pool size in the case of the *purH* mutant. Only 40% of the alpha-ketoglutarate molecules detected show full labeling after 5 min in the wild type strain and 60% of the alpha-ketoglutarate molecules detected show full labeling after 15 min in the *purH* mutant. The pool sizes have a fold change of 0.66 (p value= 1.04×10^{-3}). Succinate molecules showed full labeling in 80% of the molecules detected in the wild type strain and in the mutant strain after 20 min. The pool sizes have a fold change of 0.43 (p value= 3.30×10^{-5}). Succinyl-coA did not show labeling in the case of the *purH* mutant or in the wild type strain. Succinyl-coA was not detected within the 5 ppm error range used for pool size analysis. Fumarate did not display any labeling in the wild type strain, but 70% of the fumarate molecules detected showed full labeling after 20 min in the *purH* mutant strain. The pool sizes have a fold change of 0.28 (p value= 0.27). Fumarate is involved in the urea cycle. Malate shows isotopic labeling in both the wild type and the *purH* mutant strains and shows a larger pool size in the *purH* mutant. Malate showed full labeling in 70% of the molecules detected after 20 min in the wild type strain and the *purH* mutant strain The pool sizes have a fold change of 3.17 (p value= 0.14). Malate is also involved in other metabolic pathways Figure 3.13 shows the citric acid cycle with colors indicating relative increase, decrease, or no change in metabolic flux for each metabolite and Figure 3.14 shows the flux and pool size graphs for the metabolites involved in the citric acid cycle.

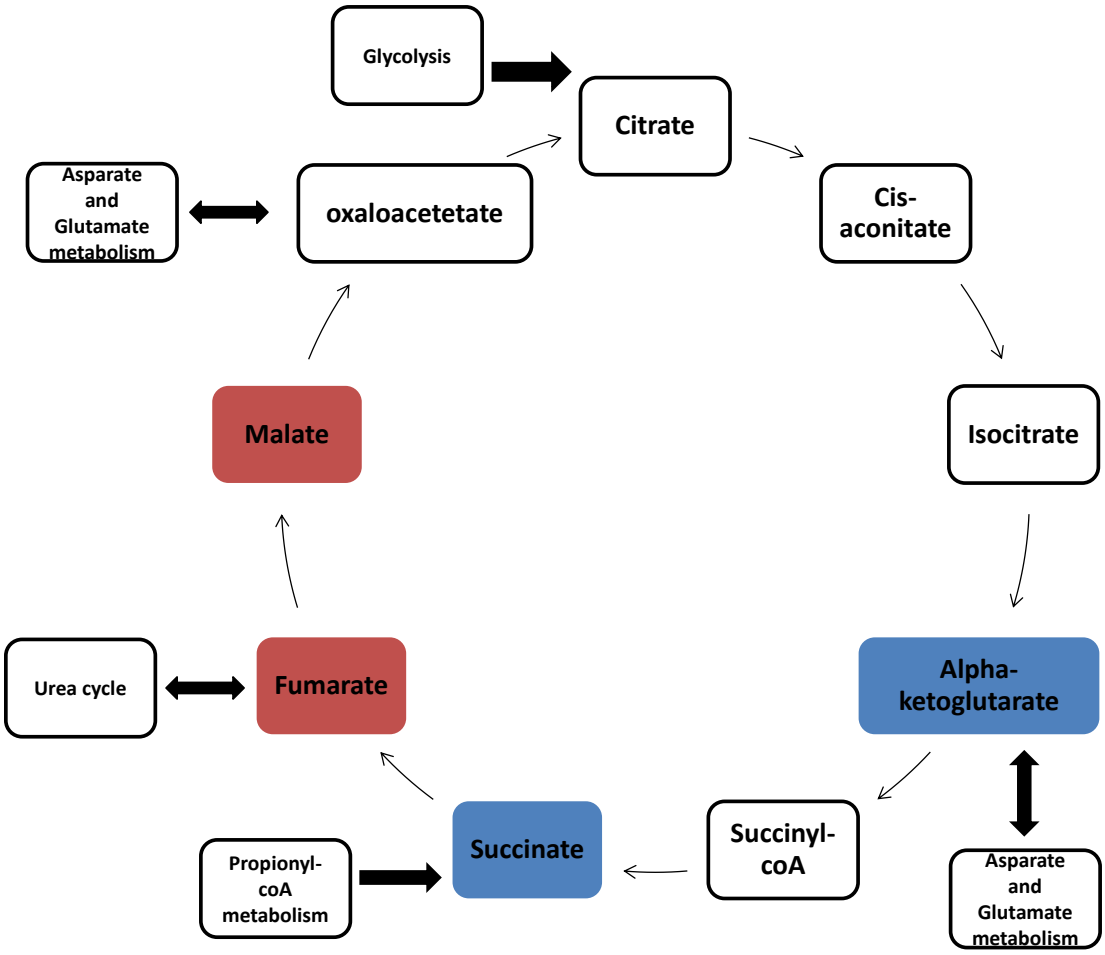

Figure 3-5. The citric acid cycle is shown above. White boxes in the cycle indicate metabolites that were not detected. Blue boxes indicate metabolites with slower or less complete labeling and smaller pool size in the *purH* mutant. Red boxes indicate metabolites with faster or more complete labeling and larger pool size in the *purH* mutant. White boxes are tangentially connected to the citric acid cycle in order to show metabolites involved in multiple pathways.

Alpha-ketoglutarate

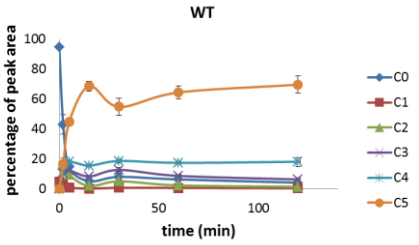

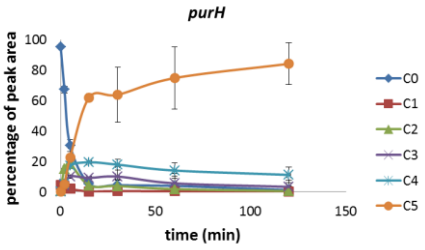

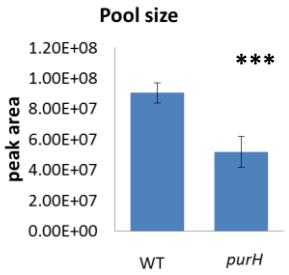

Succinate

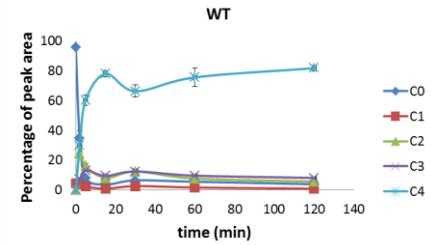

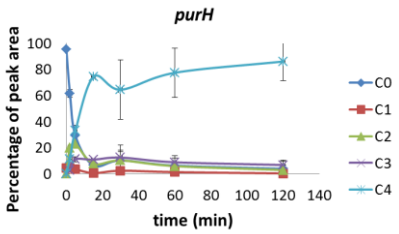

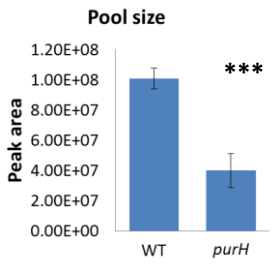

Fumarate

Labeling not detected
in WT strain

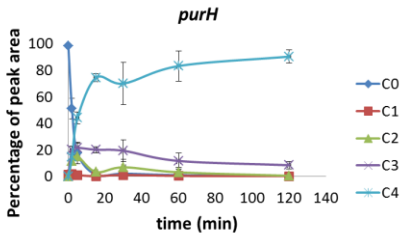

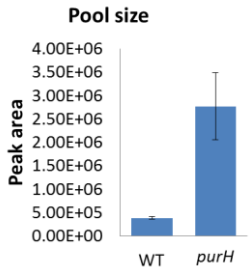

Malate

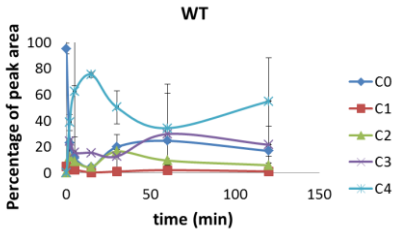

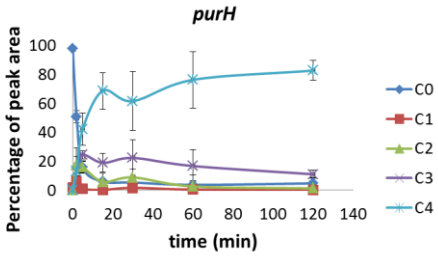

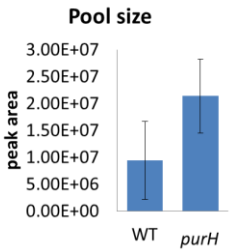

Figure 3-6. The flux graphs for the metabolites involved in the citric acid cycle are shown. *** refers to a comparison with a p value ≤ 0.01. ** refers to a comparison with a p value ≤ 0.05. * refers to a p value ≤ 0.1.

In the oxidative part of the pentose phosphate pathway, glucose-6-phosphate and 6-phospho-D-gluconate show comparable labeling patterns and a larger pool size in the *purH* mutant. 6-phosphogluconate showed full labeling in 90% of the molecules detected after 2 min in the wild type and the *purH* mutant strains. The pool sizes have a fold change of 1.64×10^3 (p value= 0.07). 6-phosphogluconolactone was not detected in this experiment. In the non-oxidative part of the pentose phosphate pathway, for every metabolite that was detected, except erthyrose-4-phosphate, full isotopic labeling was found in the wild type and *purH* mutant, with larger pool sizes being found in the *purH* mutant strain. Ribose/ ribulose/ xyulose-5-phosphate showed full labeling in 90% of the molecules detected after 2 min in the *purH* mutant, but labeling was detected for the wild type strain. Ribose/ ribulose/ xyulose-5-phosphate was not detected within the 5 ppm error window used for the pool size analysis. Sedoheptulose-1/7-phosphate showed full labeling in 95% of the molecules detected after 2 min in the wild type and the *purH* mutant strains. The pool sizes have a fold change of1.20 (p value= 0.56). Erythrose-4-phosphate showed no isotopic labeling in the wild type or the *purH* mutant strains. The pool sizes have a fold change of 0.87 (p value= 0.80). This data shows that the pentose phosphate pathway is being unregulated in the *purH* mutant strain of *S. enterica*. The pentose phosphate pathway may be allowing the *purH* mutant to continue to function without the presence of fructose-1,6-bisphosphatase. The pentose phosphate pathway is shown in Figure 3.18 with colored boxes indicating which metabolite had faster or more complete labeling, as well as a larger pool size and Figure 3.19 shows the flux and pool size graphs for the metabolites involved in the pentose phosphate pathway.

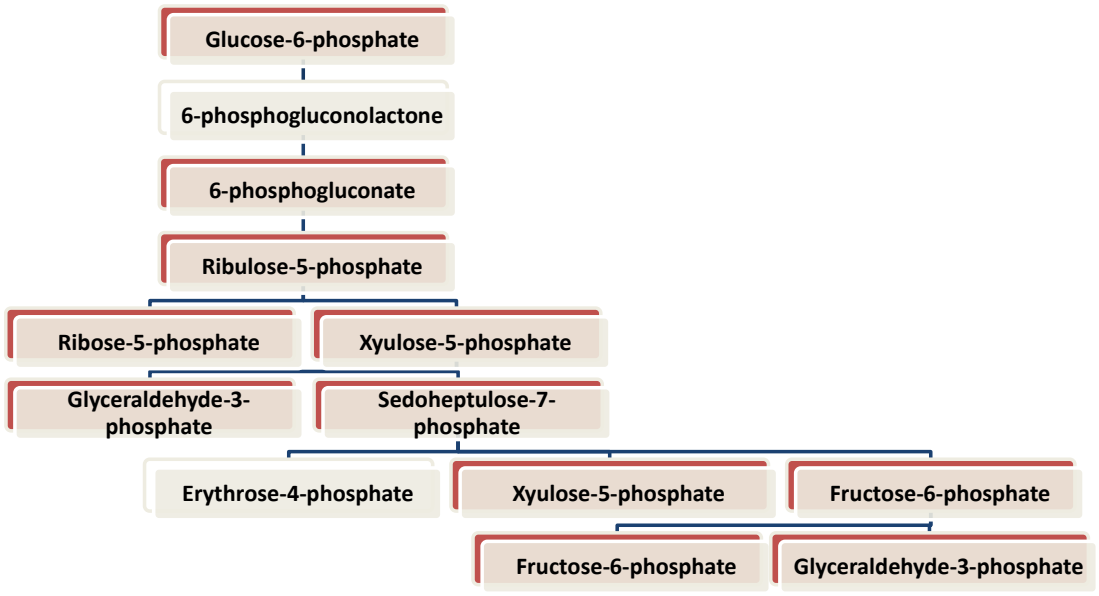

Figure 3-9. The pentose phosphate pathway is shown above. Red boxes indicate metabolites with faster or more complete labeling and larger pool size in the *purH* mutant. Grey boxes in the pathway indicate metabolites that were not detected. Black boxes in the pathway indicate that there was no significant difference between the wild type and *purH* mutant.

6-phosphogluconate

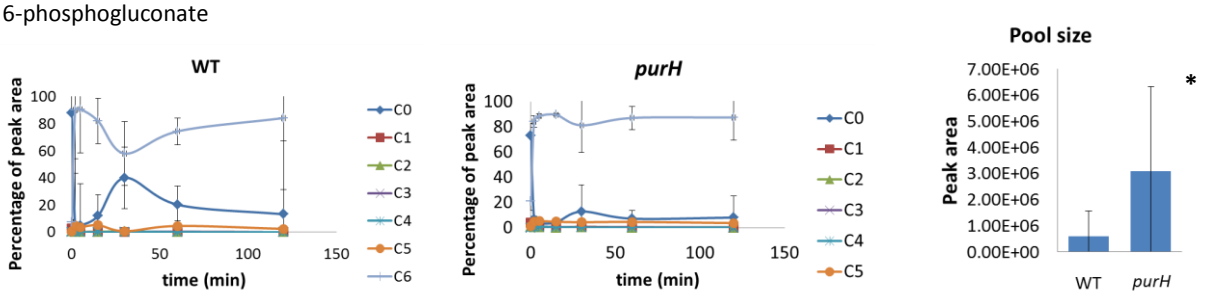

Ribose/ ribulose/ xyulose-5-phosphate

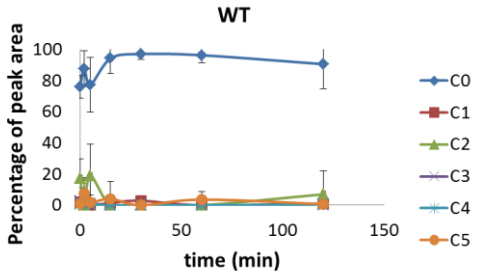

Labeling not detected in *purH* strain

Not detected within the 5 ppm error window used in pool size analysis

Sedoheptulose-1/7-phosphate

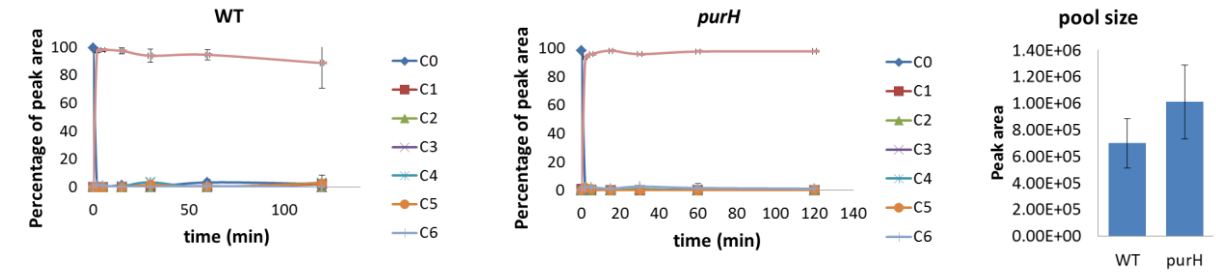

Figure 3-10. The flux graphs for the metabolites involved in the pentose phosphate pathway that were not already shown are shown here. *** refers to a comparison with a p value ≤ 0.01. ** refers to a comparison with a p value ≤ 0.05. * refers to a p value ≤ 0.1.

Due to the mutation found in the *purH* mutant, the mutant is unable to synthesize purines and so purine metabolism was also studied in this experiment. 5-phosphoribosyl-1-pyrophosphate showed slower or less complete labeling or smaller pool sizes in the *purH* mutant as compared to the wild type strain. 5-phosphoribosyl-1-pyrophosphate, phosphoribosylamine, glycinamide ribonucleotide, *N*-formylglycinamide ribonucleotide, *N*-formylglycinamidine ribonucleotide, carboxyaminoimidazole ribonucleotide, *N*-succinocarboxyamide-5-aminoimidazole ribonucleotide and FICAR were not detected in this series of experiments. AICAR molecules showed labeling with 6 ^{13}Cin 80% of the molecules detected in the wild type strain after 2 min. AICAR molecules showed labeling with 5 ^{13}C in 60% of the molecules detected after 60 min. AICAR was not detected within the 5 ppm error window used in the pool size analysis. IMP did not display a significant difference between the wild type and *purH* mutant strains. Labeling of IMP was not detected in the wild type or the *purH* mutant strains; IMP was not detected within the 5 ppm error window used for the pool size analysis. In the experiments done here, purine and thiamine were added to the media containing the cells, since that should provide the cells with the end product for the pathway affected by the mutation. Even with the end products added to the media, phenotypic and metabolic differences are seen between the wild type and *purH* mutant strains. The purine pathway is involved in making the purine nucleic acids, guanine and adenine. Thiamine also intersects the purine metabolic pathway and so the cell has no reason to make thiamine since the media was supplemented. This probably explains why most of the metabolites involved in the purine metabolic pathway do not show any labeling with ^{13}C. AICAR is involved in a number of other pathways and so the labeling pattern is explainable. Figure 3.22 summarizes the metabolites involved in purine metabolism and Figure 3.23 shows the flux graphs for the metabolites involved in purine metabolism.

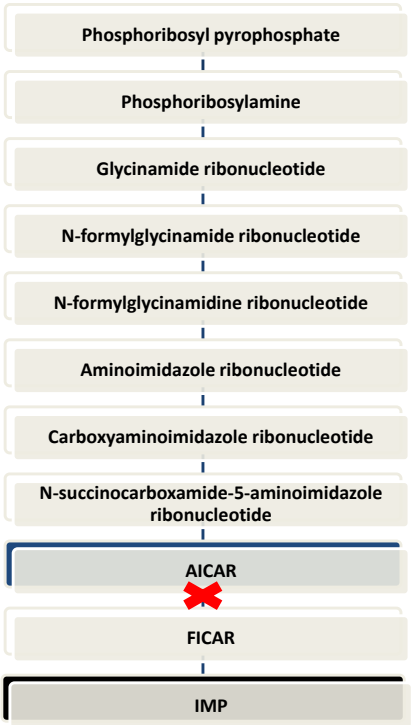

Figure 3-11. A schematic of purine metabolism is shown. Red boxes indicate that there was faster or more complete labeling or a larger pool size in the *purH* mutant. Blue boxes indicate that there was slower or less complete labeling or smaller pool sizes in the *purH* mutant. White boxes indicate that the compound was not detected in this experiment. Grey boxes indicate that there was no significant difference in the labeling patterns or pool sizes between the wild type and the *purH* mutant strains.

AICAR

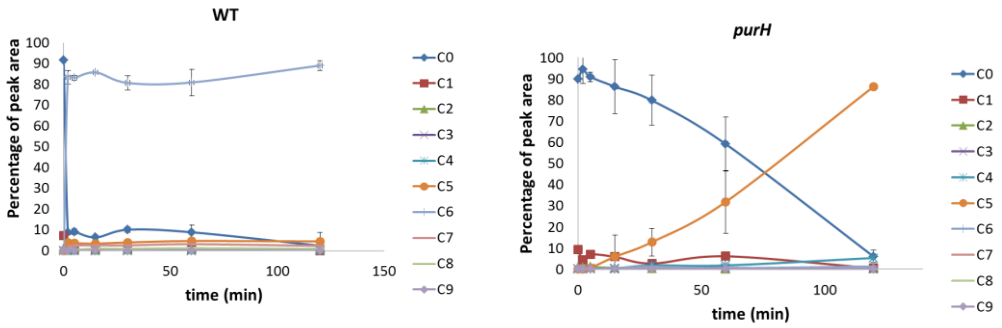

Not detected within the 5 ppm error window used in pool size analysis

Figure 3-12. The flux graphs for AICAR are shown.

Other metabolites that were of interest include acetyl-CoA, NADH, NAD^+, NADPH, $NADP^+$, ATP, and ADP. Acetyl-CoA shows labeling in the *purH* mutant, but not in the wild type strain. Approximately 80% of the acetyl-CoA molecules detected showed labeling with 2 or 3 ^{13}C after 20 min in the *purH* mutant. This labeling pattern makes sense since the acetyl group is relatively easy to label, while the 21 carbons involved in the Coenzyme A molecules are more difficult to label. The pool sizes have a fold change of 4.57×10^{-3} (p value= 0.78). NADH molecules showed labeling with 16 ^{13}C in the 30% of the molecules detected after 120 min in the wild type strain, while 40% of the NADH molecules detected showed labeling with 14 ^{13}C after 120 min in the *purH* mutant strain. The pool sizes have a fold change of 0.75 (p value= 0.07). No labeling of NADPH occurred in the wild type strain, while 15% of the NADPH molecules detected showed labeling with 16 ^{13}C after 120 min. The pool sizes have a fold change of 3.85 (p value= 1.05×10^{-4}). NAD^+ shows isotopic labeling in the wild type and the *purH* mutant. NAD^+ molecules show labeling with 16 ^{13}C in 20% of the molecules detected after 120 min in the wild type strain; while 30% of the NAD^+ molecules detected show labeling with 16 ^{13}C after 120 min. The pool sizes have a fold change of 0.95 (p value= 0.04). $NADP^+$ molecules showed labeling with 1 ^{13}C in 15% of the molecules detected after 120 min in the wild type strain, while 20% of the $NADP^+$ molecules detected showed labeling with 16 ^{13}C after 120 min in the *purH* mutant strain. The pool sizes have a fold change of 3.83 (p value= 0.12). ATP molecules showed labeling with 5 ^{13}C in 30% of the molecules detected after 30 min in the wild type strain, while 40% of the ATP molecules detected showed labeling with 5 ^{13}C after 30 min in the *purH* mutant strain. ATP was not detected within the 5 ppm error window used for pool size analysis. ADP was not detected in this set of experiments. Half of the flux and pool size graphs for the metabolites of interest listed here are shown in Figure 3. 13 and the second half of the flux and pool size graphs for the metabolites listed here are shown in Figure 3.14.

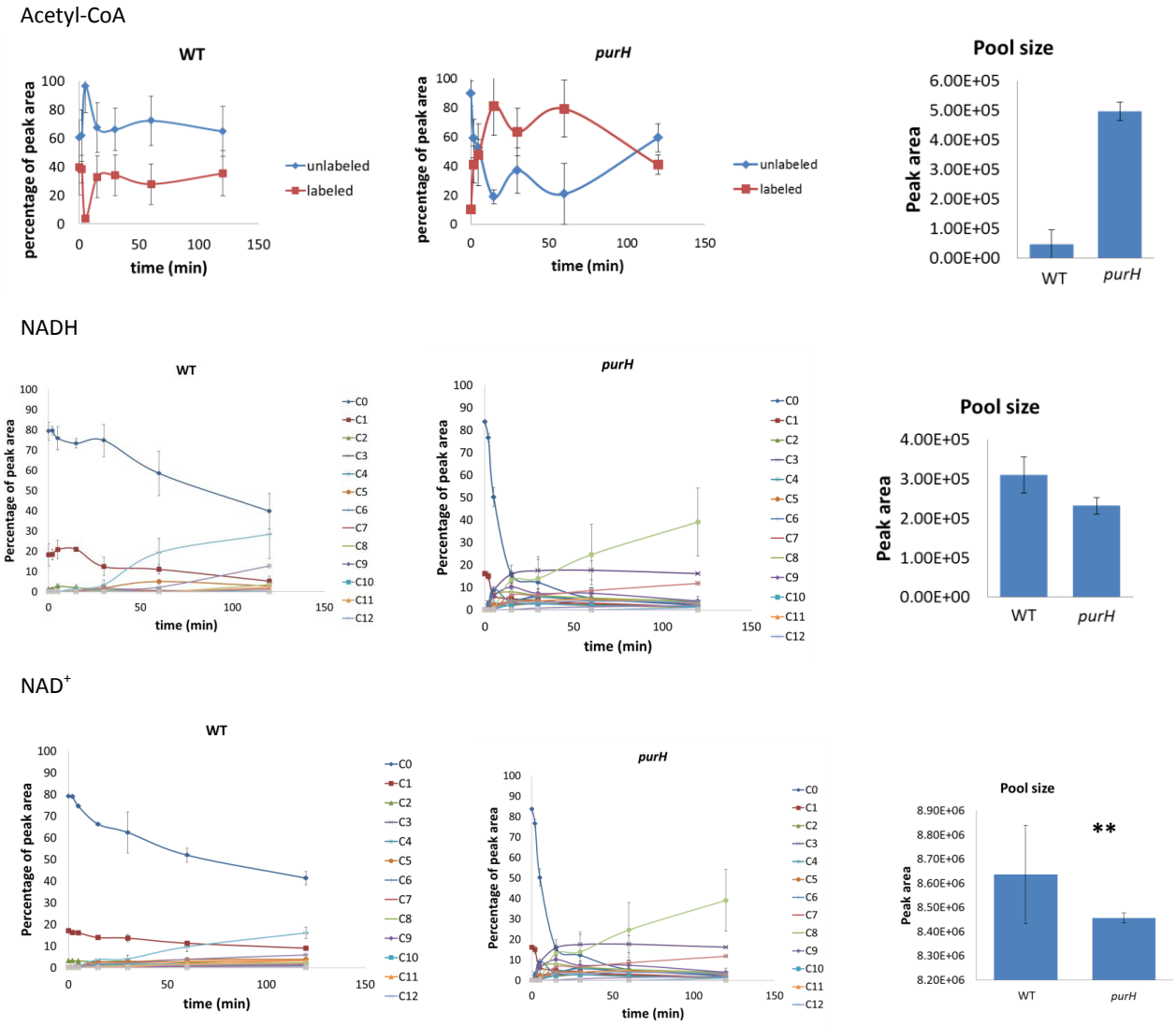

Figure 3-13. The flux graphs for acetyl coenzyme A, NADH, and NAD+ are shown. *** refers to a comparison with a p value ≤ 0.01. ** refers to a comparison with a p value ≤ 0.05. * refers to a p value ≤ 0.1.

NADPH

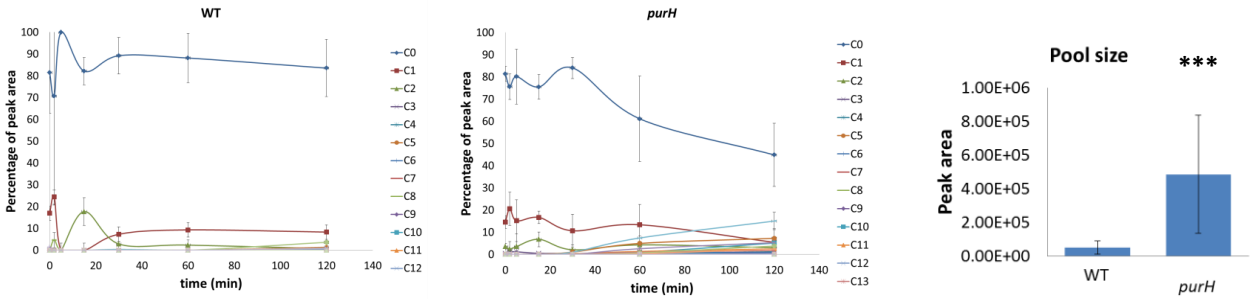

$NADP^+$

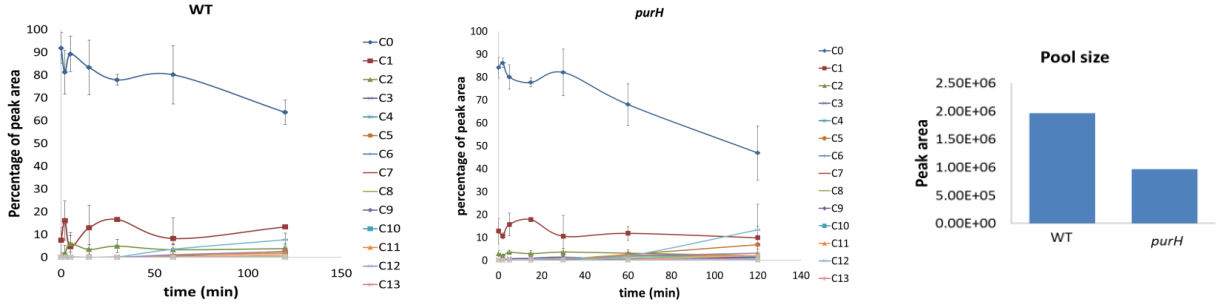

ATP

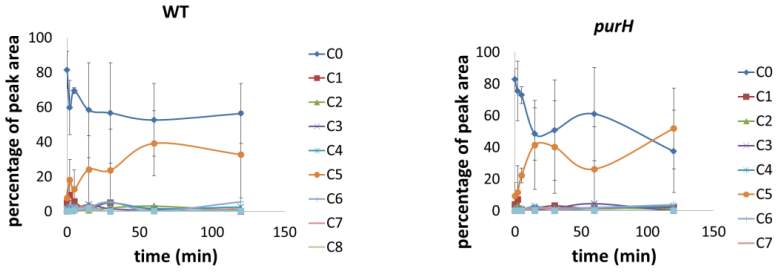

Not detected within the 5 ppm error window used in pool size analysis

Figure 3-14. Flux graphs for NADPH, $NADP^+$, ATP, and ADP. *** refers to a comparison with a p value ≤ 0.01. ** refers to a comparison with a p value ≤ 0.05. * refers to a p value ≤ 0.1.

Conclusion

The *purH* mutant differs from the WT strain of *S. enterica* due to the removal of the gene coding for the production of AICAR transformylase/IMP cyclohydrolase. Glycolysis showed a slowdown in the *purH* mutant after the production of 1,3-diphosphoglycerate. The slowdown in the *purH* mutant strain continued through the citric acid cycle, except in some cases where the metabolites were involved in more than one pathway or between two metabolites that were involved in more than one pathway. Acetyl-CoA, succinyl-CoA, fumarate, and malate all show a larger pool size in the *purH* mutant strain and comparable labeling patterns to the wild type strain. The pentose phosphate pathway shows larger pool sizes and comparable labeling patterns to the wild type strain, indicating that perhaps sugars are moving through the pentose phosphate pathway instead of glycolysis and the citric acid cycle in the *purH* mutant strain. AICAR labels to a lesser degree in the *purH* mutant, which is expected since AICAR transformylase/ IMP cyclohydrolase does not form properly due to the insertion mutation of the genome in the *purH* mutant.

CHAPTER 4 CONCLUSION

Conclusion

Cold shock metabolomics showed that the wild type strain of *S. enterica* had less efficient labeling and smaller pool sizes at lower temperatures in central carbon metabolism. Metabolites that were detected in the pentose phosphate pathway show less efficient labeling and smaller pool sizes. Proteins may also be degrading into amino acids. Conversely enzymes may be denaturing leading to slower rates of enzymatic turnover. Transcription and translation may also be occurring at slower rates due to the change in temperature. Further work could be done in order to determine the effect of cold shock on lipids, fatty acids, and proteins in the wild type strain of *S. enterica*. The effect of cold shock on macromolecule synthesis rates could also be studied. Other organisms may also be exposed to cold shock and their metabolites quantified in order to see if the metabolic changes due to cold shock are fairly universal or if they differ between species, classes, or families of organisms.

The *purH* mutant had the gene coding for AICAR transformylase/IMP cyclohydrolase altered. The *purH* mutant showed a slowdown in the glycolysis pathway and throughout the citric acid cycle after the production of 1, 3-diphosphoglycerate. Sugars may be broken down in the mutant strain through the use of the pentose phosphate pathway, as demonstrated by the larger pool sizes and similar labeling patterns in the *purH* mutant strain. In future studies, other strains of *S. enterica* may be studied in order to determine the metabolic differences caused by other mutations to the genome or the accumulation of AICAR caused by the *purH* mutation could be harnessed into an anti-cancer drug with differential lowering of body areas in areas affected by tumors.

LIST OF REFERENCES

1. Kitano, H., Systems biology: A brief overview. *Science* **2002,** *295* (5560), 1662-1664.
2. Calvert, J., Systems biology, big science and grand challenges. *BioSocieties* **2013,** *8* (4), 466-479.
3. Rabinowitz, J. D., Cellular metabolomics of Escherchia coli. *Expert Rev. Proteomics* **2007,** *4* (2), 187-198.
4. Patti, G. J.; Yanes, O.; Siuzdak, G., Metabolomics: the apogee of the omics trilogy. *Nat. Rev. Mol. Cell Biol.* **2012,** *13* (4), 263-269.
5. Yuan, J. B., B. ; Rabinowitz, J. , Kinetic flux profiling for quantitation of cellular metabolic fluxes. *Nature protocols* **2008,** *3* (8), 1328-1340.
6. Fiehn, O., Combining genomics, metabolome analysis, and biochemical modelling to understand metabolic networks. *Comparatuve and functional genomics* **2001,** *2*, 155-168.
7. Clasquin, M. M., E. ; Singer, A. ; Gooding, J. ; Xu, X. ; Dong, A. ; Cui, H. ; Campanga, S. ; Savchenko, A. ; Yakunin, A. ; Rabinowitz, J. ; Caudy, A., Riboneogenesis in Yeast. *Cell* **2011,** *145*, 969-980.
8. Raamsdonk, L. T., B. ; Broadhurst, D. ; Zhang, N. ; Hayes, A. ; Walsh, M. ; Berden, J. ; Brindle, K. ; Kell, D. ; Rowland. J. ; Westerhoff, H. ; van Dam, K. ; Oliver, S., A functional genomics strategy that uses metabolome data to reveal the phenotype of silent mutations. *Nature Biotechnology* **2001,** *19*, 45-50.
9. Kaddurah, R. K., B. ; Weinshilboum, R. , Metabolomics: A Global Biochemical Approach to Drug Response and Disease. *Annual Review of Pharmacology and Toxicology* **2008,** *48*, 653-683.
10. Campagna, S. G., J. ; May, A. , Direct Quantitation of the Quorum Sensing Signal, Autoinducer-2, in Clincally Relevant Samples by Liquid Chromatography-Tandem Mass Spectrometry. *Analytical chemistry* **2009,** *81*, 6374-6381.
11. Wenk, M., The emerging field of lipidomics. *Nature Reviews: Drug Discovery* **2005,** *4*, 594-610.
12. Qeuhenberger, O. A., A. ; Brown, A. ; Milne, S. ; Myers, D. ; Merrill, A. ; Bandyopadhyay, S. ; Jones, K. ; Kelly, S. ; Shaner, R. ; Sullards, C. ; Wang, E. ; Murphy, R. ; Barkley, R. ; Leiker, T. ; Raetz, C. ; Guan, Z. ; Laird, G. ; Six, D. ; Russell, D. ; McDonald, J. ; Subramamiam, S. ; Fahy, E. ; Dennis, E. , Lipidomics reveals a remarkable diversity of lipids in human plasma. *Journal of Lipid Research* **2010,** *51*, 3299-3305.
13. Lu, W. b., Bryson D. ; Rabinowitz, Joshua D., Analytical strategies for LC-MS-based targeted metabolomics. *Journal of Chromatography B: Technology Biomedical Life Science* **2008,** *871* (2), 236-242.
14. Cevallos-Cevallos, J. R.-d.-C., J. ; Etxeberria, E. ; Danyluk, M. ; Rodrick, G., Metabolomic analysis in food science: a review. *Trends in food science and technology* **2009,** *20*, 557-566.
15. Dunn, W. E., A. ; Weber, R. ; Creek, D. ; Brown, M. Breitling, R. ; Hankemeier, T. ; Goodacre, R. ; Neumann, S. ; Kopka, J. ; Viant, M. , Mass appeal: metabolite

identification in mass spectrometry-focused untargeted metabolomics. *Metabolomics* **2012**.
16. Pinel, G. W., S. ; Antignac, J.P. ; Mooney, M. ; Elliott, C. ; Nielen, M. ; Le Bizec, B., Targeted and untargeted profiling of biological fluids to screen for anabolic practices in cattle. *Trends in analytical chemistry* **2010,** *29*, 1269-1280.
17. Vogeser, M. S., C., A decade of HPLC–MS/MS in the routine clinical laboratory — Goals for further developments. *Clincal Biochemistry* **2008,** *41*, 649-662.
18. Wikoff, W. G., J. ; Barshop, B. ; Siuzdak, G., Metabolomics identifies perturbations in human disorders of propionate metabolism. *Clincal Chemistry* **2007,** *53* (12), 2169-2176.
19. Tohge, T. N., Y. ; Hirai, M. ; Yano, M. ; Nakajima, J. ; Awazuhara, M. ; Inoue, E. ; Takahashi, H. ; Goodenowe, D. ; Kitayama, M. ; Noji, M. ; Yamazaki, M. ; Saito, K., Functional genomics by integrated analysis of metabolome and trasncriptome of Arabidopsis plants over-expressing an MYB transcritpion factor. *The plant journal* **2005,** *42*, 218-235.
20. Bennett, B. K., E. ; Gao, M. ; Osterhout, R. ; Van Dten, S. ; Rabinowitz, J., Absolute metabolite concentrations and implied enzyme active site occupancy in *Escherichia coli*. *nature chemical biology* **2009,** *5* (8), 593-599.
21. Flores-Valverde, A. H., E., Methodology for Profiling the Steroid Metabolome in Animal Tissues Using Ultraperformance Liquid Chromatography-Electrospray-Time-of-Flight Mass Spectrometry. *Analytical chemistry* **2008,** *80*, 8771-8779.
22. Lissarre, M. O., M. ; Sato, A. ; Miura, K. , Cold-responsive gene regulation during cold acclimation in plants. *Plant Signaling & Behavior* **2010,** *5* (8), 948-952.
23. Orman, M. A., J. ; Berthiaume, F. ; Ierapetritou, M., Metabolic network analysis of perfused livers under fed and fasted states: Incorporating thermodynamic and futile-cycle-associated regulatory constraints. *Journal of theoretical biology* **2012,** *293*, 101-110.
24. Lu, W. C., M. ; Melamud, E. ; Amador-Noguez, D. ; Caudy, A. ; Rabinowitz, J., Metabolomic analysis via reversed-phase ion-pairing liquid chromatography coupled to a stand alone orbitrap mass spectrometer. *Analytical chemistry* **2010,** *82*, 3212-3221.
25. Bennett, B. Y., J. ; Kimball, E. ; Rabinowitz, J., Absolute quantitation of intracellular metabolite concentrations by an isotope ratio-based approach. *Nature protocols* **2008,** *3* (8), 1299-1311.
26. Xia, J. P., N. ; Young, N. ; Wishart, D. , MetaboAnalyst: a web server for metabolomic data analysis and interpretation. *Nucleic acids research* **2009,** *37*, W652-W660.
27. Dietmair, S., Timmins, N. , Gray, P. , Nielsen, L. , Kromer, J., Towards quantitative metabolomics of mammalian cells: Development of a metabolite extraction protocol. *Analytical Biochemistry* **2010,** *404*, 155-164.
28. Lindon, J. H., E. ; Nicholson, J., Metabonomics in pharmaceutical R & D. *FEBS Journal* **2007,** *274*, 1140-1151.

29. Clasquin, M. M., E. ; Rabinowitz, J., LC-MS Data Processing with MAVEN: A Metabolomic Analysis and Visualization Engine. *Current Protocols in Bioinformatics* **2012,** *14*, 14.11.1-14.11.23.
30. Sheperd, L. A., C. ; Sungurtas, J. ; McNicol, J. ; Stewart, D. ; Davies, H., Metabolomic analysis of the potato tuber life cycle. *Metabolomics* **2009**.
31. Bogdanov, M.; Matson, W. R.; Wang, L.; Matson, T.; Saunders-Pullman, R.; Bressman, S. S.; Beal, M. F., Metabolomic profiling to develop blood biomarkers for Parkinson's disease. *Brain* **2008,** *131*, 389-396.
32. Miller, J., *Chromatography: Concepts and Contrasts*. 2 ed.; John Wiley & sons, Inc.: Hoboken, NJ, 2005.
33. Karamani, A. A.; Fiamegos, Y. C.; Vartholomatos, G.; Stalikas, C. D., Fluoroacetylation/fluoroethylesterification as a derivatization approach for gas chromatography-mass spectrometry in metabolomics: Preliminary study of lymphohyperplastic diseases. *J. Chromatogr. A* **2013,** *1302*, 125-132.
34. The Theory of HPLC: Introduction. http://www.google.com/url?sa=t&rct=j&q=&esrc=s&source=web&cd=10&ved=0CHsQFjAJ&url=http%3A%2F%2Fforensicscienceeducation.org%2Fwp-content%2Fuploads%2F2013%2F04%2FTheory_Of_HPLC_Introduction.pdf&ei=ub1CU4D5EMug0gG6w4Fo&usg=AFQjCNFybtb-vvf4q2phL6Otdpm59Ta6IA&sig2=mjxJzs62syh2qJCvxsReMQ&bvm=bv.64125504,d.dmQ.
35. Skoog, D. H., F.; Crouch, S., *Principles of Instrumental Analysis*. 6 ed.; Brooks/ cole, Cengage learning: 2007.
36. Banerjee, S.; Mazumdar, S., Electrospray Ionization Mass Spectrometry: A Technique to Access the Information beyond the Molecular Weight of the Analyte. *Int. J. Anal. Chem.* **2012**.
37. Tassetti, C. M.; Mahieu, R.; Danel, J. S.; Peyssonneaux, O.; Progent, F.; Polizzi, J. P.; Machuron-Mandard, X.; Duraffourg, L., A MEMS electron impact ion source integrated in a microtime-of-flight mass spectrometer. *Sens. Actuator B-Chem.* **2013,** *189*, 173-178.
38. Perry, R. H.; Cooks, R. G.; Noll, R. J., ORBITRAP MASS SPECTROMETRY: INSTRUMENTATION, ION MOTION AND APPLICATIONS. *Mass Spectrom. Rev.* **2008,** *27* (6), 661-699.
39. Thermo Polaris Q - An Ion Trap GC/MS. http://departments.agri.huji.ac.il/zabam/Polaris-Q.html.
40. Lewis, J. W., J. ; Siuzdak, G., Matrix-assisted Laser Desorption/Ionization Mass Spectrometry in Peptide and Protein Analysis. In *Encyclopedia of Analytical Chemistry*, Meyers, R. A., Ed. John Wiley & Sons Ltd: Chichester, England, 2000; pp 5880-5894.
41. Domon, B., Aebersold, R., Mass Spectrometry and Protein Analysis. *Science* **2006,** *312*, 212-127.
42. TOF FUNDAMENTALS TUTORIAL. http://www.rmjordan.com/tt1.html.
43. Introduction to Time-of-Flight Mass Spectrometry. http://www.kore.co.uk/tutorial.htm.

44. Q Exactive Hybrid Quadrupole-Orbitrap Mass Spectrometer from Thermo Scientific. http://www.biocompare.com/11381-Complete-LC-MS-Systems/3722049-Q-Exactive-Hybrid-Quadrupole-Orbitrap-Mass-Spectrometer/ (accessed February 19, 2014).
45. Lu, W.; Bennett, B. D.; Rabinowitz, J. D., Analytical strategies for LC-MS-based targeted metabolomics. *J. Chromatogr. B* **2008,** *871* (2), 236-242.
46. Jozefczuk, S.; Klie, S.; Catchpole, G.; Szymanski, J.; Cuadros-Inostroza, A.; Steinhauser, D.; Selbig, J.; Willmitzer, L., Metabolomic and transcriptomic stress response of Escherichia coli. *Mol. Syst. Biol.* **2010,** *6*.
47. Gadgil, M.; Kapur, V.; Hu, W. S., Transcriptional response of Escherichia coli to temperature shift. *Biotechnol. Prog.* **2005,** *21* (3), 689-699.
48. Phadtare, S.; Inouye, M., Genome-wide transcriptional analysis of the cold shock response in wild-type and cold-sensitive, quadruple-csp-deletion strains of Escherichia coli. *J. Bacteriol.* **2004,** *186* (20), 7007-7014.
49. Zheng, M.; Wang, X.; Templeton, L. J.; Smulski, D. R.; LaRossa, R. A.; Storz, G., DNA microarray-mediated transcriptional profiling of the Escherichia coli response to hydrogen peroxide. *J. Bacteriol.* **2001,** *183* (15), 4562-4570.
50. Kral'ova, K.; Jampilek, J.; Ostrovsky, I., METABOLOMICS - USEFUL TOOL FOR STUDY OF PLANT RESPONSES TO ABIOTIC STRESSES. *Ecol. Chem. Eng. S-* **2012,** *19* (2), 133-161.
51. Lowe, R. G. T.; Lord, M.; Rybak, K.; Trengove, R. D.; Oliver, R. P.; Solomon, P. S., A metabolomic approach to dissecting osmotic stress in the wheat pathogen Stagonospora nodorum. *Fungal Genet. Biol.* **2008,** *45* (11), 1479-1486.
52. R, H.-A., *Bacterial Stress Responses*. ASM Press: 2000.
53. Kaplan, F. K., D. ; Haskell, D. ; Zhao, W. ; Schiller, K.C. ; Gatzke, N. ; Sung, D. ; Guy, C., Exploring the Temperature-Stress Metabolome of Arabidopsis[1[w]]. *Plant Physiology* **2004,** *136* (4159-4168).
54. Hincha, D. K.; Espinoza, C.; Zuther, E., *Transcriptomic and metabolomic approaches to the analysis of plant freezing tolerance and cold acclimation*. WILEY-VCH Verlag GMBH & Co. KGaA: Weinheim, Germany, 2012; p 255-287.
55. Kaplan, F.; Kopka, J.; Haskell, D. W.; Zhao, W.; Schiller, K. C.; Gatzke, N.; Sung, D. Y.; Guy, C. L., Exploring the temperature-stress metabolome of Arabidopsis. *Plant Physiol.* **2004,** *136* (4), 4159-4168.
56. Teets, N. M.; Peyton, J. T.; Ragland, G. J.; Colinet, H.; Renault, D.; Hahn, D. A.; Denlinger, D. L., Combined transcriptomic and metabolomic approach uncovers molecular mechanisms of cold tolerance in a temperate flesh fly. *Physiol. Genomics* **2012,** *44* (15), 764-777.
57. Michaud, M. R.; Benoit, J. B.; Lopez-Martinez, G.; Elnitsky, M. A.; Lee, R. E.; Denlinger, D. L., Metabolomics reveals unique and shared metabolic changes in response to heat shock, freezing and desiccation in the Antarctic midge, Belgica antarctica. *J. Insect Physiol.* **2008,** *54* (4), 645-655.
58. Colinet, H.; Larvor, V.; Laparie, M.; Renault, D., Exploring the plastic response to cold acclimation through metabolomics. *Funct. Ecol.* **2012,** *26* (3), 711-722.

59. Dougherty, M. J.; Boyd, J. M.; Downs, D. M., Inhibition of fructose-1,6-bisphosphatase by aminoimidazole carboxamide ribotide prevents growth of Salmonella enterica purH mutants on glycerol. *J. Biol. Chem.* **2006,** *281* (45), 33892-33899.
60. Bennett, B. D.; Yuan, J.; Kimball, E. H.; Rabinowitz, J. D., Absolute quantitation of intracellular metabolite concentrations by an isotope ratio-based approach. *Nat. Protoc.* **2008,** *3* (8), 1299-1311.
61. Lu, W. Y.; Clasquin, M. F.; Melamud, E.; Amador-Noguez, D.; Caudy, A. A.; Rabinowitz, J. D., Metabolomic Analysis via Reversed-Phase Ion-Pairing Liquid Chromatography Coupled to a Stand Alone Orbitrap Mass Spectrometer. *Anal. Chem.* **2010,** *82* (8), 3212-3221.
62. Kessner, D.; Chambers, M.; Burke, R.; Agusand, D.; Mallick, P., ProteoWizard: open source software for rapid proteomics tools development. *Bioinformatics* **2008,** *24* (21), 2534-2536.
63. Clasquin, M. F.; Melamud, E.; Rabinowitz, J. D., LC-MS data processing with MAVEN: a metabolomic analysis and visualization engine. *Current protocols in bioinformatics / editoral board, Andreas D. Baxevanis ... [et al.]* **2012,** *Chapter 14*, Unit14.11.
64. de Hoon, M. J. L.; Imoto, S.; Nolan, J.; Miyano, S., Open source clustering software. *Bioinformatics* **2004,** *20* (9), 1453-1454.
65. Saldanha, A. J., Java Treeview-extensible visualization of microarray data. *Bioinformatics* **2004,** *20* (17), 3246-3248.
66. Fiehn, O., Combining genomics, metabolome analysis, and biochemical modelling to understand metabolic networks. *Compar. Funct. Genom.* **2001,** *2* (3), 155-168.

APPENDIX

Table A-1. The pool size data and p values for the metabolites detected in the temperature experiment are shown.

Metabolite	median *m/z*	37 °C/25 °C	37 °C/3 °C	25 °C/3 °C	37 °C/25 °C p value	37 °C/3 °C p value	25 °C/3 °C p value
Pyruvate	870	0.729	0.000717	0.000983	0.658	0.183	0.183
Sarcosine	880	1	4.39×10^{-14}	4.39×10^{-14}	1	0.00253	0.00253
alanine	88	1	4.39×10^{-14}	4.39×10^{-14}	1	0.00253	0.00253
lactate	89	2.74×10^{-11}	8.71×10^{-16}	0.0000318	0.198	0.13	0.13
acetoacetate	101	4.32×10^{-10}	3.22×10^{-15}	7.44×10^{-06}	0.423	0.0111	0.0111
4-aminobutyrate	102	6.54×10^{-11}	4.55×10^{-15}	0.0000697	0.0658	0.0139	0.0139
L-Serine	104	4.35×10^{11}	0.193	4.44×10^{-13}	0.423	0.0706	0.06
Uracil	111	2.92×10^{13}	511	1.75×10^{-11}	0.225	0.226	0.0715
L-Proline	114	236	1.32	0.00557	0.424	0.833	0.0215
fumarate	115	2.96×10^{14}	13.9	4.71×10^{-14}	0.0345	0.0396	0.011
2-ketoisovalerate	115	17000	1.38	0.0000811	0.0344	0.281	0.00667
L-Valine	116	68900	0.534	7.74×10^{-06}	0.0532	0.0473	0.00836
Succinate	117	410000	31.1	0.0000759	0.161	0.169	0.0382
Methylmalonic acid	117	410000	31.1	0.0000759	0.161	0.169	0.0382
L-Threonine	118	2.23×10^{13}	0.35	1.57×10^{-14}	0.263	0.084	0.0171
homoserine	118	2.23×10^{13}	0.35	1.57×10^{-14}	0.263	0.084	0.0171
purine	119	1	4.77×10^{-15}	4.77×10^{-15}	1	0.423	0.423
Nicotinate	122	6.74×10^{13}	0.196	2.92×10^{-15}	0.0788	0.00369	0.00873
Thymine	125	1.65×10^{13}	16.9	1.03×10^{-12}	0.00626	0.00429	0.124
Citraconic acid	129	42500	4.39	0.000103	0.0074	0.00396	0.0393
N-Acetyl-L-alanine	130	11800	730	0.0618	0.376	0.377	0.0647
leucine/isoleucine	130	11200	1.08	0.0000963	0.119	0.878	0.046
asparagine	131	0.0215	0.188	8.74	0.0216	0.00426	0.0265
Hydroxyisocaproic acid	131	622	0.799	0.00128	0.0474	0.429	0.0186

Table A-1 continued.

Metabolite	median *m/z*	37 °C/25 °C	37 °C/3 °C	25 °C/3 °C	37 °C/25 °C p value	37 °C/3 °C p value	25 °C/3 °C p value
aspartate	132	103000	0.429	4.16×10^{-6}	0.117	0.0585	0.00313
malate	133	258000	15.5	6.02×10^{-5}	0.000909	3.49×10^{-5}	0.0943
Methylcysteine	134	93	1.95	0.021	0.37	0.63	0.0536
hypoxanthine	135	7290	159	0.0218	0.24	0.242	0.165
4-Aminobenzoate	136	6.51×10^{-12}	5.29 x 10-^{12}	0.814	0.186	0.21	0.8
p-hydroxybenzoate	137	3.07×10^{13}	14.7	4.80×10^{-13}	0.00154	0.000969	0.0223
acetylphosphate	139	0.305	18.9	62	0.0228	0.0271	0.0172
Carbamoyl phosphate	140	0.483	0.0111	0.0229	0.675	0.0897	0.091
alpha-ketoglutarate	145	60900	3.25	5.34×10^{-5}	0.133	0.225	0.185
glutamine	145	1.38×10^{14}	1.38×10^{14}	1	0.195	0.195	1
O-Acetyl-L-serine	146	33	0.463	0.014	0.111	0.158	0.058
glutamate	146	33200	0.465	0.000014	0.122	0.0768	0.0101
2-Hydroxy-2-methylbutanedioic acid	147	570	4.45	0.0078	0.00892	0.0088	0.0202
methionine	148	2.55×10^{12}	0.178	6.98×10^{-14}	0.02	0.0492	0.0356
3-methylphenylacetic acid	149	2.3×10^{12}	35.5	1.54×10^{-11}	0.00138	0.000489	0.164
guanine	150	4930	9180	1.86	0.255	0.255	0.563
Xanthine	151	233	3.77×10^{11}	1.62×10^{9}	0.306	0.304	0.423
Hydroxyphenylacetic acid	151	331	966	2.92	0.0016	0.00161	0.379
2,3-dihydroxybenzoic acid	153	4×10^{13}	4×10^{13}	1	0.0387	0.0387	1
Orotate	155	186	33200	178	0.0438	0.0434	0.139
allantoin	157	3.66×10^{-10}	1.63×10^{-12}	0.00445	0.423	0.039	0.0393
Phenylpyruvate	163	0.0000555	0.2	3600	0.00146	0.354	0.00146
Methionine sulfoxide	164	21200	7.7×10^{13}	3.64×10^{9}	0.0631	0.0631	0.423
Phosphoenolpyruvate	167	1	6.63×10^{-13}	6.63×10^{-13}	1	0.241	0.241
D-glyceraldehdye-3-phosphate	169	1	2.13×10^{-13}	2.13×10^{-13}	1	0.0268	0.0268
N-carbamoyl-L-aspartate	175	42300	22.6	0.000533	0.394	0.411	0.401

Table A-1 continued.

Metabolite	median *m/z*	37 °C/25 °C	37 °C/3 °C	25 °C/3 °C	37 °C/25 °C p value	37 °C/3 °C p value	25 °C/3 °C p value
Diphosphate	177	0.932	2.63	2.82	0.61	0.00354	0.00908
L-Tyrosine	180	4780	4460	0.933	0.00108	0.00108	0.957
3-phosphoglycerate	185	2×10^{11}	0.257	1.29×10^{-12}	0.41	0.117	0.0688
D-erythrose-4-phosphate	199	3.2×10^{12}	0.672	2.1×10^{-13}	0.153	0.474	0.0739
D-glucarate	209	1.35×10^{11}	0.0695	5.16×10^{-13}	0.177	0.0944	0.0848
deoxyribose-phosphate	213	1.15×10^{11}	0.0807	7.04×10^{-13}	0.423	0.00514	0.0145
Chorismate	225	905	3.27×10^{12}	3.62×10^{9}	0.003	0.00301	0.423
D-Ribose 5-phosphate	229	4.28×10^{13}	4.28×10^{13}	1	0.302	0.302	1
Uridine	243	9.28×10^{11}	12.4	1.34×10^{-11}	0.00834	0.00795	0.0467
Shikimate 3-phosphate	253	1.14×10^{13}	161	1.41×10^{-11}	0.197	0.199	0.349
D-glucosamine-1-phosphate	258	2.75×10^{12}	2.76	1×10^{-12}	0.00331	0.00169	0.0281
D-glucosamine-6-phosphate	258	3.09×10^{12}	31.2	1.01×10^{-11}	0.0631	0.0664	0.192
glucose-6-phosphate	259	0.703	0.77	1.1	0.179	0.359	0.596
2,3-Diphosphoglyceric acid	265	1.31	39.2	29.9	0.411	0.0332	0.0548
S-Ribosyl-L-homocysteine	266	1.62	13.4	8.27	0.427	0.135	0.0527
inosine	267	0.805	1.89	2.35	0.655	0.17	0.238
6-phospho-D-gluconate	275	0.449	157	350	0.11	0.174	0.0186
Xanthosine	283	1.75	0.598	0.341	0.232	0.218	0.0813
D-sedoheptulose-1/7-phosphate	289	0.452	0.525	1.16	0.0659	0.185	0.607
N-acetyl-glucosamine-1/6-phosphate	300	5.95	21.8	3.66	0.0507	0.0426	0.0831
glutathione	306	1.44	1.58	1.1	0.641	0.563	0.855
Octoluse 8/1P	319	0.112	0.136	1.21	0.181	0.158	0.764
dTMP	321	0.165	0.62	3.76	0.0766	0.704	0.104
CMP	322	0.985	2.26	2.29	0.981	0.387	0.158
UMP	323	1.14	1.87	1.64	0.893	0.615	0.201
cyclic-AMP	328	21.3	565	26.5	0.173	0.162	0.194

Table A-1 continued.

Metabolite	median *m/z*	37 °C/25 °C	37 °C/3 °C	25 °C/3 °C	37 °C/25 °C p value	37 °C/3 °C p value	25 °C/3 °C p value
aminoimidazole carboxamide ribonucleotide	337	0.548	38	69.3	0.393	0.291	0.072
fructose-1,6-bisphosphate	339	1.53	24.9	16.2	0.375	0.0822	0.0505
Sucrose	341	1	0.953	0.952	0.997	0.889	0.71
Cellobiose	341	1	0.953	0.952	0.997	0.889	0.71
dGMP	346	2.53	29.5	11.7	0.136	0.0673	0.095
IMP	347	0.413	55.4	134	0.0139	0.0542	0.00227
S-Adenosylmethioninamine	354	0.491	27.9	56.8	0.239	0.244	0.0453
GMP	362	0.234	0.757	3.24	0.22	0.793	0.259
Xanthosine 5--phosphate	363	0.65	0.164	0.252	0.439	0.352	0.394
Orotidine 5-phosphate	367	0.528	26.1	49.4	0.358	0.202	0.112
Sedoheptoluse bisphosphate	369	0.565	50.4	89.3	0.504	0.297	0.154
Riboflavin	375	4.06	8.36	2.06	0.00155	0.00122	0.215
dCDP	386	1.79	83.6	46.7	0.391	0.127	0.121
Octoluse Bisphosphate	399	0.267	8.42	31.5	0.281	0.312	0.195
dTDP	401	3.92	37.6	9.61	0.318	0.228	0.179
CDP	402	2.46	1.5	0.61	0.0898	0.264	0.189
UDP	403	1.76	127	72.2	0.348	0.108	0.0291
adenosine 5-phosphosulfate	426	0.43	2	4.65	0.159	0.507	0.00275
ADP	426	3.12	118	37.8	0.0498	0.0311	0.0403
GDP	442	1.94	16.6	8.57	0.384	0.163	0.0843
FMN	455	1.76	29.9	17	0.471	0.165	0.205
dCTP	466	2.55	15.8	6.21	0.577	0.413	0.217
dTTP	481	3.33	12.9	3.89	0.491	0.381	0.45
CTP	482	6.76	21.3	3.16	0.127	0.109	0.249
UTP	483	1.33	23.7	17.8	0.665	0.133	0.184
Taurodeoxycholate	498	1.57	1.89	1.21	0.692	0.607	0.686

Table A-1. continued.

Metabolite	median *m/z*	37 °C/25 °C	37 °C/3 °C	25 °C/3 °C	37 °C/25 °C p value	37 °C/3 °C p value	25 °C/3 °C p value
ATP	506	1.24	36.4	29.3	0.677	0.103	0.0996
UDP-glucose	565	0.878	0.407	0.464	0.608	0.00863	0.0128
UDP-glucuronate	579	0.971	0.685	0.705	0.906	0.212	0.184
ADP-D-glucose	588	71.8	25.8	0.36	0.0743	0.0777	0.0645
guanosine 5-diphosphate-3-diphosphate	596	8.92×10^{10}	8.92×10^{10}	1	0.423	0.423	1
UDP-N-acetyl-D-glucosamine	606	0.805	1.12	1.39	0.488	0.762	0.109
glutathione disulfide	611	7.42	2.79	0.375	0.356	0.473	0.331
NAD+	662	1.26	1.63	1.29	0.434	0.204	0.0622
NADH	664	1.26	11.7	9.32	0.262	0.0205	0.00784
NADP+	742	2.06	16.3	7.91	0.109	0.0357	0.00121
NADPH	744	0.646	54.2	83.9	0.451	0.23	0.0231
FAD	784	1.42	1.54	1.09	0.0365	0.0533	0.671
acetyl-CoA	808	1.11	145	130	0.776	0.0871	0.00285
succinyl-CoA/methylmalonyl-CoA	866	0.336	3.57	10.6	0.152	0.335	0.0875

Table A-2. The fold changes and p values for the metabolites in the heat map for the purH vs wild type study are shown.

Metabolite	median *m/z*	*purH*/WT	p value
S-methyl-5-thioadenosine	296.0818	0.865	0.669
L-arginino-succinate	289.1147	1.09	0.717
D-sedoheptulose-1/7-phosphate	289.0321	1.2	0.555
xanthosine	283.0676	2.88	0.0199
6-phospho-D-gluconate	275.0171	1640	0.067
inosine	267.0729	6.25	0.00644
adenosine	241.8991	0.0281	0.00254
S-ribosyl-L-homocysteine	266.0699	0.607	0.0159
1,3-diphopshateglycerate	264.9514	0.529	0.127
2,3-Diphosphoglyceric acid	264.9514	0.529	0.127
glutathione	306.0758	0.747	0.0211
dUMP	307.0331	51.9	0.0396
Geranyl-PP	313.0603	1.09	0.836
cyclic-AMP	328.0446	0.0675	0.0266
trehalose/sucrose	341.1082	0.978	0.887
Cellobiose	341.1082	0.978	0.887
D-erythrose-4-phosphate	199.0012	0.868	0.801
Acetylcarnitine	203.1172	1.4	0.196
Kynurenine	207.0775	0.831	0.0145
D-glucarate	209.0301	0.865	0.439
deoxyadenosine	250.095	3.49	0.089
deoxyinosine	251.0789	0.126	0.323
glucose-1/6-phosphate	259.0215	0.655	0.0428
NAD+	259.0215	0.949	0.0428
Taurodeoxycholic acid	662.1006	3.04	0.227
UDP-D-glucose	498.2883	1.14	0.215
UDP-D-glucuronate	565.0467	1.05	0.268
ADP-D-glucose	579.0261	0.131	0.448
UDP-N-acetyl-glucosamine	588.0737	1.14	0.00103
glutathione disulfide	606.0734	2.84	0.076
NADH	611.1442	0.748	0.199
cyclic bis(3-->5-) dimeric GMP	664.1169	1.67	0.0581
NADP+	689.0862	3.83	0.121
NADPH	742.0673	3.85	0.000105
FAD	744.0826	0.982	0.0147
acetyl-CoA	784.1494	0.00457	0.779
butyryl-CoA	808.1168	4.61	0.0121

Table A-2 continued.

Metabolite	median *m/z*	*purH*/WT	p value
GMP	836.1508	21.5	0.413
xanthosine-5-phosphate	362.051	3.95	0.363
orotidine-5-phosphate	363.0341	1.78	0.05
riboflavin	367.0177	0.514	0.104
S-adenosyl-L-homoCysteine	375.1302	0.42	0.00266
UDP	383.1131	1.4	0.0954
Cholic acid	402.994	3.55	0.125
adenosine 5-phosphosulfate	407.2802	0.446	0.212
Deoxycholic acid	426.0125	1.1	0.00608
cholesteryl sulfate	448.3061	0.395	0.0781
ornithine	465.3043	1.78	0.387
nicotinamide	131.0823	0.715	0.0657
nicotinate	121.0404	1.71	0.189
taurine	122.0246	0.108	0.0191
thymine	93.00521	0.298	0.338
Pyroglutamic acid	125.0352	0.257	0.319
Citraconic acid	128.0352	0.0795	0.424
N-Acetyl-L-alanine	129.0193	0.0026	0.000107
leucine/isoleucine	130.0507	3.29	0.207
asparagine	130.0873	0.743	0.0000287
Hydroxyisocaproic acid	131.0459	0.645	0.499
aspartate	131.0713	0.692	0.134
malate	132.0302	3.17	0.14
anthranilate	133.0143	0.638	0.00313
p-aminobenzoate	136.04	0.638	0.0000973
p-hydroxybenzoate	136.04	0.368	0.0000973
acetylphosphate	137.0243	0.581	0.0298
Carbamoyl phosphate	138.9799	0.239	0.145
histidinol	139.9753	0.312	0.211
a-ketoglutarate	140.0827	0.661	0.00104
2-oxobutanoate	145.0141	0.647	0.0113
acetoacetate	101.024	0.647	0.598
dimethylglycine	101.024	0.387	0.598
4-aminobutyrate	102.0557	0.387	0.0617
serine	102.0557	0.00192	0.0617
glycerate	104.035	0.943	0.365
uracil	105.0189	7.35	0.878
proline	111.0196	21.5	0.413

Table A-2 continued.

Metabolite	median *m/z*	*purH*/WT	p value
fumarate	114.0556	0.284	0.271
2-keto-isovalerate	115.0034	3.13	0.00174
indole	115.0398	1.86	0.00311
betaine	116.0502	15.1	0.185
valine	116.0714	15.1	0.0000321
Methylmalonic acid	116.0714	0.433	0.0000321
succinate	117.0191	0.433	0.000033
threonine	117.0191	4.31	0.000033
homoserine	118.0505	4.31	0.0000959
D-glyceraldehdye-3-phosphate	118.0505	0.118	0.0000959
arginine	168.9901	0.392	0.000333
Ascorbic acid	173.1045	0.764	0.0262
N-carbamoyl-L-aspartate	175.0249	0.623	0.00465
allantoate	175.0364	1.21	0.436
glucono-Î´-lactone	175.0479	0.0411	0.369
hydroxyphenylpyruvate	177.0408	1.05	0.235
dihydroxy-acetone-phosphate	179.0348	0.118	0.836
3-phosphoglycerate	168.9901	0.325	0.000445
Acetyllysine	184.9865	0.478	0.196
allantoin	187.1085	0.948	0.116
glutamine	157.0368	1.18	0.854
glutamate	145.0616	0.836	0.0981
O-acetyl-L-serine	146.0456	0.931	0.386
2-Hydroxy-2-methylbutanedioic acid	146.0456	0.317	0.46
methionine	147.0298	0.169	0.000000457
xanthine	148.0435	0.87	0.00292
2,3-dihydroxybenzoic acid	137.297	0.663	0.797
dihydroorotate	153.019	1.06	0.0241
Uric acid	157.0252	0.0125	0.792
Pyridoxamine	167.0208	0.00501	0.0177
fructose-1,6-bisphosphate	167.0823	1.96	0.00674
sedoheptulose-bisphosphate	338.9886	8.15	0.107
Octulose-1-phosphate-	368.9979	0.0406	0.0382

Table A-3. The average ion counts plus or minus the standard deviation counts for each metabolite discussed and their isotopomers for the 37 °C experiment for the 0, 2, 5, and 15 minute time points are shown.

Metabolite	labeling pattern	0 min	2 min	5 min	15 min
glucose/fructose-6-phosphate	^{12}C	$1.28 \pm 0.55 \times 10^{6}$	$1.28 \pm 0.8 \times 10^{5}$	$1.54 \pm 0.6 \times 10^{5}$	$9.37 \pm 4.0 \times 10^{4}$
glucose/fructose-6-phosphate	$^{13}C_1$	$7.09 \pm 3.4 \times 10^{4}$	$0 \pm 0.0 \times 10^{0}$	$0 \pm 0.0 \times 10^{0}$	$0 \pm 0.0 \times 10^{0}$
glucose/fructose-6-phosphate	$^{13}C_2$	$0 \pm 0.0 \times 10^{0}$	$0 \pm 0.0 \times 10^{0}$	$0 \pm 0.0 \times 10^{0}$	$0 \pm 0.0 \times 10^{0}$
glucose/fructose-6-phosphate	$^{13}C_3$	$0 \pm 0.0 \times 10^{0}$	$0 \pm 0.0 \times 10^{0}$	$0 \pm 0.0 \times 10^{0}$	$0 \pm 0.0 \times 10^{0}$
glucose/fructose-6-phosphate	$^{13}C_4$	$0 \pm 0.0 \times 10^{0}$	$0 \pm 0.0 \times 10^{0}$	$0 \pm 0.0 \times 10^{0}$	$0 \pm 0.0 \times 10^{0}$
glucose/fructose-6-phosphate	$^{13}C_5$	$0 \pm 0.0 \times 10^{0}$	$2.79 \pm 4.8 \times 10^{4}$	$6.15 \pm 2.0 \times 10^{4}$	$4.41 \pm 3.8 \times 10^{4}$
glucose/fructose-6-phosphate	$^{13}C_6$	$0 \pm 0.0 \times 10^{0}$	$9.47 \pm 8.9 \times 10^{5}$	$1.52 \pm 0.6 \times 10^{6}$	$1.07 \pm 0.9 \times 10^{6}$
fructose-1-6-bisphosphate	^{12}C	$2.52 \pm 1.2 \times 10^{6}$	$4.40 \pm 2.2 \times 10^{4}$	$4.88 \pm 2.4 \times 10^{4}$	$5.59 \pm 3.4 \times 10^{4}$
fructose-1-6-bisphosphate	$^{13}C_1$	$1.37 \pm 0.69 \times 10^{5}$	$2.70 \pm 2.3 \times 10^{3}$	$1.72 \pm 1.0 \times 10^{3}$	$2.52 \pm 1.8 \times 10^{3}$
fructose-1-6-bisphosphate	$^{13}C_2$	$4.39 \pm 2.0 \times 10^{4}$	$1.88 \pm 1.5 \times 10^{3}$	$1.86 \pm 1.0 \times 10^{3}$	$1.09 \pm 0.2 \times 10^{3}$
fructose-1-6-bisphosphate	$^{13}C_3$	$1.62 \pm 0.9 \times 10^{3}$	$5.18 \pm 2.5 \times 10^{4}$	$4.28 \pm 2.0 \times 10^{4}$	$1.48 \pm 0.2 \times 10^{4}$
fructose-1-6-bisphosphate	$^{13}C_4$	$3.08 \pm 4.3 \times 10^{2}$	$1.24 \pm 0.8 \times 10^{4}$	$1.29 \pm 0.6 \times 10^{4}$	$4.55 \pm 2.5 \times 10^{3}$
fructose-1-6-bisphosphate	$^{13}C_5$	$9.21 \pm 1.3 \times 10^{3}$	$1.79 \pm 0.5 \times 10^{5}$	$2.07 \pm 0.5 \times 10^{5}$	$1.33 \pm 0.2 \times 10^{5}$
fructose-1-6-bisphosphate	$^{13}C_6$	$1.86 \pm 0.04 \times 10^{5}$	$3.60 \pm 0.9 \times 10^{6}$	$4.44 \pm 1.1 \times 10^{6}$	$2.96 \pm 0.5 \times 10^{6}$
1,3-Diphosphoglyceric acid	^{12}C	$5.44 \pm 1.1 \times 10^{4}$	$8.24 \pm 1.8 \times 10^{2}$	$1.52 \pm 1.0 \times 10^{3}$	$1.80 \pm 1.0 \times 10^{3}$
1,3-Diphosphoglyceric acid	$^{13}C_1$	$0 \pm 0.0 \times 10^{0}$	$0 \pm 0.0 \times 10^{0}$	$0 \pm 0.0 \times 10^{0}$	$0 \pm 0.0 \times 10^{0}$
1,3-Diphosphoglyceric acid	$^{13}C_2$	$0 \pm 0.0 \times 10^{0}$	$0 \pm 0.0 \times 10^{0}$	$0 \pm 0.0 \times 10^{0}$	$0 \pm 0.0 \times 10^{0}$
1,3-Diphosphoglyceric acid	$^{13}C_3$	$0 \pm 0.0 \times 10^{0}$	$0 \pm 0.0 \times 10^{0}$	$0 \pm 0.0 \times 10^{0}$	$0 \pm 0.0 \times 10^{0}$
Pyruvate	^{12}C	$6.06 \pm 5.4 \times 10^{7}$	$7.35 \pm 3.2 \times 10^{6}$	$5.50 \pm 2.3 \times 10^{6}$	$1.10 \pm 0.6 \times 10^{6}$
Pyruvate	$^{13}C_1$	$1.57 \pm 1.1 \times 10^{6}$	$2.79 \pm 1.4 \times 10^{5}$	$1.37 \pm 1.5 \times 10^{5}$	$0 \pm 0.0 \times 10^{0}$
Pyruvate	$^{13}C_2$	$0 \pm 0.0 \times 10^{0}$	$2.03 \pm 0.4 \times 10^{6}$	$2.26 \pm 0.7 \times 10^{6}$	$7.59 \pm 3.1 \times 10^{5}$
Pyruvate	$^{13}C_3$	$0 \pm 0.0 \times 10^{0}$	$4.23 \pm 3.8 \times 10^{7}$	$7.38 \pm 3.1 \times 10^{7}$	$2.80 \pm 1.2 \times 10^{7}$
alpha-ketoglutarate	^{12}C	$8.36 \pm 5.5 \times 10^{6}$	$4.35 \pm 0.5 \times 10^{6}$	$4.35 \pm 0.9 \times 10^{6}$	$1.09 \pm 0.1 \times 10^{6}$
alpha-ketoglutarate	$^{13}C_1$	$4.42 \pm 3.4 \times 10^{5}$	$3.45 \pm 0.9 \times 10^{5}$	$2.47 \pm 1.0 \times 10^{5}$	$4.04 \pm 0.5 \times 10^{4}$
alpha-ketoglutarate	$^{13}C_2$	$1.52 \pm 1.5 \times 10^{3}$	$1.15 \pm 0.4 \times 10^{6}$	$1.13 \pm 0.3 \times 10^{6}$	$4.03 \pm 1.2 \times 10^{5}$
alpha-ketoglutarate	$^{13}C_3$	$0 \pm 0.0 \times 10^{0}$	$1.35 \pm 0.6 \times 10^{6}$	$1.60 \pm 0.4 \times 10^{6}$	$8.29 \pm 0.3 \times 10^{5}$
alpha-ketoglutarate	$^{13}C_4$	$5.45 \pm 4.7 \times 10^{2}$	$7.80 \pm 3.6 \times 10^{5}$	$1.36 \pm 0.3 \times 10^{6}$	$1.19 \pm 0.1 \times 10^{6}$
alpha-ketoglutarate	$^{13}C_5$	$2.32 \pm 2.0 \times 10^{2}$	$1.86 \pm 1.1 \times 10^{6}$	$4.33 \pm 1.0 \times 10^{6}$	$6.65 \pm 0.5 \times 10^{6}$
succinyl-CoA	^{12}C	$3.25 \pm 0.9 \times 10^{4}$	$1.95 \pm 0.4 \times 10^{4}$	$9.56 \pm 5.3 \times 10^{3}$	$9.22 \pm 16.0 \times 10^{2}$
succinyl-CoA	$^{13}C_1$	$0 \pm 0.0 \times 10^{0}$	$0 \pm 0.0 \times 10^{0}$	$0 \pm 0.0 \times 10^{0}$	$0 \pm 0.0 \times 10^{0}$
succinyl-CoA	$^{13}C_2$	$0 \pm 0.0 \times 10^{0}$	$0 \pm 0.0 \times 10^{0}$	$0 \pm 0.0 \times 10^{0}$	$0 \pm 0.0 \times 10^{0}$
succinyl-CoA	$^{13}C_3$	$0 \pm 0.0 \times 10^{0}$	$0 \pm 0.0 \times 10^{0}$	$0 \pm 0.0 \times 10^{0}$	$0 \pm 0.0 \times 10^{0}$
succinyl-CoA	$^{13}C_4$	$0 \pm 0.0 \times 10^{0}$	$0 \pm 0.0 \times 10^{0}$	$0 \pm 0.0 \times 10^{0}$	$0 \pm 0.0 \times 10^{0}$
succinyl-CoA	$^{13}C_5$	$0 \pm 0.0 \times 10^{0}$	$0 \pm 0.0 \times 10^{0}$	$0 \pm 0.0 \times 10^{0}$	$0 \pm 0.0 \times 10^{0}$

Table A-3 continued.

Metabolite	labeling pattern	0 min	2 min	5 min	15 min
succinyl-CoA	$^{13}C_6$	$0 \pm 0.0 \times 10^0$	$0 \pm 0.0 \times 10^0$	$0 \pm 0.0 \times 10^0$	$0 \pm 0.0 \times 10^0$
succinyl-CoA	$^{13}C_7$	$0 \pm 0.0 \times 10^0$	$0 \pm 0.0 \times 10^0$	$0 \pm 0.0 \times 10^0$	$0 \pm 0.0 \times 10^0$
succinyl-CoA	$^{13}C_8$	$0 \pm 0.0 \times 10^0$	$0 \pm 0.0 \times 10^0$	$0 \pm 0.0 \times 10^0$	$0 \pm 0.0 \times 10^0$
succinyl-CoA	$^{13}C_9$	$0 \pm 0.0 \times 10^0$	$0 \pm 0.0 \times 10^0$	$0 \pm 0.0 \times 10^0$	$0 \pm 0.0 \times 10^0$
succinyl-CoA	$^{13}C_{10}$	$0 \pm 0.0 \times 10^0$	$0 \pm 0.0 \times 10^0$	$0 \pm 0.0 \times 10^0$	$0 \pm 0.0 \times 10^0$
succinyl-CoA	$^{13}C_{11}$	$0 \pm 0.0 \times 10^0$	$0 \pm 0.0 \times 10^0$	$0 \pm 0.0 \times 10^0$	$0 \pm 0.0 \times 10^0$
succinyl-CoA	$^{13}C_{12}$	$0 \pm 0.0 \times 10^0$	$0 \pm 0.0 \times 10^0$	$0 \pm 0.0 \times 10^0$	$0 \pm 0.0 \times 10^0$
succinyl-CoA	$^{13}C_{13}$	$0 \pm 0.0 \times 10^0$	$0 \pm 0.0 \times 10^0$	$0 \pm 0.0 \times 10^0$	$0 \pm 0.0 \times 10^0$
succinyl-CoA	$^{13}C_{14}$	$0 \pm 0.0 \times 10^0$	$0 \pm 0.0 \times 10^0$	$0 \pm 0.0 \times 10^0$	$0 \pm 0.0 \times 10^0$
succinyl-CoA	$^{13}C_{15}$	$0 \pm 0.0 \times 10^0$	$0 \pm 0.0 \times 10^0$	$0 \pm 0.0 \times 10^0$	$0 \pm 0.0 \times 10^0$
succinyl-CoA	$^{13}C_{16}$	$0 \pm 0.0 \times 10^0$	$0 \pm 0.0 \times 10^0$	$0 \pm 0.0 \times 10^0$	$0 \pm 0.0 \times 10^0$
succinyl-CoA	$^{13}C_{17}$	$0 \pm 0.0 \times 10^0$	$0 \pm 0.0 \times 10^0$	$0 \pm 0.0 \times 10^0$	$0 \pm 0.0 \times 10^0$
succinyl-CoA	$^{13}C_{18}$	$0 \pm 0.0 \times 10^0$	$0 \pm 0.0 \times 10^0$	$0 \pm 0.0 \times 10^0$	$0 \pm 0.0 \times 10^0$
succinyl-CoA	$^{13}C_{19}$	$0 \pm 0.0 \times 10^0$	$0 \pm 0.0 \times 10^0$	$0 \pm 0.0 \times 10^0$	$0 \pm 0.0 \times 10^0$
succinyl-CoA	$^{13}C_{20}$	$0 \pm 0.0 \times 10^0$	$0 \pm 0.0 \times 10^0$	$0 \pm 0.0 \times 10^0$	$0 \pm 0.0 \times 10^0$
succinyl-CoA	$^{13}C_{21}$	$0 \pm 0.0 \times 10^0$	$0 \pm 0.0 \times 10^0$	$0 \pm 0.0 \times 10^0$	$0 \pm 0.0 \times 10^0$
succinyl-CoA	$^{13}C_{22}$	$0 \pm 0.0 \times 10^0$	$0 \pm 0.0 \times 10^0$	$0 \pm 0.0 \times 10^0$	$0 \pm 0.0 \times 10^0$
succinyl-CoA	$^{13}C_{23}$	$0 \pm 0.0 \times 10^0$	$0 \pm 0.0 \times 10^0$	$0 \pm 0.0 \times 10^0$	$0 \pm 0.0 \times 10^0$
succinyl-CoA	$^{13}C_{24}$	$0 \pm 0.0 \times 10^0$	$0 \pm 0.0 \times 10^0$	$0 \pm 0.0 \times 10^0$	$0 \pm 0.0 \times 10^0$
succinyl-CoA	$^{13}C_{25}$	$0 \pm 0.0 \times 10^0$	$0 \pm 0.0 \times 10^0$	$0 \pm 0.0 \times 10^0$	$0 \pm 0.0 \times 10^0$
Succinate	^{12}C	$1.44 \pm 1.0 \times 10^8$	$6.86 \pm 3.0 \times 10^6$	$3.24 \pm 0.8 \times 10^6$	$1.67 \pm 1.0 \times 10^6$
Succinate	$^{13}C_1$	$6.71 \pm 5.0 \times 10^6$	$7.34 \pm 2.2 \times 10^5$	$5.03 \pm 0.7 \times 10^5$	$2.48 \pm 2.0 \times 10^5$
Succinate	$^{13}C_2$	$3.81 \pm 3.3 \times 10^4$	$3.77 \pm 1.8 \times 10^6$	$3.39 \pm 1.1 \times 10^6$	$1.81 \pm 0.2 \times 10^6$
Succinate	$^{13}C_3$	$0 \pm 0.0 \times 10^0$	$2.20 \pm 1.8 \times 10^6$	$2.10 \pm 0.3 \times 10^6$	$2.86 \pm 1.5 \times 10^6$
Succinate	$^{13}C_4$	$0 \pm 0.0 \times 10^0$	$9.00 \pm 4.9 \times 10^6$	$1.20 \pm 0.1 \times 10^7$	$2.88 \pm 1.1 \times 10^7$
fumarate	^{12}C	$3.57 \pm 1.6 \times 10^6$	$4.16 \pm 1.2 \times 10^5$	$1.61 \pm 0.6 \times 10^5$	$5.72 \pm 5.5 \times 10^4$
fumarate	$^{13}C_1$	$1.42 \pm 0.9 \times 10^5$	$3.61 \pm 1.9 \times 10^4$	$2.04 \pm 0.8 \times 10^4$	$8.72 \pm 1.8 \times 10^3$
fumarate	$^{13}C_2$	$0 \pm 0.0 \times 10^0$	$3.05 \pm 1.6 \times 10^5$	$2.45 \pm 1.1 \times 10^5$	$1.03 \pm 0.2 \times 10^5$
fumarate	$^{13}C_3$	$0 \pm 0.0 \times 10^0$	$4.74 \pm 0.7 \times 10^5$	$3.78 \pm 0.8 \times 10^5$	$4.80 \pm 1.5 \times 10^5$
fumarate	$^{13}C_4$	$0 \pm 0.0 \times 10^0$	$1.37 \pm 0.5 \times 10^6$	$1.55 \pm 0.4 \pm 10^6$	$2.93 \pm 0.5 \times 10^6$
malate	^{12}C	$3.99 \pm 0.3 \times 10^7$	$6.24 \pm 1.9 \times 10^6$	$2.87 \pm 0.6 \times 10^6$	$1.03 \pm 0.4 \times 10^6$
malate	$^{13}C_1$	$1.74 \pm 0.2 \times 10^6$	$9.64 \pm 2.2 \times 10^5$	$6.53 \pm 1.61 \times 10^5$	$2.20 \pm 0.5 \times 10^5$
malate	$^{13}C_2$	$8.86 \pm 2.1 \times 10^3$	$7.74 \pm 1.0 \times 10^6$	$6.67 \pm 1.2 \times 10^6$	$5.97 \pm 0.5 \times 10^6$
malate	$^{13}C_3$	$1.32 \pm 0.2 \times 10^5$	$2.21 \pm 0.6 \times 10^7$	$2.71 \pm 0.6 \times 10^7$	$5.56 \pm 0.4 \times 10^7$
6-phospho-D-gluconate	^{12}C	$9.17 \pm 6.4 \times 10^5$	$3.56 \pm 0.4 \times 10^4$	$3.41 \pm 0.7 \times 10^4$	$2.50 \pm 0.4 \times 10^4$
6-phospho-D-gluconate	$^{13}C_1$	$4.29 \pm 3.1 \times 10^4$	$0 \pm 0.0 \times 10^0$	$0 \pm 0.0 \times 10^0$	$0 \pm 0.0 \times 10^0$

Table A-3 continued.

Metabolite	labeling pattern	0 min	2 min	5 min	15 min
6-phospho-D-gluconate	$^{13}C_2$	$6.36 \pm 11.0 \times 10^3$	$0 \pm 0.0 \times 10^0$	$0 \pm 0.0 \times 10^0$	$0 \pm 0.0 \times 10^0$
6-phospho-D-gluconate	$^{13}C_3$	$0 \pm 0.0 \times 10^0$	$0 \pm 0.0 \times 10^0$	$0 \pm 0.0 \times 10^0$	$0 \pm 0.0 \times 10^0$
6-phospho-D-gluconate	$^{13}C_4$	$0 \pm 0.0 \times 10^0$	$0 \pm 0.0 \times 10^0$	$0 \pm 0.0 \times 10^0$	$0 \pm 0.0 \times 10^0$
6-phospho-D-gluconate	$^{13}C_5$	$0 \pm 0.0 \times 10^0$	$5.04 \pm 4.7 \times 10^4$	$8.82 \pm 1.4 \times 10^4$	$0 \pm 0.0 \times 10^0$
6-phospho-D-gluconate	$^{13}C_6$	$0 \pm 0.0 \times 10^0$	$1.26 \pm 1.1 \times 10^6$	$2.16 \pm 0.3 \times 10^6$	$5.33 \pm 9.2 \times 10^5$
D-xylulose 5-phosphate	^{12}C	$5.54 \pm 9.6 \times 10^1$	$0 \pm 0.0 \times 10^0$	$1.57 \pm 1.4 \times 10^2$	$5.38 \pm 4.6 \times 10^2$
D-xylulose 5-phosphate	$^{13}C_1$	$0 \pm 0.0 \times 10^0$	$0 \pm 0.0 \times 10^0$	$0 \pm 0.0 \times 10^0$	$0 \pm 0.0 \times 10^0$
D-xylulose 5-phosphate	$^{13}C_2$	$0 \pm 0.0 \times 10^0$	$0 \pm 0.0 \times 10^0$	$0 \pm 0.0 \times 10^0$	$0 \pm 0.0 \times 10^0$
D-xylulose 5-phosphate	$^{13}C_3$	$0 \pm 0.0 \times 10^0$	$0 \pm 0.0 \times 10^0$	$0 \pm 0.0 \times 10^0$	$0 \pm 0.0 \times 10^0$
D-xylulose 5-phosphate	$^{13}C_4$	$0 \pm 0.0 \times 10^0$	$0 \pm 0.0 \times 10^0$	$0 \pm 0.0 \times 10^0$	$0 \pm 0.0 \times 10^0$
D-xylulose 5-phosphate	$^{13}C_5$	$0 \pm 0.0 \times 10^0$	$0 \pm 0.0 \times 10^0$	$0 \pm 0.0 \times 10^0$	$0 \pm 0.0 \times 10^0$
D-sedoheptulose-1/7-phosphate	^{12}C	$8.18 \pm 3.6 \times 10^4$	$1.62 \pm 2.9 \times 10^2$	$1.86 \pm 2.2 \times 10^3$	$7.63 \pm 13.2 \times 10^2$
D-sedoheptulose-1/7-phosphate	$^{13}C_1$	$2.17 \pm 0.9 \times 10^3$	$0 \pm 0.0 \times 10^0$	$0.69 \pm 1.2 \times 10^2$	$0 \pm 0.0 \times 10^0$
D-sedoheptulose-1/7-phosphate	$^{13}C_2$	$0 \pm 0.0 \times 10^0$	$0 \pm 0.0 \times 10^0$	$0 \pm 0.0 \times 10^0$	$0 \pm 0.0 \times 10^0$
D-sedoheptulose-1/7-phosphate	$^{13}C_3$	$0 \pm 0.0 \times 10^0$	$0 \pm 0.0 \times 10^0$	$0 \pm 0.0 \times 10^0$	$0 \pm 0.0 \times 10^0$
D-sedoheptulose-1/7-phosphate	$^{13}C_4$	$0 \pm 0.0 \times 10^0$	$0 \pm 0.0 \times 10^0$	$0.59 \pm 1.0 \times 10^3$	$0 \pm 0.0 \times 10^0$
D-sedoheptulose-1/7-phosphate	$^{13}C_5$	$0 \pm 0.0 \times 10^0$	$6.70 \pm 1.2 \times 10^2$	$0 \pm 0.0 \times 10^0$	$0 \pm 0.0 \times 10^0$
D-sedoheptulose-1/7-phosphate	$^{13}C_6$	$0 \pm 0.0 \times 10^0$	$3.65 \pm 4.1 \times 10^3$	$3.20 \pm 3.0 \times 10^3$	$4.34 \pm 5.0 \times 10^3$
D-sedoheptulose-1/7-phosphate	$^{13}C_7$	$0 \pm 0.0 \times 10^0$	$8.00 \pm 7.9 \times 10^4$	$6.40 \pm 9.0 \times 10^4$	$9.85 \pm 7.7 \times 10^4$
glutamate	^{12}C	$1.98 \pm 1.3 \times 10^7$	$1.19 \pm 0.3 \times 10^7$	$5.12 \pm 1.2 \times 10^6$	$4.63 \pm 3.5 \times 10^5$
glutamate	$^{13}C_1$	$1.08 \pm 0.7 \times 10^6$	$1.21 \pm 0.002 \times 10^6$	$7.66 \pm 0.7 \times 10^5$	$6.79 \pm 5.4 \times 10^4$
glutamate	$^{13}C_2$	$4.38 \pm 2.8 \times 10^3$	$5.43 \pm 0.2 \times 10^6$	$4.56 \pm 0.7 \times 10^6$	$8.22 \pm 5.2 \times 10^5$
glutamate	$^{13}C_3$	$2.70 \pm 3.1 \times 10^3$	$5.80 \pm 1.2 \times 10^6$	$6.08 \pm 0.4 \times 10^6$	$2.40 \pm 1.7 \times 10^6$
glutamate	$^{13}C_4$	$2.07 \pm 0.2 \times 10^3$	$3.65 \pm 0.9 \times 10^6$	$5.86 \pm 0.3 \times 10^6$	$3.94 \pm 2.6 \times 10^6$
glutamate	$^{13}C_5$	$1.23 \pm 0.4 \times 10^4$	$8.38 \pm 3.0 \times 10^6$	$1.87 \pm 0.009 \times 10^7$	$2.31 \pm 1.6 \times 10^7$
glutamine	^{12}C	$1.49 \pm 1.24 \times 10^6$	$1.12 \pm 0.1 \times 10^6$	$3.03 \pm 1.5 \times 10^5$	$2.00 \pm 0.5 \times 10^4$
glutamine	$^{13}C_1$	$2.67 \pm 2.0 \times 10^4$	$3.73 \pm 0.2 \times 10^4$	$1.68 \pm 0.6 \times 10^4$	$3.14 \pm 0.5 \times 10^3$
glutamine	$^{13}C_2$	$2.71 \pm 4.7 \times 10^2$	$3.90 \pm 0.7 \times 10^5$	$2.46 \pm 1.2 \times 10^5$	$2.18 \pm 0.4 \times 10^4$
glutamine	$^{13}C_3$	$1.95 \pm 1.7 \times 10^2$	$4.15 \pm 1.6 \times 10^5$	$4.17 \pm 1.7 \times 10^5$	$8.51 \pm 2.0 \times 10^4$
glutamine	$^{13}C_4$	$1.13 \pm 2.0 \times 10^2$	$2.42 \pm 1.3 \times 10^5$	$3.75 \pm 1.3 \times 10^5$	$2.06 \pm 0.2 \times 10^5$
glutamine	$^{13}C_5$	$1.72 \pm 1.0 \times 10^3$	$7.20 \pm 3.6 \times 10^5$	$1.50 \pm 0.3 \times 10^6$	$1.98 \pm 0.3 \times 10^6$
aspartate	^{12}C	$1.50 \pm 0.8 \times 10^6$	$4.85 \pm 1.0 \times 10^5$	$1.77 \pm 0.7 \times 10^5$	$8.99 \pm 4.8 \times 10^4$

Table A-3 continued.

Metabolite	labeling pattern	0 min	2 min	5 min	15 min
aspartate	$^{13}C_1$	$2.17 \pm 1.2 \times 10^4$	$2.80 \pm 0.6 \times 10^4$	$1.79 \pm 0.5 \times 10^4$	$6.09 \pm 10.6 \times 10^3$
aspartate	$^{13}C_2$	$0 \pm 0.0 \times 10^0$	$1.81 \pm 1.3 \times 10^5$	$1.67 \pm 0.9 \times 10^5$	$0 \pm 0.0 \times 10^0$
aspartate	$^{13}C_3$	$0 \pm 0.0 \times 10^0$	$5.29 \pm 0.7 \times 10^5$	$3.93 \pm 1.2 \times 10^5$	$0 \pm 0.0 \times 10^0$
aspartate	$^{13}C_4$	$0 \pm 0.0 \times 10^0$	$1.38 \pm 0.4 \times 10^6$	$1.43 \pm 0.5 \times 10^6$	$8.70 \pm 15.1 \times 10^5$
leucine/isoleucine	^{12}C	$4.34 \pm 1.8 \times 10^5$	$1.94 \pm 0.7 \times 10^4$	$1.68 \pm 0.5 \times 10^4$	$2.61 \pm 2.2 \times 10^4$
leucine/isoleucine	$^{13}C_1$	$8.26 \pm 3.0 \times 10^3$	$0 \pm 0.0 \times 10^0$	$0 \pm 0.0 \times 10^0$	$8.74 \pm 15.1 \times 10^2$
leucine/isoleucine	$^{13}C_2$	$0 \pm 0.0 \times 10^0$	$2.79 \pm 0.9 \times 10^4$	$1.55 \pm 0.6 \times 10^4$	$5.98 \pm 5.3 \times 10^3$
leucine/isoleucine	$^{13}C_3$	$0 \pm 0.0 \times 10^0$	$2.06 \pm 3.6 \times 10^3$	$2.17 \pm 3.8 \times 10^3$	$5.77 \pm 10.0 \times 10^2$
leucine/isoleucine	$^{13}C_4$	$0 \pm 0.0 \times 10^0$	$1.83 \pm 0.9 \times 10^4$	$1.85 \pm 0.8 \times 10^4$	$6.91 \pm 6.2 \times 10^3$
leucine/isoleucine	$^{13}C_5$	$0 \pm 0.0 \times 10^0$	$2.38 \pm 2.12 \times 10^4$	$3.23 \pm 1.4 \times 10^4$	$1.80 \pm 1.7 \times 10^4$
leucine/isoleucine	$^{13}C_6$	$0 \pm 0.0 \times 10^0$	$1.57 \pm 1.2 \times 10^5$	$2.68 \pm 0.7 \times 10^5$	$2.54 \pm 2.3 \times 10^5$
alanine	^{12}C	$5.92 \pm 2.2 \times 10^5$	$2.51 \pm 2.7 \times 10^4$	$7.46 \pm 6.5 \times 10^3$	$2.81 \pm 2.7 \times 10^3$
alanine	$^{13}C_1$	$6.75 \pm 12.0 \times 10^2$	$0 \pm 0.0 \times 10^0$	$0 \pm 0.0 \times 10^0$	$0 \pm 0.0 \times 10^0$
alanine	$^{13}C_2$	$0 \pm 0.0 \times 10^0$	$0 \pm 0.0 \times 10^0$	$0 \pm 0.0 \times 10^0$	$0 \pm 0.0 \times 10^0$
alanine	$^{13}C_3$	$0 \pm 0.0 \times 10^0$	$3.53 \pm 0.6 \times 10^5$	$4.39 \pm 0.6 \times 10^5$	$1.76 \pm 3.0 \times 10^5$
L-Valine	^{12}C	$5.38 \pm 1.7 \times 10^6$	$1.70 \pm 0.1 \times 10^6$	$5.62 \pm 1.1 \times 10^5$	$1.79 \pm 1.3 \times 10^5$
L-Valine	$^{13}C_1$	$2.82 \pm 1.1 \times 10^5$	$7.84 \pm 1.1 \times 10^4$	$1.67 \pm 0.5 \times 10^4$	$3.84 \pm 3.6 \times 10^3$
L-Valine	$^{13}C_2$	$1.68 \pm 1.6 \times 10^3$	$2.31 \pm 0.4 \times 10^5$	$1.44 \pm 0.03 \times 10^5$	$5.50 \pm 7.3 \times 10^4$
L-Valine	$^{13}C_3$	$0 \pm 0.0 \times 10^0$	$2.60 \pm 0.4 \times 10^5$	$1.69 \pm 0.07 \times 10^5$	$6.13 \pm 7.8 \times 10^4$
L-Valine	$^{13}C_4$	$0 \pm 0.0 \times 10^0$	$1.48 \pm 0.7 \times 10^5$	$1.72 \pm 0.2 \times 10^5$	$1.42 \pm 1.5 \times 10^5$
L-Valine	$^{13}C_5$	$0 \pm 0.0 \times 10^0$	$2.98 \pm 1.0 \times 10^6$	$3.29 \pm 0.2 \times 10^6$	$3.04 \pm 2.8 \times 10^6$

Table A-4. The average ion counts plus or minus the standard deviation for the metabolites discussed and their isotopomers are displayed for the 37 °C experiment at 30, 60, and 120 minutes.

Metabolite	labeling pattern	30 min	60 min	120 min
glucose/fructose-6-phosphate	^{12}C	$9.90 \pm 2.0 \times 10^4$	$7.62 \pm 0.7 \times 10^4$	$5.90 \pm 2.3 \times 10^4$
glucose/fructose-6-phosphate	$^{13}C_1$	$0 \pm 0.0 \times 10^0$	$0 \pm 0.0 \times 10^0$	$0 \pm 0.0 \times 10^0$
glucose/fructose-6-phosphate	$^{13}C_2$	$0 \pm 0.0 \times 10^0$	$0 \pm 0.0 \times 10^0$	$0 \pm 0.0 \times 10^0$
glucose/fructose-6-phosphate	$^{13}C_3$	$0 \pm 0.0 \times 10^0$	$0 \pm 0.0 \times 10^0$	$0 \pm 0.0 \times 10^0$
glucose/fructose-6-phosphate	$^{13}C_4$	$0 \pm 0.0 \times 10^0$	$0 \pm 0.0 \times 10^0$	$0 \pm 0.0 \times 10^0$
glucose/fructose-6-phosphate	$^{13}C_5$	$1.94 \pm 3.4 \times 10^4$	$0 \pm 0.0 \times 10^0$	$0 \pm 0.0 \times 10^0$
glucose/fructose-6-phosphate	$^{13}C_6$	$1.31 \pm 0.002 \times 10^6$	$5.24 \pm 9.1 \times 10^5$	$0 \pm 0.0 \times 10^0$
fructose-1-6-bisphosphate	^{12}C	$1.13 \pm 1.6 \times 10^5$	$2.32 \pm 1.6 \times 10^4$	$8.17 \pm 9.6 \times 10^4$
fructose-1-6-bisphosphate	$^{13}C_1$	$4.99 \pm 7.1 \times 10^3$	$1.81 \pm 0.8 \times 10^3$	$3.42 \pm 5.2 \times 10^3$
fructose-1-6-bisphosphate	$^{13}C_2$	$7.59 \pm 13.1 \times 10^2$	$8.58 \pm 7.5 \times 10^2$	$1.84 \pm 1.6 \times 10^3$
fructose-1-6-bisphosphate	$^{13}C_3$	$1.13 \pm 0.6 \times 10^4$	$6.05 \pm 1.2 \times 10^3$	$3.31 \pm 2.6 \times 10^3$
fructose-1-6-bisphosphate	$^{13}C_4$	$3.36 \pm 0.3 \times 10^3$	$1.96 \pm 0.4 \times 10^3$	$1.78 \pm 1.4 \times 10^3$
fructose-1-6-bisphosphate	$^{13}C_5$	$1.11 \pm 0.1 \times 10^5$	$7.12 \pm 2.7 \times 10^4$	$3.92 \pm 3.1 \times 10^4$
fructose-1-6-bisphosphate	$^{13}C_6$	$2.74 \pm 0.5 \times 10^6$	$1.59 \pm 0.6 \times 10^6$	$8.61 \pm 7.6 \times 10^5$
1,3-Diphosphoglyceric acid	^{12}C	$2.54 \pm 1.4 \times 10^3$	$2.90 \pm 2.7 \times 10^3$	$1.17 \pm 0.7 \times 10^3$
1,3-Diphosphoglyceric acid	$^{13}C_1$	$0 \pm 0.0 \times 10^0$	$0 \pm 0.0 \times 10^0$	$0 \pm 0.0 \times 10^0$
1,3-Diphosphoglyceric acid	$^{13}C_2$	$0 \pm 0.0 \times 10^0$	$0 \pm 0.0 \times 10^0$	$0 \pm 0.0 \times 10^0$
1,3-Diphosphoglyceric acid	$^{13}C_3$	$0 \pm 0.0 \times 10^0$	$0 \pm 0.0 \times 10^0$	$0 \pm 0.0 \times 10^0$
Pyruvate	^{12}C	$4.53 \pm 1.3 \times 10^5$	$1.32 \pm 1.2 \times 10^5$	$1.47 \pm 1.0 \times 10^5$
Pyruvate	$^{13}C_1$	$0 \pm 0.0 \times 10^0$	$0 \pm 0.0 \times 10^0$	$0 \pm 0.0 \times 10^0$
Pyruvate	$^{13}C_2$	$1.38 \pm 0.9 \times 10^5$	$1.20 \pm 1.05 \times 10^4$	$0 \pm 0.0 \times 10^0$
Pyruvate	$^{13}C_3$	$7.45 \pm 2.6 \times 10^6$	$1.64 \pm 1.42 \times 10^6$	$1.55 \pm 1.4 \times 10^6$
alpha-ketoglutarate	^{12}C	$6.86 \pm 0.8 \times 10^5$	$3.55 \pm 0.5 \times 10^5$	$1.42 \pm 0.5 \times 10^5$
alpha-ketoglutarate	$^{13}C_1$	$2.08 \pm 0.4 \times 10^4$	$8.92 \pm 1.1 \times 10^3$	$4.40 \pm 2.2 \times 10^3$
alpha-ketoglutarate	$^{13}C_2$	$1.59 \pm 0.5 \times 10^5$	$5.21 \pm 1.3 \times 10^4$	$1.43 \pm 0.3 \times 10^4$
alpha-ketoglutarate	$^{13}C_3$	$4.85 \pm 0.6 \times 10^5$	$2.34 \pm 0.5 \times 10^5$	$8.86 \pm 4.4 \times 10^4$
alpha-ketoglutarate	$^{13}C_4$	$7.80 \pm 1.0 \times 10^5$	$5.26 \pm 0.7 \times 10^5$	$3.98 \pm 1.5 \times 10^5$
alpha-ketoglutarate	$^{13}C_5$	$5.27 \pm 0.5 \times 10^6$	$3.98 \pm 0.6 \times 10^6$	$3.35 \pm 1.2 \times 10^6$
succinyl-CoA	^{12}C	$2.50 \pm 1.4 \times 10^3$	$6.62 \pm 11.5 \times 10^2$	$7.17 \pm 4.9 \times 10^3$
succinyl-CoA	$^{13}C_1$	$0 \pm 0.0 \times 10^0$	$0 \pm 0.0 \times 10^0$	$0 \pm 0.0 \times 10^0$
succinyl-CoA	$^{13}C_2$	$0 \pm 0.0 \times 10^0$	$0 \pm 0.0 \times 10^0$	$0 \pm 0.0 \times 10^0$
succinyl-CoA	$^{13}C_3$	$0 \pm 0.0 \times 10^0$	$0 \pm 0.0 \times 10^0$	$0 \pm 0.0 \times 10^0$
succinyl-CoA	$^{13}C_4$	$0 \pm 0.0 \times 10^0$	$0 \pm 0.0 \times 10^0$	$0 \pm 0.0 \times 10^0$
succinyl-CoA	$^{13}C_5$	$0 \pm 0.0 \times 10^0$	$0 \pm 0.0 \times 10^0$	$0 \pm 0.0 \times 10^0$
succinyl-CoA	$^{13}C_6$	$0 \pm 0.0 \times 10^0$	$0 \pm 0.0 \times 10^0$	$0 \pm 0.0 \times 10^0$
succinyl-CoA	$^{13}C_7$	$0 \pm 0.0 \times 10^0$	$0 \pm 0.0 \times 10^0$	$0 \pm 0.0 \times 10^0$
succinyl-CoA	$^{13}C_8$	$0 \pm 0.0 \times 10^0$	$0 \pm 0.0 \times 10^0$	$0 \pm 0.0 \times 10^0$

Table A-4 continued.

Metabolite	labeling pattern	30 min	60 min	120 min
succinyl-CoA	$^{13}C_9$	$0 \pm 0.0 \times 10^0$	$0 \pm 0.0 \times 10^0$	$0 \pm 0.0 \times 10^0$
succinyl-CoA	$^{13}C_{10}$	$0 \pm 0.0 \times 10^0$	$0 \pm 0.0 \times 10^0$	$0 \pm 0.0 \times 10^0$
succinyl-CoA	$^{13}C_{11}$	$0 \pm 0.0 \times 10^0$	$0 \pm 0.0 \times 10^0$	$0 \pm 0.0 \times 10^0$
succinyl-CoA	$^{13}C_{12}$	$0 \pm 0.0 \times 10^0$	$0 \pm 0.0 \times 10^0$	$0 \pm 0.0 \times 10^0$
succinyl-CoA	$^{13}C_{13}$	$0 \pm 0.0 \times 10^0$	$0 \pm 0.0 \times 10^0$	$0 \pm 0.0 \times 10^0$
succinyl-CoA	$^{13}C_{14}$	$0 \pm 0.0 \times 10^0$	$0 \pm 0.0 \times 10^0$	$0 \pm 0.0 \times 10^0$
succinyl-CoA	$^{13}C_{15}$	$0 \pm 0.0 \times 10^0$	$0 \pm 0.0 \times 10^0$	$0 \pm 0.0 \times 10^0$
succinyl-CoA	$^{13}C_{16}$	$0 \pm 0.0 \times 10^0$	$0 \pm 0.0 \times 10^0$	$0 \pm 0.0 \times 10^0$
succinyl-CoA	$^{13}C_{17}$	$0 \pm 0.0 \times 10^0$	$6.17 \pm 10.7 \times 10^2$	$0 \pm 0.0 \times 10^0$
succinyl-CoA	$^{13}C_{18}$	$0 \pm 0.0 \times 10^0$	$0 \pm 0.0 \times 10^0$	$0 \pm 0.0 \times 10^0$
succinyl-CoA	$^{13}C_{19}$	$0 \pm 0.0 \times 10^0$	$0 \pm 0.0 \times 10^0$	$0 \pm 0.0 \times 10^0$
succinyl-CoA	$^{13}C_{20}$	$0 \pm 0.0 \times 10^0$	$0 \pm 0.0 \times 10^0$	$0 \pm 0.0 \times 10^0$
succinyl-CoA	$^{13}C_{21}$	$0 \pm 0.0 \times 10^0$	$0 \pm 0.0 \times 10^0$	$0 \pm 0.0 \times 10^0$
succinyl-CoA	$^{13}C_{22}$	$0 \pm 0.0 \times 10^0$	$0 \pm 0.0 \times 10^0$	$0 \pm 0.0 \times 10^0$
succinyl-CoA	$^{13}C_{23}$	$0 \pm 0.0 \times 10^0$	$0 \pm 0.0 \times 10^0$	$0 \pm 0.0 \times 10^0$
succinyl-CoA	$^{13}C_{24}$	$0 \pm 0.0 \times 10^0$	$0 \pm 0.0 \times 10^0$	$0 \pm 0.0 \times 10^0$
succinyl-CoA	$^{13}C_{25}$	$0 \pm 0.0 \times 10^0$	$0 \pm 0.0 \times 10^0$	$0 \pm 0.0 \times 10^0$
Succinate	^{12}C	$1.08 \pm 0.008 \times 10^6$	$1.22 \pm 0.7 \times 10^6$	$6.63 \pm 2.5 \times 10^5$
Succinate	$^{13}C_1$	$1.28 \pm 0.6 \times 10^5$	$2.06 \pm 2.4 \times 10^5$	$2.05 \pm 2.9 \times 10^5$
Succinate	$^{13}C_2$	$1.48 \pm 0.09 \times 10^6$	$1.46 \pm 0.2 \times 10^6$	$9.85 \pm 1.5 \times 10^5$
Succinate	$^{13}C_3$	$2.10 \pm 0.5 \times 10^6$	$4.57 \pm 4.5 \times 10^6$	$3.80 \pm 3.6 \times 10^6$
Succinate	$^{13}C_4$	$2.67 \pm 0.3 \times 10^7$	$6.66 \pm 6.3 \times 10^7$	$5.60 \pm 4.7 \times 10^7$
fumarate	^{12}C	$1.98 \pm 0.2 \times 10^4$	$2.46 \pm 1.8 \times 10^4$	$1.14 \pm 0.007 \times 10^4$
fumarate	$^{13}C_1$	$6.75 \pm 0.6 \times 10^3$	$5.24 \pm 5.4 \times 10^3$	$0 \pm 0.0 \times 10^0$
fumarate	$^{13}C_2$	$5.72 \pm 1.0 \times 10^4$	$4.20 \pm 0.3 \times 10^4$	$1.12 \pm 1.0 \times 10^4$
fumarate	$^{13}C_3$	$3.09 \pm 0.3 \times 10^5$	$3.38 \pm 0.9 \times 10^5$	$2.09 \pm 0.4 \times 10^5$
fumarate	$^{13}C_4$	$2.61 \pm 0.2 \times 10^6$	$3.12 \pm 1.2 \times 10^6$	$2.22 \pm 0.3 \times 10^6$
malate	^{12}C	$6.20 \pm 0.2 \times 10^5$	$6.85 \pm 3.6 \times 10^5$	$2.88 \pm 2.8 \times 10^5$
malate	$^{13}C_1$	$1.65 \pm 0.2 \times 10^5$	$1.10 \pm 0.2 \times 10^5$	$8.55 \pm 2.1 \times 10^4$
malate	$^{13}C_2$	$4.39 \pm 0.5 \times 10^6$	$3.95 \pm 0.005 \times 10^6$	$3.08 \pm 1.9 \times 10^6$
malate	$^{13}C_3$	$3.38 \pm 0.3 \times 10^7$	$3.24 \pm 0.4 \times 10^7$	$2.79 \pm 0.009 \times 10^7$
6-phospho-D-gluconate	^{12}C	$2.63 \pm 0.1 \times 10^4$	$2.65 \pm 0.5 \times 10^4$	$4.12 \pm 2.0 \times 10^4$
6-phospho-D-gluconate	$^{13}C_1$	$0 \pm 0.0 \times 10^0$	$0 \pm 0.0 \times 10^0$	$0 \pm 0.0 \times 10^0$
6-phospho-D-gluconate	$^{13}C_2$	$0 \pm 0.0 \times 10^0$	$0 \pm 0.0 \times 10^0$	$0 \pm 0.0 \times 10^0$
6-phospho-D-gluconate	$^{13}C_3$	$0 \pm 0.0 \times 10^0$	$0 \pm 0.0 \times 10^0$	$0 \pm 0.0 \times 10^0$
6-phospho-D-gluconate	$^{13}C_4$	$0 \pm 0.0 \times 10^0$	$0 \pm 0.0 \times 10^0$	$0 \pm 0.0 \times 10^0$
6-phospho-D-gluconate	$^{13}C_5$	$0 \pm 0.0 \times 10^0$	$0 \pm 0.0 \times 10^0$	$0 \pm 0.0 \times 10^0$
6-phospho-D-gluconate	$^{13}C_6$	$0 \pm 0.0 \times 10^0$	$0 \pm 0.0 \times 10^0$	$0 \pm 0.0 \times 10^0$

Table A-4 continued.

Metabolite	labeling pattern	30 min	60 min	120 min
D-xylulose 5-phosphate	^{12}C	$9.37 \pm 0.3 \times 10^{2}$	$7.40 \pm 6.6 \times 10^{2}$	$9.75 \pm 2.03 \times 10^{2}$
D-xylulose 5-phosphate	$^{13}C_1$	$0 \pm 0.0 \times 10^{0}$	$0 \pm 0.0 \times 10^{0}$	$0 \pm 0.0 \times 10^{0}$
D-xylulose 5-phosphate	$^{13}C_2$	$0 \pm 0.0 \times 10^{0}$	$0 \pm 0.0 \times 10^{0}$	$0 \pm 0.0 \times 10^{0}$
D-xylulose 5-phosphate	$^{13}C_3$	$0 \pm 0.0 \times 10^{0}$	$0 \pm 0.0 \times 10^{0}$	$0 \pm 0.0 \times 10^{0}$
D-xylulose 5-phosphate	$^{13}C_4$	$0 \pm 0.0 \times 10^{0}$	$0 \pm 0.0 \times 10^{0}$	$0 \pm 0.0 \times 10^{0}$
D-xylulose 5-phosphate	$^{13}C_5$	$0 \pm 0.0 \times 10^{0}$	$0 \pm 0.0 \times 10^{0}$	$0 \pm 0.0 \times 10^{0}$
D-sedoheptulose-1/7-phosphate	^{12}C	$1.75 \pm 2.4 \times 10^{3}$	$0 \pm 0.0 \times 10^{0}$	$1.05 \pm 1.8 \times 10^{2}$
D-sedoheptulose-1/7-phosphate	$^{13}C_1$	$0 \pm 0.0 \times 10^{0}$	$0 \pm 0.0 \times 10^{0}$	$0 \pm 0.0 \times 10^{0}$
D-sedoheptulose-1/7-phosphate	$^{13}C_2$	$0 \pm 0.0 \times 10^{0}$	$0 \pm 0.0 \times 10^{0}$	$0 \pm 0.0 \times 10^{0}$
D-sedoheptulose-1/7-phosphate	$^{13}C_3$	$0 \pm 0.0 \times 10^{0}$	$0 \pm 0.0 \times 10^{0}$	$0 \pm 0.0 \times 10^{0}$
D-sedoheptulose-1/7-phosphate	$^{13}C_4$	$0 \pm 0.0 \times 10^{0}$	$0 \pm 0.0 \times 10^{0}$	$0 \pm 0.0 \times 10^{0}$
D-sedoheptulose-1/7-phosphate	$^{13}C_5$	$0 \pm 0.0 \times 10^{0}$	$0 \pm 0.0 \times 10^{0}$	$0 \pm 0.0 \times 10^{0}$
D-sedoheptulose-1/7-phosphate	$^{13}C_6$	$3.87 \pm 6.7 \times 10^{3}$	$8.62 \pm 14.9 \times 10^{2}$	$6.82 \pm 11.8 \times 10^{2}$
D-sedoheptulose-1/7-phosphate	$^{13}C_7$	$3.15 \pm 5.5 \times 10^{4}$	$5.26 \pm 1.8 \times 10^{3}$	$2.92 \pm 3.0 \times 10^{3}$
glutamate	^{12}C	$5.54 \pm 2.4 \times 10^{5}$	$4.69 \pm 1.4 \times 10^{5}$	$2.63 \pm 0.6 \times 10^{5}$
glutamate	$^{13}C_1$	$7.46 \pm 4.4 \times 10^{4}$	$4.13 \pm 1.5 \times 10^{4}$	$2.42 \pm 1.2 \times 10^{4}$
glutamate	$^{13}C_2$	$8.09 \pm 1.0 \times 10^{5}$	$8.71 \pm 3.0 \times 10^{5}$	$5.35 \pm 2.6 \times 10^{5}$
glutamate	$^{13}C_3$	$2.39 \pm 0.2 \times 10^{6}$	$2.10 \pm 0.9 \times 10^{6}$	$1.91 \pm 1.0 \times 10^{6}$
glutamate	$^{13}C_4$	$4.37 \pm 0.4 \times 10^{6}$	$4.43 \pm 1.7 \times 10^{6}$	$4.39 \pm 2.2 \times 10^{6}$
glutamate	$^{13}C_5$	$2.88 \pm 0.3 \times 10^{7}$	$3.27 \pm 0.8 \times 10^{7}$	$3.53 \pm 1.2 \times 10^{7}$
glutamine	^{12}C	$1.79 \pm 0.6 \times 10^{4}$	$2.11 \pm 0.7 \times 10^{4}$	$1.21 \pm 0.6 \times 10^{4}$
glutamine	$^{13}C_1$	$2.49 \pm 2.4 \times 10^{3}$	$1.83 \pm 1.3 \times 10^{3}$	$7.64 \pm 8.4 \times 10^{2}$
glutamine	$^{13}C_2$	$1.28 \pm 0.4 \times 10^{4}$	$9.80 \pm 2.9 \times 10^{3}$	$6.93 \pm 3.6 \times 10^{3}$
glutamine	$^{13}C_3$	$4.66 \pm 0.6 \times 10^{4}$	$3.03 \pm 1.3 \times 10^{4}$	$2.83 \pm 1.6 \times 10^{4}$
glutamine	$^{13}C_4$	$1.51 \pm 0.2 \times 10^{5}$	$1.18 \pm 0.5 \times 10^{5}$	$1.21 \pm 0.8 \times 10^{5}$
glutamine	$^{13}C_5$	$1.74 \pm 0.1 \times 10^{6}$	$1.53 \pm 0.3 \times 10^{6}$	$1.54 \pm 0.7 \times 10^{6}$
aspartate	^{12}C	$1.32 \pm 0.7 \times 10^{5}$	$9.10 \pm 4.1 \times 10^{4}$	$8.14 \pm 4.3 \times 10^{4}$
aspartate	$^{13}C_1$	$1.43 \pm 1.4 \times 10^{4}$	$3.13 \pm 5.4 \times 10^{3}$	$0 \pm 0.0 \times 10^{0}$
aspartate	$^{13}C_2$	$3.63 \pm 6.3 \times 10^{4}$	$0 \pm 0.0 \times 10^{0}$	$0 \pm 0.0 \times 10^{0}$
aspartate	$^{13}C_3$	$1.42 \pm 2.45 \times 10^{5}$	$0 \pm 0.0 \times 10^{0}$	$0 \pm 0.0 \times 10^{0}$
aspartate	$^{13}C_4$	$9.28 \pm 16.1 \times 10^{5}$	$0 \pm 0.0 \times 10^{0}$	$0 \pm 0.0 \times 10^{0}$
leucine/isoleucine	^{12}C	$9.23 \pm 6.6 \times 10^{4}$	$2.20 \pm 1.4 \times 10^{5}$	$4.49 \pm 3.8 \times 10^{5}$
leucine/isoleucine	$^{13}C_1$	$3.04 \pm 1.4 \times 10^{3}$	$6.03 \pm 2.1 \times 10^{3}$	$1.24 \pm 1.1 \times 10^{4}$
leucine/isoleucine	$^{13}C_2$	$7.71 \pm 0.9 \times 10^{3}$	$1.56 \pm 0.7 \times 10^{4}$	$3.13 \pm 2.3 \times 10^{4}$
leucine/isoleucine	$^{13}C_3$	$1.21 \pm 1.0 \times 10^{3}$	$0 \pm 0.0 \times 10^{0}$	$0 \pm 0.0 \times 10^{0}$
leucine/isoleucine	$^{13}C_4$	$9.97 \pm 1.8 \times 10^{3}$	$2.16 \pm 1.3 \times 10^{4}$	$1.09 \pm 0.9 \times 10^{5}$
leucine/isoleucine	$^{13}C_5$	$2.15 \pm 0.1 \times 10^{4}$	$3.40 \pm 1.7 \times 10^{4}$	$1.58 \pm 1.2 \times 10^{5}$
leucine/isoleucine	$^{13}C_6$	$3.30 \pm 0.2 \times 10^{5}$	$5.06 \pm 1.6 \times 10^{5}$	$9.87 \pm 6.2 \times 10^{5}$

Table A-4 continued.

Metabolite	labeling pattern	30 min	60 min	120 min
alanine	^{12}C	$9.57 \pm 16.6 \times 10^{2}$	$9.11 \pm 15.8 \times 10^{2}$	$2.37 \pm 2.5 \times 10^{3}$
alanine	$^{13}C_1$	$0 \pm 0.0 \times 10^{0}$	$0 \pm 0.0 \times 10^{0}$	$0 \pm 0.0 \times 10^{0}$
alanine	$^{13}C_2$	$0 \pm 0.0 \times 10^{0}$	$0 \pm 0.0 \times 10^{0}$	$0 \pm 0.0 \times 10^{0}$
alanine	$^{13}C_3$	$0 \pm 0.0 \times 10^{0}$	$4.13 \pm 7.2 \times 10^{4}$	$7.96 \pm 12.1 \times 10^{4}$
L-Valine	^{12}C	$1.85 \pm 2.1 \times 10^{5}$	$3.40 \pm 2.6 \times 10^{4}$	$1.27 \pm 0.6 \times 10^{4}$
L-Valine	$^{13}C_1$	$4.69 \pm 6.2 \times 10^{3}$	$0 \pm 0.0 \times 10^{0}$	$0 \pm 0.0 \times 10^{0}$
L-Valine	$^{13}C_2$	$8.40 \pm 1.2 \times 10^{3}$	$9.85 \pm 6.1 \times 10^{3}$	$0 \pm 0.0 \times 10^{0}$
L-Valine	$^{13}C_3$	$1.08 \pm 0.2 \times 10^{4}$	$7.65 \pm 2.4 \times 10^{3}$	$0 \pm 0.0 \times 10^{0}$
L-Valine	$^{13}C_4$	$3.12 \pm 0.6 \times 10^{4}$	$2.25 \pm 0.7 \times 10^{4}$	$4.09 \pm 7.1 \times 10^{3}$
L-Valine	$^{13}C_5$	$9.67 \pm 1.1 \times 10^{5}$	$5.82 \pm 1.2 \times 10^{5}$	$8.31 \pm 3.8 \times 10^{5}$

Table A-5. The average ion counts plus or minus the standard deviation for the metabolites discussed and their isotopomers for the 25 °C experiment at 0, 2, 5, and 15 minutes are shown.

metabolite	labeling pattern	0 min	2 min	5 min	15 min
glucose/fructose-6-phosphate	^{12}C	$1.75 \pm 0.006 \times 10^{6}$	$1.58 \pm 0.3 \times 10^{4}$	$1.17 \pm 0.2 \times 10^{5}$	$9.14 \pm 1.1 \times 10^{4}$
glucose/fructose-6-phosphate	$^{13}C_1$	$1.02 \pm 0.1 \times 10^{5}$	$0 \pm 0.0 \times 10^{0}$	$0 \pm 0.0 \times 10^{0}$	$0 \pm 0.0 \times 10^{0}$
glucose/fructose-6-phosphate	$^{13}C_2$	$0 \pm 0.0 \times 10^{0}$	$0 \pm 0.0 \times 10^{0}$	$0 \pm 0.0 \times 10^{0}$	$0 \pm 0.0 \times 10^{0}$
glucose/fructose-6-phosphate	$^{13}C_3$	$0 \pm 0.0 \times 10^{0}$	$0 \pm 0.0 \times 10^{0}$	$0 \pm 0.0 \times 10^{0}$	$0 \pm 0.0 \times 10^{0}$
glucose/fructose-6-phosphate	$^{13}C_4$	$0 \pm 0.0 \times 10^{0}$	$0 \pm 0.0 \times 10^{0}$	$0 \pm 0.0 \times 10^{0}$	$0 \pm 0.0 \times 10^{0}$
glucose/fructose-6-phosphate	$^{13}C_5$	$0 \pm 0.0 \times 10^{0}$	$6.79 \pm 1.2 \times 10^{4}$	$5.53 \pm 4.8 \times 10^{4}$	$5.99 \pm 5.3 \times 10^{4}$
glucose/fructose-6-phosphate	$^{13}C_6$	$0 \pm 0.0 \times 10^{0}$	$1.23 \pm 0.05 \times 10^{6}$	$1.57 \pm 0.2 \times 10^{6}$	$1.58 \pm 1.4 \times 10^{6}$
fructose-1-6-bisphosphate	^{12}C	$1.71 \pm 0.6 \times 10^{6}$	$5.80 \pm 2.4 \times 10^{4}$	$6.48 \pm 3.6 \times 10^{4}$	$5.40 \pm 0.7 \times 10^{4}$
fructose-1-6-bisphosphate	$^{13}C_1$	$8.86 \pm 2.8 \times 10^{4}$	$3.54 \pm 3.3 \times 10^{3}$	$3.69 \pm 3.0 \times 10^{3}$	$3.32 \pm 0.1 \times 10^{3}$
fructose-1-6-bisphosphate	$^{13}C_2$	$2.87 \pm 0.9 \times 10^{4}$	$5.17 \pm 3.3 \times 10^{3}$	$2.15 \pm 1.4 \times 10^{3}$	$2.45 \pm 0.7 \times 10^{3}$
fructose-1-6-bisphosphate	$^{13}C_3$	$1.05 \pm 0.3 \times 10^{4}$	$9.63 \pm 4.3 \times 10^{4}$	$7.00 \pm 1.4 \times 10^{4}$	$6.60 \pm 1.2 \times 10^{4}$
fructose-1-6-bisphosphate	$^{13}C_4$	$1.14 \pm 0.9 \times 10^{3}$	$1.64 \pm 0.6 \times 10^{4}$	$1.26 \pm 0.5 \times 10^{4}$	$1.60 \pm 0.3 \times 10^{4}$
fructose-1-6-bisphosphate	$^{13}C_5$	$1.51 \pm 0.4 \times 10^{4}$	$7.18 \pm 3.1 \times 10^{4}$	$7.24 \pm 1.3 \times 10^{4}$	$1.31 \pm 0.2 \times 10^{5}$
fructose-1-6-bisphosphate	$^{13}C_6$	$2.66 \pm 0.08 \times 10^{5}$	$1.28 \pm 0.6 \times 10^{6}$	$1.40 \pm 0.3 \times 10^{6}$	$2.66 \pm 0.4 \times 10^{6}$
1,3-Diphosphoglyceric acid	^{12}C	$3.50 \pm 1.3 \times 10^{4}$	$1.32 \pm 0.008 \times 10^{3}$	$2.05 \pm 1.4 \times 10^{3}$	$9.93 \pm 2.9 \times 10^{2}$
1,3-Diphosphoglyceric acid	$^{13}C_1$	$0 \pm 0.0 \times 10^{0}$	$0 \pm 0.0 \times 10^{0}$	$0 \pm 0.0 \times 10^{0}$	$0 \pm 0.0 \times 10^{0}$
1,3-Diphosphoglyceric acid	$^{13}C_2$	$0 \pm 0.0 \times 10^{0}$	$0 \pm 0.0 \times 10^{0}$	$0 \pm 0.0 \times 10^{0}$	$0 \pm 0.0 \times 10^{0}$
1,3-Diphosphoglyceric acid	$^{13}C_3$	$0 \pm 0.0 \times 10^{0}$	$0 \pm 0.0 \times 10^{0}$	$0 \pm 0.0 \times 10^{0}$	$0 \pm 0.0 \times 10^{0}$
Pyruvate	^{12}C	$1.62 \pm 2.8 \times 10^{4}$	$2.02 \pm 3.5 \times 10^{3}$	$2.45 \pm 2.1 \times 10^{3}$	$1.55 \pm 0.6 \times 10^{3}$
Pyruvate	$^{13}C_1$	$0 \pm 0.0 \times 10^{0}$	$0 \pm 0.0 \times 10^{0}$	$0 \pm 0.0 \times 10^{0}$	$0 \pm 0.0 \times 10^{0}$
Pyruvate	$^{13}C_2$	$0 \pm 0.0 \times 10^{0}$	$0 \pm 0.0 \times 10^{0}$	$0 \pm 0.0 \times 10^{0}$	$0 \pm 0.0 \times 10^{0}$
Pyruvate	$^{13}C_3$	$0 \pm 0.0 \times 10^{0}$	$0 \pm 0.0 \times 10^{0}$	$0 \pm 0.0 \times 10^{0}$	$0 \pm 0.0 \times 10^{0}$
alpha-ketoglutarate	^{12}C	$8.54 \pm 6.1 \times 10^{2}$	$6.23 \pm 2.3 \times 10^{2}$	$3.88 \pm 1.2 \times 10^{2}$	$4.02 \pm 0.5 \times 10^{2}$
alpha-ketoglutarate	$^{13}C_1$	$0 \pm 0.0 \times 10^{0}$	$4.26 \pm 5.5 \times 10^{2}$	$0 \pm 0.0 \times 10^{0}$	$0 \pm 0.0 \times 10^{0}$
alpha-ketoglutarate	$^{13}C_2$	$0 \pm 0.0 \times 10^{0}$	$6.37 \pm 11.0 \times 10^{1}$	$0 \pm 0.0 \times 10^{0}$	$0 \pm 0.0 \times 10^{0}$
alpha-ketoglutarate	$^{13}C_3$	$0 \pm 0.0 \times 10^{0}$	$7.80 \pm 13.5 \times 10^{1}$	$0 \pm 0.0 \times 10^{0}$	$0 \pm 0.0 \times 10^{0}$
alpha-ketoglutarate	$^{13}C_4$	$1.98 \pm 1.7 \times 10^{2}$	$0 \pm 0.0 \times 10^{0}$	$0 \pm 0.0 \times 10^{0}$	$0 \pm 0.0 \times 10^{0}$
alpha-ketoglutarate	$^{13}C_5$	$1.06 \pm 1.8 \times 10^{2}$	$1.54 \pm 1.3 \times 10^{2}$	$8.39 \pm 14.5 \times 10^{1}$	$6.33 \pm 11.0 \times 10^{1}$
succinyl-CoA	^{12}C	$7.36 \pm 0.9 \times 10^{4}$	$6.19 \pm 2.7 \times 10^{4}$	$2.42 \pm 0.8 \times 10^{4}$	$1.59 \pm 1.1 \times 10^{4}$
succinyl-CoA	$^{13}C_1$	$0 \pm 0.0 \times 10^{0}$	$0 \pm 0.0 \times 10^{0}$	$0 \pm 0.0 \times 10^{0}$	$0 \pm 0.0 \times 10^{0}$
succinyl-CoA	$^{13}C_2$	$0 \pm 0.0 \times 10^{0}$	$1.52 \pm 2.6 \times 10^{4}$	$4.35 \pm 7.6 \times 10^{3}$	$0 \pm 0.0 \times 10^{0}$
succinyl-CoA	$^{13}C_3$	$0 \pm 0.0 \times 10^{0}$	$0 \pm 0.0 \times 10^{0}$	$0 \pm 0.0 \times 10^{0}$	$0 \pm 0.0 \times 10^{0}$
succinyl-CoA	$^{13}C_4$	$0 \pm 0.0 \times 10^{0}$	$0 \pm 0.0 \times 10^{0}$	$0 \pm 0.0 \times 10^{0}$	$0 \pm 0.0 \times 10^{0}$
succinyl-CoA	$^{13}C_5$	$0 \pm 0.0 \times 10^{0}$	$0 \pm 0.0 \times 10^{0}$	$0 \pm 0.0 \times 10^{0}$	$0 \pm 0.0 \times 10^{0}$
succinyl-CoA	$^{13}C_6$	$0 \pm 0.0 \times 10^{0}$	$0 \pm 0.0 \times 10^{0}$	$0 \pm 0.0 \times 10^{0}$	$0 \pm 0.0 \times 10^{0}$
succinyl-CoA	$^{13}C_7$	$0 \pm 0.0 \times 10^{0}$	$0 \pm 0.0 \times 10^{0}$	$0 \pm 0.0 \times 10^{0}$	$0 \pm 0.0 \times 10^{0}$
succinyl-CoA	$^{13}C_8$	$0 \pm 0.0 \times 10^{0}$	$0 \pm 0.0 \times 10^{0}$	$0 \pm 0.0 \times 10^{0}$	$0 \pm 0.0 \times 10^{0}$
succinyl-CoA	$^{13}C_9$	$0 \pm 0.0 \times 10^{0}$	$0 \pm 0.0 \times 10^{0}$	$0 \pm 0.0 \times 10^{0}$	$0 \pm 0.0 \times 10^{0}$
succinyl-CoA	$^{13}C_{10}$	$0 \pm 0.0 \times 10^{0}$	$0 \pm 0.0 \times 10^{0}$	$0 \pm 0.0 \times 10^{0}$	$0 \pm 0.0 \times 10^{0}$
succinyl-CoA	$^{13}C_{11}$	$0 \pm 0.0 \times 10^{0}$	$0 \pm 0.0 \times 10^{0}$	$0 \pm 0.0 \times 10^{0}$	$0 \pm 0.0 \times 10^{0}$
succinyl-CoA	$^{13}C_{12}$	$0 \pm 0.0 \times 10^{0}$	$0 \pm 0.0 \times 10^{0}$	$0 \pm 0.0 \times 10^{0}$	$0 \pm 0.0 \times 10^{0}$

Table A-5 continued.

metabolite	labeling pattern	0 min	2 min	5 min	15 min
succinyl-CoA	$^{13}C_{13}$	$0 \pm 0.0 \times 10^{0}$	$0 \pm 0.0 \times 10^{0}$	$0 \pm 0.0 \times 10^{0}$	$0 \pm 0.0 \times 10^{0}$
succinyl-CoA	$^{13}C_{14}$	$0 \pm 0.0 \times 10^{0}$	$0 \pm 0.0 \times 10^{0}$	$0 \pm 0.0 \times 10^{0}$	$0 \pm 0.0 \times 10^{0}$
succinyl-CoA	$^{13}C_{15}$	$0 \pm 0.0 \times 10^{0}$	$0 \pm 0.0 \times 10^{0}$	$0 \pm 0.0 \times 10^{0}$	$0 \pm 0.0 \times 10^{0}$
succinyl-CoA	$^{13}C_{16}$	$0 \pm 0.0 \times 10^{0}$	$0 \pm 0.0 \times 10^{0}$	$0 \pm 0.0 \times 10^{0}$	$0 \pm 0.0 \times 10^{0}$
succinyl-CoA	$^{13}C_{17}$	$0 \pm 0.0 \times 10^{0}$	$0 \pm 0.0 \times 10^{0}$	$0 \pm 0.0 \times 10^{0}$	$0 \pm 0.0 \times 10^{0}$
succinyl-CoA	$^{13}C_{18}$	$0 \pm 0.0 \times 10^{0}$	$0 \pm 0.0 \times 10^{0}$	$0 \pm 0.0 \times 10^{0}$	$0 \pm 0.0 \times 10^{0}$
succinyl-CoA	$^{13}C_{19}$	$0 \pm 0.0 \times 10^{0}$	$0 \pm 0.0 \times 10^{0}$	$0 \pm 0.0 \times 10^{0}$	$0 \pm 0.0 \times 10^{0}$
succinyl-CoA	$^{13}C_{20}$	$0 \pm 0.0 \times 100$	$0 \pm 0.0 \times 10^{0}$	$0 \pm 0.0 \times 10^{0}$	$0 \pm 0.0 \times 10^{0}$
succinyl-CoA	$^{13}C_{21}$	$0 \pm 0.0 \times 10^{0}$	$0 \pm 0.0 \times 10^{0}$	$0 \pm 0.0 \times 10^{0}$	$0 \pm 0.0 \times 10^{0}$
succinyl-CoA	$^{13}C_{22}$	$0 \pm 0.0 \times 10^{0}$	$0 \pm 0.0 \times 10^{0}$	$0 \pm 0.0 \times 10^{0}$	$0 \pm 0.0 \times 10^{0}$
succinyl-CoA	$^{13}C_{23}$	$0 \pm 0.0 \times 10^{0}$	$0 \pm 0.0 \times 10^{0}$	$0 \pm 0.0 \times 10^{0}$	$0 \pm 0.0 \times 10^{0}$
succinyl-CoA	$^{13}C_{24}$	$0 \pm 0.0 \times 10^{0}$	$0 \pm 0.0 \times 10^{0}$	$0 \pm 0.0 \times 10^{0}$	$0 \pm 0.0 \times 10^{0}$
succinyl-CoA	$^{13}C_{25}$	$0 \pm 0.0 \times 10^{0}$	$0 \pm 0.0 \times 10^{0}$	$0 \pm 0.0 \times 10^{0}$	$0 \pm 0.0 \times 10^{0}$
Succinate	^{12}C	$1.82 \pm 2.1 \times 10^{3}$	$1.97 \pm 0.4 \times 10^{5}$	$2.75 \pm 0.2 \times 10^{5}$	$2.39 \pm 0.6 \times 10^{5}$
Succinate	$^{13}C_{1}$	$0 \pm 0.0 \times 10^{0}$	$4.33 \pm 0.6 \times 10^{5}$	$4.32 \pm 0.3 \times 10^{5}$	$6.02 \pm 0.7 \times 10^{5}$
Succinate	$^{13}C_{2}$	$0 \pm 0.0 \times 10^{0}$	$4.18 \pm 0.7 \times 10^{5}$	$6.30 \pm 0.8 \times 10^{5}$	$1.81 \pm 0.1 \times 10^{6}$
Succinate	$^{13}C_{3}$	$0 \pm 0.0 \times 10^{0}$	$0 \pm 0.0 \times 10^{0}$	$0 \pm 0.0 \times 10^{0}$	$0 \pm 0.0 \times 10^{0}$
Succinate	$^{13}C_{4}$	$0 \pm 0.0 \times 10^{0}$	$0 \pm 0.0 \times 10^{0}$	$0 \pm 0.0 \times 10^{0}$	$0 \pm 0.0 \times 10^{0}$
fumarate	^{12}C	$0 \pm 0.0 \times 10^{0}$	$1.86 \pm 1.6 \times 10^{2}$	$1.52 \pm 2.6 \times 10^{2}$	$6.37 \pm 11.0 \times 10^{1}$
fumarate	$^{13}C_{1}$	$0 \pm 0.0 \times 10^{0}$	$0 \pm 0.0 \times 10^{0}$	$0 \pm 0.0 \times 10^{0}$	$0 \pm 0.0 \times 10^{0}$
fumarate	$^{13}C_{2}$	$0 \pm 0.0 \times 10^{0}$	$0 \pm 0.0 \times 10^{0}$	$0 \pm 0.0 \times 10^{0}$	$0 \pm 0.0 \times 10^{0}$
fumarate	$^{13}C_{3}$	$0 \pm 0.0 \times 10^{0}$	$0 \pm 0.0 \times 10^{0}$	$0 \pm 0.0 \times 10^{0}$	$0 \pm 0.0 \times 10^{0}$
fumarate	$^{13}C_{4}$	$0 \pm 0.0 \times 10^{0}$	$0 \pm 0.0 \times 10^{0}$	$0 \pm 0.0 \times 10^{0}$	$0 \pm 0.0 \times 10^{0}$
malate	^{12}C	$0 \pm 0.0 \times 10^{0}$	$0 \pm 0.0 \times 10^{0}$	$0 \pm 0.0 \times 10^{0}$	$0 \pm 0.0 \times 10^{0}$
malate	$^{13}C_{1}$	$0 \pm 0.0 \times 10^{0}$	$0 \pm 0.0 \times 10^{0}$	$0 \pm 0.0 \times 10^{0}$	$1.09 \pm 1.9 \times 10^{2}$
malate	$^{13}C_{2}$	$1.67 \pm 0.3 \times 10^{4}$	$2.43 \pm 0.4 \times 10^{4}$	$1.89 \pm 0.3 \times 10^{4}$	$6.54 \pm 1.7 \times 10^{4}$
malate	$^{13}C_{3}$	$5.29 \pm 1.3 \times 10^{2}$	$7.75 \pm 8.5 \times 10^{2}$	$4.41 \pm 2.1 \times 10^{2}$	$3.84 \pm 2.2 \times 10^{3}$
6-phospho-D-gluconate	^{12}C	$1.64 \pm 0.3 \times 10^{6}$	$1.14 \pm 0.2 \times 10^{5}$	$9.71 \pm 5.1 \times 10^{4}$	$1.10 \pm 0.4 \times 10^{5}$
6-phospho-D-gluconate	$^{13}C_{1}$	$8.49 \pm 1.6 \times 10^{4}$	$4.69 \pm 4.1 \times 10^{3}$	$2.62 \pm 4.5 \times 10^{3}$	$2.51 \pm 4.3 \times 10^{3}$
6-phospho-D-gluconate	$^{13}C_{2}$	$2.17 \pm 0.3 \times 10^{4}$	$0 \pm 0.0 \times 10^{0}$	$0 \pm 0.0 \times 10^{0}$	$0 \pm 0.0 \times 10^{0}$
6-phospho-D-gluconate	$^{13}C_{3}$	$0 \pm 0.0 \times 10^{0}$	$8.74 \pm 1.3 \times 10^{3}$	$2.30 \pm 4.0 \times 10^{3}$	$0 \pm 0.0 \times 10^{0}$
6-phospho-D-gluconate	$^{13}C_{4}$	$0 \pm 0.0 \times 10^{0}$	$2.66 \pm 4.61 \times 10^{3}$	$2.52 \pm 4.4 \times 10^{3}$	$6.16 \pm 5.3 \times 10^{3}$
6-phospho-D-gluconate	$^{13}C_{5}$	$0 \pm 0.0 \times 10^{0}$	$5.44 \pm 1.0 \times 10^{4}$	$7.24 \pm 2.2 \times 10^{4}$	$1.74 \pm 0.3 \times 10^{5}$
6-phospho-D-gluconate	$^{13}C_{6}$	$0 \pm 0.0 \times 10^{0}$	$1.18 \pm 0.2 \times 10^{6}$	$1.58 \pm 0.5 \times 10^{6}$	$3.68 \pm 0.5 \times 10^{6}$
D-Xylulose 5-phosphate	^{12}C	$0 \pm 0.0 \times 10^{0}$	$0 \pm 0.0 \times 10^{0}$	$0 \pm 0.0 \times 10^{0}$	$0 \pm 0.0 \times 10^{0}$
D-Xylulose 5-phosphate	$^{13}C_{1}$	$0 \pm 0.0 \times 10^{0}$	$0 \pm 0.0 \times 10^{0}$	$0 \pm 0.0 \times 10^{0}$	$0 \pm 0.0 \times 10^{0}$
D-Xylulose 5-phosphate	$^{13}C_{2}$	$0 \pm 0.0 \times 10^{0}$	$0 \pm 0.0 \times 10^{0}$	$0 \pm 0.0 \times 10^{0}$	$0 \pm 0.0 \times 10^{0}$
D-Xylulose 5-phosphate	$^{13}C_{3}$	$0 \pm 0.0 \times 10^{0}$	$0 \pm 0.0 \times 10^{0}$	$0 \pm 0.0 \times 10^{0}$	$0 \pm 0.0 \times 10^{0}$
D-Xylulose 5-phosphate	$^{13}C_{4}$	$0 \pm 0.0 \times 10^{0}$	$0 \pm 0.0 \times 10^{0}$	$0 \pm 0.0 \times 10^{0}$	$0 \pm 0.0 \times 10^{0}$
D-Xylulose 5-phosphate	$^{13}C_{5}$	$0 \pm 0.0 \times 10^{0}$	$0 \pm 0.0 \times 10^{0}$	$0 \pm 0.0 \times 10^{0}$	$0 \pm 0.0 \times 10^{0}$
D-sedoheptulose-1/7-phosphate	^{12}C	$1.68 \pm 0.1 \times 10^{5}$	$9.68 \pm 16.8 \times 10^{2}$	$0 \pm 0.0 \times 10^{0}$	$0 \pm 0.0 \times 10^{0}$

Table A-5 continued.

metabolite	labeling pattern	0 min	2 min	5 min	15 min
D-sedoheptulose-1/7-phosphate	$^{13}C_1$	4.25 ± 0.3 x 10^3	0 ± 0.0 x 10^0	0 ± 0.0 x 10^0	0 ± 0.0 x 10^0
D-sedoheptulose-1/7-phosphate	$^{13}C_2$	0 ± 0.0 x 10^0	5.46 ± 9.5 x 10^2	0 ± 0.0 x 10^0	7.25 ± 12.6 x 10^2
D-sedoheptulose-1/7-phosphate	$^{13}C_3$	0 ± 0.0 x 10^0	1.26 ± 1.1 x 10^3	0 ± 0.0 x 10^0	0 ± 0.0 x 10^0
D-sedoheptulose-1/7-phosphate	$^{13}C_4$	0 ± 0.0 x 10^0	3.96 ± 2.0 x 10^3	1.43 ± 2.5 x 10^3	6.29 ± 10.9 x 10^2
D-sedoheptulose-1/7-phosphate	$^{13}C_5$	0 ± 0.0 x 10^0	9.41 ± 5.5 x 10^3	4.41 ± 0.9 x 10^3	3.70 ± 0.9 x 10^2
D-sedoheptulose-1/7-phosphate	$^{13}C_6$	0 ± 0.0 x 10^0	4.20 ± 1.2 x 10^3	1.05 ± 0.2 x 10^4	1.26 ± 0.4 x 10^3
D-sedoheptulose-1/7-phosphate	$^{13}C_7$	0 ± 0.0 x 10^0	6.78 ± 0.3 x 10^4	1.27 ± 0.2 x 10^5	1.89 ± 0.3 x 10^5
glutamate	^{12}C	3.03 ± 1.8 x 10^3	9.87 ± 9.4 x 10^2	7.30 ± 6.4 x 10^2	2.36 ± 0.4 x 10^2
glutamate	$^{13}C_1$	1.22 ± 0.6 x 10^4	1.09 ± 0.9 x 10^4	5.18 ± 2.8 x 10^3	2.26 ± 1.7 x 10^3
glutamate	$^{13}C_2$	1.16 ± 1.3 x 10^3	4.38 ± 3.1 x 10^2	3.42 ± 5.9 x 10^2	1.51 ± 1.4 x 10^2
glutamate	$^{13}C_3$	6.80 ± 2.3 x 10^3	6.04 ± 5.4 x 10^3	6.97 ± 11.8 x 10^4	1.52 ± 2.6 x 10^5
glutamate	$^{13}C_4$	1.89 ± 2.9 x 10^3	9.55 ± 16.5 x 10^1	9.63 ± 12.5 x 10^2	4.11 ± 5.5 x 10^3
glutamate	$^{13}C_5$	4.27 ± 1.6 x 10^2	6.94 ± 12.0 x 10^1	0 ± 0.0 x 10^0	1.32 ± 1.3 x 10^3
glutamine	^{12}C	4.79 ± 26.1 x 10^5	3.75 ± 15.8 x 10^5	7.03 ± 157.0 x 10^4	4.69 ± 8.3 x 10^5
glutamine	$^{13}C_1$	7.99 ± 436.0 x 10^2	3.30 ± 40.7 x 10^3	6.91 ± 51.5 x 10^3	6.18 ± 52.3 x 10^3
glutamine	$^{13}C_2$	1.18 ± 44.9 x 10^3	2.23 ± 12.7 x 10^4	4.82 ± 35.8 x 10^4	2.55 ± 35.0 x 10^4
glutamine	$^{13}C_3$	2.14 ± 4.8 x 10^3	1.03 ± 13.5 x 10^3	5.70 ± 40.7 x 10^3	1.44 ± 65.6 x 10^3
glutamine	$^{13}C_4$	2.21 ± 6.5 x 10^2	5.65 ± 36.5 x 10^2	4.59 ± 1.3 x 10^3	1.19 ± 0.009 x 10^3
glutamine	$^{13}C_5$	1.25 ± 2.0 x 10^3	6.98 ± 9.5 x 10^2	2.24 ± 15.2 x 10^2	5.51 ± 32.8 x 10^2
aspartate	^{12}C	2.23 ± 0.2 x 10^2	4.77 ± 1.6 x 10^2	5.14 ± 0.3 x 10^2	3.82 ± 0.3 x 10^2
aspartate	$^{13}C_1$	0 ± 0.0 x 10^0	0 ± 0.0 x 10^0	0 ± 0.0 x 10^0	0 ± 0.0 x 10^0
aspartate	$^{13}C_2$	0 ± 0.0 x 10^0	0 ± 0.0 x 10^0	0 ± 0.0 x 10^0	0 ± 0.0 x 10^0
aspartate	$^{13}C_3$	0 ± 0.0 x 10^0	0 ± 0.0 x 10^0	0 ± 0.0 x 10^0	0 ± 0.0 x 10^0
aspartate	$^{13}C_4$	0 ± 0.0 x 10^0	0 ± 0.0 x 10^0	0 ± 0.0 x 10^0	0 ± 0.0 x 10^0
leucine/isoleucine	^{12}C	1.39 ± 1.3 x 10^2	2.16 ± 58.5 x 10^2	1.39 ± 1.2 x 10^2	1.84 ± 0.2 x 10^2
leucine/isoleucine	$^{13}C_1$	0 ± 0.0 x 10^0	0 ± 0.0 x 10^0	0 ± 0.0 x 10^0	0 ± 0.0 x 10^0
leucine/isoleucine	$^{13}C_2$	0 ± 0.0 x 10^0	0 ± 0.0 x 10^0	0 ± 0.0 x 10^0	0 ± 0.0 x 10^0
leucine/isoleucine	$^{13}C_3$	0 ± 0.0 x 10^0	0 ± 0.0 x 10^0	0 ± 0.0 x 10^0	0 ± 0.0 x 10^0
leucine/isoleucine	$^{13}C_4$	0 ± 0.0 x 10^0	0 ± 0.0 x 10^0	0 ± 0.0 x 10^0	0 ± 0.0 x 10^0
leucine/isoleucine	$^{13}C_5$	0 ± 0.0 x 10^0	0 ± 0.0 x 10^0	0 ± 0.0 x 10^0	0 ± 0.0 x 10^0
leucine/isoleucine	$^{13}C_6$	0 ± 0.0 x 10^0	0 ± 0.0 x 10^0	0 ± 0.0 x 10^0	0 ± 0.0 x 10^0
alanine	^{12}C	0 ± 0.0 x 10^0	1.07 ± 0.2 x 10^3	1.43 ± 1.4 x 10^3	1.74 ± 0.8 x 10^3
alanine	$^{13}C_1$	0 ± 0.0 x 10^0	0 ± 0.0 x 10^0	0 ± 0.0 x 10^0	0 ± 0.0 x 10^0
alanine	$^{13}C_2$	0 ± 0.0 x 10^0	0 ± 0.0 x 10^0	0 ± 0.0 x 10^0	0 ± 0.0 x 10^0
alanine	$^{13}C_3$	0 ± 0.0 x 10^0	0 ± 0.0 x 10^0	0 ± 0.0 x 10^0	0 ± 0.0 x 10^0
L-Valine	^{12}C	4.26 ± 3.7 x 10^2	4.34 ± 1.2 x 10^3	9.34 ± 1.2 x 10^3	3.62 ± 0.5 x 10^3
L-Valine	$^{13}C_1$	0 ± 0.0 x 10^0	0 ± 0.0 x 10^0	0 ± 0.0 x 10^0	0 ± 0.0 x 10^0
L-Valine	$^{13}C_2$	0 ± 0.0 x 10^0	0 ± 0.0 x 10^0	4.97 ± 4.4 x 10^3	0 ± 0.0 x 10^0

Table A-5 continued.

metabolite	labeling pattern	0 min	2 min	5 min	15 min
L-Valine	$^{13}C_3$	$0 \pm 0.0 \times 10^0$	$0 \pm 0.0 \times 10^0$	$2.82 \pm 4.9 \times 10^3$	$0 \pm 0.0 \times 10^0$
L-Valine	$^{13}C_4$	$0 \pm 0.0 \times 10^0$	$0 \pm 0.0 \times 10^0$	$0 \pm 0.0 \times 10^0$	$0 \pm 0.0 \times 10^0$
L-Valine	$^{13}C_5$	$0 \pm 0.0 \times 10^0$	$0 \pm 0.0 \times 10^0$	$0 \pm 0.0 \times 10^0$	$0 \pm 0.0 \times 10^0$

Table A-6. The average ion counts plus or minus the standard deviation for the metabolites discussed and their isotopomers for the 25 °C experiment at 30, 60, and 120 minutes are shown.

metabolite	labeling pattern	30 min	60 min	120 min
glucose/fructose-6-phosphate	^{12}C	$7.68 \pm 2.0 \times 10^{4}$	$7.10 \pm 4.3 \times 10^{4}$	$5.92 \pm 0.8 \times 10^{4}$
glucose/fructose-6-phosphate	$^{13}C_1$	$0 \pm 0.0 \times 10^{0}$	$0 \pm 0.0 \times 10^{0}$	$0 \pm 0.0 \times 10^{0}$
glucose/fructose-6-phosphate	$^{13}C_2$	$0 \pm 0.0 \times 10^{0}$	$0 \pm 0.0 \times 10^{0}$	$0 \pm 0.0 \times 10^{0}$
glucose/fructose-6-phosphate	$^{13}C_3$	$0 \pm 0.0 \times 10^{0}$	$0 \pm 0.0 \times 10^{0}$	$0 \pm 0.0 \times 10^{0}$
glucose/fructose-6-phosphate	$^{13}C_4$	$0 \pm 0.0 \times 10^{0}$	$0 \pm 0.0 \times 10^{0}$	$0 \pm 0.0 \times 10^{0}$
glucose/fructose-6-phosphate	$^{13}C_5$	$2.19 \pm 3.8 \times 10^{4}$	$0 \pm 0.0 \times 10^{0}$	$0 \pm 0.0 \times 10^{0}$
glucose/fructose-6-phosphate	$^{13}C_6$	$1.10 \pm 1.0 \times 10^{6}$	$0 \pm 0.0 \times 10^{0}$	$0 \pm 0.0 \times 10^{0}$
fructose-1-6-bisphosphate	^{12}C	$1.61 \pm 1.7 \times 10^{5}$	$7.26 \pm 4.7 \times 10^{4}$	$1.61 \pm 1.2 \times 10^{5}$
fructose-1-6-bisphosphate	$^{13}C_1$	$9.45 \pm 8.1 \times 10^{3}$	$2.55 \pm 0.2 \times 10^{3}$	$8.71 \pm 8.2 \times 10^{3}$
fructose-1-6-bisphosphate	$^{13}C_2$	$2.68 \pm 2.5 \times 10^{3}$	$1.42 \pm 0.7 \times 10^{3}$	$2.18 \pm 1.6 \times 10^{3}$
fructose-1-6-bisphosphate	$^{13}C_3$	$5.21 \pm 1.4 \times 10^{4}$	$3.83 \pm 1.3 \times 10^{4}$	$1.89 \pm 0.2 \times 10^{4}$
fructose-1-6-bisphosphate	$^{13}C_4$	$1.57 \pm 0.4 \times 10^{4}$	$1.23 \pm 0.5 \times 10^{4}$	$5.18 \pm 2.3 \times 10^{3}$
fructose-1-6-bisphosphate	$^{13}C_5$	$1.67 \pm 0.3 \times 10^{5}$	$1.64 \pm 0.1 \times 10^{5}$	$1.02 \pm 0.1 \times 10^{5}$
fructose-1-6-bisphosphate	$^{13}C_6$	$3.43 \pm 0.7 \times 10^{6}$	$3.37 \pm 0.4 \times 10^{6}$	$2.25 \pm 0.2 \times 10^{6}$
1,3-Diphosphoglyceric acid	^{12}C	$1.26 \pm 0.9 \times 10^{3}$	$5.12 \pm 0.5 \times 10^{2}$	$2.22 \pm 1.1 \times 10^{3}$
1,3-Diphosphoglyceric acid	$^{13}C_1$	$0 \pm 0.0 \times 10^{0}$	$0 \pm 0.0 \times 10^{0}$	$0 \pm 0.0 \times 10^{0}$
1,3-Diphosphoglyceric acid	$^{13}C_2$	$0 \pm 0.0 \times 10^{0}$	$0 \pm 0.0 \times 10^{0}$	$0 \pm 0.0 \times 10^{0}$
1,3-Diphosphoglyceric acid	$^{13}C_3$	$0 \pm 0.0 \times 10^{0}$	$0 \pm 0.0 \times 10^{0}$	$0 \pm 0.0 \times 10^{0}$
Pyruvate	^{12}C	$0 \pm 0.0 \times 10^{0}$	$1.04 \pm 1.8 \times 10^{2}$	$0 \pm 0.0 \times 10^{0}$
Pyruvate	$^{13}C_1$	$0 \pm 0.0 \times 10^{0}$	$0 \pm 0.0 \times 10^{0}$	$0 \pm 0.0 \times 10^{0}$
Pyruvate	$^{13}C_2$	$0 \pm 0.0 \times 10^{0}$	$0 \pm 0.0 \times 10^{0}$	$0 \pm 0.0 \times 10^{0}$
Pyruvate	$^{13}C_3$	$0 \pm 0.0 \times 10^{0}$	$0 \pm 0.0 \times 10^{0}$	$0 \pm 0.0 \times 10^{0}$
alpha-ketoglutarate	^{12}C	$7.49 \pm 0.4 \times 10^{2}$	$7.00 \pm 3.1 \times 10^{2}$	$3.61 \pm 0.6 \times 10^{2}$
alpha-ketoglutarate	$^{13}C_1$	$0 \pm 0.0 \times 10^{0}$	$0 \pm 0.0 \times 10^{0}$	$0 \pm 0.0 \times 10^{0}$
alpha-ketoglutarate	$^{13}C_2$	$0 \pm 0.0 \times 10^{0}$	$7.50 \pm 13.0 \times 10^{1}$	$9.54 \pm 16.5 \times 10^{1}$
alpha-ketoglutarate	$^{13}C_3$	$0 \pm 0.0 \times 10^{0}$	$8.49 \pm 14.7 \times 10^{1}$	$8.98 \pm 15.5 \times 10^{1}$
alpha-ketoglutarate	$^{13}C_4$	$0 \pm 0.0 \times 10^{0}$	$0 \pm 0.0 \times 10^{0}$	$0 \pm 0.0 \times 10^{0}$
alpha-ketoglutarate	$^{13}C_5$	$0 \pm 0.0 \times 10^{0}$	$9.81 \pm 17.0 \times 10^{1}$	$1.02 \pm 1.8 \times 10^{2}$
succinyl-CoA	^{12}C	$1.39 \pm 1.6 \times 10^{4}$	$2.97 \pm 5.1 \times 10^{3}$	$1.03 \pm 0.9 \times 10^{4}$
succinyl-CoA	$^{13}C_1$	$0 \pm 0.0 \times 10^{0}$	$0 \pm 0.0 \times 10^{0}$	$0 \pm 0.0 \times 10^{0}$
succinyl-CoA	$^{13}C_2$	$0 \pm 0.0 \times 10^{0}$	$0 \pm 0.0 \times 10^{0}$	$0 \pm 0.0 \times 10^{0}$
succinyl-CoA	$^{13}C_3$	$0 \pm 0.0 \times 10^{0}$	$0 \pm 0.0 \times 10^{0}$	$0 \pm 0.0 \times 10^{0}$
succinyl-CoA	$^{13}C_4$	$0 \pm 0.0 \times 10^{0}$	$0 \pm 0.0 \times 10^{0}$	$0 \pm 0.0 \times 10^{0}$
succinyl-CoA	$^{13}C_5$	$0 \pm 0.0 \times 10^{0}$	$0 \pm 0.0 \times 10^{0}$	$0 \pm 0.0 \times 10^{0}$
succinyl-CoA	$^{13}C_6$	$0 \pm 0.0 \times 10^{0}$	$0 \pm 0.0 \times 10^{0}$	$0 \pm 0.0 \times 10^{0}$
succinyl-CoA	$^{13}C_7$	$0 \pm 0.0 \times 10^{0}$	$0 \pm 0.0 \times 10^{0}$	$0 \pm 0.0 \times 10^{0}$
succinyl-CoA	$^{13}C_8$	$0 \pm 0.0 \times 10^{0}$	$0 \pm 0.0 \times 10^{0}$	$0 \pm 0.0 \times 10^{0}$
succinyl-CoA	$^{13}C_9$	$0 \pm 0.0 \times 10^{0}$	$0 \pm 0.0 \times 10^{0}$	$0 \pm 0.0 \times 10^{0}$

Table A-6 continued.

metabolite	labeling pattern	30 min	60 min	120 min
succinyl-CoA	$^{13}C_{10}$	$0 \pm 0.0 \times 10^{0}$	$0 \pm 0.0 \times 10^{0}$	$0 \pm 0.0 \times 10^{0}$
succinyl-CoA	$^{13}C_{11}$	$0 \pm 0.0 \times 10^{0}$	$0 \pm 0.0 \times 10^{0}$	$0 \pm 0.0 \times 10^{0}$
succinyl-CoA	$^{13}C_{12}$	$0 \pm 0.0 \times 10^{0}$	$0 \pm 0.0 \times 10^{0}$	$0 \pm 0.0 \times 10^{0}$
succinyl-CoA	$^{13}C_{13}$	$0 \pm 0.0 \times 10^{0}$	$0 \pm 0.0 \times 10^{0}$	$0 \pm 0.0 \times 10^{0}$
succinyl-CoA	$^{13}C_{14}$	$0 \pm 0.0 \times 10^{0}$	$0 \pm 0.0 \times 10^{0}$	$0 \pm 0.0 \times 10^{0}$
succinyl-CoA	$^{13}C_{15}$	$0 \pm 0.0 \times 10^{0}$	$0 \pm 0.0 \times 10^{0}$	$0 \pm 0.0 \times 10^{0}$
succinyl-CoA	$^{13}C_{16}$	$0 \pm 0.0 \times 10^{0}$	$0 \pm 0.0 \times 10^{0}$	$0 \pm 0.0 \times 10^{0}$
succinyl-CoA	$^{13}C_{17}$	$0 \pm 0.0 \times 10^{0}$	$0 \pm 0.0 \times 10^{0}$	$0 \pm 0.0 \times 10^{0}$
succinyl-CoA	$^{13}C_{18}$	$0 \pm 0.0 \times 10^{0}$	$0 \pm 0.0 \times 10^{0}$	$0 \pm 0.0 \times 10^{0}$
succinyl-CoA	$^{13}C_{19}$	$0 \pm 0.0 \times 10^{0}$	$0 \pm 0.0 \times 10^{0}$	$0 \pm 0.0 \times 10^{0}$
succinyl-CoA	$^{13}C_{20}$	$0 \pm 0.0 \times 10^{0}$	$0 \pm 0.0 \times 10^{0}$	$0 \pm 0.0 \times 10^{0}$
succinyl-CoA	$^{13}C_{21}$	$0 \pm 0.0 \times 10^{0}$	$0 \pm 0.0 \times 10^{0}$	$0 \pm 0.0 \times 10^{0}$
succinyl-CoA	$^{13}C_{22}$	$0 \pm 0.0 \times 10^{0}$	$0 \pm 0.0 \times 10^{0}$	$0 \pm 0.0 \times 10^{0}$
succinyl-CoA	$^{13}C_{23}$	$0 \pm 0.0 \times 10^{0}$	$0 \pm 0.0 \times 10^{0}$	$0 \pm 0.0 \times 10^{0}$
succinyl-CoA	$^{13}C_{24}$	$0 \pm 0.0 \times 10^{0}$	$0 \pm 0.0 \times 10^{0}$	$0 \pm 0.0 \times 10^{0}$
succinyl-CoA	$^{13}C_{25}$	$0 \pm 0.0 \times 10^{0}$	$0 \pm 0.0 \times 10^{0}$	$0 \pm 0.0 \times 10^{0}$
Succinate	^{12}C	$8.98 \pm 2.0 \times 10^{4}$	$2.55 \pm 0.5 \times 10^{4}$	$2.40 \pm 0.2 \times 10^{4}$
Succinate	$^{13}C_{1}$	$5.65 \pm 1.8 \times 10^{5}$	$2.53 \pm 0.4 \times 10^{5}$	$1.93 \pm 0.4 \times 10^{5}$
Succinate	$^{13}C_{2}$	$2.34 \pm 0.1 \times 10^{6}$	$1.72 \pm 0.2 \times 10^{6}$	$2.24 \pm 0.2 \times 10^{6}$
Succinate	$^{13}C_{3}$	$0 \pm 0.0 \times 10^{0}$	$0 \pm 0.0 \times 10^{0}$	$0 \pm 0.0 \times 10^{0}$
Succinate	$^{13}C_{4}$	$0 \pm 0.0 \times 10^{0}$	$0 \pm 0.0 \times 10^{0}$	$0 \pm 0.0 \times 10^{0}$
fumarate	^{12}C	$1.37 \pm 2.4 \times 10^{2}$	$0 \pm 0.0 \times 10^{0}$	$0 \pm 0.0 \times 10^{0}$
fumarate	$^{13}C_{1}$	$0 \pm 0.0 \times 10^{0}$	$0 \pm 0.0 \times 10^{0}$	$0 \pm 0.0 \times 10^{0}$
fumarate	$^{13}C_{2}$	$0 \pm 0.0 \times 10^{0}$	$0 \pm 0.0 \times 10^{0}$	$0 \pm 0.0 \times 10^{0}$
fumarate	$^{13}C_{3}$	$0 \pm 0.0 \times 10^{0}$	$0 \pm 0.0 \times 10^{0}$	$0 \pm 0.0 \times 10^{0}$
fumarate	$^{13}C_{4}$	$0 \pm 0.0 \times 10^{0}$	$0 \pm 0.0 \times 10^{0}$	$0 \pm 0.0 \times 10^{0}$
malate	^{12}C	$0 \pm 0.0 \times 10^{0}$	$0 \pm 0.0 \times 10^{0}$	$0 \pm 0.0 \times 10^{0}$
malate	$^{13}C_{1}$	$0 \pm 0.0 \times 10^{0}$	$6.86 \pm 11.9 \times 10^{1}$	$1.74 \pm 3.0 \times 10^{2}$
malate	$^{13}C_{2}$	$4.22 \pm 0.7 \times 10^{4}$	$2.09 \pm 0.2 \times 10^{4}$	$4.65 \pm 0.9 \times 10^{4}$
malate	$^{13}C_{3}$	$2.82 \pm 2.1 \times 10^{3}$	$1.53 \pm 1.1 \times 10^{3}$	$6.07 \pm 0.6 \times 10^{3}$
6-phospho-D-gluconate	^{12}C	$1.62 \pm 1.5 \times 10^{5}$	$4.78 \pm 1.3 \times 10^{4}$	$8.41 \pm 5.8 \times 10^{4}$
6-phospho-D-gluconate	$^{13}C_{1}$	$5.83 \pm 10.1 \times 10^{3}$	$0 \pm 0.0 \times 10^{0}$	$0 \pm 0.0 \times 10^{0}$
6-phospho-D-gluconate	$^{13}C_{2}$	$0 \pm 0.0 \times 10^{0}$	$0 \pm 0.0 \times 10^{0}$	$0 \pm 0.0 \times 10^{0}$
6-phospho-D-gluconate	$^{13}C_{3}$	$0 \pm 0.0 \times 10^{0}$	$0 \pm 0.0 \times 10^{0}$	$0 \pm 0.0 \times 10^{0}$
6-phospho-D-gluconate	$^{13}C_{4}$	$2.87 \pm 5.0 \times 10^{3}$	$0 \pm 0.0 \times 10^{0}$	$0 \pm 0.0 \times 10^{0}$
6-phospho-D-gluconate	$^{13}C_{5}$	$1.99 \pm 0.6 \times 10^{5}$	$1.06 \pm 0.2 \times 10^{5}$	$1.86 \pm 3.2 \times 10^{4}$
6-phospho-D-gluconate	$^{13}C_{6}$	$4.13 \pm 1.1 \times 10^{6}$	$2.37 \pm 0.3 \times 10^{6}$	$3.85 \pm 6.7 \times 10^{5}$
D-Xylulose 5-phosphate	^{12}C	$5.42\ 9.4 \times 10^{1}$	$5.86 \pm 10.2 \times 10^{1}$	$0 \pm 0.0 \times 10^{0}$
D-Xylulose 5-phosphate	$^{13}C_{1}$	$0 \pm 0.0 \times 10^{0}$	$0 \pm 0.0 \times 10^{0}$	$0 \pm 0.0 \times 10^{0}$
D-Xylulose 5-phosphate	$^{13}C_{2}$	$0 \pm 0.0 \times 10^{0}$	$0 \pm 0.0 \times 10^{0}$	$0 \pm 0.0 \times 10^{0}$
D-Xylulose 5-phosphate	$^{13}C_{3}$	$0 \pm 0.0 \times 10^{0}$	$0 \pm 0.0 \times 10^{0}$	$0 \pm 0.0 \times 10^{0}$
D-Xylulose 5-phosphate	$^{13}C_{4}$	$0 \pm 0.0 \times 10^{0}$	$0 \pm 0.0 \times 10^{0}$	$0 \pm 0.0 \times 10^{0}$

Table A-6 continued.

metabolite	labeling pattern	30 min	60 min	120 min
D-Xylulose 5-phosphate	$^{13}C_5$	$0 \pm 0.0 \times 10^0$	$0 \pm 0.0 \times 10^0$	$0 \pm 0.0 \times 10^0$
D-sedoheptulose-1/7-phosphate	^{12}C	$0 \pm 0.0 \times 10^0$	$1.21 \pm 2.1 \times 10^3$	$0 \pm 0.0 \times 10^0$
D-sedoheptulose-1/7-phosphate	$^{13}C_1$	$0 \pm 0.0 \times 10^0$	$0 \pm 0.0 \times 10^0$	$0 \pm 0.0 \times 10^0$
D-sedoheptulose-1/7-phosphate	$^{13}C_2$	$0 \pm 0.0 \times 10^0$	$0 \pm 0.0 \times 10^0$	$0 \pm 0.0 \times 10^0$
D-sedoheptulose-1/7-phosphate	$^{13}C_3$	$0 \pm 0.0 \times 10^0$	$0 \pm 0.0 \times 10^0$	$0 \pm 0.0 \times 10^0$
D-sedoheptulose-1/7-phosphate	$^{13}C_4$	$0 \pm 0.0 \times 10^0$	$0 \pm 0.0 \times 10^0$	$6.97 \pm 12.1 \times 10^2$
D-sedoheptulose-1/7-phosphate	$^{13}C_5$	$2.72 \pm 2.6 \times 10^3$	$0 \pm 0.0 \times 10^0$	$0 \pm 0.0 \times 10^0$
D-sedoheptulose-1/7-phosphate	$^{13}C_6$	$7.51 \pm 4.3 \times 10^3$	$8.01 \pm 13.9 \times 10^2$	$7.75 \pm 3.6 \times 10^3$
D-sedoheptulose-1/7-phosphate	$^{13}C_7$	$1.89 \pm 0.2 \times 10^5$	$7.10 \pm 10.1 \times 10^3$	$1.68 \pm 0.3 \times 10^5$
glutamate	^{12}C	$1.71 \pm 1.6 \times 10^2$	$3.34 \pm 2.3 \times 10^2$	$2.32 \pm 0.3 \times 10^2$
glutamate	$^{13}C_1$	$1.86 \pm 0.9 \times 10^3$	$1.52 \pm 0.5 \times 10^3$	$1.66 \pm 0.6 \times 10^3$
glutamate	$^{13}C_2$	$0 \pm 0.0 \times 10^0$	$7.65 \pm 13.2 \times 10^1$	$1.50 \pm 1.3 \times 10^2$
glutamate	$^{13}C_3$	$7.50 \pm 11.4 \times 10^3$	$1.91 \pm 3.2 \times 10^5$	$1.23 \pm 1.9 \times 10^5$
glutamate	$^{13}C_4$	$7.10 \pm 4.2 \times 10^2$	$3.47 \pm 5.3 \times 10^3$	$6.57 \pm 8.4 \times 10^2$
glutamate	$^{13}C_5$	$8.07 \pm 9.5 \times 10^2$	$9.51 \pm 7.1 \times 10^2$	$3.33 \pm 1.4 \times 10^2$
glutamine	^{12}C	$7.29 \pm 6.9 \times 10^5$	$3.53 \pm 0.007 \times 10^5$	$3.33 \pm 1.4 \times 10^2$
glutamine	$^{13}C_1$	$1.44 \pm 5.7 \times 10^4$	$1.87 \pm 0.7 \times 10^4$	$8.94 \pm 0.4 \times 10^2$
glutamine	$^{13}C_2$	$1.18 \pm 5.1 \times 10^5$	$1.30 \pm 0.01 \times 10^5$	$7.86 \pm 13.6 \times 10^1$
glutamine	$^{13}C_3$	$6.03 \pm 115.0 \times 10^3$	$0 \pm 0.0 \times 10^0$	$6.35 \pm 11.0 \times 10^1$
glutamine	$^{13}C_4$	$1.63 \pm 5.4 \times 10^2$	$5.47 \pm 8.2 \times 10^2$	4.93 ± 2.3 x 103
glutamine	$^{13}C_5$	$1.99 \pm 0.8 \times 10^3$	$7.41 \pm 7.5 \times 10^2$	$3.02 \pm 3.0 \times 10^2$
aspartate	^{12}C	$3.63 \pm 1.0 \times 10^2$	$5.26 \pm 4.3 \times 10^2$	$3.46 \pm 0.9 \times 10^2$
aspartate	$^{13}C_1$	$0 \pm 0.0 \times 10^0$	$0 \pm 0.0 \times 10^0$	$0 \pm 0.0 \times 10^0$
aspartate	$^{13}C_2$	$0 \pm 0.0 \times 10^0$	$0 \pm 0.0 \times 10^0$	$0 \pm 0.0 \times 10^0$
aspartate	$^{13}C_3$	$0 \pm 0.0 \times 10^0$	$0 \pm 0.0 \times 10^0$	$0 \pm 0.0 \times 10^0$
aspartate	$^{13}C_4$	$0 \pm 0.0 \times 10^0$	$0 \pm 0.0 \times 10^0$	$0 \pm 0.0 \times 10^0$
leucine/isoleucine	^{12}C	$1.70 \pm 0.08 \times 10^2$	$2.86 \pm 1.2 \times 10^2$	$2.18 \pm 0.6 \times 10^2$
leucine/isoleucine	$^{13}C_1$	$0 \pm 0.0 \times 10^0$	$0 \pm 0.0 \times 10^0$	$0 \pm 0.0 \times 10^0$
leucine/isoleucine	$^{13}C_2$	$0 \pm 0.0 \times 10^0$	$0 \pm 0.0 \times 10^0$	$0 \pm 0.0 \times 10^0$
leucine/isoleucine	$^{13}C_3$	$0 \pm 0.0 \times 10^0$	$0 \pm 0.0 \times 10^0$	$0 \pm 0.0 \times 10^0$
leucine/isoleucine	$^{13}C_4$	$0 \pm 0.0 \times 10^0$	$0 \pm 0.0 \times 10^0$	$0 \pm 0.0 \times 10^0$
leucine/isoleucine	$^{13}C_5$	$0 \pm 0.0 \times 10^0$	$0 \pm 0.0 \times 10^0$	$0 \pm 0.0 \times 10^0$
leucine/isoleucine	$^{13}C_6$	$0 \pm 0.0 \times 10^0$	$0 \pm 0.0 \times 10^0$	$0 \pm 0.0 \times 10^0$
alanine	^{12}C	$1.20 \pm 1.0 \times 10^3$	$8.26 \pm 2.8 \times 10^2$	$7.11 \pm 0.8 \times 10^2$
alanine	$^{13}C_1$	$0 \pm 0.0 \times 10^0$	$0 \pm 0.0 \times 10^0$	$0 \pm 0.0 \times 10^0$
alanine	$^{13}C_2$	$0 \pm 0.0 \times 10^0$	$0 \pm 0.0 \times 10^0$	$0 \pm 0.0 \times 10^0$
alanine	$^{13}C_3$	$0 \pm 0.0 \times 10^0$	$0 \pm 0.0 \times 10^0$	$0 \pm 0.0 \times 10^0$
L-Valine	^{12}C	$3.80 \pm 1.1 \times 10^2$	$5.43 \pm 1.9 \times 10^2$	$5.31 \pm 4.9 \times 10^2$
L-Valine	$^{13}C_1$	$0 \pm 0.0 \times 10^0$	$0 \pm 0.0 \times 10^0$	$0 \pm 0.0 \times 10^0$
L-Valine	$^{13}C_2$	$0 \pm 0.0 \times 10^0$	$0 \pm 0.0 \times 10^0$	$0 \pm 0.0 \times 10^0$
L-Valine	$^{13}C_3$	$0 \pm 0.0 \times 10^0$	$0 \pm 0.0 \times 10^0$	$0 \pm 0.0 \times 10^0$
L-Valine	$^{13}C_4$	$0 \pm 0.0 \times 10^0$	$0 \pm 0.0 \times 10^0$	$0 \pm 0.0 \times 10^0$

Table A-6 continued.

metabolite	labeling pattern	30 min	60 min	120 min
L-Valine	$^{13}C_5$	$0 \pm 0.0 \times 10^0$	$0 \pm 0.0 \times 10^0$	$0 \pm 0.0 \times 10^0$

Table A-7. The average ion counts plus or minus the standard deviation for the metabolites discussed and their isotopomers for the 3 °C experiment at 0, 2, 5, and 15 minutes are shown.

metabolite	labeling pattern	0 min	2 min	5 min	15 min
glucose/fructose-6-phosphate	^{12}C	$1.68 \pm 0.4 \times 10^{6}$	$6.45 \pm 1.0 \times 10^{5}$	$4.21 \pm 2.0 \times 10^{5}$	$2.99 \pm 0.7 \times 10^{5}$
glucose/fructose-6-phosphate	$^{13}C_1$	$8.73 \pm 1.8 \times 10^{4}$	$4.83 \pm 0.6 \times 10^{4}$	$2.85 \pm 2.5 \times 10^{4}$	$2.36 \pm 2.2 \times 10^{4}$
glucose/fructose-6-phosphate	$^{13}C_2$	$0 \pm 0.0 \times 10^{0}$	$0 \pm 0.0 \times 10^{0}$	$1.49 \pm 2.6 \times 10^{4}$	$1.65 \pm 2.9 \times 10^{4}$
glucose/fructose-6-phosphate	$^{13}C_3$	$0 \pm 0.0 \times 10^{0}$	$0 \pm 0.0 \times 10^{0}$	$1.04 \pm 0.2 \times 10^{5}$	$1.09 \pm 0.2 \times 10^{5}$
glucose/fructose-6-phosphate	$^{13}C_4$	$0 \pm 0.0 \times 10^{0}$	$0 \pm 0.0 \times 10^{0}$	$6.53 \pm 11.3 \times 10^{3}$	$3.40 \pm 3.3 \times 10^{4}$
glucose/fructose-6-phosphate	$^{13}C_5$	$0 \pm 0.0 \times 10^{0}$	$0 \pm 0.0 \times 10^{0}$	$7.16 \pm 0.8 \times 10^{4}$	$1.22 \pm 0.2 \times 10^{5}$
glucose/fructose-6-phosphate	$^{13}C_6$	$0 \pm 0.0 \times 10^{0}$	$5.68 \pm 0.3 \times 10^{5}$	$8.68 \pm 1.8 \times 10^{5}$	$1.30 \pm 0.4 \times 10^{6}$
fructose-1-6-bisphosphate	^{12}C	$1.97 \pm 1.8 \times 10^{5}$	$8.38 \pm 7.9 \times 10^{5}$	$2.31 \pm 3.9 \times 10^{5}$	$1.54 \pm 1.8 \times 10^{5}$
fructose-1-6-bisphosphate	$^{13}C_1$	$1.62 \pm 1.4 \times 10^{4}$	$6.20 \pm 5.8 \times 10^{4}$	$1.97 \pm 3.3 \times 10^{4}$	$1.50 \pm 1.4 \times 10^{4}$
fructose-1-6-bisphosphate	$^{13}C_2$	$1.18 \pm 1.0 \times 10^{4}$	$4.30 \pm 3.3 \times 10^{4}$	$1.90 \pm 3.0 \times 10^{4}$	$1.67 \pm 1.4 \times 10^{4}$
fructose-1-6-bisphosphate	$^{13}C_3$	$1.87 \pm 1.4 \times 10^{5}$	$7.56 \pm 6.5 \times 10^{5}$	$8.59 \pm 14.9 \times 10^{3}$	$2.46 \pm 2.4 \times 10^{5}$
fructose-1-6-bisphosphate	$^{13}C_4$	$1.75 \pm 1.1 \times 10^{4}$	$5.62 \pm 4.37 \times 10^{4}$	$2.73 \pm 4.4 \times 10^{4}$	$2.46 \pm 2.0 \times 10^{4}$
fructose-1-6-bisphosphate	$^{13}C_5$	$2.75 \pm 1.7 \times 10^{4}$	$8.28 \pm 6.7 \times 10^{4}$	$4.44 \pm 7.42 \times 10^{4}$	$4.08 \pm 3.7 \times 10^{4}$
fructose-1-6-bisphosphate	$^{13}C_6$	$2.98 \pm 2.1 \times 10^{5}$	$9.70 \pm 7.7 \times 10^{5}$	$4.44 \pm 7.3 \times 10^{5}$	$4.21 \pm 4.4 \times 10^{5}$
1,3-Diphosphoglyceric acid	^{12}C	$1.64 \pm 1.3 \times 10^{3}$	$4.75 \pm 2.9 \times 10^{3}$	$1.17 \pm 1.6 \times 10^{3}$	$1.26 \pm 1.6 \times 10^{3}$
1,3-Diphosphoglyceric acid	$^{13}C_1$	$0 \pm 0.0 \times 10^{0}$	$0 \pm 0.0 \times 10^{0}$	$0 \pm 0.0 \times 10^{0}$	$0 \pm 0.0 \times 10^{0}$
1,3-Diphosphoglyceric acid	$^{13}C_2$	$0 \pm 0.0 \times 10^{0}$	$0 \pm 0.0 \times 10^{0}$	$0 \pm 0.0 \times 10^{0}$	$0 \pm 0.0 \times 10^{0}$
1,3-Diphosphoglyceric acid	$^{13}C_3$	$0 \pm 0.0 \times 10^{0}$	$0 \pm 0.0 \times 10^{0}$	$0 \pm 0.0 \times 10^{0}$	$0 \pm 0.0 \times 10^{0}$
Pyruvate	^{12}C	$9.77 \pm 7.8 \times 10^{6}$	$8.35 \pm 1.5 \times 10^{5}$	$6.00 \pm 2.8 \times 10^{5}$	$2.80 \pm 1.3 \times 10^{5}$
Pyruvate	$^{13}C_1$	$2.41 \pm 3.1 \times 10^{5}$	$0 \pm 0.0 \times 10^{0}$	$2.85 \pm 4.9 \times 10^{3}$	$0 \pm 0.0 \times 10^{0}$
Pyruvate	$^{13}C_2$	$0 \pm 0.0 \times 10^{0}$	$0 \pm 0.0 \times 10^{0}$	$0 \pm 0.0 \times 10^{0}$	$3.30 \pm 5.7 \times 10^{3}$
Pyruvate	$^{13}C_3$	$0 \pm 0.0 \times 10^{0}$	$2.4 \pm 1.2 \times 10^{5}$	$3.51 \pm 2.1 \times 10^{5}$	$5.00 \pm 2.0 \times 10^{5}$
alpha-ketoglutarate	^{12}C	$3.84 \pm 1.1 \times 10^{6}$	$2.10 \pm 0.3 \times 10^{6}$	$1.34 \pm 0.1 \times 10^{6}$	$7.91 \pm 2.0 \times 10^{5}$
alpha-ketoglutarate	$^{13}C_1$	$1.73 \pm 0.8 \times 10^{5}$	$5.22 \pm 2.2 \times 10^{4}$	$2.68 \pm 0.2 \times 10^{4}$	$1.52 \pm 0.4 \times 10^{4}$
alpha-ketoglutarate	$^{13}C_2$	$1.06 \pm 0.3 \times 10^{4}$	$1.34 \pm 0.2 \times 10^{4}$	$3.64 \pm 0.5 \times 10^{4}$	$7.90 \pm 3.7 \times 10^{4}$
alpha-ketoglutarate	$^{13}C_3$	$1.60 \pm 2.8 \times 10^{2}$	$1.09 \pm 0.2 \times 10^{3}$	$4.69 \pm 1.4 \times 10^{3}$	$8.63 \pm 4.2 \times 10^{3}$
alpha-ketoglutarate	$^{13}C_4$	$5.44 \pm 3.6 \times 10^{2}$	$4.4 \pm 0.4 \times 10^{2}$	$8.01 \pm 5.7 \times 10^{2}$	$3.96 \pm 0.4 \times 10^{2}$
alpha-ketoglutarate	$^{13}C_5$	$0 \pm 0.0 \times 10^{0}$	$7.69 \pm 13.3 \times 10^{1}$	$0 \pm 0.0 \times 10^{0}$	$0 \pm 0.0 \times 10^{0}$
succinyl-CoA	^{12}C	$6.74 \pm 8.7 \times 10^{3}$	$4.32 \pm 5.6 \times 10^{4}$	$2.69 \pm 4.7 \times 10^{4}$	$2.10 \pm 3.6 \times 10^{3}$
succinyl-CoA	$^{13}C_1$	$0 \pm 0.0 \times 10^{0}$	$0 \pm 0.0 \times 10^{0}$	$0 \pm 0.0 \times 10^{0}$	$0 \pm 0.0 \times 10^{0}$
succinyl-CoA	$^{13}C_2$	$0 \pm 0.0 \times 10^{0}$	$0 \pm 0.0 \times 10^{0}$	$0 \pm 0.0 \times 10^{0}$	$0 \pm 0.0 \times 10^{0}$
succinyl-CoA	$^{13}C_3$	$0 \pm 0.0 \times 10^{0}$	$0 \pm 0.0 \times 10^{0}$	$0 \pm 0.0 \times 10^{0}$	$0 \pm 0.0 \times 10^{0}$
succinyl-CoA	$^{13}C_4$	$0 \pm 0.0 \times 10^{0}$	$0 \pm 0.0 \times 10^{0}$	$0 \pm 0.0 \times 10^{0}$	$0 \pm 0.0 \times 10^{0}$
succinyl-CoA	$^{13}C_5$	$0 \pm 0.0 \times 10^{0}$	$0 \pm 0.0 \times 10^{0}$	$0 \pm 0.0 \times 10^{0}$	$0 \pm 0.0 \times 10^{0}$
succinyl-CoA	$^{13}C_6$	$0 \pm 0.0 \times 10^{0}$	$0 \pm 0.0 \times 10^{0}$	$0 \pm 0.0 \times 10^{0}$	$0 \pm 0.0 \times 10^{0}$
succinyl-CoA	$^{13}C_7$	$0 \pm 0.0 \times 10^{0}$	$0 \pm 0.0 \times 10^{0}$	$0 \pm 0.0 \times 10^{0}$	$0 \pm 0.0 \times 10^{0}$
succinyl-CoA	$^{13}C_8$	$0 \pm 0.0 \times 10^{0}$	$0 \pm 0.0 \times 10^{0}$	$0 \pm 0.0 \times 10^{0}$	$0 \pm 0.0 \times 10^{0}$
succinyl-CoA	$^{13}C_9$	$0 \pm 0.0 \times 10^{0}$	$0 \pm 0.0 \times 10^{0}$	$0 \pm 0.0 \times 10^{0}$	$0 \pm 0.0 \times 10^{0}$
succinyl-CoA	$^{13}C_{10}$	$0 \pm 0.0 \times 10^{0}$	$0 \pm 0.0 \times 10^{0}$	$0 \pm 0.0 \times 10^{0}$	$0 \pm 0.0 \times 10^{0}$
succinyl-CoA	$^{13}C_{11}$	$0 \pm 0.0 \times 10^{0}$	$0 \pm 0.0 \times 10^{0}$	$0 \pm 0.0 \times 10^{0}$	$0 \pm 0.0 \times 10^{0}$
succinyl-CoA	$^{13}C_{12}$	$0 \pm 0.0 \times 10^{0}$	$0 \pm 0.0 \times 10^{0}$	$0 \pm 0.0 \times 10^{0}$	$0 \pm 0.0 \times 10^{0}$
succinyl-CoA	$^{13}C_{13}$	$0 \pm 0.0 \times 10^{0}$	$0 \pm 0.0 \times 10^{0}$	$0 \pm 0.0 \times 10^{0}$	$0 \pm 0.0 \times 10^{0}$

Table A-7 continued.

metabolite	labeling pattern	0 min	2 min	5 min	15 min
succinyl-CoA	$^{13}C_{14}$	$0 \pm 0.0 \times 10^{0}$	$0 \pm 0.0 \times 10^{0}$	$0 \pm 0.0 \times 10^{0}$	$0 \pm 0.0 \times 10^{0}$
succinyl-CoA	$^{13}C_{15}$	$0 \pm 0.0 \times 10^{0}$	$0 \pm 0.0 \times 10^{0}$	$0 \pm 0.0 \times 10^{0}$	$0 \pm 0.0 \times 10^{0}$
succinyl-CoA	$^{13}C_{16}$	$0 \pm 0.0 \times 10^{0}$	$0 \pm 0.0 \times 10^{0}$	$0 \pm 0.0 \times 10^{0}$	$0 \pm 0.0 \times 10^{0}$
succinyl-CoA	$^{13}C_{17}$	$0 \pm 0.0 \times 10^{0}$	$0 \pm 0.0 \times 10^{0}$	$0 \pm 0.0 \times 10^{0}$	$0 \pm 0.0 \times 10^{0}$
succinyl-CoA	$^{13}C_{18}$	$0 \pm 0.0 \times 10^{0}$	$0 \pm 0.0 \times 10^{0}$	$0 \pm 0.0 \times 10^{0}$	$0 \pm 0.0 \times 10^{0}$
succinyl-CoA	$^{13}C_{19}$	$0 \pm 0.0 \times 10^{0}$	$0 \pm 0.0 \times 10^{0}$	$0 \pm 0.0 \times 10^{0}$	$0 \pm 0.0 \times 10^{0}$
succinyl-CoA	$^{13}C_{20}$	$0 \pm 0.0 \times 10^{0}$	$0 \pm 0.0 \times 10^{0}$	$0 \pm 0.0 \times 10^{0}$	$0 \pm 0.0 \times 10^{0}$
succinyl-CoA	$^{13}C_{21}$	$0 \pm 0.0 \times 10^{0}$	$0 \pm 0.0 \times 10^{0}$	$0 \pm 0.0 \times 10^{0}$	$0 \pm 0.0 \times 10^{0}$
succinyl-CoA	$^{13}C_{22}$	$0 \pm 0.0 \times 10^{0}$	$0 \pm 0.0 \times 10^{0}$	$0 \pm 0.0 \times 10^{0}$	$0 \pm 0.0 \times 10^{0}$
succinyl-CoA	$^{13}C_{23}$	$0 \pm 0.0 \times 10^{0}$	$0 \pm 0.0 \times 10^{0}$	$0 \pm 0.0 \times 10^{0}$	$0 \pm 0.0 \times 10^{0}$
succinyl-CoA	$^{13}C_{24}$	$0 \pm 0.0 \times 10^{0}$	$0 \pm 0.0 \times 10^{0}$	$0 \pm 0.0 \times 10^{0}$	$0 \pm 0.0 \times 10^{0}$
succinyl-CoA	$^{13}C_{25}$	$0 \pm 0.0 \times 10^{0}$	$0 \pm 0.0 \times 10^{0}$	$0 \pm 0.0 \times 10^{0}$	$0 \pm 0.0 \times 10^{0}$
Succinate	^{12}C	$7.20 \pm 2.2 \times 10^{6}$	$7.55 \pm 2.5 \times 10^{6}$	$5.03 \pm 2.4 \times 10^{6}$	$3.64 \pm 1.3 \times 10^{6}$
Succinate	$^{13}C_{1}$	$3.25 \pm 1.1 \times 10^{5}$	$3.45 \pm 1.1 \times 10^{5}$	$2.28 \pm 1.3 \times 10^{5}$	$1.81 \pm 0.8 \times 10^{5}$
Succinate	$^{13}C_{2}$	$0 \pm 0.0 \times 10^{0}$	$4.36 \pm 1.3 \times 10^{4}$	$2.54 \pm 1.1 \times 10^{5}$	$5.21 \pm 2.1 \times 10^{5}$
Succinate	$^{13}C_{3}$	$0 \pm 0.0 \times 10^{0}$	$0 \pm 0.0 \times 10^{0}$	$4.70 \pm 0.7 \times 10^{3}$	$1.84 \pm 0.7 \times 10^{4}$
Succinate	$^{13}C_{4}$	$0 \pm 0.0 \times 10^{0}$	$2.16 \pm 0.8 \times 10^{4}$	$7.23 \pm 3.1 \times 10^{4}$	$2.93 \pm 1.2 \times 10^{5}$
fumarate	^{12}C	$3.34 \pm 0.7 \times 10^{5}$	$2.61 \pm 0.7 \times 10^{5}$	$1.41 \pm 0.3 \times 10^{5}$	$9.11 \pm 1.9 \times 10^{4}$
fumarate	$^{13}C_{1}$	$3.57 \pm 3.1 \times 10^{3}$	$0 \pm 0.0 \times 10^{0}$	$0 \pm 0.0 \times 10^{0}$	$0 \pm 0.0 \times 10^{0}$
fumarate	$^{13}C_{2}$	$0 \pm 0.0 \times 10^{0}$	$0 \pm 0.0 \times 10^{0}$	$5.30 \pm 9.2 \times 10^{2}$	$4.62 \pm 4.2 \times 10^{3}$
fumarate	$^{13}C_{3}$	$0 \pm 0.0 \times 10^{0}$	$9.26 \pm 10.1 \times 10^{3}$	$2.29 \pm 0.2 \times 10^{4}$	$5.04 \pm 2.0 \times 10^{4}$
fumarate	$^{13}C_{4}$	$0 \pm 0.0 \times 10^{0}$	$0 \pm 0.0 \times 10^{0}$	$0 \pm 0.0 \times 10^{0}$	$0 \pm 0.0 \times 10^{0}$
malate	^{12}C	$1.61 \pm 1.0 \times 10^{6}$	$2.12 \pm 1.8 \times 10^{6}$	$8.36 \pm 9.7 \times 10^{5}$	$3.17 \pm 5.5 \times 10^{5}$
malate	$^{13}C_{1}$	$2.09 \pm 1.0 \times 10^{4}$	$3.82 \pm 1.7 \times 10^{4}$	$1.91 \pm 1.7 \times 10^{4}$	$1.55 \pm 0.7 \times 10^{4}$
malate	$^{13}C_{2}$	$2.34 \pm 1.4 \times 10^{5}$	$3.61 \pm 1.3 \times 10^{5}$	$2.55 \pm 3.6 \times 10^{5}$	$5.29 \pm 2.1 \times 10^{5}$
malate	$^{13}C_{3}$	$2.64 \pm 2.1 \times 10^{4}$	$1.05 \pm 0.3 \times 10^{4}$	$1.27 \pm 1.4 \times 10^{4}$	$3.44 \pm 1.4 \times 10^{4}$
6-phospho-D-gluconate	^{12}C	$1.91 \pm 1.1 \times 10^{3}$	$3.83 \pm 2.9 \times 10^{4}$	$2.48 \pm 0.6 \times 10^{4}$	$2.02 \pm 0.1 \times 10^{4}$
6-phospho-D-gluconate	$^{13}C_{1}$	$0 \pm 0.0 \times 10^{0}$	$0 \pm 0.0 \times 10^{0}$	$0 \pm 0.0 \times 10^{0}$	$0 \pm 0.0 \times 10^{0}$
6-phospho-D-gluconate	$^{13}C_{2}$	$0 \pm 0.0 \times 10^{0}$	$0 \pm 0.0 \times 10^{0}$	$0 \pm 0.0 \times 10^{0}$	$0 \pm 0.0 \times 10^{0}$
6-phospho-D-gluconate	$^{13}C_{3}$	$0 \pm 0.0 \times 10^{0}$	$3.36 \pm 5.8 \times 10^{3}$	$0 \pm 0.0 \times 10^{0}$	$0 \pm 0.0 \times 10^{0}$
6-phospho-D-gluconate	$^{13}C_{4}$	$0 \pm 0.0 \times 10^{0}$	$0 \pm 0.0 \times 10^{0}$	$0 \pm 0.0 \times 10^{0}$	$0 \pm 0.0 \times 10^{0}$
6-phospho-D-gluconate	$^{13}C_{5}$	$0 \pm 0.0 \times 10^{0}$	$4.01 \pm 7.0 \times 10^{3}$	$0 \pm 0.0 \times 10^{0}$	$0 \pm 0.0 \times 10^{0}$
6-phospho-D-gluconate	$^{13}C_{6}$	$0 \pm 0.0 \times 10^{0}$	$4.23 \pm 7.3 \times 10^{4}$	$1.80 \pm 3.1 \times 10^{4}$	$0 \pm 0.0 \times 10^{0}$
D-Xylulose 5-phosphate	^{12}C	$0 \pm 0.0 \times 10^{0}$	$0 \pm 0.0 \times 10^{0}$	$0 \pm 0.0 \times 10^{0}$	$0 \pm 0.0 \times 10^{0}$
D-Xylulose 5-phosphate	$^{13}C_{1}$	$0 \pm 0.0 \times 10^{0}$	$0 \pm 0.0 \times 10^{0}$	$0 \pm 0.0 \times 10^{0}$	$0 \pm 0.0 \times 10^{0}$
D-Xylulose 5-phosphate	$^{13}C_{2}$	$0 \pm 0.0 \times 10^{0}$	$0 \pm 0.0 \times 10^{0}$	$0 \pm 0.0 \times 10^{0}$	$0 \pm 0.0 \times 10^{0}$
D-Xylulose 5-phosphate	$^{13}C_{3}$	$0 \pm 0.0 \times 10^{0}$	$0 \pm 0.0 \times 10^{0}$	$0 \pm 0.0 \times 10^{0}$	$0 \pm 0.0 \times 10^{0}$
D-Xylulose 5-phosphate	$^{13}C_{4}$	$0 \pm 0.0 \times 10^{0}$	$0 \pm 0.0 \times 10^{0}$	$0 \pm 0.0 \times 10^{0}$	$0 \pm 0.0 \times 10^{0}$
D-Xylulose 5-phosphate	$^{13}C_{5}$	$0 \pm 0.0 \times 10^{0}$	$0 \pm 0.0 \times 10^{0}$	$0 \pm 0.0 \times 10^{0}$	$0 \pm 0.0 \times 10^{0}$
D-sedoheptulose-1/7-phosphate	^{12}C	$1.8 \pm 0.7 \times 10^{5}$	$4.55 \pm 0.4 \times 10^{4}$	$1.47 \pm 1.2 \times 10^{4}$	$6.41 \pm 1.1 \times 10^{3}$
D-sedoheptulose-1/7-phosphate	$^{13}C_{1}$	$9.54 \pm 2.5 \times 10^{3}$	$4.23 \pm 0.6 \times 10^{3}$	$4.53 \pm 2.3 \times 10^{3}$	$1.73 \pm 1.6 \times 10^{3}$
D-sedoheptulose-1/7-phosphate	$^{13}C_{2}$	$0 \pm 0.0 \times 10^{0}$	$9.80 \pm 3.1 \times 10^{3}$	$1.20 \pm 1.0 \times 10^{4}$	$9.88 \pm 6.0 \times 10^{3}$

Table A-7 continued.

metabolite	labeling pattern	0 min	2 min	5 min	15 min
D-sedoheptulose-1/7-phosphate	$^{13}C_3$	0 ± 0.0 x 10^0	4.23 ± 2.9 x 10^3	1.19 ± 0.005 x 10^4	1.42 ± 0.4 x 10^4
D-sedoheptulose-1/7-phosphate	$^{13}C_4$	0 ± 0.0 x 10^0	3.42 ± 0.9 x 10^3	1.71 ± 1.1 x 10^4	2.84 ± 0.7 x 10^4
D-sedoheptulose-1/7-phosphate	$^{13}C_5$	0 ± 0.0 x 10^0	3.66 ± 1.1 x 10^3	2.32 ± 0.7 x 10^4	3.02 ± 0.5 x 10^4
D-sedoheptulose-1/7-phosphate	$^{13}C_6$	0 ± 0.0 x 10^0	2.04 ± 2.3 x 10^3	8.64 ± 4.6 x 10^3	1.54 ± 0.8 x 10^4
D-sedoheptulose-1/7-phosphate	$^{13}C_7$	0 ± 0.0 x 10^0	3.54 ± 1.1 x 10^3	2.67 ± 0.2 x 10^4	4.12 ± 2.3 x 10^4
glutamate	^{12}C	3.91 ± 0.1 x 10^7	2.34 ± 0.8 x 10^7	3.01 ± 2.0 x 10^7	1.64 ± 0.3 x 10^7
glutamate	$^{13}C_1$	2.16 ± 0.01 x 10^6	1.26 ± 0.4 x 10^6	1.72 ± 1.1 x 10^6	9.98 ± 1.5 x 10^5
glutamate	$^{13}C_2$	2.42 ± 0.03 x 10^3	1.48 ± 0.5 x 10^5	1.60 ± 0.8 x 10^6	2.91 ± 0.2 x 10^6
glutamate	$^{13}C_3$	6.17 ± 0.5 x 10^3	5.82 ± 4.7 x 10^3	1.56 ± 0.2 x 10^3	1.93 ± 1.2 x 10^3
glutamate	$^{13}C_4$	1.46 ± 0.6 x 10^3	1.36 ± 0.4 x 10^3	1.50 ± 0.5 x 10^3	1.39 ± 0.2 x 10^3
glutamate	$^{13}C_5$	2.07 ± 0.3 x 10^4	1.45 ± 0.1 x 10^4	8.01 ± 3.8 x 10^3	8.90 ± 7.2 x 10^3
glutamine	^{12}C	2.07 ± 0.3 x 10^4	1.45 ± 0.1 x 10^4	8.01 ± 3.8 x 10^3	8.90 ± 7.2 x 10^3
glutamine	$^{13}C_1$	4.15 ± 0.2 x 10^6	2.34 ± 0.5 x 10^6	2.61 ± 0.4 x 10^6	1.58 ± 0.07 x 10^6
glutamine	$^{13}C_2$	7.60 ± 1.7 x 10^4	4.20 ± 0.08 x 10^4	4.36 ± 0.3 x 10^4	4.07 ± 0.7 x 10^4
glutamine	$^{13}C_3$	1.19 ± 0.1 x 10^5	2.72 ± 0.1 x 10^4	2.29 ± 2.2 x 10^4	1.27 ± 0.5 x 10^5
glutamine	$^{13}C_4$	4.54 ± 1.3 x 10^3	2.53 ± 2.1 x 10^3	4.83 ± 1.0 x 10^3	1.35 ± 0.6 x 10^4
glutamine	$^{13}C_5$	7.31 ± 10.7 x 10^2	1.37 ± 0.2 x 10^3	6.49 ± 5.7 x 10^2	3.65 ± 4.6 x 10^3
aspartate	^{12}C	3.51 ± 0.03 x 10^6	1.68 ± 0.6 x 10^6	1.57 ± 0.3 x 10^6	8.93 ± 1.5 x 10^5
aspartate	$^{13}C_1$	4.57 ± 0.5 x 10^4	2.52 ± 0.8 x 10^4	3.98 ± 1.3 x 10^4	2.96 ± 0.5 x 10^4
aspartate	$^{13}C_2$	0 ± 0.0 x 10^0	0 ± 0.0 x 10^0	2.64 ± 0.8 x 10^4	4.90 ± 0.7 x 10^4
aspartate	$^{13}C_3$	0 ± 0.0 x 10^0	6.95 ± 1.8 x 10^4	6.02 ± 1.7 x 10^5	8.31 ± 0.5 x 10^5
aspartate	$^{13}C_4$	0 ± 0.0 x 10^0	0 ± 0.0 x 10^0	1.03 ± 0.3 x 10^4	2.92 ± 0.4 x 10^4
leucine/isoleucine	^{12}C	8.36 ± 1.9 x 10^5	9.31 ± 0.5 x 10^5	8.36 ± 2.0 x 10^5	8.50 ± 0.7 x 10^5
leucine/isoleucine	$^{13}C_1$	1.62 ± 0.4 x 10^4	1.82 ± 0.2 x 10^4	1.67 ± 0.1 x 10^4	1.80 ± 0.3 x 10^4
leucine/isoleucine	$^{13}C_2$	0 ± 0.0 x 10^0	0 ± 0.0 x 10^0	7.38 ± 5.4 x 10^3	8.66 ± 1.9 x 10^3
leucine/isoleucine	$^{13}C_3$	0 ± 0.0 x 10^0	0 ± 0.0 x 10^0	0 ± 0.0 x 10^0	0 ± 0.0 x 10^0
leucine/isoleucine	$^{13}C_4$	0 ± 0.0 x 10^0	0 ± 0.0 x 10^0	0 ± 0.0 x 10^0	0 ± 0.0 x 10^0
leucine/isoleucine	$^{13}C_5$	0 ± 0.0 x 10^0	0 ± 0.0 x 10^0	0 ± 0.0 x 10^0	0 ± 0.0 x 10^0
leucine/isoleucine	$^{13}C_6$	0 ± 0.0 x 10^0	0 ± 0.0 x 10^0	0 ± 0.0 x 10^0	0 ± 0.0 x 10^0
alanine	^{12}C	3.31 ± 0.4 x 10^5	4.49 ± 1.7 x 10^4	1.19 ± 1.0 x 10^5	4.21 ± 1.5 x 10^4
alanine	$^{13}C_1$	0 ± 0.0 x 10^0	2.25 ± 3.9 x 10^5	0 ± 0.0 x 10^0	3.12 ± 5.4 x 10^5
alanine	$^{13}C_2$	0 ± 0.0 x 10^0	0 ± 0.0 x 10^0	0 ± 0.0 x 10^0	0 ± 0.0 x 10^0
alanine	$^{13}C_3$	0 ± 0.0 x 10^0	0 ± 0.0 x 10^0	7.96 ± 6.9 x 10^3	2.67 ± 0.4 x 10^4
L-Valine	^{12}C	9.67 ± 1.5 x 10^6	5.98 ± 0.5 x 10^6	5.99 ± 0.9 x 10^6	4.07 ± 0.06 x 10^6
L-Valine	$^{13}C_1$	5.52 ± 0.08 x 10^5	3.13 ± 0.3 x 10^5	3.41 ± 0.7 x 10^5	2.45 ± 0.1 x 10^5
L-Valine	$^{13}C_2$	4.05 ± 0.5 x 10^3	1.27 ± 0.3 x 10^4	2.21 ± 0.5 x 10^5	4.05 ± 0.5 x 10^5
L-Valine	$^{13}C_3$	0 ± 0.0 x 10^0	8.24 ± 1.2 x 10^3	2.21 ± 0.4 x 10^5	4.30 ± 0.4 x 10^5
L-Valine	$^{13}C_4$	0 ± 0.0 x 10^0	0 ± 0.0 x 10^0	8.36 ± 4.0 x 10^3	2.90 ±0.5 x 10^4
L-Valine	$^{13}C_5$	0 ± 0.0 x 10^0	8.88 ± 15.4 x 10^2	1.40 ± 0.5 x 10^5	5.26 ± 0.6 x 10^5

Table A-8. The average ion counts plus or minus the standard deviation for the metabolites discussed and their isotopomers for the 3 °C experiment at 30, 60 and 120 minutes are shown.

metabolite	labeling pattern	30 min	60 min	120 min
glucose/fructose-6-phosphate	^{12}C	$1.86 \pm 0.5 \times 10^5$	$1.32 \pm 0.5 \times 10^5$	$9.54 \pm 0.9 \times 10^4$
glucose/fructose-6-phosphate	$^{13}C_1$	$0 \pm 0.0 \times 10^0$	$0 \pm 0.0 \times 10^0$	$0 \pm 0.0 \times 10^0$
glucose/fructose-6-phosphate	$^{13}C_2$	$0 \pm 0.0 \times 10^0$	$0 \pm 0.0 \times 10^0$	$0 \pm 0.0 \times 10^0$
glucose/fructose-6-phosphate	$^{13}C_3$	$6.91 \pm 1.8 \times 10^4$	$3.61 \pm 3.2 \times 10^4$	$0 \pm 0.0 \times 10^0$
glucose/fructose-6-phosphate	$^{13}C_4$	$1.71 \pm 3.0 \times 10^4$	$2.16 \pm 3.7 \times 10^4$	$0 \pm 0.0 \times 10^0$
glucose/fructose-6-phosphate	$^{13}C_5$	$9.26 \pm 1.8 \times 10^4$	$7.10 \pm 6.3 \times 10^4$	$8.49 \pm 1.7 \times 10^4$
glucose/fructose-6-phosphate	$^{13}C_6$	$1.27 \pm 0.3 \times 10^6$	$1.32 \pm 0.4 \times 10^6$	$1.23 \pm 0.2 \times 10^6$
fructose-1-6-bisphosphate	^{12}C	$4.60 \pm 3.5 \times 10^5$	$4.05 \pm 4.6 \times 10^5$	$2.96 \pm 1.7 \times 10^5$
fructose-1-6-bisphosphate	$^{13}C_1$	$3.43 \pm 2.3 \times 10^4$	$3.23 \pm 3.6 \times 10^4$	$2.36 \pm 1.0 \times 10^4$
fructose-1-6-bisphosphate	$^{13}C_2$	$3.11 \pm 2.0 \times 10^4$	$2.09 \pm 2.2 \times 10^4$	$2.39 \pm 1.0 \times 10^4$
fructose-1-6-bisphosphate	$^{13}C_3$	$5.26 \pm 3.6 \times 10^5$	$3.87 \pm 4.1 \times 10^5$	$3.83 \pm 1.5 \times 10^5$
fructose-1-6-bisphosphate	$^{13}C_4$	$5.19 \pm 3.6 \times 10^4$	$3.11 \pm 3.2 \times 10^4$	$2.80 \pm 3.1 \times 10^4$
fructose-1-6-bisphosphate	$^{13}C_5$	$9.34 \pm 7.0 \times 10^4$	$5.48 \pm 5.3 \times 10^4$	$5.59 \pm 4.3 \times 10^4$
fructose-1-6-bisphosphate	$^{13}C_6$	$9.56 \pm 7.2 \times 10^5$	$6.24 \pm 6.4 \times 10^5$	$6.56 \pm 4.7 \times 10^5$
1,3-Diphosphoglyceric acid	^{12}C	$1.10 \pm 0.1 \times 10^3$	$4.33 \pm 3.8 \times 10^2$	$5.03 \pm 0.4 \times 10^2$
1,3-Diphosphoglyceric acid	$^{13}C_1$	$0 \pm 0.0 \times 10^0$	$0 \pm 0.0 \times 10^0$	$0 \pm 0.0 \times 10^0$
1,3-Diphosphoglyceric acid	$^{13}C_2$	$0 \pm 0.0 \times 10^0$	$0 \pm 0.0 \times 10^0$	$0 \pm 0.0 \times 10^0$
1,3-Diphosphoglyceric acid	$^{13}C_3$	$0 \pm 0.0 \times 10^0$	$0 \pm 0.0 \times 10^0$	$0 \pm 0.0 \times 10^0$
Pyruvate	^{12}C	$1.40 \pm 0.1 \times 10^5$	$1.48 \pm 0.7 \times 10^5$	$5.13 \pm 0.8 \times 10^4$
Pyruvate	$^{13}C_1$	$0 \pm 0.0 \times 10^0$	$0 \pm 0.0 \times 10^0$	$0 \pm 0.0 \times 10^0$
Pyruvate	$^{13}C_2$	$0 \pm 0.0 \times 10^0$	$5.03 \pm 8.7 \times 10^3$	$0 \pm 0.0 \times 10^0$
Pyruvate	$^{13}C_3$	$2.40 \pm 2.0 \times 10^5$	$3.95 \pm 3.7 \times 10^5$	$0 \pm 0.0 \times 10^0$
alpha-ketoglutarate	^{12}C	$6.27 \pm 1.3 \times 10^5$	$5.83 \pm 2.5 \times 10^5$	$3.88 \pm 1.2 \times 10^5$
alpha-ketoglutarate	$^{13}C_1$	$1.25 \pm 0.2 \times 10^4$	$1.52 \pm 0.5 \times 10^4$	$8.60 \pm 4.0 \times 10^3$
alpha-ketoglutarate	$^{13}C_2$	$1.10 \pm 0.4 \times 10^5$	$2.51 \pm 1.0 \times 10^5$	$2.20 \pm 0.4 \times 10^5$
alpha-ketoglutarate	$^{13}C_3$	$1.36 \pm 0.3 \times 10^4$	$4.53 \pm 1.8 \times 10^4$	$6.38 \pm 0.1 \times 10^4$
alpha-ketoglutarate	$^{13}C_4$	$4.89 \pm 1.1 \times 10^2$	$4.29 \pm 0.4 \times 10^2$	$4.57 \pm 2.2 \times 10^2$
alpha-ketoglutarate	$^{13}C_5$	$1.21 \pm 2.1 \times 10^2$	$1.10 \pm 1.9 \times 10^2$	$2.70 \pm 2.8 \times 10^2$
succinyl-CoA	^{12}C	$3.10 \pm 2.8 \times 10^4$	$1.47 \pm 2.2 \times 10^4$	$1.63 \pm 2.8 \times 10^4$
succinyl-CoA	$^{13}C_1$	$0 \pm 0.0 \times 10^0$	$0 \pm 0.0 \times 10^0$	$0 \pm 0.0 \times 10^0$
succinyl-CoA	$^{13}C_2$	$0 \pm 0.0 \times 10^0$	$0 \pm 0.0 \times 10^0$	$0 \pm 0.0 \times 10^0$
succinyl-CoA	$^{13}C_3$	$0 \pm 0.0 \times 10^0$	$0 \pm 0.0 \times 10^0$	$0 \pm 0.0 \times 10^0$
succinyl-CoA	$^{13}C_4$	$0 \pm 0.0 \times 10^0$	$0 \pm 0.0 \times 10^0$	$0 \pm 0.0 \times 10^0$
succinyl-CoA	$^{13}C_5$	$0 \pm 0.0 \times 10^0$	$0 \pm 0.0 \times 10^0$	$0 \pm 0.0 \times 10^0$
succinyl-CoA	$^{13}C_6$	$0 \pm 0.0 \times 10^0$	$0 \pm 0.0 \times 10^0$	$0 \pm 0.0 \times 10^0$
succinyl-CoA	$^{13}C_7$	$0 \pm 0.0 \times 10^0$	$0 \pm 0.0 \times 10^0$	$0 \pm 0.0 \times 10^0$
succinyl-CoA	$^{13}C_8$	$0 \pm 0.0 \times 10^0$	$0 \pm 0.0 \times 10^0$	$0 \pm 0.0 \times 10^0$
succinyl-CoA	$^{13}C_9$	$0 \pm 0.0 \times 10^0$	$0 \pm 0.0 \times 10^0$	$0 \pm 0.0 \times 10^0$
succinyl-CoA	$^{13}C_{10}$	$0 \pm 0.0 \times 10^0$	$0 \pm 0.0 \times 10^0$	$0 \pm 0.0 \times 10^0$
succinyl-CoA	$^{13}C_{11}$	$0 \pm 0.0 \times 10^0$	$0 \pm 0.0 \times 10^0$	$0 \pm 0.0 \times 10^0$

Table A-8 continued.

metabolite	labeling pattern	30 min	60 min	120 min
succinyl-CoA	$^{13}C_{12}$	$0 \pm 0.0 \times 10^{0}$	$0 \pm 0.0 \times 10^{0}$	$0 \pm 0.0 \times 10^{0}$
succinyl-CoA	$^{13}C_{13}$	$0 \pm 0.0 \times 10^{0}$	$0 \pm 0.0 \times 10^{0}$	$0 \pm 0.0 \times 10^{0}$
succinyl-CoA	$^{13}C_{14}$	$0 \pm 0.0 \times 10^{0}$	$0 \pm 0.0 \times 10^{0}$	$0 \pm 0.0 \times 10^{0}$
succinyl-CoA	$^{13}C_{15}$	$0 \pm 0.0 \times 10^{0}$	$0 \pm 0.0 \times 10^{0}$	$0 \pm 0.0 \times 10^{0}$
succinyl-CoA	$^{13}C_{16}$	$0 \pm 0.0 \times 10^{0}$	$0 \pm 0.0 \times 10^{0}$	$0 \pm 0.0 \times 10^{0}$
succinyl-CoA	$^{13}C_{17}$	$0 \pm 0.0 \times 10^{0}$	$0 \pm 0.0 \times 10^{0}$	$0 \pm 0.0 \times 10^{0}$
succinyl-CoA	$^{13}C_{18}$	$0 \pm 0.0 \times 10^{0}$	$0 \pm 0.0 \times 10^{0}$	$0 \pm 0.0 \times 10^{0}$
succinyl-CoA	$^{13}C_{19}$	$0 \pm 0.0 \times 10^{0}$	$0 \pm 0.0 \times 10^{0}$	$0 \pm 0.0 \times 10^{0}$
succinyl-CoA	$^{13}C_{20}$	$0 \pm 0.0 \times 10^{0}$	$0 \pm 0.0 \times 10^{0}$	$0 \pm 0.0 \times 10^{0}$
succinyl-CoA	$^{13}C_{21}$	$0 \pm 0.0 \times 10^{0}$	$0 \pm 0.0 \times 10^{0}$	$0 \pm 0.0 \times 10^{0}$
succinyl-CoA	$^{13}C_{22}$	$0 \pm 0.0 \times 10^{0}$	$0 \pm 0.0 \times 10^{0}$	$0 \pm 0.0 \times 10^{0}$
succinyl-CoA	$^{13}C_{23}$	$0 \pm 0.0 \times 10^{0}$	$0 \pm 0.0 \times 10^{0}$	$0 \pm 0.0 \times 10^{0}$
succinyl-CoA	$^{13}C_{24}$	$0 \pm 0.0 \times 10^{0}$	$0 \pm 0.0 \times 10^{0}$	$0 \pm 0.0 \times 10^{0}$
succinyl-CoA	$^{13}C_{25}$	$0 \pm 0.0 \times 10^{0}$	$0 \pm 0.0 \times 10^{0}$	$0 \pm 0.0 \times 10^{0}$
Succinate	^{12}C	$3.02 \pm 0.4 \times 10^{6}$	$2.01 \pm 0.3 \times 10^{6}$	$1.83 \pm 0.1 \times 10^{6}$
Succinate	$^{13}C_{1}$	$1.60 \pm 0.2 \times 10^{5}$	$1.20 \pm 0.2 \times 10^{5}$	$1.24 \pm 0.03 \times 10^{5}$
Succinate	$^{13}C_{2}$	$7.83 \pm 0.7 \times 10^{5}$	$8.06 \pm 1.3 \times 10^{5}$	$1.03 \pm 0.1 \times 10^{6}$
Succinate	$^{13}C_{3}$	$1.13 \pm 0.2 \times 10^{5}$	$2.18 \pm 0.3 \times 10^{5}$	$4.49 \pm 0.6 \times 10^{5}$
Succinate	$^{13}C_{4}$	$8.06 \pm 1.1 \times 10^{5}$	$1.62 \pm 0.4 \times 10^{6}$	$3.22 \pm 0.7 \times 10^{6}$
fumarate	^{12}C	$6.73 \pm 0.6 \times 10^{4}$	$3.99 \pm 0.8 \times 10^{4}$	$2.45 \pm 0.8 \times 10^{4}$
fumarate	$^{13}C_{1}$	$0 \pm 0.0 \times 10^{0}$	$0 \pm 0.0 \times 10^{0}$	$0 \pm 0.0 \times 10^{0}$
fumarate	$^{13}C_{2}$	$7.53 \pm 1.4 \times 10^{3}$	$5.83 \pm 5.1 \times 10^{3}$	$6.60 \pm 5.8 \times 10^{3}$
fumarate	$^{13}C_{3}$	$8.52 \pm 1.0 \times 10^{4}$	$9.88 \pm 2.0 \times 10^{4}$	$1.17 \pm 0.2 \times 10^{5}$
fumarate	$^{13}C_{4}$	$1.01 \pm 0.2 \times 10^{4}$	$1.75 \pm 0.2 \times 10^{4}$	$4.21 \pm 1.2 \times 10^{4}$
malate	^{12}C	$6.47 \pm 5.7 \times 10^{5}$	$4.48 \pm 4.4 \times 10^{5}$	$0 \pm 0.0 \times 10^{0}$
malate	$^{13}C_{1}$	$2.29 \pm 0.8 \times 10^{4}$	$1.65 \pm 0.5 \times 10^{4}$	$1.34 \pm 0.5 \times 10^{4}$
malate	$^{13}C_{2}$	$8.24 \pm 0.3 \times 10^{5}$	$8.21 \pm 4.4 \times 10^{5}$	$1.03 \pm 0.5 \times 10^{6}$
malate	$^{13}C_{3}$	$9.52 \pm 7.3 \times 10^{4}$	$1.74 \pm 1.3 \times 10^{5}$	$3.63 \pm 2.0 \times 10^{5}$
6-phospho-D-gluconate	^{12}C	$2.92 \pm 1.8 \times 10^{4}$	$2.27 \pm 0.3 \times 10^{4}$	$2.05 \pm 0.1 \times 10^{4}$
6-phospho-D-gluconate	$^{13}C_{1}$	$0 \pm 0.0 \times 10^{0}$	$0 \pm 0.0 \times 10^{0}$	$0 \pm 0.0 \times 10^{0}$
6-phospho-D-gluconate	$^{13}C_{2}$	$0 \pm 0.0 \times 10^{0}$	$0 \pm 0.0 \times 10^{0}$	$0 \pm 0.0 \times 10^{0}$
6-phospho-D-gluconate	$^{13}C_{3}$	$0 \pm 0.0 \times 10^{0}$	$0 \pm 0.0 \times 10^{0}$	$0 \pm 0.0 \times 10^{0}$
6-phospho-D-gluconate	$^{13}C_{4}$	$0 \pm 0.0 \times 10^{0}$	$0 \pm 0.0 \times 10^{0}$	$0 \pm 0.0 \times 10^{0}$
6-phospho-D-gluconate	$^{13}C_{5}$	$0 \pm 0.0 \times 10^{0}$	$0 \pm 0.0 \times 10^{0}$	$0 \pm 0.0 \times 10^{0}$
6-phospho-D-gluconate	$^{13}C_{6}$	$3.20 \pm 3.7 \times 10^{4}$	$0 \pm 0.0 \times 10^{0}$	$0 \pm 0.0 \times 10^{0}$
D-Xylulose 5-phosphate	^{12}C	$0 \pm 0.0 \times 10^{0}$	$0 \pm 0.0 \times 10^{0}$	$0 \pm 0.0 \times 10^{0}$
D-Xylulose 5-phosphate	$^{13}C_{1}$	$0 \pm 0.0 \times 10^{0}$	$0 \pm 0.0 \times 10^{0}$	$0 \pm 0.0 \times 10^{0}$
D-Xylulose 5-phosphate	$^{13}C_{2}$	$0 \pm 0.0 \times 10^{0}$	$0 \pm 0.0 \times 10^{0}$	$0 \pm 0.0 \times 10^{0}$
D-Xylulose 5-phosphate	$^{13}C_{3}$	$0 \pm 0.0 \times 10^{0}$	$0 \pm 0.0 \times 10^{0}$	$0 \pm 0.0 \times 10^{0}$
D-Xylulose 5-phosphate	$^{13}C_{4}$	$0 \pm 0.0 \times 10^{0}$	$0 \pm 0.0 \times 10^{0}$	$0 \pm 0.0 \times 10^{0}$
D-Xylulose 5-phosphate	$^{13}C_{5}$	$0 \pm 0.0 \times 10^{0}$	$0 \pm 0.0 \times 10^{0}$	$0 \pm 0.0 \times 10^{0}$
D-sedoheptulose-1/7-phosphate	^{12}C	$1.49 \pm 1.0 \times 10^{3}$	$0 \pm 0.0 \times 10^{0}$	$2.42 \pm 4.2 \times 10^{2}$

Table A-8 continued.

metabolite	labeling pattern	30 min	60 min	120 min
D-sedoheptulose-1/7-phosphate	$^{13}C_1$	$0 \pm 0.0 \times 10^{0}$	$0 \pm 0.0 \times 10^{0}$	$0 \pm 0.0 \times 10^{0}$
D-sedoheptulose-1/7-phosphate	$^{13}C_2$	$1.45 \pm 1.3 \times 10^{3}$	$1.07 \pm 10.7 \times 10^{2}$	$7.17 \pm 12.4 \times 10^{2}$
D-sedoheptulose-1/7-phosphate	$^{13}C_3$	$3.47 \pm 3.0 \times 10^{3}$	$1.81 \pm 1.6 \times 10^{3}$	$0 \pm 0.0 \times 10^{0}$
D-sedoheptulose-1/7-phosphate	$^{13}C_4$	$1.08 \pm 1.3 \times 10^{4}$	$6.20 \pm 5.2 \times 10^{3}$	$1.94 \pm 1.8 \times 10^{3}$
D-sedoheptulose-1/7-phosphate	$^{13}C_5$	$1.33 \pm 1.6 \times 10^{4}$	$4.87 \pm 3.4 \times 10^{3}$	$5.21 \pm 4.6 \times 10^{3}$
D-sedoheptulose-1/7-phosphate	$^{13}C_6$	$1.48 \pm 1.4 \times 10^{4}$	$3.94 \pm 0.5 \times 10^{3}$	$1.02 \pm 1.0 \times 10^{4}$
D-sedoheptulose-1/7-phosphate	$^{13}C_7$	$5.96 \pm 6.0 \times 10^{4}$	$9.36 \pm 1.1 \times 10^{4}$	$6.34 \pm 5.8 \times 10^{4}$
glutamate	^{12}C	$1.58 \pm 0.5 \times 10^{7}$	$1.07 \pm 0.5 \times 10^{7}$	$7.03 \pm 2.1 \times 10^{6}$
glutamate	$^{13}C_1$	$1.11 \pm 0.3 \times 10^{6}$	$9.03 \pm 3.9 \times 10^{5}$	$7.30 \pm 2.0 \times 10^{5}$
glutamate	$^{13}C_2$	$5.01 \pm 1.2 \times 10^{6}$	$6.20 \pm 1.8 \times 10^{6}$	$6.37 \pm 0.9 \times 10^{6}$
glutamate	$^{13}C_3$	$9.84 \pm 17.1 \times 10^{1}$	$1.38 \pm 2.0 \times 10^{3}$	$1.43 \pm 0.6 \times 10^{3}$
glutamate	$^{13}C_4$	$1.09 \pm 1.9 \times 10^{2}$	$1.74 \pm 3.0 \times 10^{3}$	$1.36 \pm 0.3 \times 10^{4}$
glutamate	$^{13}C_5$	$4.89 \pm 7.3 \times 10^{3}$	$3.40 \pm 2.8 \times 10^{3}$	$7.76 \pm 2.8 \times 10^{3}$
glutamine	^{12}C	$4.89 \pm 7.3 \times 10^{3}$	$3.40 \pm 2.8 \times 10^{3}$	$7.76 \pm 2.8 \times 10^{3}$
glutamine	$^{13}C_1$	$1.57 \pm 0.5 \times 10^{6}$	$8.30 \pm 7.3 \times 10^{5}$	$6.87 \pm 3.5 \times 10^{5}$
glutamine	$^{13}C_2$	$5.15 \pm 0.6 \times 10^{4}$	$5.23 \pm 1.4 \times 10^{4}$	$5.73 \pm 1.9 \times 10^{4}$
glutamine	$^{13}C_3$	$3.58 \pm 0.3 \times 10^{5}$	$3.50 \pm 1.2 \times 10^{5}$	$5.11 \pm 1.3 \times 10^{5}$
glutamine	$^{13}C_4$	$4.07 \pm 0.1 \times 10^{4}$	$6.56 \pm 0.6 \times 10^{4}$	$1.15 \pm 0.2 \times 10^{5}$
glutamine	$^{13}C_5$	$1.29 \pm 1.2 \times 10^{3}$	$9.44 \pm 16.3 \times 10^{1}$	$5.36 \pm 5.5 \times 10^{2}$
aspartate	^{12}C	$8.20 \pm 1.3 \times 10^{5}$	$4.64 \pm 1.7 \times 10^{5}$	$2.97 \pm 1.0 \times 10^{5}$
aspartate	$^{13}C_1$	$3.74 \pm 0.2 \times 10^{4}$	$2.32 \pm 0.6 \times 10^{4}$	$2.53 \pm 0.1 \times 10^{4}$
aspartate	$^{13}C_2$	$1.63 \pm 0.5 \times 10^{5}$	$1.70 \pm 1.0 \times 10^{5}$	$2.61 \pm 0.6 \times 10^{5}$
aspartate	$^{13}C_3$	$1.43 \pm 0.3 \times 10^{6}$	$1.65 \pm 0.4 \times 10^{6}$	$2.30 \pm 0.1 \times 10^{6}$
aspartate	$^{13}C_4$	$1.31 \pm 0.6 \times 10^{5}$	$3.23 \pm 0.7 \times 10^{5}$	$7.20 \pm 0.4 \times 10^{5}$
leucine/isoleucine	^{12}C	$9.01 \pm 1.6 \times 10^{5}$	$7.52 \pm 0.5 \times 10^{5}$	$8.84 \pm 1.0 \times 10^{5}$
leucine/isoleucine	$^{13}C_1$	$1.75 \pm 0.08 \times 10^{4}$	$1.47 \pm 0.2 \times 10^{4}$	$2.04 \pm 0.4 \times 10^{4}$
leucine/isoleucine	$^{13}C_2$	$1.16 \pm 1.0 \times 10^{4}$	$1.51 \pm 1.3 \times 10^{4}$	$4.65 \pm 8.1 \times 10^{4}$
leucine/isoleucine	$^{13}C_3$	$0 \pm 0.0 \times 10^{0}$	$0 \pm 0.0 \times 10^{0}$	$0 \pm 0.0 \times 10^{0}$
leucine/isoleucine	$^{13}C_4$	$6.75 \pm 0.5 \times 10^{3}$	$1.36 \pm 0.3 \times 10^{4}$	$3.62 \pm 0.8 \times 10^{4}$
leucine/isoleucine	$^{13}C_5$	$0 \pm 0.0 \times 10^{0}$	$0 \pm 0.0 \times 10^{0}$	$0 \pm 0.0 \times 10^{0}$
leucine/isoleucine	$^{13}C_6$	$2.99 \pm 2.8 \times 10^{3}$	$1.92 \pm 0.6 \times 10^{4}$	$1.26 \pm 0.4 \times 10^{5}$
alanine	^{12}C	$7.51 \pm 5.0 \times 10^{4}$	$3.20 \pm 0.4 \times 10^{4}$	$1.77 \pm 0.1 \times 10^{4}$
alanine	$^{13}C_1$	$0 \pm 0.0 \times 10^{0}$	$0 \pm 0.0 \times 10^{0}$	$3.40 \pm 5.9 \times 10^{5}$
alanine	$^{13}C_2$	$1.49 \pm 2.6 \times 10^{3}$	$0 \pm 0.0 \times 10^{0}$	$0 \pm 0.0 \times 10^{0}$
alanine	$^{13}C_3$	$8.32 \pm 4.8 \times 10^{4}$	$1.93 \pm 0.4 \times 10^{5}$	$1.35 \pm 1.2 \times 10^{5}$
L-Valine	^{12}C	$4.53 \pm 1.0 \times 10^{6}$	$3.11 \pm 0.9 \times 10^{6}$	$2.80 \pm 0.5 \times 10^{6}$
L-Valine	$^{13}C_1$	$2.84 \pm 0.7 \times 10^{5}$	$1.95 \pm 0.6 \times 10^{5}$	$1.87 \pm 0.3 \times 10^{5}$
L-Valine	$^{13}C_2$	$7.49 \pm 0.7 \times 10^{5}$	$8.46 \pm 1.0 \times 10^{5}$	$9.38 \pm 0.9 \times 10^{5}$
L-Valine	$^{13}C_3$	$8.23 \pm 0.6 \times 10^{5}$	$9.74 \pm 1.0 \times 10^{5}$	$1.10 \pm 0.1 \times 10^{6}$
L-Valine	$^{13}C_4$	$1.87 \pm 0.3 \times 10^{5}$	$3.78 \pm 0.8 \times 10^{5}$	$7.34 \pm 0.4 \times 10^{5}$
L-Valine	$^{13}C_5$	$1.88 \pm 0.3 \times 10^{6}$	$3.77 \pm 0.5 \times 10^{6}$	$6.78 \pm 0.7 \times 10^{6}$

Table A-9. The average ion counts plus or minus the standard deviation for the metabolites discussed and their isotopomers for the wild type *Salmonella enterica* study at 0, 2, 5, and 15 minutes are shown.

metabolite	labeling pattern	0 min	2 min	5 min	15 min
glucose/fructose-6-phosphate	^{12}C	$5.37 \pm 1.3 \times 10^5$	$1.84 \pm 0.4 \times 10^5$	$1.70 \pm 0.6 \times 10^5$	$1.36 \pm 0.5 \times 10^5$
glucose/fructose-6-phosphate	$^{13}C_1$	$1.46 \pm 1.7 \times 10^4$	$6.04 \pm 10.5 \times 10^3$	$0 \pm 0.0 \times 10^0$	$8.03 \pm 0.9 \times 10$
glucose/fructose-6-phosphate	$^{13}C_2$	$0 \pm 0.0 \times 10^0$	$0 \pm 0.0 \times 10^0$	$0 \pm 0.0 \times 10^0$	$0 \pm 0.0 \times 10^0$
glucose/fructose-6-phosphate	$^{13}C_3$	$0 \pm 0.0 \times 10^0$	$0 \pm 0.0 \times 10^0$	$0 \pm 0.0 \times 10^0$	$0 \pm 0.0 \times 10^0$
glucose/fructose-6-phosphate	$^{13}C_4$	$0 \pm 0.0 \times 10^0$	$0 \pm 0.0 \times 10^0$	$0 \pm 0.0 \times 10^0$	$0 \pm 0.0 \times 10^0$
glucose/fructose-6-phosphate	$^{13}C_5$	$0 \pm 0.0 \times 10^0$	$2.75 \pm 2.9 \times 10^4$	$4.47 \pm 2.3 \times 10^4$	$2.7 \pm 2.5 \times 10^4$
glucose/fructose-6-phosphate	$^{13}C_6$	$5.76 \pm 10.0 \times 10^3$	$4.64 \pm 6.8 \times 10^5$	$6.69 \pm 4.3 \times 10^5$	$1.65 \pm 1.6 \times 10^5$
fructose-1-6-bisphosphate	^{12}C	$2.29 \pm 1.8 \times 10^5$	$5.29 \pm 2.1 \times 10^4$	$1.01 \pm 1.3 \times 10^5$	$1.63 \pm 0.5 \times 10^5$
fructose-1-6-bisphosphate	$^{13}C_1$	$9.57 \pm 9.4 \times 10^3$	$2.89 \pm 4.1 \times 10^3$	$2.31 \pm 0.6 \times 10^3$	$1.20 \pm 2.4 \times 10^4$
fructose-1-6-bisphosphate	$^{13}C_2$	$5.11 \pm 5.7 \times 10^3$	$1.45 \pm 2.5 \times 10^3$	$2.02 \pm 3.5 \times 10^3$	$6.28 \pm 4.7 \times 10^3$
fructose-1-6-bisphosphate	$^{13}C_3$	$3.54 \pm 3.1 \times 10^3$	$6.21 \pm 7.7 \times 10^3$	$9.35 \pm 11.3 \times 10^3$	$7.20 \pm 1.3 \times 10^3$
fructose-1-6-bisphosphate	$^{13}C_4$	$4.19 \pm 7.3 \times 10^2$	$3.38 \pm 3.1 \times 10^3$	$3.31 \pm 2.7 \times 10^3$	$2.32 \pm 3.2 \times 10^3$
fructose-1-6-bisphosphate	$^{13}C_5$	$1.22 \pm 1.1 \times 10^4$	$1.14 \pm 1.0 \times 10^4$	$7.90 \pm 4.6 \times 10^3$	$1.35 \pm 0.5 \times 10^4$
fructose-1-6-bisphosphate	$^{13}C_6$	$1.82 \pm 1.6 \times 10^5$	$3.37 \pm 2.9 \times 10^5$	$3.99 \pm 3.2 \times 10^5$	$2.52 \pm 0.6 \times 10^5$
D-glyceraldehdye-3-phosphate	^{12}C	$4.06 \pm 0.6 \times 10^6$	$2.46 \pm 0.7 \times 10^6$	$2.04 \pm 0.5 \times 10^6$	$1.31 \pm 0.5 \times 10^6$
D-glyceraldehdye-3-phosphate	$^{13}C_1$	$3.62 \pm 0.9 \times 10^4$	$3.00 \pm 2.8 \times 10^4$	$2.25 \pm 0.4 \times 10^4$	$2.65 \pm 0.8 \times 10^4$
D-glyceraldehdye-3-phosphate	$^{13}C_2$	$4.46 \pm 2.5 \times 10^3$	$5.30 \pm 3.5 \times 10^3$	$3.54 \pm 1.2 \times 10^3$	$7.10 \pm 3.3 \times 10^3$
D-glyceraldehdye-3-phosphate	$^{13}C_3$	$0 \pm 0.0 \times 10^0$	$8.51 \pm 14.7 \times 10^3$	$1.23 \pm 1.1 \times 10^5$	$4.81 \pm 1.5 \times 10^5$
1,3-diphopshateglycerate	^{12}C	$7.01 \pm 5.7 \times 10^3$	$4.02 \pm 5.0 \times 10^3$	$4.33 \pm 1.3 \times 10^3$	$7.67 \pm 1.1 \times 10^3$
1,3-diphopshateglycerate	$^{13}C_1$	$0 \pm 0.0 \times 10^0$	$0 \pm 0.0 \times 10^0$	$0 \pm 0.0 \times 10^0$	$0 \pm 0.0 \times 10^0$
1,3-diphopshateglycerate	$^{13}C_2$	$1.40 \pm 2.4 \times 10^3$	$2.90 \pm 5.0 \times 10^3$	$1.91 \pm 2.1 \times 10^3$	$3.53 \pm 6.1 \times 10^2$
1,3-diphopshateglycerate	$^{13}C_3$	$5.23 \pm 9.1 \times 10^2$	$4.19 \pm 7.3 \times 10^3$	$1.38 \pm 1.4 \times 10^4$	$9.67 \pm 8.5 \times 10^3$
3/2-phosphoglycerate	^{12}C	$4.81 \pm 3.4 \times 10^4$	$2.31 \pm 1.1 \times 10^4$	$2.77 \pm 2.1 \times 10^4$	$1.47 \pm 1.0 \times 10^4$
3/2-phosphoglycerate	$^{13}C_1$	$2.76 \pm 2.8 \times 10^2$	$0 \pm 0.0 \times 10^0$	$3.86 \pm 6.7 \times 10^2$	$3.24 \pm 5.6 \times 10^2$
3/2-phosphoglycerate	$^{13}C_2$	$0 \pm 0.0 \times 10^0$	$0 \pm 0.0 \times 10^0$	$0 \pm 0.0 \times 10^0$	$0 \pm 0.0 \times 10^0$
3/2-phosphoglycerate	$^{13}C_3$	$0 \pm 0.0 \times 10^0$	$0 \pm 0.0 \times 10^0$	$0 \pm 0.0 \times 10^0$	$0 \pm 0.0 \times 10^0$
pyruvate	^{12}C	$2.43 \pm 1.2 \times 10^8$	$3.41 \pm 3.0 \times 10^7$	$1.18 \pm 0.6 \times 10^7$	$6.78 \pm 2.8 \times 10^6$
pyruvate	$^{13}C_1$	$8.83 \pm 4.5 \times 10^6$	$1.89 \pm 2.0 \times 10^6$	$2.05 \pm 3.3 \times 10^5$	$4.77 \pm 2.8 \times 10^4$
pyruvate	$^{13}C_2$	$2.60 \pm 0.5 \times 10^4$	$3.38 \pm 3.0 \times 10^6$	$2.28 \pm 3.5 \times 10^6$	$8.85 \pm 7.6 \times 10^4$
pyruvate	$^{13}C_3$	$0 \pm 0.0 \times 10^0$	$9.37 \pm 8.0 \times 10^7$	$6.67 \pm 8.3 \times 10^7$	$1.03 \pm 0.6 \times 10^7$
alpha-ketoglutarate	^{12}C	$9.04 \pm 0.6 \times 10^7$	$3.99 \pm 1.6 \times 10^7$	$1.09 \pm 0.5 \times 10^7$	$2.18 \pm 0.9 \times 10^6$
alpha-ketoglutarate	$^{13}C_1$	$4.54 \pm 0.3 \times 10^6$	$2.93 \pm 1.3 \times 10^6$	$7.33 \pm 4.1 \times 10^5$	$9.99 \pm 1.5 \times 10^4$
alpha-ketoglutarate	$^{13}C_2$	$3.24 \pm 0.3 \times 10^5$	$1.48 \pm 0.4 \times 10^7$	$6.94 \pm 2.2 \times 10^6$	$7.92 \pm 4.1 \times 10^5$
alpha-ketoglutarate	$^{13}C_3$	$6.09 \pm 0.7 \times 10^3$	$9.57 \pm 2.3 \times 10^6$	$9.15 \pm 2.7 \times 10^6$	$3.50 \pm 1.0 \times 10^6$

Table A-9 continued.

metabolite	labeling pattern	0 min	2 min	5 min	15 min
alpha-ketoglutarate	$^{13}C_4$	$0 \pm 0.0 \times 10^0$	$1.03 \pm 0.2 \times 10^7$	$1.34 \pm 0.4 \times 10^7$	$6.52 \pm 1.7 \times 10^6$
alpha-ketoglutarate	$^{13}C_5$	$0 \pm 0.0 \times 10^0$	$1.53 \pm 0.1 \times 10^7$	$3.33 \pm 1.2 \times 10^7$	$2.88 \pm 0.5 \times 10^7$
succinyl-CoA	^{12}C	$9.64 \pm 14.7 \times 10^3$	$1.10 \pm 1.9 \times 10^3$	$3.47 \pm 6.0 \times 10^3$	$2.65 \pm 1.2 \times 10^4$
succinyl-CoA	$^{13}C_1$	$0 \pm 0.0 \times 10^0$	$0 \pm 0.0 \times 10^0$	$0 \pm 0.0 \times 10^0$	$2.22 \pm 2.2 \times 10^3$
succinyl-CoA	$^{13}C_2$	$0 \pm 0.0 \times 10^0$	$0 \pm 0.0 \times 10^0$	$0 \pm 0.0 \times 10^0$	$0 \pm 0.0 \times 10^0$
succinyl-CoA	$^{13}C_3$	$0 \pm 0.0 \times 10^0$	$0 \pm 0.0 \times 10^0$	$0 \pm 0.0 \times 10^0$	$0 \pm 0.0 \times 10^0$
succinyl-CoA	$^{13}C_4$	$0 \pm 0.0 \times 10^0$	$3.13 \pm 5.4 \times 10^3$	$0 \pm 0.0 \times 10^0$	$0 \pm 0.0 \times 10^0$
succinyl-CoA	$^{13}C_5$	$0 \pm 0.0 \times 10^0$	$0 \pm 0.0 \times 10^0$	$0 \pm 0.0 \times 10^0$	$0 \pm 0.0 \times 10^0$
succinyl-CoA	$^{13}C_6$	$0 \pm 0.0 \times 10^0$	$0 \pm 0.0 \times 10^0$	$0 \pm 0.0 \times 10^0$	$0 \pm 0.0 \times 10^0$
succinyl-CoA	$^{13}C_7$	$0 \pm 0.0 \times 10^0$	$0 \pm 0.0 \times 10^0$	$0 \pm 0.0 \times 10^0$	$0 \pm 0.0 \times 10^0$
succinyl-CoA	$^{13}C_8$	$0 \pm 0.0 \times 10^0$	$0 \pm 0.0 \times 10^0$	$0 \pm 0.0 \times 10^0$	$0 \pm 0.0 \times 10^0$
succinyl-CoA	$^{13}C_9$	$0 \pm 0.0 \times 10^0$	$0 \pm 0.0 \times 10^0$	$0 \pm 0.0 \times 10^0$	$0 \pm 0.0 \times 10^0$
succinyl-CoA	$^{13}C_{10}$	$0 \pm 0.0 \times 10^0$	$0 \pm 0.0 \times 10^0$	$0 \pm 0.0 \times 10^0$	$0 \pm 0.0 \times 10^0$
succinyl-CoA	$^{13}C_{11}$	$0 \pm 0.0 \times 10^0$	$0 \pm 0.0 \times 10^0$	$0 \pm 0.0 \times 10^0$	$0 \pm 0.0 \times 10^0$
succinyl-CoA	$^{13}C_{12}$	$0 \pm 0.0 \times 10^0$	$0 \pm 0.0 \times 10^0$	$0 \pm 0.0 \times 10^0$	$0 \pm 0.0 \times 10^0$
succinyl-CoA	$^{13}C_{13}$	$0 \pm 0.0 \times 10^0$	$0 \pm 0.0 \times 10^0$	$0 \pm 0.0 \times 10^0$	$0 \pm 0.0 \times 10^0$
succinyl-CoA	$^{13}C_{14}$	$0 \pm 0.0 \times 10^0$	$0 \pm 0.0 \times 10^0$	$0 \pm 0.0 \times 10^0$	$0 \pm 0.0 \times 10^0$
succinyl-CoA	$^{13}C_{15}$	$0 \pm 0.0 \times 10^0$	$0 \pm 0.0 \times 10^0$	$0 \pm 0.0 \times 10^0$	$0 \pm 0.0 \times 10^0$
succinyl-CoA	$^{13}C_{16}$	$0 \pm 0.0 \times 10^0$	$0 \pm 0.0 \times 10^0$	$0 \pm 0.0 \times 10^0$	$0 \pm 0.0 \times 10^0$
succinyl-CoA	$^{13}C_{17}$	$0 \pm 0.0 \times 10^0$	$0 \pm 0.0 \times 10^0$	$0 \pm 0.0 \times 10^0$	$0 \pm 0.0 \times 10^0$
succinyl-CoA	$^{13}C_{18}$	$0 \pm 0.0 \times 10^0$	$0 \pm 0.0 \times 10^0$	$0 \pm 0.0 \times 10^0$	$0 \pm 0.0 \times 10^0$
succinyl-CoA	$^{13}C_{19}$	$0 \pm 0.0 \times 10^0$	$0 \pm 0.0 \times 10^0$	$0 \pm 0.0 \times 10^0$	$0 \pm 0.0 \times 10^0$
succinyl-CoA	$^{13}C_{20}$	$0 \pm 0.0 \times 10^0$	$0 \pm 0.0 \times 10^0$	$0 \pm 0.0 \times 10^0$	$0 \pm 0.0 \times 10^0$
succinyl-CoA	$^{13}C_{21}$	$0 \pm 0.0 \times 10^0$	$0 \pm 0.0 \times 10^0$	$0 \pm 0.0 \times 10^0$	$0 \pm 0.0 \times 10^0$
succinyl-CoA	$^{13}C_{22}$	$0 \pm 0.0 \times 10^0$	$0 \pm 0.0 \times 10^0$	$0 \pm 0.0 \times 10^0$	$0 \pm 0.0 \times 10^0$
succinyl-CoA	$^{13}C_{23}$	$0 \pm 0.0 \times 10^0$	$0 \pm 0.0 \times 10^0$	$0 \pm 0.0 \times 10^0$	$0 \pm 0.0 \times 10^0$
succinyl-CoA	$^{13}C_{24}$	$0 \pm 0.0 \times 10^0$	$0 \pm 0.0 \times 10^0$	$0 \pm 0.0 \times 10^0$	$0 \pm 0.0 \times 10^0$
succinyl-CoA	$^{13}C_{25}$	$0 \pm 0.0 \times 10^0$	$0 \pm 0.0 \times 10^0$	$0 \pm 0.0 \times 10^0$	$0 \pm 0.0 \times 10^0$
succinate	^{12}C	$1.01 \pm 0.07 \times 10^8$	$3.63 \pm 0.7 \times 10^7$	$9.15 \pm 1.9 \times 10^6$	$3.33 \pm 1.0 \times 10^6$
succinate	$^{13}C_1$	$4.66 \pm 0.3 \times 10^6$	$5.43 \pm 0.5 \times 10^6$	$2.66 \pm 0.4 \times 10^6$	$7.94 \pm 1.2 \times 10^5$
succinate	$^{13}C_2$	$6.72 \pm 6.0 \times 10^3$	$2.57 \pm 0.2 \times 10^7$	$1.81 \pm 0.2 \times 10^7$	$7.23 \pm 0.5 \times 10^6$
succinate	$^{13}C_3$	$4.65 \pm 4.2 \times 10^3$	$7.36 \pm 0.9 \times 10^6$	$1.48 \pm 0.2 \times 10^7$	$8.48 \pm 0.1 \times 10^6$
succinate	$^{13}C_4$	$0 \pm 0.0 \times 10^0$	$3.12 \pm 0.3 \times 10^7$	$6.79 \pm 1.3 \times 10^7$	$6.95 \pm 0.2 \times 10^7$
fumarate	^{12}C	$6.27 \pm 0.5 \times 10^6$	$1.78 \pm 0.5 \times 10^6$	$2.26 \pm 0.7 \times 10^5$	$3.17 \pm 2.0 \times 10^4$
fumarate	$^{13}C_1$	$1.32 \pm 0.1 \times 10^5$	$1.14 \pm 0.3 \times 10^5$	$5.39 \pm 1.7 \times 10^4$	$1.07 \pm 0.2 \times 10^4$
fumarate	$^{13}C_2$	$6.55 \pm 11.3 \times 10^2$	$1.29 \pm 0.2 \times 10^6$	$7.09 \pm 2.1 \times 10^5$	$1.57 \pm 0.4 \times 10^5$

Table A-9 continued.

metabolite	labeling pattern	0 min	2 min	5 min	15 min
fumarate	$^{13}C_3$	$6.55 \pm 2.6 \times 10^2$	$1.67 \pm 0.3 \times 10^6$	$1.20 \pm 0.5 \times 10^6$	$5.41 \pm 0.8 \times 10^5$
fumarate	$^{13}C_4$	$1.14 \pm 1.6 \times 10^3$	$3.31 \pm 0.5 \times 10^6$	$3.66 \pm 2.3 \times 10^6$	$2.39 \pm 0.3 \times 10^6$
malate	^{12}C	$9.38 \pm 7.3 \times 10^6$	$3.27 \pm 3.3 \times 10^6$	$9.89 \pm 4.4 \times 10^5$	$5.59 \pm 1.3 \times 10^5$
malate	$^{13}C_1$	$4.67 \pm 7.8 \times 10^5$	$3.04 \pm 3.7 \times 10^5$	$2.04 \pm 1.8 \times 10^5$	$4.59 \pm 2.3 \times 10^4$
malate	$^{13}C_2$	$1.36 \pm 2.2 \times 10^4$	$1.73 \pm 2.6 \times 10^6$	$7.56 \pm 13.1 \times 10^5$	$5.72 \pm 2.7 \times 10^5$
malate	$^{13}C_3$	$3.00 \pm 5.2 \times 10^3$	$3.43 \pm 3.6 \times 10^6$	$1.38 \pm 2.4 \times 10^6$	$1.90 \pm 0.4 \times 10^6$
malate	$^{13}C_4$	$2.05 \pm 3.56 \times 10^3$	$5.51 \pm 5.1 \times 10^6$	$5.49 \pm 9.5 \times 10^6$	$9.29 \pm 1.7 \times 10^6$
6-phospho-D-gluconate	^{12}C	$6.06 \pm 9.5 \times 10^5$	$5.21 \pm 5.2 \times 10^4$	$1.29 \pm 1.4 \times 10^5$	$8.34 \pm 8.9 \times 10^4$
6-phospho-D-gluconate	$^{13}C_1$	$1.75 \pm 1.9 \times 10^4$	$1.37 \pm 1.3 \times 10^3$	$1.04 \pm 1.8 \times 10^3$	$2.34 \pm 4.1 \times 10^3$
6-phospho-D-gluconate	$^{13}C_2$	$5.05 \pm 6.1 \times 10^3$	$0 \pm 0.0 \times 10^0$	$2.26 \pm 3.9 \times 10^3$	$2.09 \pm 3.6 \times 10^3$
6-phospho-D-gluconate	$^{13}C_3$	$8.52 \pm 8.2 \times 10^2$	$0 \pm 0.0 \times 10^0$	$1.93 \pm 3.3 \times 10^3$	$0 \pm 0.0 \times 10^0$
6-phospho-D-gluconate	$^{13}C_4$	$0 \pm 0.0 \times 10^0$	$3.86 \pm 6.7 \times 10^3$	$4.43 \pm 7.7 \times 10^3$	$0 \pm 0.0 \times 10^0$
6-phospho-D-gluconate	$^{13}C_5$	$4.38 \pm 6.7 \times 10^3$	$5.21 \pm 8.7 \times 10^4$	$9.72 \pm 11.3 \times 10^5$	$3.58 \pm 0.6 \times 10^4$
6-phospho-D-gluconate	$^{13}C_6$	$5.26 \pm 4.6 \times 10^4$	$1.00 \pm 1.7 \times 10^6$	$2.32 \pm 3.6 \times 10^6$	$5.63 \pm 2.5 \times 10^5$
ribose/ ribulose/ xyulose-phosphate	^{12}C	$1.62 \pm 0.9 \times 10^4$	$1.51 \pm 0.7 \times 10^4$	$2.40 \pm 0.7 \times 10^4$	$1.99 \pm 1.7 \times 10^4$
ribose/ ribulose/ xyulose-phosphate	$^{13}C_1$	$4.45 \pm 7.7 \times 10^2$	$5.06 \pm 7.0 \times 10^2$	$0 \pm 0.0 \times 10^0$	$3.11 \pm 1.7 \times 10^4$
ribose/ ribulose/ xyulose-phosphate	$^{13}C_2$	$3.68 \pm 3.4 \times 10^3$	$0 \pm 0.0 \times 10^0$	$5.86 \pm 10.2 \times 10^3$	$0 \pm 0.0 \times 10^0$
ribose/ ribulose/ xyulose-phosphate	$^{13}C_3$	$5.96 \pm 5.6 \times 10^2$	$2.47 \pm 4.3 \times 10^2$	$3.78 \pm 3.3 \times 10^2$	$0 \pm 0.0 \times 10^0$
ribose/ ribulose/ xyulose-phosphate	$^{13}C_4$	$1.51 \pm 2.6 \times 10^2$	$1.59 \pm 2.8 \times 10^2$	$1.88 \pm 3.3 \times 10^2$	$0 \pm 0.0 \times 10^0$
ribose/ ribulose/ xyulose-phosphate	$^{13}C_5$	$1.81 \pm 3.1 \times 10^2$	$1.32 \pm 1.8 \times 10^3$	$6.02 \pm 10.4 \times 10^2$	$8.79 \pm 15.2 \times 10^2$
D-sedoheptulose-1/7-phosphate	^{12}C	$2.81 \pm 4.2 \times 10^5$	$2.29 \pm 2.5 \times 10^4$	$6.28 \pm 9.9 \times 10^4$	$1.39 \pm 0.9 \times 10^5$
D-sedoheptulose-1/7-phosphate	$^{13}C_1$	$6.03 \pm 10.4 \times 10^2$	$0 \pm 0.0 \times 10^0$	$4.95 \pm 8.6 \times 10^2$	$9.79 \pm 17.0 \times 10^2$
D-sedoheptulose-1/7-phosphate	$^{13}C_2$	$0 \pm 0.0 \times 10^0$	$0 \pm 0.0 \times 10^0$	$0 \pm 0.0 \times 10^0$	$0 \pm 0.0 \times 10^0$
D-sedoheptulose-1/7-phosphate	$^{13}C_3$	$0 \pm 0.0 \times 10^0$	$0 \pm 0.0 \times 10^0$	$0 \pm 0.0 \times 10^0$	$0 \pm 0.0 \times 10^0$
D-sedoheptulose-1/7-phosphate	$^{13}C_4$	$0 \pm 0.0 \times 10^0$	$0 \pm 0.0 \times 10^0$	$0 \pm 0.0 \times 10^0$	$0 \pm 0.0 \times 10^0$
D-sedoheptulose-1/7-phosphate	$^{13}C_5$	$0 \pm 0.0 \times 10^0$	$0 \pm 0.0 \times 10^0$	$0 \pm 0.0 \times 10^0$	$0 \pm 0.0 \times 10^0$
D-sedoheptulose-1/7-phosphate	$^{13}C_6$	$0 \pm 0.0 \times 10^0$	$4.33 \pm 4.5 \times 10^3$	$1.00 \pm 1.2 \times 10^4$	$6.47 \pm 5.0 \times 10^3$
D-sedoheptulose-1/7-phosphate	$^{13}C_7$	$5.90 \pm 6.5 \times 10^4$	$4.48 \pm 6.9 \times 10^5$	$6.42 \pm 8.9 \times 10^5$	$2.68 \pm 1.1 \times 10^5$
D-erythrose-4-phosphate	^{12}C	$5.10 \pm 4.3 \times 10^4$	$5.74 \pm 4.1 \times 10^4$	$2.23 \pm 2.2 \times 10^4$	$3.97 \pm 2.7 \times 10^4$
D-erythrose-4-phosphate	$^{13}C_1$	$9.04 \pm 8.5 \times 10^2$	$1.04 \pm 1.2 \times 10^3$	$0 \pm 0.0 \times 10^0$	$3.12 \pm 5.4 \times 10^2$
D-erythrose-4-phosphate	$^{13}C_2$	$0 \pm 0.0 \times 10^0$	$0 \pm 0.0 \times 10^0$	$0 \pm 0.0 \times 10^0$	$0 \pm 0.0 \times 10^0$
D-erythrose-4-phosphate	$^{13}C_3$	$0 \pm 0.0 \times 10^0$	$0 \pm 0.0 \times 10^0$	$0 \pm 0.0 \times 10^0$	$0 \pm 0.0 \times 10^0$
D-erythrose-4-phosphate	$^{13}C_4$	$0 \pm 0.0 \times 10^0$	$0 \pm 0.0 \times 10^0$	$0 \pm 0.0 \times 10^0$	$0 \pm 0.0 \times 10^0$

Table A-10. The average ion counts plus or minus the standard deviation for each metabolite discussed and their isotopomers wild type *Salmonella enterica* experiment at 30, 60, and 120 minutes are shown.

metabolite	labeling pattern	30 min	60 min	120 min
glucose/fructose-6-phosphate	^{12}C	$2.63 \pm 1.2 \times 10^{5}$	$8.30 \pm 1.8 \times 10^{5}$	$1.49 \pm 0.3 \times 10^{6}$
glucose/fructose-6-phosphate	$^{13}C_1$	$7.37 \pm 12.8 \times 10^{3}$	$1.35 \pm 1.5 \times 10^{4}$	$6.69 \pm 0.9 \times 10^{4}$
glucose/fructose-6-phosphate	$^{13}C_2$	$0 \pm 0.0 \times 10^{0}$	$0 \pm 0.0 \times 10^{0}$	$2.20 \pm 3.8 \times 10^{3}$
glucose/fructose-6-phosphate	$^{13}C_3$	$0 \pm 0.0 \times 10^{0}$	$0 \pm 0.0 \times 10^{0}$	$0 \pm 0.0 \times 10^{0}$
glucose/fructose-6-phosphate	$^{13}C_4$	$0 \pm 0.0 \times 10^{0}$	$0 \pm 0.0 \times 10^{0}$	$0 \pm 0.0 \times 10^{0}$
glucose/fructose-6-phosphate	$^{13}C_5$	$2.94 \pm 0.4 \times 10^{4}$	$1.87 \pm 3.2 \times 10^{4}$	$1.34 \pm 1.2 \times 10^{4}$
glucose/fructose-6-phosphate	$^{13}C_6$	$3.23 \pm 1.3 \times 10^{5}$	$4.07 \pm 7.1 \times 10^{5}$	$1.45 \pm 1.3 \times 10^{5}$
fructose-1-6-bisphosphate	^{12}C	$1.65 \pm 1.5 \times 10^{5}$	$8.49 \pm 7.2 \times 10^{4}$	$7.51 \pm 4.9 \times 10^{4}$
fructose-1-6-bisphosphate	$^{13}C_1$	$5.03 \pm 2.2 \times 10^{3}$	$4.98 \pm 3.8 \times 10^{3}$	$5.01 \pm 3.5 \times 10^{3}$
fructose-1-6-bisphosphate	$^{13}C_2$	$8.66 \pm 10.2 \times 10^{2}$	$2.21 \pm 1.3 \times 10^{3}$	$2.76 \pm 4.8 \times 10^{2}$
fructose-1-6-bisphosphate	$^{13}C_3$	$1.20 \pm 0.4 \times 10^{4}$	$1.66 \pm 1.1 \times 10^{4}$	$6.65 \pm 8.2 \times 10^{3}$
fructose-1-6-bisphosphate	$^{13}C_4$	$2.99 \pm 0.5 \times 10^{3}$	$4.92 \pm 2.6 \times 10^{3}$	$4.20 \pm 7.3 \times 10^{2}$
fructose-1-6-bisphosphate	$^{13}C_5$	$7.48 \pm 3.9 \times 10^{3}$	$2.04 \pm 1.8 \times 10^{4}$	$1.15 \pm 1.5 \times 10^{4}$
fructose-1-6-bisphosphate	$^{13}C_6$	$2.91 \pm 1.5 \times 10^{5}$	$5.15 \pm 1.5 \times 10^{5}$	$2.45 \pm 1.8 \times 10^{5}$
D-glyceraldehdye-3-phosphate	^{12}C	$4.04 \pm 0.6 \times 10^{5}$	$3.64 \pm 1.3 \times 10^{5}$	$4.85 \pm 0.9 \times 10^{5}$
D-glyceraldehdye-3-phosphate	$^{13}C_1$	$2.61 \pm 2.6 \times 10^{4}$	$0 \pm 0.0 \times 10^{0}$	$9.67 \pm 16.7 \times 10^{3}$
D-glyceraldehdye-3-phosphate	$^{13}C_2$	$4.49 \pm 0.6 \times 10^{3}$	$7.19 \pm 3.6 \times 10^{3}$	$2.45 \pm 0.4 \times 10^{4}$
D-glyceraldehdye-3-phosphate	$^{13}C_3$	$1.76 \pm 0.4 \times 10^{5}$	$5.62 \pm 2.0 \times 10^{5}$	$1.42 \pm 0.1 \times 10^{6}$
1,3-diphopshateglycerate	^{12}C	$1.36 \pm 1.0 \times 10^{4}$	$1.81 \pm 0.6 \times 10^{4}$	$3.08 \pm 1.5 \times 10^{4}$
1,3-diphopshateglycerate	$^{13}C_1$	$1.66 \pm 2.9 \times 10^{3}$	$1.94 \pm 1.7 \times 10^{3}$	$1.52 \pm 2.6 \times 10^{3}$
1,3-diphopshateglycerate	$^{13}C_2$	$9.64 \pm 16.7 \times 10^{2}$	$7.25 \pm 12.6 \times 10^{2}$	$7.65 \pm 3.7 \times 10^{3}$
1,3-diphopshateglycerate	$^{13}C_3$	$1.31 \pm 1.2 \times 10^{4}$	$0 \pm 0.0 \times 10^{0}$	$1.42 \pm 2.1 \times 10^{4}$
3/2-phosphoglycerate	^{12}C	$2.39 \pm 0.8 \times 10^{4}$	$6.38 \pm 4.2 \times 10^{3}$	$8.24 \pm 8.9 \times 10^{3}$
3/2-phosphoglycerate	$^{13}C_1$	$0 \pm 0.0 \times 10^{0}$	$9.64 \pm 16.7 \times 10^{2}$	$3.27 \pm 5.7 \times 10^{2}$
3/2-phosphoglycerate	$^{13}C_2$	$0 \pm 0.0 \times 10^{0}$	$0 \pm 0.0 \times 10^{0}$	$0 \pm 0.0 \times 10^{0}$
3/2-phosphoglycerate	$^{13}C_3$	$0 \pm 0.0 \times 10^{0}$	$0 \pm 0.0 \times 10^{0}$	$0 \pm 0.0 \times 10^{0}$
pyruvate	^{12}C	$5.22 \pm 0.4 \times 10^{6}$	$3.41 \pm 2.1 \times 10^{6}$	$3.37 \pm 1.8 \times 10^{6}$
pyruvate	$^{13}C_1$	$4.75 \pm 1.2 \times 10^{4}$	$3.86 \pm 2.7 \times 10^{4}$	$1.86 \pm 1.7 \times 10^{4}$
pyruvate	$^{13}C_2$	$3.15 \pm 0.7 \times 10^{4}$	$1.99 \pm 1.3 \times 10^{4}$	$2.36 \pm 2.3 \times 10^{4}$
pyruvate	$^{13}C_3$	$3.15 \pm 1.4 \times 10^{6}$	$3.34 \pm 0.6 \times 10^{6}$	$3.34 \pm 0.6 \times 10^{6}$
alpha-ketoglutarate	^{12}C	$2.02 \pm 0.7 \times 10^{6}$	$1.11 \pm 0.6 \times 10^{6}$	$7.86 \pm 1.7 \times 10^{5}$
alpha-ketoglutarate	$^{13}C_1$	$1.70 \pm 0.4 \times 10^{5}$	$1.17 \pm 0.7 \times 10^{5}$	$7.78 \pm 1.0 \times 10^{4}$
alpha-ketoglutarate	$^{13}C_2$	$1.28 \pm 0.4 \times 10^{6}$	$4.16 \pm 1.9 \times 10^{5}$	$2.56 \pm 0.4 \times 10^{5}$
alpha-ketoglutarate	$^{13}C_3$	$3.19 \pm 0.7 \times 10^{6}$	$1.53 \pm 0.2 \times 10^{6}$	$1.19 \pm 0.1 \times 10^{6}$

Table A.10 continued.

metabolite	labeling pattern	30 min	60 min	120 min
alpha-ketoglutarate	$^{13}C_4$	$4.68 \pm 1.0 \times 10^6$	$3.06 \pm 0.3 \times 10^6$	$3.42 \pm 0.2 \times 10^6$
alpha-ketoglutarate	$^{13}C_5$	$1.38 \pm 0.2 \times 10^7$	$1.13 \pm 0.1 \times 10^7$	$1.32 \pm 0.3 \times 10^7$
succinyl-CoA	^{12}C	$1.94 \pm 1.8 \times 10^4$	$2.05 \pm 1.8 \times 10^3$	$1.62 \pm 2.8 \times 10^3$
succinyl-CoA	$^{13}C_1$	$0 \pm 0.0 \times 10^0$	$1.01 \pm 1.8 \times 10^3$	$0 \pm 0.0 \times 10^0$
succinyl-CoA	$^{13}C_2$	$0 \pm 0.0 \times 10^0$	$0 \pm 0.0 \times 10^0$	$0 \pm 0.0 \times 10^0$
succinyl-CoA	$^{13}C_3$	$0 \pm 0.0 \times 10^0$	$0 \pm 0.0 \times 10^0$	$0 \pm 0.0 \times 10^0$
succinyl-CoA	$^{13}C_4$	$0 \pm 0.0 \times 10^0$	$0 \pm 0.0 \times 10^0$	$0 \pm 0.0 \times 10^0$
succinyl-CoA	$^{13}C_5$	$1.75 \pm 3.0 \times 10^3$	$0 \pm 0.0 \times 10^0$	$6.90 \pm 12.0 \times 10^2$
succinyl-CoA	$^{13}C_6$	$0 \pm 0.0 \times 10^0$	$0 \pm 0.0 \times 10^0$	$9.18 \pm 15.9 \times 10^2$
succinyl-CoA	$^{13}C_7$	$0 \pm 0.0 \times 10^0$	$1.26 \pm 2.2 \times 10^3$	$0 \pm 0.0 \times 10^0$
succinyl-CoA	$^{13}C_8$	$0 \pm 0.0 \times 10^0$	$0 \pm 0.0 \times 10^0$	$0 \pm 0.0 \times 10^0$
succinyl-CoA	$^{13}C_9$	$0 \pm 0.0 \times 10^0$	$0 \pm 0.0 \times 10^0$	$0 \pm 0.0 \times 10^0$
succinyl-CoA	$^{13}C_{10}$	$0 \pm 0.0 \times 10^0$	$0 \pm 0.0 \times 10^0$	$0 \pm 0.0 \times 10^0$
succinyl-CoA	$^{13}C_{11}$	$0 \pm 0.0 \times 10^0$	$0 \pm 0.0 \times 10^0$	$0 \pm 0.0 \times 10^0$
succinyl-CoA	$^{13}C_{12}$	$0 \pm 0.0 \times 10^0$	$0 \pm 0.0 \times 10^0$	$0 \pm 0.0 \times 10^0$
succinyl-CoA	$^{13}C_{13}$	$0 \pm 0.0 \times 10^0$	$0 \pm 0.0 \times 10^0$	$0 \pm 0.0 \times 10^0$
succinyl-CoA	$^{13}C_{14}$	$0 \pm 0.0 \times 10^0$	$0 \pm 0.0 \times 10^0$	$0 \pm 0.0 \times 10^0$
succinyl-CoA	$^{13}C_{15}$	$0 \pm 0.0 \times 10^0$	$0 \pm 0.0 \times 10^0$	$0 \pm 0.0 \times 10^0$
succinyl-CoA	$^{13}C_{16}$	$0 \pm 0.0 \times 10^0$	$0 \pm 0.0 \times 10^0$	$0 \pm 0.0 \times 10^0$
succinyl-CoA	$^{13}C_{17}$	$0 \pm 0.0 \times 10^0$	$0 \pm 0.0 \times 10^0$	$0 \pm 0.0 \times 10^0$
succinyl-CoA	$^{13}C_{18}$	$0 \pm 0.0 \times 10^0$	$0 \pm 0.0 \times 10^0$	$0 \pm 0.0 \times 10^0$
succinyl-CoA	$^{13}C_{19}$	$0 \pm 0.0 \times 10^0$	$0 \pm 0.0 \times 10^0$	$0 \pm 0.0 \times 10^0$
succinyl-CoA	$^{13}C_{20}$	$0 \pm 0.0 \times 10^0$	$0 \pm 0.0 \times 10^0$	$0 \pm 0.0 \times 10^0$
succinyl-CoA	$^{13}C_{21}$	$0 \pm 0.0 \times 10^0$	$0 \pm 0.0 \times 10^0$	$0 \pm 0.0 \times 10^0$
succinyl-CoA	$^{13}C_{22}$	$0 \pm 0.0 \times 10^0$	$0 \pm 0.0 \times 10^0$	$0 \pm 0.0 \times 10^0$
succinyl-CoA	$^{13}C_{23}$	$0 \pm 0.0 \times 10^0$	$0 \pm 0.0 \times 10^0$	$0 \pm 0.0 \times 10^0$
succinyl-CoA	$^{13}C_{24}$	$0 \pm 0.0 \times 10^0$	$0 \pm 0.0 \times 10^0$	$0 \pm 0.0 \times 10^0$
succinyl-CoA	$^{13}C_{25}$	$0 \pm 0.0 \times 10^0$	$0 \pm 0.0 \times 10^0$	$0 \pm 0.0 \times 10^0$
succinate	^{12}C	$3.38 \pm 0.2 \times 10^6$	$3.43 \pm 1.7 \times 10^6$	$2.13 \pm 0.9 \times 10^6$
succinate	$^{13}C_1$	$1.37 \pm 0.3 \times 10^6$	$1.04 \pm 0.3 \times 10^6$	$4.94 \pm 1.4 \times 10^5$
succinate	$^{13}C_2$	$6.47 \pm 0.8 \times 10^6$	$4.77 \pm 0.6 \times 10^6$	$3.09 \pm 0.8 \times 10^6$
succinate	$^{13}C_3$	$6.49 \pm 0.2 \times 10^6$	$5.95 \pm 0.3 \times 10^6$	$4.45 \pm 1.4 \times 10^6$
succinate	$^{13}C_4$	$3.46 \pm 0.5 \times 10^7$	$4.66 \pm 0.9 \times 10^7$	$4.50 \pm 1.9 \times 10^7$
fumarate	^{12}C	$2.42 \pm 2.1 \times 10^4$	$2.64 \pm 2.0 \times 10^4$	$2.23 \pm 1.4 \times 10^4$
fumarate	$^{13}C_1$	$2.11 \pm 0.4 \times 10^4$	$9.62 \pm 8.2 \times 10^3$	$6.22 \pm 5.7 \times 10^3$
fumarate	$^{13}C_2$	$1.24 \pm 0.3 \times 10^5$	$4.80 \pm 1.2 \times 10^4$	$2.57 \pm 0.5 \times 10^4$

Table A-10 continued.

metabolite	labeling pattern	30 min	60 min	120 min
fumarate	$^{13}C_3$	$3.45 \pm 0.5 \times 10^5$	$2.01 \pm 0.05 \times 10^5$	$2.40 \pm 0.7 \times 10^5$
fumarate	$^{13}C_4$	$1.15 \pm 0.2 \times 10^6$	$1.08 \pm 0.05 \times 10^6$	$1.02 \pm 0.4 \times 10^6$
malate	^{12}C	$6.71 \pm 2.9 \times 10^5$	$8.44 \pm 2.9 \times 10^5$	$5.15 \pm 0.9 \times 10^5$
malate	$^{13}C_1$	$3.42 \pm 1.8 \times 10^4$	$7.19 \pm 9.0 \times 10^4$	$3.44 \pm 1.8 \times 10^4$
malate	$^{13}C_2$	$5.56 \pm 2.1 \times 10^5$	$3.24 \pm 2.9 \times 10^5$	$1.79 \pm 1.0 \times 10^5$
malate	$^{13}C_3$	$4.29 \pm 7.4 \times 10^5$	$1.02 \pm 1.0 \times 10^6$	$6.58 \pm 6.1 \times 10^5$
malate	$^{13}C_4$	$1.70 \pm 1.5 \times 10^6$	$1.18 \pm 1.2 \times 10^6$	$1.68 \pm 1.9 \times 10^6$
6-phospho-D-gluconate	^{12}C	$1.25 \pm 0.9 \times 10^5$	$8.16 \pm 5.1 \times 10^4$	$4.37 \pm 2.7 \times 10^4$
6-phospho-D-gluconate	$^{13}C_1$	$0 \pm 0.0 \times 10^0$	$7.80 \pm 13.5 \times 10^2$	$0 \pm 0.0 \times 10^0$
6-phospho-D-gluconate	$^{13}C_2$	$2.05 \pm 1.8 \times 10^3$	$0 \pm 0.0 \times 10^0$	$0 \pm 0.0 \times 10^0$
6-phospho-D-gluconate	$^{13}C_3$	$3.42 \pm 5.9 \times 10^2$	$1.34 \pm 2.3 \times 10^3$	$0 \pm 0.0 \times 10^0$
6-phospho-D-gluconate	$^{13}C_4$	$9.19 \pm 15.9 \times 10^2$	$4.09 \pm 7.1 \times 10^2$	$0 \pm 0.0 \times 10^0$
6-phospho-D-gluconate	$^{13}C_5$	$2.26 \pm 2.9 \times 10^3$	$1.86 \pm 1.8 \times 10^4$	$8.18 \pm 10.3 \times 10^3$
6-phospho-D-gluconate	$^{13}C_6$	$1.81 \pm 0.9 \times 10^5$	$2.99 \pm 0.7 \times 10^5$	$2.78 \pm 2.7 \times 10^5$
ribose/ ribulose/ xyulose-phosphate	^{12}C	$1.70 \pm 0.5 \times 10^4$	$1.08 \pm 0.4 \times 10^4$	$3.20 \pm 1.8 \times 10^4$
ribose/ ribulose/ xyulose-phosphate	$^{13}C_1$	$5.06 \pm 5.1 \times 10^2$	$0 \pm 0.0 \times 10^0$	$3.72 \pm 6.5 \times 10^2$
ribose/ ribulose/ xyulose-phosphate	$^{13}C_2$	$0 \pm 0.0 \times 10^0$	$0 \pm 0.0 \times 10^0$	$2.48 \pm 4.3 \times 10^3$
ribose/ ribulose/ xyulose-phosphate	$^{13}C_3$	$0 \pm 0.0 \times 10^0$	$0 \pm 0.0 \times 10^0$	$0 \pm 0.0 \times 10^0$
ribose/ ribulose/ xyulose-phosphate	$^{13}C_4$	$0 \pm 0.0 \times 10^0$	$0 \pm 0.0 \times 10^0$	$1.75 \pm 3.0 \times 10^2$
ribose/ ribulose/ xyulose-phosphate	$^{13}C_5$	$0 \pm 0.0 \times 10^0$	$4.06 \pm 7.0 \times 10^2$	$2.67 \pm 4.6 \times 10^2$
D-sedoheptulose-1/7-phosphate	^{12}C	$1.63 \pm 1.9 \times 10^5$	$3.40 \pm 2.1 \times 10^4$	$2.60 \pm 2.6 \times 10^4$
D-sedoheptulose-1/7-phosphate	$^{13}C_1$	$0 \pm 0.0 \times 10^0$	$4.48 \pm 7.8 \times 10^2$	$0 \pm 0.0 \times 10^0$
D-sedoheptulose-1/7-phosphate	$^{13}C_2$	$0 \pm 0.0 \times 10^0$	$0 \pm 0.0 \times 10^0$	$0 \pm 0.0 \times 10^0$
D-sedoheptulose-1/7-phosphate	$^{13}C_3$	$0 \pm 0.0 \times 10^0$	$0 \pm 0.0 \times 10^0$	$0 \pm 0.0 \times 10^0$
D-sedoheptulose-1/7-phosphate	$^{13}C_4$	$0 \pm 0.0 \times 10^0$	$0 \pm 0.0 \times 10^0$	$0 \pm 0.0 \times 10^0$
D-sedoheptulose-1/7-phosphate	$^{13}C_5$	$0 \pm 0.0 \times 10^0$	$0 \pm 0.0 \times 10^0$	$0 \pm 0.0 \times 10^0$
D-sedoheptulose-1/7-phosphate	$^{13}C_6$	$5.36 \pm 2.3 \times 10^3$	$5.41 \pm 3.8 \times 10^3$	$3.49 \pm 1.2 \times 10^3$
D-sedoheptulose-1/7-phosphate	$^{13}C_7$	$2.06 \pm 1.8 \times 10^5$	$5.78 \pm 4.7 \times 10^5$	$3.89 \pm 3.1 \times 10^5$
D-erythrose-4-phosphate	^{12}C	$1.33 \pm 0.8 \times 10^4$	$1.08 \pm 0.9 \times 10^4$	$3.13 \pm 2.4 \times 10^4$
D-erythrose-4-phosphate	$^{13}C_1$	$0 \pm 0.0 \times 10^0$	$0 \pm 0.0 \times 10^0$	$0 \pm 0.0 \times 10^0$
D-erythrose-4-phosphate	$^{13}C_2$	$0 \pm 0.0 \times 10^0$	$0 \pm 0.0 \times 10^0$	$0 \pm 0.0 \times 10^0$
D-erythrose-4-phosphate	$^{13}C_3$	$0 \pm 0.0 \times 10^0$	$0 \pm 0.0 \times 10^0$	$0 \pm 0.0 \times 10^0$
D-erythrose-4-phosphate	$^{13}C_4$	$0 \pm 0.0 \times 10^0$	$0 \pm 0.0 \times 10^0$	$0 \pm 0.0 \times 10^0$

Table A-11. The average ion counts plus or minus the standard deviation for the metabolites discussed and their isotopomers is the *purH Salmonella enterica* experiment at 0, 2, 5, and 15 minutes are shown.

metabolite	labeling pattern	0 min	2 min	5 min	15 min
glucose/fructose-6-phosphate	^{12}C	$7.67 \pm 1.7 \times 10^{5}$	$1.79 \pm 0.2 \times 10^{5}$	$1.05 \pm 1.4 \times 10^{5}$	$1.67 \pm 0.5 \times 10^{5}$
glucose/fructose-6-phosphate	$^{13}C_1$	$8.19 \pm 1.0 \times 10^{4}$	$0 \pm 0.0 \times 10^{0}$	$1.03 \pm 0.6 \times 10^{4}$	$0 \pm 0.0 \times 10^{0}$
glucose/fructose-6-phosphate	$^{13}C_2$	$3.86 \pm 6.7 \times 10^{3}$	$0 \pm 0.0 \times 10^{0}$	$0 \pm 0.0 \times 10^{0}$	$0 \pm 0.0 \times 10^{0}$
glucose/fructose-6-phosphate	$^{13}C_3$	$0 \pm 0.0 \times 10^{0}$	$2.86 \pm 5.0 \times 10^{3}$	$0 \pm 0.0 \times 10^{0}$	$0 \pm 0.0 \times 10^{0}$
glucose/fructose-6-phosphate	$^{13}C_4$	$0 \pm 0.0 \times 10^{0}$	$0 \pm 0.0 \times 10^{0}$	$0 \pm 0.0 \times 10^{0}$	$2.67 \pm 4.6 \times 10^{3}$
glucose/fructose-6-phosphate	$^{13}C_5$	$0 \pm 0.0 \times 10^{0}$	$8.25 \pm 4.0 \times 10^{4}$	$6.34 \pm 7.3 \times 10^{4}$	$1.68 \pm 2.9 \times 10^{4}$
glucose/fructose-6-phosphate	$^{13}C_6$	$0 \pm 0.0 \times 10^{0}$	$4.82 \pm 3.5 \times 10^{5}$	$4.03 \pm 6.1 \times 10^{5}$	$4.97 \pm 5.2 \times 10^{5}$
fructose-1-6-bisphosphate	^{12}C	$2.57 \pm 1.9 \times 10^{6}$	$9.38 \pm 8.8 \times 10^{4}$	$6.48 \pm 8.4 \times 10^{4}$	$1.66 \pm 1.7 \times 10^{5}$
fructose-1-6-bisphosphate	$^{13}C_1$	$5.85 \pm 7.5 \times 10^{4}$	$5.76 \pm 7.5 \times 10^{3}$	$1.22 \pm 1.1 \times 10^{4}$	$1.89 \pm 3.3 \times 10^{3}$
fructose-1-6-bisphosphate	$^{13}C_2$	$2.93 \pm 2.2 \times 10^{4}$	$2.08 \pm 2.6 \times 10^{4}$	$0 \pm 0.0 \times 10^{0}$	$1.13 \pm 1.6 \times 10^{4}$
fructose-1-6-bisphosphate	$^{13}C_3$	$1.25 \pm 1.6 \times 10^{4}$	$1.24 \pm 1.6 \times 10^{5}$	$2.14 \pm 2.2 \times 10^{5}$	$8.98 \pm 4.0 \times 10^{4}$
fructose-1-6-bisphosphate	$^{13}C_4$	$1.19 \pm 0.6 \times 10^{4}$	$2.23 \pm 3.9 \times 10^{4}$	$2.15 \pm 2.2 \times 10^{4}$	$6.73 \pm 11.7 \times 10^{3}$
fructose-1-6-bisphosphate	$^{13}C_5$	$5.88 \pm 8.8 \times 10^{3}$	$5.57 \pm 6.5 \times 10^{4}$	$2.57 \pm 1.5 \times 10^{5}$	$1.43 \pm 1.5 \times 10^{5}$
fructose-1-6-bisphosphate	$^{13}C_6$	$1.32 \pm 1.2 \times 10^{5}$	$1.40 \pm 1.0 \times 10^{6}$	$1.13 \pm 2.1 \times 10^{6}$	$1.80 \pm 1.8 \times 10^{6}$
D-glyceraldehdye-3-phosphate	^{12}C	$1.41 \pm 0.2 \times 10^{6}$	$8.91 \pm 1.9 \times 10^{5}$	$3.25 \pm 10.0 \times 10^{5}$	$5.65 \pm 1.6 \times 10^{5}$
D-glyceraldehdye-3-phosphate	$^{13}C_1$	$1.32 \pm 0.2 \times 10^{4}$	$1.09 \pm 0.5 \times 10^{4}$	$1.32 \pm 1.4 \times 10^{4}$	$1.24 \pm 0.6 \times 10^{4}$
D-glyceraldehdye-3-phosphate	$^{13}C_2$	$2.17 \pm 1.0 \times 10^{3}$	$0 \pm 0.0 \times 10^{0}$	$7.12 \pm 6.8 \times 10^{2}$	$2.31 \pm 0.1 \times 10^{3}$
D-glyceraldehdye-3-phosphate	$^{13}C_3$	$0 \pm 0.0 \times 10^{0}$	$5.55 \pm 9.6 \times 10^{2}$	$6.10 \pm 13.2 \times 10^{3}$	$1.00 \pm 0.3 \times 10^{5}$
1,3-diphopshateglycerate	^{12}C	$9.31 \pm 4.4 \times 10^{4}$	$5.05 \pm 1.6 \times 10^{4}$	$1.20 \pm 0.8 \times 10^{5}$	$1.11 \pm 0.5 \times 10^{4}$
1,3-diphopshateglycerate	$^{13}C_1$	$8.60 \pm 14.9 \times 10^{2}$	$7.47 \pm 6.5 \times 10^{3}$	$1.48 \pm 0.9 \times 10^{4}$	$0 \pm 0.0 \times 10^{0}$
1,3-diphopshateglycerate	$^{13}C_2$	$9.96 \pm 6.3 \times 10^{3}$	$1.96 \pm 1.3 \times 10^{4}$	$7.92 \pm 7.7 \times 10^{3}$	$0 \pm 0.0 \times 10^{0}$
1,3-diphopshateglycerate	$^{13}C_3$	$9.29 \pm 2.5 \times 10^{4}$	$3.09 \pm 1.9 \times 10^{5}$	$2.68 \pm 2.0 \times 10^{5}$	$5.89 \pm 1.8 \times 10^{4}$
3/2-phosphoglycerate	^{12}C	$3.85 \pm 4.9 \times 10^{4}$	$4.04 \pm 1.7 \times 10^{4}$	$1.40 \pm 4.6 \times 10^{4}$	$4.08 \pm 1.2 \times 10^{4}$
3/2-phosphoglycerate	$^{13}C_1$	$1.82 \pm 1.2 \times 10^{7}$	$1.16 \pm 0.5 \times 10^{7}$	$1.02 \pm 4.8 \times 10^{6}$	$5.38 \pm 2.0 \times 10^{6}$
3/2-phosphoglycerate	$^{13}C_2$	$4.79 \pm 6.7 \times 10^{5}$	$1.52 \pm 1.1 \times 10^{5}$	$3.30 \pm 4.5 \times 10^{4}$	$2.68 \pm 1.8 \times 10^{4}$
3/2-phosphoglycerate	$^{13}C_3$	$0 \pm 0.0 \times 10^{0}$	$2.52 \pm 2.5 \times 10^{5}$	$1.64 \pm 1.7 \times 10^{4}$	$5.41 \pm 7.1 \times 10^{5}$
pyruvate	^{12}C	$0 \pm 0.0 \times 10^{0}$	$1.31 \pm 0.8 \times 10^{7}$	$6.92 \pm 9.2 \times 10^{6}$	$2.44 \pm 1.5 \times 10^{7}$
pyruvate	$^{13}C_1$	$5.19 \pm 1.0 \times 10^{7}$	$3.04 \pm 0.5 \times 10^{7}$	$1.75 \pm 14.9 \times 10^{6}$	$3.13 \pm 0.2 \times 10^{6}$
pyruvate	$^{13}C_2$	$2.39 \pm 0.6 \times 10^{6}$	$1.70 \pm 0.5 \times 10^{6}$	$3.49 \pm 9.2 \times 10^{5}$	$1.38 \pm 0.3 \times 10^{5}$
pyruvate	$^{13}C_3$	$1.64 \pm 0.4 \times 10^{5}$	$6.80 \pm 1.1 \times 10^{6}$	$1.87 \pm 9.0 \times 10^{6}$	$2.50 \pm 0.7 \times 10^{6}$
alpha-ketoglutarate	^{12}C	$1.85 \pm 1.1 \times 10^{3}$	$1.87 \pm 0.3 \times 10^{6}$	$1.74 \pm 4.9 \times 10^{6}$	$5.43 \pm 0.6 \times 10^{6}$

Table A-11 continued.

metabolite	labeling pattern	0 min	2 min	5 min	15 min
alpha-ketoglutarate	$^{13}C_1$	$0 \pm 0.0 \times 10^0$	$2.41 \pm 0.4 \times 10^6$	$2.10 \pm 8.3 \times 10^6$	$1.16 \pm 0.1 \times 10^7$
alpha-ketoglutarate	$^{13}C_2$	$1.62 \pm 2.8 \times 10^3$	$2.16 \pm 0.7 \times 10^6$	$3.90 \pm 11.1 \times 10^6$	$3.70 \pm 0.3 \times 10^7$
alpha-ketoglutarate	$^{13}C_3$	$1.77 \pm 0.9 \times 10^5$	$1.66 \pm 2.1 \times 10^4$	$3.35 \pm 3.8 \times 10^4$	$6.61 \pm 6.7 \times 10^3$
alpha-ketoglutarate	$^{13}C_4$	$3.93 \pm 2.1 \times 10^4$	$0 \pm 0.0 \times 10^0$	$0 \pm 0.0 \times 10^0$	$0 \pm 0.0 \times 10^0$
alpha-ketoglutarate	$^{13}C_5$	$0 \pm 0.0 \times 10^0$	$1.08 \pm 1.9 \times 10^4$	$1.90 \pm 1.1 \times 10^4$	$1.84 \pm 3.2 \times 10^3$
succinyl-CoA	^{12}C	$0 \pm 0.0 \times 10^0$	$1.97 \pm 3.4 \times 10^3$	$1.25 \pm 0.9 \times 10^4$	$2.58 \pm 4.5 \times 10^3$
succinyl-CoA	$^{13}C_1$	$0 \pm 0.0 \times 10^0$	$1.85 \pm 3.2 \times 10^3$	$0 \pm 0.0 \times 10^0$	$1.41 \pm 2.5 \times 10^4$
succinyl-CoA	$^{13}C_2$	$0 \pm 0.0 \times 10^0$	$0 \pm 0.0 \times 10^0$	$0 \pm 0.0 \times 10^0$	$0 \pm 0.0 \times 10^0$
succinyl-CoA	$^{13}C_3$	$0 \pm 0.0 \times 10^0$	$0 \pm 0.0 \times 10^0$	$0 \pm 0.0 \times 10^0$	$0 \pm 0.0 \times 10^0$
succinyl-CoA	$^{13}C_4$	$0 \pm 0.0 \times 10^0$	$0 \pm 0.0 \times 10^0$	$0 \pm 0.0 \times 10^0$	$0 \pm 0.0 \times 10^0$
succinyl-CoA	$^{13}C_5$	$0 \pm 0.0 \times 10^0$	$0 \pm 0.0 \times 10^0$	$0 \pm 0.0 \times 10^0$	$0 \pm 0.0 \times 10^0$
succinyl-CoA	$^{13}C_6$	$0 \pm 0.0 \times 10^0$	$0 \pm 0.0 \times 10^0$	$0 \pm 0.0 \times 10^0$	$2.28 \pm 4.0 \times 10^3$
succinyl-CoA	$^{13}C_7$	$0 \pm 0.0 \times 10^0$	$0 \pm 0.0 \times 10^0$	$0 \pm 0.0 \times 10^0$	$0 \pm 0.0 \times 10^0$
succinyl-CoA	$^{13}C_8$	$0 \pm 0.0 \times 10^0$	$0 \pm 0.0 \times 10^0$	$0 \pm 0.0 \times 10^0$	$0 \pm 0.0 \times 10^0$
succinyl-CoA	$^{13}C_9$	$0 \pm 0.0 \times 10^0$	$0 \pm 0.0 \times 10^0$	$0 \pm 0.0 \times 10^0$	$0 \pm 0.0 \times 10^0$
succinyl-CoA	$^{13}C_{10}$	$0 \pm 0.0 \times 10^0$	$0 \pm 0.0 \times 10^0$	$0 \pm 0.0 \times 10^0$	$0 \pm 0.0 \times 10^0$
succinyl-CoA	$^{13}C_{11}$	$0 \pm 0.0 \times 10^0$	$0 \pm 0.0 \times 10^0$	$0 \pm 0.0 \times 10^0$	$0 \pm 0.0 \times 10^0$
succinyl-CoA	$^{13}C_{12}$	$0 \pm 0.0 \times 10^0$	$0 \pm 0.0 \times 10^0$	$0 \pm 0.0 \times 10^0$	$0 \pm 0.0 \times 10^0$
succinyl-CoA	$^{13}C_{13}$	$0 \pm 0.0 \times 10^0$	$0 \pm 0.0 \times 10^0$	$0 \pm 0.0 \times 10^0$	$0 \pm 0.0 \times 10^0$
succinyl-CoA	$^{13}C_{14}$	$0 \pm 0.0 \times 10^0$	$0 \pm 0.0 \times 10^0$	$0 \pm 0.0 \times 10^0$	$0 \pm 0.0 \times 10^0$
succinyl-CoA	$^{13}C_{15}$	$0 \pm 0.0 \times 10^0$	$0 \pm 0.0 \times 10^0$	$0 \pm 0.0 \times 10^0$	$0 \pm 0.0 \times 10^0$
succinyl-CoA	$^{13}C_{16}$	$1.15 \pm 2.0 \times 10^3$	$0 \pm 0.0 \times 10^0$	$0 \pm 0.0 \times 10^0$	$0 \pm 0.0 \times 10^0$
succinyl-CoA	$^{13}C_{17}$	$1.13 \pm 2.0 \times 10^3$	$1.38 \pm 2.4 \times 10^3$	$0 \pm 0.0 \times 10^0$	$0 \pm 0.0 \times 10^0$
succinyl-CoA	$^{13}C_{18}$	$0 \pm 0.0 \times 10^0$	$0 \pm 0.0 \times 10^0$	$0 \pm 0.0 \times 10^0$	$0 \pm 0.0 \times 10^0$
succinyl-CoA	$^{13}C_{19}$	$0 \pm 0.0 \times 10^0$	$0 \pm 0.0 \times 10^0$	$0 \pm 0.0 \times 10^0$	$0 \pm 0.0 \times 10^0$
succinyl-CoA	$^{13}C_{20}$	$0 \pm 0.0 \times 10^0$	$0 \pm 0.0 \times 10^0$	$0 \pm 0.0 \times 10^0$	$0 \pm 0.0 \times 10^0$
succinyl-CoA	$^{13}C_{21}$	$0 \pm 0.0 \times 10^0$	$0 \pm 0.0 \times 10^0$	$0 \pm 0.0 \times 10^0$	$0 \pm 0.0 \times 10^0$
succinyl-CoA	$^{13}C_{22}$	$0 \pm 0.0 \times 10^0$	$0 \pm 0.0 \times 10^0$	$0 \pm 0.0 \times 10^0$	$0 \pm 0.0 \times 10^0$
succinyl-CoA	$^{13}C_{23}$	$3.99 \pm 1.1 \times 10^7$	$2.07 \pm 1.0 \times 10^7$	$3.91 \pm 11.8 \times 10^6$	$1.71 \pm 0.6 \times 10^6$
succinyl-CoA	$^{13}C_{24}$	$1.80 \pm 0.5 \times 10^6$	$1.44 \pm 0.8 \times 10^6$	$3.73 \pm 14.6 \times 10^5$	$1.62 \pm 1.4 \times 10^5$
succinyl-CoA	$^{13}C_{25}$	$1.68 \pm 0.7 \times 10^4$	$6.72 \pm 2.8 \times 10^6$	$2.51 \pm 9.3 \times 10^6$	$2.05 \pm 1.8 \times 10^6$
succinate	^{12}C	$1.29 \pm 2.2 \times 10^3$	$9.24 \pm 5.2 \times 10^5$	$1.74 \pm 4.5 \times 10^6$	$2.89 \pm 2.5 \times 10^6$
succinate	$^{13}C_1$	$4.40 \pm 7.6 \times 10^4$	$3.81 \pm 1.7 \times 10^6$	$5.19 \pm 13.3 \times 10^6$	$1.97 \pm 1.7 \times 10^7$
succinate	$^{13}C_2$	$2.77 \pm 0.7 \times 10^6$	$1.04 \pm 0.5 \times 10^6$	$1.11 \pm 2.6 \times 10^5$	$2.27 \pm 0.3 \times 10^4$
succinate	$^{13}C_3$	$3.76 \pm 1.4 \times 10^4$	$3.69 \pm 2.1 \times 10^4$	$9.03 \pm 16.8 \times 10^3$	$5.76 \pm 4.4 \times 10^3$

Table A-11 continued.

metabolite	labeling pattern	0 min	2 min	5 min	15 min
succinate	$^{13}C_4$	$8.12 \pm 10.5 \times 10^{2}$	$2.38 \pm 1.3 \times 10^{5}$	$1.22 \pm 2.2 \times 10^{5}$	$5.30 \pm 0.3 \times 10^{4}$
fumarate	^{12}C	$7.56 \pm 8.6 \times 10^{2}$	$4.16 \pm 2.3 \times 10^{5}$	$1.98 \pm 3.2 \times 10^{5}$	$3.07 \pm 0.2 \times 10^{5}$
fumarate	$^{13}C_1$	$2.49 \pm 2.8 \times 10^{3}$	$3.02 \pm 2.1 \times 10^{5}$	$3.94 \pm 6.5 \times 10^{5}$	$1.13 \pm 0.2 \times 10^{6}$
fumarate	$^{13}C_2$	$2.14 \pm 0.7 \times 10^{7}$	$3.93 \pm 3.0 \times 10^{6}$	$8.41 \pm 22.6 \times 10^{5}$	$5.75 \pm 0.8 \times 10^{5}$
fumarate	$^{13}C_3$	$4.26 \pm 5.8 \times 10^{5}$	$4.91 \pm 6.1 \times 10^{5}$	$1.73 \pm 1.6 \times 10^{5}$	$3.14 \pm 3.7 \times 10^{4}$
fumarate	$^{13}C_4$	$3.02 \pm 2.8 \times 10^{4}$	$1.33 \pm 0.9 \times 10^{6}$	$1.02 \pm 2.3 \times 10^{6}$	$5.60 \pm 7.3 \times 10^{5}$
malate	^{12}C	$3.62 \pm 3.3 \times 10^{3}$	$9.96 \pm 11.9 \times 10^{5}$	$1.71 \pm 3.5 \times 10^{6}$	$1.80 \pm 2.1 \times 10^{6}$
malate	$^{13}C_1$	$6.69 \pm 11.6 \times 10^{3}$	$1.01 \pm 1.5 \times 10^{6}$	$3.48 \pm 6.0 \times 10^{6}$	$6.54 \pm 9.2 \times 10^{6}$
malate	$^{13}C_2$	$4.47 \pm 2.2 \times 10^{3}$	$4.77 \pm 3.5 \times 10^{3}$	$2.00 \pm 3.0 \times 10^{3}$	$4.89 \pm 1.3 \times 10^{3}$
malate	$^{13}C_3$	$0 \pm 0.0 \times 10^{0}$	$0 \pm 0.0 \times 10^{0}$	$0 \pm 0.0 \times 10^{0}$	$0 \pm 0.0 \times 10^{0}$
malate	$^{13}C_4$	$0 \pm 0.0 \times 10^{0}$	$0 \pm 0.0 \times 10^{0}$	$0 \pm 0.0 \times 10^{0}$	$0 \pm 0.0 \times 10^{0}$
6-phospho-D-gluconate	^{12}C	$0 \pm 0.0 \times 10^{0}$	$0 \pm 0.0 \times 10^{0}$	$0 \pm 0.0 \times 10^{0}$	$0 \pm 0.0 \times 10^{0}$
6-phospho-D-gluconate	$^{13}C_1$	$0 \pm 0.0 \times 10^{0}$	$0 \pm 0.0 \times 10^{0}$	$0 \pm 0.0 \times 10^{0}$	$0 \pm 0.0 \times 10^{0}$
6-phospho-D-gluconate	$^{13}C_2$	$3.10 \pm 3.2 \times 10^{6}$	$4.46 \pm 3.4 \times 10^{4}$	$1.53 \pm 1.2 \times 10^{5}$	$1.19 \pm 1.0 \times 10^{5}$
6-phospho-D-gluconate	$^{13}C_3$	$1.75 \pm 2.2 \times 10^{5}$	$2.94 \pm 5.1 \times 10^{3}$	$1.19 \pm 0.9 \times 10^{4}$	$5.04 \pm 4.9 \times 10^{3}$
6-phospho-D-gluconate	$^{13}C_4$	$2.82 \pm 4.1 \times 10^{4}$	$1.17 \pm 2.0 \times 10^{3}$	$2.16 \pm 2.5 \times 10^{3}$	$2.94 \pm 5.1 \times 10^{2}$
6-phospho-D-gluconate	$^{13}C_5$	$1.25 \pm 2.2 \times 10^{3}$	$1.77 \pm 2.0 \times 10^{4}$	$4.39 \pm 3.1 \times 10^{4}$	$1.82 \pm 1.0 \times 10^{4}$
6-phospho-D-gluconate	$^{13}C_6$	$0 \pm 0.0 \times 10^{0}$	$1.99 \pm 2.7 \times 10^{3}$	$4.55 \pm 2.9 \times 10^{4}$	$1.29 \pm 0.6 \times 10^{4}$
ribose/ ribulose/ xyulose-phosphate	^{12}C	$4.70 \pm 4.2 \times 10^{4}$	$3.29 \pm 3.0 \times 10^{4}$	$2.50 \pm 1.7 \times 10^{5}$	$1.31 \pm 0.6 \times 10^{5}$
ribose/ ribulose/ xyulose-phosphate	$^{13}C_1$	$8.96 \pm 11.3 \times 10^{5}$	$5.40 \pm 4.3 \times 10^{5}$	$4.06 \pm 2.8 \times 10^{6}$	$2.47 \pm 1.3 \times 10^{6}$
ribose/ ribulose/ xyulose-phosphate	$^{13}C_2$	$1.33 \pm 1.0 \times 10^{4}$	$1.32 \pm 0.5 \times 10^{4}$	$1.94 \pm 1.7 \times 10^{4}$	$2.10 \pm 1.5 \times 10^{4}$
ribose/ ribulose/ xyulose-phosphate	$^{13}C_3$	$3.62 \pm 3.2 \times 10^{2}$	$1.57 \pm 2.7 \times 10^{2}$	$3.72 \pm 2.2 \times 10^{2}$	$0 \pm 0.0 \times 10^{0}$
ribose/ ribulose/ xyulose-phosphate	$^{13}C_4$	$4.55 \pm 7.9 \times 10^{3}$	$2.74 \pm 4.8 \times 10^{3}$	$5.92 \pm 3.4 \times 10^{3}$	$1.14 \pm 0.1 \times 10^{4}$
ribose/ ribulose/ xyulose-phosphate	$^{13}C_5$	$0 \pm 0.0 \times 10^{0}$	$1.88 \pm 3.3 \times 10^{2}$	$6.83 \pm 7.8 \times 10^{2}$	$3.04 \pm 0.6 \times 10^{3}$
D-sedoheptulose-1/7-phosphate	^{12}C	$0 \pm 0.0 \times 10^{0}$	$0 \pm 0.0 \times 10^{0}$	$3.13 \pm 1.8 \times 102$	$1.74 \pm 3.0 \times 10^{2}$
D-sedoheptulose-1/7-phosphate	$^{13}C_1$	$1.65 \pm 2.9 \times 10^{2}$	$1.93 \pm 3.3 \times 10^{3}$	$0 \pm 0.0 \times 10^{0}$	$1.17 \pm 2.0 \times 10^{3}$
D-sedoheptulose-1/7-phosphate	$^{13}C_2$	$2.39 \pm 1.0 \times 10^{6}$	$1.65 \pm 1.5 \times 10^{4}$	$5.75 \pm 4.1 \times 10^{4}$	$8.40 \pm 8.9 \times 10^{4}$
D-sedoheptulose-1/7-phosphate	$^{13}C_3$	$4.76 \pm 4.3 \times 10^{4}$	$0 \pm 0.0 \times 10^{0}$	$2.03 \pm 1.8 \times 10^{3}$	$9.43 \pm 16.3 \times 10^{2}$
D-sedoheptulose-1/7-phosphate	$^{13}C_4$	$0 \pm 0.0 \times 10^{0}$	$0 \pm 0.0 \times 10^{0}$	$0 \pm 0.0 \times 10^{0}$	$0 \pm 0.0 \times 10^{0}$
D-sedoheptulose-1/7-phosphate	$^{13}C_5$	$0 \pm 0.0 \times 10^{0}$	$0 \pm 0.0 \times 10^{0}$	$0 \pm 0.0 \times 10^{0}$	$0 \pm 0.0 \times 10^{0}$
D-sedoheptulose-1/7-phosphate	$^{13}C_6$	$0 \pm 0.0 \times 10^{0}$	$0 \pm 0.0 \times 10^{0}$	$0 \pm 0.0 \times 10^{0}$	$0 \pm 0.0 \times 10^{0}$
D-sedoheptulose-1/7-phosphate	$^{13}C_7$	$0 \pm 0.0 \times 10^{0}$	$0 \pm 0.0 \times 10^{0}$	$0 \pm 0.0 \times 10^{0}$	$0 \pm 0.0 \times 10^{0}$
D-erythrose-4-phosphate	^{12}C	$4.24 \pm 2.9 \times 10^{3}$	$6.22 \pm 4.0 \times 10^{4}$	$1.23 \pm 1.2 \times 10^{5}$	$5.41 \pm 0.8 \times 10^{4}$

Table A-11 continued.

metabolite	labeling pattern	0 min	2 min	5 min	15 min
D-erythrose-4-phosphate	$^{13}C_1$	$2.00 \pm 1.2 \times 10^5$	$1.20 \pm 0.5 \times 10^6$	$1.34 \pm 2.1 \times 10^6$	$1.79 \pm 0.2 \times 10^6$
D-erythrose-4-phosphate	$^{13}C_2$	$7.84 \pm 0.8 \times 10^4$	$5.30 \pm 6.7 \times 10^4$	$1.95 \pm 6.7 \times 10^4$	$7.33 \pm 2.4 \times 10^4$
D-erythrose-4-phosphate	$^{13}C_3$	$0 \pm 0.0 \times 10^0$	$0 \pm 0.0 \times 10^0$	$0 \pm 0.0 \times 10^0$	$3.90 \pm 6.8 \times 10^2$
D-erythrose-4-phosphate	$^{13}C_4$	$0 \pm 0.0 \times 10^0$	$0 \pm 0.0 \times 10^0$	$0 \pm 0.0 \times 10^0$	$0 \pm 0.0 \times 10^0$

Table A-12. The average ion counts plus or minus the standard deviation for the metabolites discussed and their isotopomers for the *purH Salmonella enterica* experiment at 30, 60, and 120 minutes are shown.

metabolite	labeling pattern	30 min	60 min	120 min
glucose/fructose-6-phosphate	^{12}C	$1.91 \pm 0.5 \times 10^5$	$2.59 \pm 1.1 \times 10^5$	$4.87 \pm 2.4 \times 10^5$
glucose/fructose-6-phosphate	$^{13}C_1$	$2.85 \pm 4.9 \times 10^3$	$1.05 \pm 1.8 \times 10^4$	$8.20 \pm 8.8 \times 10^3$
glucose/fructose-6-phosphate	$^{13}C_2$	$0 \pm 0.0 \times 10^0$	$0 \pm 0.0 \times 10^0$	$0 \pm 0.0 \times 10^0$
glucose/fructose-6-phosphate	$^{13}C_3$	$0 \pm 0.0 \times 10^0$	$0 \pm 0.0 \times 10^0$	$0 \pm 0.0 \times 10^0$
glucose/fructose-6-phosphate	$^{13}C_4$	$2.63 \pm 4.6 \times 10^3$	$0 \pm 0.0 \times 10^0$	$0 \pm 0.0 \times 10^0$
glucose/fructose-6-phosphate	$^{13}C_5$	$4.38 \pm 5.9 \times 10^4$	$8.61 \pm 14.9 \times 10^3$	$4.00 \pm 5.6 \times 10^4$
glucose/fructose-6-phosphate	$^{13}C_6$	$2.91 \pm 2.4 \times 10^5$	$0 \pm 0.0 \times 10^0$	$1.67 \pm 2.4 \times 10^5$
fructose-1-6-bisphosphate	^{12}C	$4.08 \pm 6.7 \times 10^5$	$1.04 \pm 0.7 \times 10^5$	$2.75 \pm 1.9 \times 10^5$
fructose-1-6-bisphosphate	$^{13}C_1$	$7.28 \pm 9.5 \times 10^3$	$0 \pm 0.0 \times 10^0$	$1.86 \pm 1.7 \times 10^4$
fructose-1-6-bisphosphate	$^{13}C_2$	$1.79 \pm 3.1 \times 10^3$	$0 \pm 0.0 \times 10^0$	$9.28 \pm 10.1 \times 10^3$
fructose-1-6-bisphosphate	$^{13}C_3$	$1.51 \pm 1.6 \times 10^4$	$1.30 \pm 1.9 \times 10^4$	$1.18 \pm 1.1 \times 10^4$
fructose-1-6-bisphosphate	$^{13}C_4$	$1.34 \pm 1.7 \times 10^4$	$2.50 \pm 4.3 \times 10^3$	$5.39 \pm 4.9 \times 10^3$
fructose-1-6-bisphosphate	$^{13}C_5$	$2.23 \pm 3.9 \times 10^5$	$4.10 \pm 5.6 \times 10^4$	$1.15 \pm 1.7 \times 10^5$
fructose-1-6-bisphosphate	$^{13}C_6$	$1.86 \pm 3.2 \times 10^6$	$7.41 \pm 11.8 \times 10^5$	$1.00 \pm 1.4 \times 10^6$
D-glyceraldehdye-3-phosphate	^{12}C	$7.80 \pm 4.4 \times 10^5$	$4.24 \pm 0.8 \times 10^5$	$5.66 \pm 2.5 \times 10^5$
D-glyceraldehdye-3-phosphate	$^{13}C_1$	$1.08 \pm 0.5 \times 10^4$	$1.15 \pm 1.6 \times 10^4$	$1.60 \pm 1.4 \times 10^4$
D-glyceraldehdye-3-phosphate	$^{13}C_2$	$3.74 \pm 5.5 \times 10^3$	$1.40 \pm 1.7 \times 10^4$	$5.68 \pm 4.3 \times 10^4$
D-glyceraldehdye-3-phosphate	$^{13}C_3$	$2.94 \pm 3.9 \times 10^5$	$1.12 \pm 1.6 \times 10^6$	$3.63 \pm 2.8 \times 10^6$
1,3-diphopshateglycerate	^{12}C	$1.67 \pm 2.1 \times 10^4$	$8.41 \pm 4.9 \times 10^3$	$2.42 \pm 2.0 \times 10^4$
1,3-diphopshateglycerate	$^{13}C_1$	$0 \pm 0.0 \times 10^0$	$5.68 \pm 9.9 \times 10^2$	$1.82 \pm 3.2 \times 10^3$
1,3-diphopshateglycerate	$^{13}C_2$	$2.03 \pm 2.3 \times 10^3$	$2.75 \pm 3.8 \times 10^3$	$4.56 \pm 3.6 \times 10^3$
1,3-diphopshateglycerate	$^{13}C_3$	$4.90 \pm 4.9 \times 10^4$	$2.64 \pm 3.6 \times 10^4$	$1.19 \pm 1.0 \times 10^5$
3/2-phosphoglycerate	^{12}C	$6.13 \pm 5.3 \times 10^4$	$2.24 \pm 0.6 \times 10^4$	$3.70 \pm 3.8 \times 10^4$
3/2-phosphoglycerate	$^{13}C_1$	$5.22 \pm 1.4 \times 10^6$	$2.42 \pm 1.1 \times 10^6$	$2.99 \pm 0.4 \times 10^6$
3/2-phosphoglycerate	$^{13}C_2$	$1.93 \pm 1.8 \times 10^4$	$3.16 \pm 1.3 \times 10^4$	$2.40 \pm 0.7 \times 10^4$
3/2-phosphoglycerate	$^{13}C_3$	$3.47 \pm 5.8 \times 10^5$	$7.00 \pm 12.0 \times 10^5$	$8.19 \pm 11.9 \times 10^4$
pyruvate	^{12}C	$1.39 \pm 2.0 \times 10^7$	$1.74 \pm 2.9 \times 10^7$	$9.67 \pm 12.1 \times 10^6$
pyruvate	$^{13}C_1$	$1.94 \pm 0.6 \times 10^6$	$1.69 \pm 1.2 \times 10^6$	$6.66 \pm 2.3 \times 10^5$
pyruvate	$^{13}C_2$	$1.97 \pm 1.1 \times 10^5$	$1.34 \pm 0.9 \times 10^5$	$5.13 \pm 3.0 \times 10^4$
pyruvate	$^{13}C_3$	$1.67 \pm 0.9 \times 10^6$	$7.69 \pm 4.0 \times 10^5$	$2.63 \pm 1.6 \times 10^5$
alpha-ketoglutarate	^{12}C	$4.47 \pm 0.5 \times 10^6$	$2.47 \pm 0.4 \times 10^6$	$1.88 \pm 0.3 \times 10^6$
alpha-ketoglutarate	$^{13}C_1$	$7.96 \pm 3.4 \times 10^6$	$6.22 \pm 4.5 \times 10^6$	$6.47 \pm 3.8 \times 10^6$

Table A-12 continued.

metabolite	labeling pattern	30 min	60 min	120 min
alpha-ketoglutarate	$^{13}C_2$	$2.85 \pm 2.7 \times 10^7$	$3.33 \pm 4.2 \times 10^7$	$4.92 \pm 4.5 \times 10^7$
alpha-ketoglutarate	$^{13}C_3$	$1.34 \pm 1.5 \times 10^4$	$4.73 \pm 1.1 \times 10^3$	$2.06 \pm 2.9 \times 10^4$
alpha-ketoglutarate	$^{13}C_4$	$0 \pm 0.0 \times 10^0$	$0 \pm 0.0 \times 10^0$	$0 \pm 0.0 \times 10^0$
alpha-ketoglutarate	$^{13}C_5$	$2.30 \pm 2.0 \times 10^3$	$0 \pm 0.0 \times 10^0$	$0 \pm 0.0 \times 10^0$
succinyl-CoA	^{12}C	$4.25 \pm 7.4 \times 10^3$	$0 \pm 0.0 \times 10^0$	$0 \pm 0.0 \times 10^0$
succinyl-CoA	$^{13}C_1$	$0 \pm 0.0 \times 10^0$	$1.08 \pm 1.9 \times 10^3$	$0 \pm 0.0 \times 10^0$
succinyl-CoA	$^{13}C_2$	$0 \pm 0.0 \times 10^0$	$0 \pm 0.0 \times 10^0$	$0 \pm 0.0 \times 10^0$
succinyl-CoA	$^{13}C_3$	$0 \pm 0.0 \times 10^0$	$0 \pm 0.0 \times 10^0$	$0 \pm 0.0 \times 10^0$
succinyl-CoA	$^{13}C_4$	$0 \pm 0.0 \times 10^0$	$0 \pm 0.0 \times 10^0$	$0 \pm 0.0 \times 10^0$
succinyl-CoA	$^{13}C_5$	$0 \pm 0.0 \times 10^0$	$0 \pm 0.0 \times 10^0$	$0 \pm 0.0 \times 10^0$
succinyl-CoA	$^{13}C_6$	$0 \pm 0.0 \times 10^0$	$0 \pm 0.0 \times 10^0$	$1.40 \pm 2.4 \times 10^3$
succinyl-CoA	$^{13}C_7$	$0 \pm 0.0 \times 10^0$	$0 \pm 0.0 \times 10^0$	$0 \pm 0.0 \times 10^0$
succinyl-CoA	$^{13}C_8$	$0 \pm 0.0 \times 10^0$	$0 \pm 0.0 \times 10^0$	$0 \pm 0.0 \times 10^0$
succinyl-CoA	$^{13}C_9$	$0 \pm 0.0 \times 10^0$	$0 \pm 0.0 \times 10^0$	$0 \pm 0.0 \times 10^0$
succinyl-CoA	$^{13}C_{10}$	$0 \pm 0.0 \times 10^0$	$0 \pm 0.0 \times 10^0$	$0 \pm 0.0 \times 10^0$
succinyl-CoA	$^{13}C_{11}$	$0 \pm 0.0 \times 10^0$	$0 \pm 0.0 \times 10^0$	$0 \pm 0.0 \times 10^0$
succinyl-CoA	$^{13}C_{12}$	$0 \pm 0.0 \times 10^0$	$0 \pm 0.0 \times 10^0$	$0 \pm 0.0 \times 10^0$
succinyl-CoA	$^{13}C_{13}$	$0 \pm 0.0 \times 10^0$	$0 \pm 0.0 \times 10^0$	$0 \pm 0.0 \times 10^0$
succinyl-CoA	$^{13}C_{14}$	$0 \pm 0.0 \times 10^0$	$0 \pm 0.0 \times 10^0$	$0 \pm 0.0 \times 10^0$
succinyl-CoA	$^{13}C_{15}$	$0 \pm 0.0 \times 10^0$	$0 \pm 0.0 \times 10^0$	$0 \pm 0.0 \times 10^0$
succinyl-CoA	$^{13}C_{16}$	$0 \pm 0.0 \times 10^0$	$0 \pm 0.0 \times 10^0$	$0 \pm 0.0 \times 10^0$
succinyl-CoA	$^{13}C_{17}$	$0 \pm 0.0 \times 10^0$	$0 \pm 0.0 \times 10^0$	$1.47 \pm 2.6 \times 10^4$
succinyl-CoA	$^{13}C_{18}$	$0 \pm 0.0 \times 10^0$	$0 \pm 0.0 \times 10^0$	$0 \pm 0.0 \times 10^0$
succinyl-CoA	$^{13}C_{19}$	$0 \pm 0.0 \times 10^0$	$0 \pm 0.0 \times 10^0$	$0 \pm 0.0 \times 10^0$
succinyl-CoA	$^{13}C_{20}$	$1.46 \pm 2.5 \times 10^3$	$0 \pm 0.0 \times 10^0$	$0 \pm 0.0 \times 10^0$
succinyl-CoA	$^{13}C_{21}$	$0 \pm 0.0 \times 10^0$	$0 \pm 0.0 \times 10^0$	$0 \pm 0.0 \times 10^0$
succinyl-CoA	$^{13}C_{22}$	$0 \pm 0.0 \times 10^0$	$0 \pm 0.0 \times 10^0$	$0 \pm 0.0 \times 10^0$
succinyl-CoA	$^{13}C_{23}$	$4.04 \pm 2.1 \times 10^6$	$2.30 \pm 0.7 \times 10^6$	$2.59 \pm 0.3 \times 10^6$
succinyl-CoA	$^{13}C_{24}$	$9.52 \pm 8.3 \times 10^5$	$4.98 \pm 4.3 \times 10^5$	$2.26 \pm 1.8 \times 10^5$
succinyl-CoA	$^{13}C_{25}$	$4.05 \pm 2.1 \times 10^6$	$2.16 \pm 1.0 \times 10^6$	$1.96 \pm 0.1 \times 10^6$
succinate	^{12}C	$4.92 \pm 1.9 \times 10^6$	$3.2 \pm 1.1 \times 10^6$	$4.54 \pm 2.2 \times 10^6$
succinate	$^{13}C_1$	$2.54 \pm 2.0 \times 10^7$	$2.81 \pm 3.0 \times 10^7$	$5.76 \pm 4.7 \times 10^7$
succinate	$^{13}C_2$	$3.91 \pm 0.9 \times 10^4$	$1.79 \pm 0.9 \times 10^4$	$8.99 \pm 7.5 \times 10^3$
succinate	$^{13}C_3$	$2.09 \pm 1.1 \times 10^4$	$9.27 \pm 6.7 \times 10^3$	$1.48 \pm 1.3 \times 10^3$
succinate	$^{13}C_4$	$1.23 \pm 0.9 \times 10^5$	$5.24 \pm 2.5 \times 10^4$	$1.49 \pm 1.0 \times 10^4$
fumarate	^{12}C	$3.40 \pm 0.7 \times 10^5$	$1.90 \pm 0.4 \times 10^5$	$2.03 \pm 1.3 \times 10^5$

Table A-12 continued.

metabolite	labeling pattern	30 min	60 min	120 min
fumarate	$^{13}C_1$	$1.22 \pm 0.8 \times 10^6$	$1.34 \pm 1.2 \times 10^6$	$2.14 \pm 1.8 \times 10^6$
fumarate	$^{13}C_2$	$9.92 \pm 1.2 \times 10^5$	$8.51 \pm 1.3 \times 10^5$	$7.75 \pm 2.1 \times 10^5$
fumarate	$^{13}C_3$	$3.07 \pm 2.2 \times 10^5$	$1.04 \pm 1.3 \times 10^5$	$2.29 \pm 2.1 \times 10^4$
fumarate	$^{13}C_4$	$1.65 \pm 0.9 \times 10^6$	$6.05 \pm 5.0 \times 10^5$	$2.04 \pm 1.5 \times 10^5$
malate	^{12}C	$4.12 \pm 2.0 \times 10^6$	$3.81 \pm 2.2 \times 10^6$	$1.81 \pm 0.5 \times 10^6$
malate	$^{13}C_1$	$1.14 \pm 0.5 \times 10^7$	$1.74 \pm 2.2 \times 10^7$	$1.35 \pm 0.8 \times 10^7$
malate	$^{13}C_2$	$2.93 \pm 1.4 \times 10^3$	$4.02 \pm 2.8 \times 10^3$	$4.33 \pm 1.3 \times 10^3$
malate	$^{13}C_3$	$0 \pm 0.0 \times 10^0$	$1.99 \pm 3.4 \times 10^2$	$0 \pm 0.0 \times 10^0$
malate	$^{13}C_4$	$0 \pm 0.0 \times 10^0$	$0 \pm 0.0 \times 10^0$	$0 \pm 0.0 \times 10^0$
6-phospho-D-gluconate	^{12}C	$2.39 \pm 4.1 \times 10^2$	$0 \pm 0.0 \times 10^0$	$0 \pm 0.0 \times 10^0$
6-phospho-D-gluconate	$^{13}C_1$	$0 \pm 0.0 \times 10^0$	$0 \pm 0.0 \times 10^0$	$0 \pm 0.0 \times 10^0$
6-phospho-D-gluconate	$^{13}C_2$	$4.22 \pm 5.6 \times 10^5$	$1.53 \pm 1.7 \times 10^5$	$2.00 \pm 1.9 \times 10^5$
6-phospho-D-gluconate	$^{13}C_3$	$2.38 \pm 3.4 \times 10^4$	$8.99 \pm 8.7 \times 10^3$	$1.02 \pm 0.5 \times 10^4$
6-phospho-D-gluconate	$^{13}C_4$	$4.70 \pm 6.7 \times 10^3$	$9.67 \pm 10.8 \times 10^2$	$8.50 \pm 14.7 \times 10^2$
6-phospho-D-gluconate	$^{13}C_5$	$7.73 \pm 8.6 \times 10^3$	$7.53 \pm 3.6 \times 10^3$	$1.79 \pm 0.9 \times 10^3$
6-phospho-D-gluconate	$^{13}C_6$	$1.14 \pm 0.9 \times 10^4$	$3.57 \pm 4.7 \times 10^3$	$5.75 \pm 0.5 \times 10^3$
ribose/ ribulose/ xyulose-phosphate	^{12}C	$1.45 \pm 2.3 \times 10^5$	$9.75 \pm 13.8 \times 10^4$	$9.24 \pm 13.1 \times 10^4$
ribose/ ribulose/ xyulose-phosphate	$^{13}C_1$	$2.67 \pm 3.6 \times 10^6$	$1.84 \pm 2.6 \times 10^6$	$2.18 \pm 2.7 \times 10^6$
ribose/ ribulose/ xyulose-phosphate	$^{13}C_2$	$4.28 \pm 1.2 \times 10^4$	$3.20 \pm 0.3 \times 10^4$	$3.08 \pm 2.4 \times 10^4$
ribose/ ribulose/ xyulose-phosphate	$^{13}C_3$	$2.37 \pm 4.1 \times 10^2$	$0 \pm 0.0 \times 10^0$	$0 \pm 0.0 \times 10^0$
ribose/ ribulose/ xyulose-phosphate	$^{13}C_4$	$8.83 \pm 10.1 \times 10^3$	$8.02 \pm 7.4 \times 10^3$	$8.25 \pm 1.9 \times 10^3$
ribose/ ribulose/ xyulose-phosphate	$^{13}C_5$	$7.45 \pm 13.1 \times 10^2$	$0 \pm 0.0 \times 10^0$	$9.31 \pm 16.1 \times 10^2$
D-sedoheptulose-1/7-phosphate	^{12}C	$1.61 \pm 2.8 \times 10^2$	$0 \pm 0.0 \times 10^0$	$0 \pm 0.0 \times 10^0$
D-sedoheptulose-1/7-phosphate	$^{13}C_1$	$0 \pm 0.0 \times 10^0$	$1.72 \pm 2.5 \times 10^3$	$1.60 \pm 2.8 \times 10^3$
D-sedoheptulose-1/7-phosphate	$^{13}C_2$	$1.28 \pm 1.1 \times 10^5$	$2.30 \pm 2.4 \times 10^4$	$1.69 \pm 1.8 \times 10^5$
D-sedoheptulose-1/7-phosphate	$^{13}C_3$	$9.21 \pm 16.0 \times 10^2$	$0 \pm 0.0 \times 10^0$	$0 \pm 0.0 \times 10^0$
D-sedoheptulose-1/7-phosphate	$^{13}C_4$	$0 \pm 0.0 \times 10^0$	$0 \pm 0.0 \times 10^0$	$0 \pm 0.0 \times 10^0$
D-sedoheptulose-1/7-phosphate	$^{13}C_5$	$0 \pm 0.0 \times 10^0$	$0 \pm 0.0 \times 10^0$	$0 \pm 0.0 \times 10^0$
D-sedoheptulose-1/7-phosphate	$^{13}C_6$	$0 \pm 0.0 \times 10^0$	$0 \pm 0.0 \times 10^0$	$0 \pm 0.0 \times 10^0$
D-sedoheptulose-1/7-phosphate	$^{13}C_7$	$0 \pm 0.0 \times 10^0$	$0 \pm 0.0 \times 10^0$	$0 \pm 0.0 \times 10^0$
D-erythrose-4-phosphate	^{12}C	$3.18 \pm 3.9 \times 10^4$	$2.90 \pm 4.0 \times 10^4$	$3.10 \pm 4.1 \times 10^4$
D-erythrose-4-phosphate	$^{13}C_1$	$1.09 \pm 1.1 \times 10^6$	$1.00 \pm 1.2 \times 10^6$	$1.26 \pm 1.2 \times 10^6$
D-erythrose-4-phosphate	$^{13}C_2$	$8.29 \pm 4.5 \times 10^4$	$4.33 \pm 1.3 \times 10^4$	$5.19 \pm 3.09 \times 10^4$

Table A-12 continued.

metabolite	labeling pattern	30 min	60 min	120 min
D-erythrose-4-phosphate	$^{13}C_3$	$9.01 \pm 15.6 \times 10^2$	$0 \pm 0.0 \times 10^0$	$4.32 \pm 7.5 \times 10^2$
D-erythrose-4-phosphate	$^{13}C_4$	$0 \pm 0.0 \times 10^0$	$0 \pm 0.0 \times 10^0$	$0 \pm 0.0 \times 10^0$

VITA

Nicole Mooney was born in Deland, Florida. She graduated from T. DeWitt Taylor Middle-High School in 2007. She then attended the University of North Florida, pursuing a bachelor's in biology and in chemistry. She attended the University of Tennessee, pursuing a master's degree in chemistry and worked in Dr. Campagna's lab.